UNIVERSITY OF OKLAHOMA

GRADUATE COLLEGE

ORGANIC GEOCHEMICAL CHARACTERIZATION OF THE SILURIAN TANEZZUFT FORMATION AND CRUDE OILS FROM THE MURZUQ BASIN, S. W. LIBYA

A DISSERTATION

SUBMITTED TO THE GRADUATE FACULTY

in partial fulfillment of the requirements for the

Degree of

DOCTOR OF PHILOSOPHY

By

TAREK A. HODAIRI
Norman, Oklahoma
2012

ORGANIC GEOCHEMICAL CHARACTERIZATION OF THE SILURIAN TANEZZUFT FORMATION AND CRUDE OILS FROM THE MURZUQ BASIN, S. W. LIBYA

A DISSERTAION APPROVED FOR THE
CONOCOPHILIPS SCHOOL OF GEOLOGY AND GEOPHYSICS

BY

_____
Dr. R. Paul Philp, Chair

_____
Dr. Bor-Jier (Benjamin) Shiau

_____
Dr. Michael Engel

_____
Daniel Jarvie

_____
Dr. Roger Slatt

ACKNOWLEDGEMENTS

I would like to express my sincere appreciation and thank to my research advisor and graduate committee chairman, Dr. R. Paul Philp, for his knowledge, direction, and time for this research, and for his patience, guidance, assistance, and encouragement throughout my study, and also for giving me the opportunity to be one of his students.

I would like to express my deep gratitude to all members of my advisory committee, Dr. Michael H. Engel, Dr. Roger Slatt, Dr. Bor-Jier (Benjamin) Shiau, and Mr. Daniel Jarvie, for their guidance, valuable suggestions, discussion, and the time they invested to review this manuscript.

I would like to express my gratitude to the staff of Repsol (Akakus) Oil Company, the operator of El-Sharara Oil Field in the Murzuq Basin, S.W. Libya, for providing us with the shale and oil samples. This research would have not been possible without their contribution. My gratitude is extended to Dr. N. Fello and Dr. S. Lüning for their invaluable support and suggestion. I also gratefully acknowledge the financial support awarded by the Libya's Ministry of Higher Education Scholarship Programs.

My sincere thanks go also to Mr. Jonathan Allen, the technician at the Organic Geochemistry Laboratory of the School of Geology and Geophysics for his time, help and being patient with us throughout my lab work. I am very grateful to Brian J. Cardott of the Oklahoma Geological Survey at the University of Oklahoma for training me throughout the whole process of reflectance measurements and his help in obtaining the graptolite reflectance measurements. My gratitude is also extended to R. Maynard for his help in obtaining the isotopic data.

I would like to express my deep appreciation to my entire friends in our Organic Geochemistry Group at the School of Geology and Geophysics with whom I shared great moments and always helped me with my research in particular Tomasz Kuder and Coralie Biache for their valuable comments and suggestions. My gratitude is also extended to all professors and staff of the School of Geology and Geophysics at the University of Oklahoma for their kindness, support, guidance and assistance throughout my study in particular Dr. R. Elmore, Donna, Teresa, Nicky, Nancy, and Adrianne.

My special thanks are extended to my parents: Abu-Baker and Kalthoum, my brothers: Mohammed, Othman, Khalid, Shamsuddin, and Ashraf, and my sisters: Fatima, Rahma, Amina, and Ruqayya, for their love and support.

Finally, I would like to express my very special thanks to my wonderful wife “Huda” whose understanding, encouragement, support, patience, made this work possible. She has been my inspiration and motivation for continuing to improve my knowledge and move my study forward. I also thank my wonderful children: Abu-Baker and Mohammed, for always making me smile and for understanding on those weekend mornings when I was studying instead of playing games with them. I hope that one day they can read this manuscript and understand why I spent so much time in front of my computer.

TABLE OF CONTENTS

Page

LIST OF TABLES

Page

LIST OF FIGURES

Page

ABSTRACT

Source rock and crude oil samples collected from the Murzuq Basin, S.W. Libya have been investigated by a variety of organic geochemical methods, including Rock-Eval pyrolysis (RE), gas chromatography (GC), gas chromatography mass spectrometry (GCMS), and graptolite reflectance. Rock samples were collected from the Tanezzuft Formation ('cool' shales) from several wells of A-Field located in Block NC-115. Furthermore, crude oil samples were collected from A-, R-, and I-Fields in NC-115 and NC-186 Blocks. The distributions of n-alkanes, isoprenoids, terpanes, and steranes (saturate fractions) along with phenanthrenes, mono- and triaromatic steroid hydrocarbons (aromatic fractions) were studied and used to determine organic matter composition, nature of depositional environments and levels of thermal maturity for both rock and crude oil samples.

The results from the study of the rock samples show a close correlation between RE data and the biomarker parameters. Based on RE data, organic matter is characterized as being poor to fair in TOC. This is most probably due to the relative oxicity of the depositional environment. The samples are shown to be mainly Type III kerogen (gas prone) with some contribution of mixed type II and III kerogens (gas/oil prone). The predominance of nC_{17} over nC_{25} in n-alkane profiles suggests a high input of marine-derived organic matter. However, values of Pr/nC_{17} vs. Ph/nC_{18} and the stable carbon isotopic composition for saturate and aromatic hydrocarbons of selected extracts along with the predominance of C_{27} and C_{29} steranes in most of the samples indicate that organic matter in these sediments has mixed marine/terrigenous sources with a slight

influence of marine input as suggested by the presence of C_{30} steranes and a predominance of tricyclic terpanes in most samples. The values of Pr/Ph ratios (0.83–2.32) suggest that these sediments were deposited under sub-oxic conditions, which is also indicated by the presence of C_{30}-diahopane in most of the samples, low ratios of C_{35} to C_{34} homohopanes, high diasterane/sterane ratios as well as low quality organic matter manifested by low hydrogen indices. Thermal maturity parameters, including the sterane isomerization ratios $C_{29}\alpha\beta\beta/(\alpha\beta\beta+\alpha\alpha\alpha)$, $C_{29}\alpha\alpha\alpha 20S/(20S+20R)$, homohopane isomerization ratios $C_{32}22S/(22S+22R)$, Ts/(Ts+Tm) ratios, and C_{30}-moretanes/C_{30}-hopanes ($C_{30}\beta\alpha/C_{30}\alpha\beta$) ratios, together with organic petrography and Rock-Eval data (e.g. Tmax and HI vs. Tmax crossplot), support early to intermediate maturity levels for the rock samples. However, it is proposed that the Uppermost Silurian Tanezzuft Formation ('cool' shale) has not generated, or will not generate, considerable amounts of hydrocarbons in the Murzuq Basin.

Based on biomarker distributions (e.g. *n*-alkanes, isoprenoids, terpanes, and steranes), the source of crude oils is characterized by mixed marine/terrigenous organic matter indicated by the stable carbon isotopic composition for saturate and aromatic hydrocarbons of selected crude oils. The values of the Pr/Ph (1.36–2.1), C_{30}-diahopane/C_{29}Ts, and diasterane/sterane ratios together with the low values of C_{29}/C_{30}-hopane ratio and the crossplot of the dibenzothiophene/phenanthrene ratio (DBT/P) vs. Pr/Ph ratio in most of oil samples suggest that the oils were sourced from marine clay-rich sediments deposited in sub-oxic (mild anoxic) depositional environments. Assessment of thermal maturity based on phenanthrenes, aromatic steroids (e.g. monoaromatic (MA) and triaromatic (TA) steroid hydrocarbons), terpanes (e.g.

tricyclic/hopane ratios), diasterane/sterane ratios, as well as the high concentrations of pregnane and homopregnane, indicates that crude oils from A-Field are at high levels of thermal maturity, while oils from R- and I-Fields are characterized by intermediate levels of thermal maturity. Based on the distributions of *n*-alkanes (*n*-C_{11} – *n*-C_{32}) along with the absence of 25-norhopanes in all of the crude oils, the oils do not appear to have been biodegraded. Correlation of crude oils permits the establishment of one genetic family and is supported by the stable carbon isotope values. These oils can be divided into two subfamilies based on the differences in maturities as shown in the Pr/nC_{17} vs. Ph/nC_{18} crossplot. Subfamily-A is represented by all oils from A-Field-NC115, which is characterized by high levels of maturity. Subfamily-B is described by oils from R- and I-Fields that are at intermediate levels of maturity. The two subfamilies may represent two different phases of hydrocarbon generation that took place in the Murzuq Basin. In summary, the geochemical characteristics of the oil samples from A-, R-, and I-Fields from the Murzuq Basin suggested that all the crude oils were generated from similar source rocks. Depositional environment conditions and advanced thermal maturities of these oils are also consistent with the previously published geochemical interpretations of the Rhuddanian 'hot' shale Tanezzuft Formation, which is thought to be the main source rock in the Murzuq Basin.

Based on the relative concentration of biomarkers, oil/source rock correlation suggests that the Tanezzuft 'cool' shales in this study show a lack of correlation with crude oils.

CHAPTER-I

1. INTRODUCTION

1.1 GENERAL CONCEPTS OF THE MURZUQ BASIN

The Murzuq Basin, situated in southwestern Libya, is one of a number of intracratonic basins located on the North African Saharan Platform. It covers an area of about 350,000 km^2 in the southwest of Libya and extends southwards into Niger where it is known as the Djadu Basin (Figure 1.1). The basin developed during the Palaeozoic and was severely affected by mid-Devonian tectonism and subsequently by the Hercynian Orogeny during which the Al-Qarqaf Arch (Northern rim of the basin) was formed, and by further subsidence during the Mesozoic/Cenozoic (Bellini and Massa, 1980; Echikh, 1998; Yahia et al., 2000). The Palaeozoic sequence is comprised of Cambrian, Ordovician, Silurian, Devonian and Carboniferous rocks, and is unconformably overlain by up to 1500m of mainly Mesozoic continental deposits. The Lowermost Silurian Tanezzuft Formation ('hot' shale) and Middle-Late Devonian Awaynat Wanin Formation shale are thought to be the main source rocks along with other local source rocks (Echikh and Sola, 2000; Sikander et al., 2000). These have been recognized within Palaeozoic sequences and have contributed to charging of the Palaeozoic and Mesozoic reservoirs in the Murzuq Basin (Lüning et al., 2000; Sikander et al., 2000; Fello et al., 2006). Hydrocarbon generation began in the Mesozoic but peaked in the Cenozoic (Echikh and Sola, 2000).

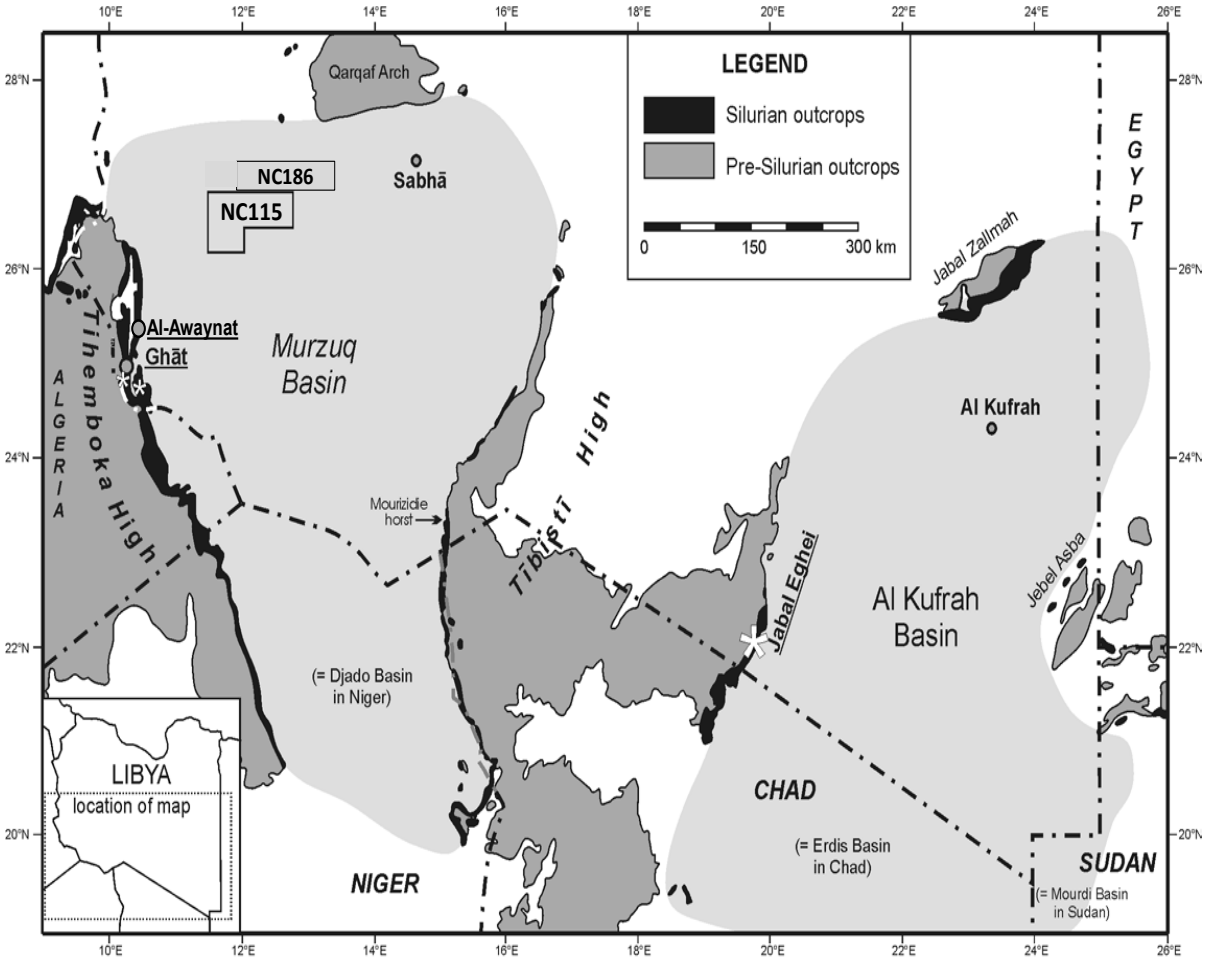

Figure 1.1. Location map of Murzuq Basin with position of the Blocks NC-115 and NC-186 selected for this study (Modified from Ghnia et al., 2008).

Oil migrated into the subjacent Mamuniyat Formation sandstones and was trapped in updip structures, which are Palaeozoic and Mesozoic anticlines, some of which are faulted, and palaeotopographic features ('buried hills') on the irregular Ordovician surface which are draped by Tanezzuft Shales (Echikh and Sola, 2000; Hallett, 2002). Only one effective petroleum system (Tanezzuft-Mamuniyat) has been found in the Murzuq Basin to date (Echikh and Sola, 2000), although others may remain to be discovered.

1.2 AIMS AND OBJECTIVE OF THE RESEARCH

Petroleum geochemistry is widely used to study the origin, migration pathways, and accumulation of petroleum. Nowadays, petroleum geochemistry techniques have become very significant geological tools in petroleum exploration due to their high efficiency, low cost, and rapid techniques for primary screening of the hydrocarbon potential of available samples. Geochemical analyses are used to determine how, where, and when organic matter in the sediments is converted into oil and/or gas. This is done by defining the concentration, quantity and quality, state of thermal evolution of organic matter, and the amounts of hydrocarbons which have been, or could be, generated from the source rock.

The main aim of this study is to obtain a better understanding of the petroleum systems contributing to hydrocarbon generation in the Murzuq Basin in order to improve the overall understanding of the potential for future production from this petroleum system. The main objectives of the study are to:

i) Characterize and assess the organic matter content, organic facies, kerogen types, and source rock potential of the sediments within the Tanezzuft Formation in the area of study (e.g. Rock-Eval pyrolysis analysis, GC, and GC-MS).

ii) Evaluate the petroleum generating potential of the source rocks.

iii) Determine the thermal maturity levels of the organic constituents.

iv) Undertake oil–oil and oil-source rock correlations.

v) Identify the effective petroleum system and the main prospective area within the basin.

1.3 PREVIOUS STUDIES ON THE MURZUQ BASIN

1.3.1 STRUCTURAL SETTING

The Murzuq Basin was subject to several compressional and extensional tectonic phases. These tectonic activities began during the Pre-Cambrian orogenesis that formed vertical basement faults, trending N-S, and counterbalanced by conjugated faults trending in a NE−SW direction (Massa and Jaeger, 1971; Bellini and Massa, 1980; Goudarzi, 1980; Echikh, 1998; Yahia et al., 2000).

The Pan-African movements were followed by three principal tectonic episodes, including the Caledonian orogeny (Wenlokian, Late-Early Silurian) and the Hercynian Orogeny that corresponds to the second major tectonic phase which has affected the Palaeozoic (Middle to Upper Carboniferous). The Hercynian Orogeny has caused folding, faulting, and strong subsidence (Bellini and Massa, 1980). The third phase was the Alpine

orogeny of the Tertiary period. Echikh and Sola (2000) stated that there are seven major tectonic elements that have been identified within the Murzuq Basin from west to east. These are the Tihemboka Arch, Alawaynat Trough, Tirinine High, Awbari Trough, Idhan Depression, Brak Bin-Ghanimah uplift, and Dur Al-Qussah Trough (Figure 1.2).

Moreover, Yahia et al. (2000) concluded that the Murzuq Basin was shaped by two main sets of faults. The first set located east of the basin is the Dur Al-Qussah complex fault set with NE-SW trend. The Dur Al-Qussah Trough is clearly visible, whereas, the Brak Ben-Ghanimah Arch, trending NW-SE was separating the Dur Al-Qussah sub-basin in the east from the main Murzuq Basin in the west (Figure 1.2). These fault sets were thought to be tectonically active during Cambro-Ordovician, Silurian, and Early Devonian times. During the Mesozoic era (Jurassic time), the eastern rim of the basin was uplifted, and since then the Dur Al-Qussah has been a mountain chain (Yahia et al., 2000). Several folded units were located along the major N-S Tihemboka Arch in the western part of the basin; these folds were separated the Murzuq Basin (SW) and the Ghadamis Basin (NE) in Libya and from the Illizi Basin in Algeria (SE).

1.3.2 STRATIGRAPHIC SETTING

The Murzuq basin has been studied stratigraphically by several geologists (Desio, 1936a; Lelubre, 1946b; Freulon, 1964; Klitzsch, 1969; Bellini and Massa, 1980; Klitzsch, 1981). Since the structural aspects of the basin were developed during the Late Proterozoic Pan-African orogenic event, this has probably affected the stratigraphic and depositional system within the predominantly Palaeozoic clastic basin- fill (Fello, 2001).

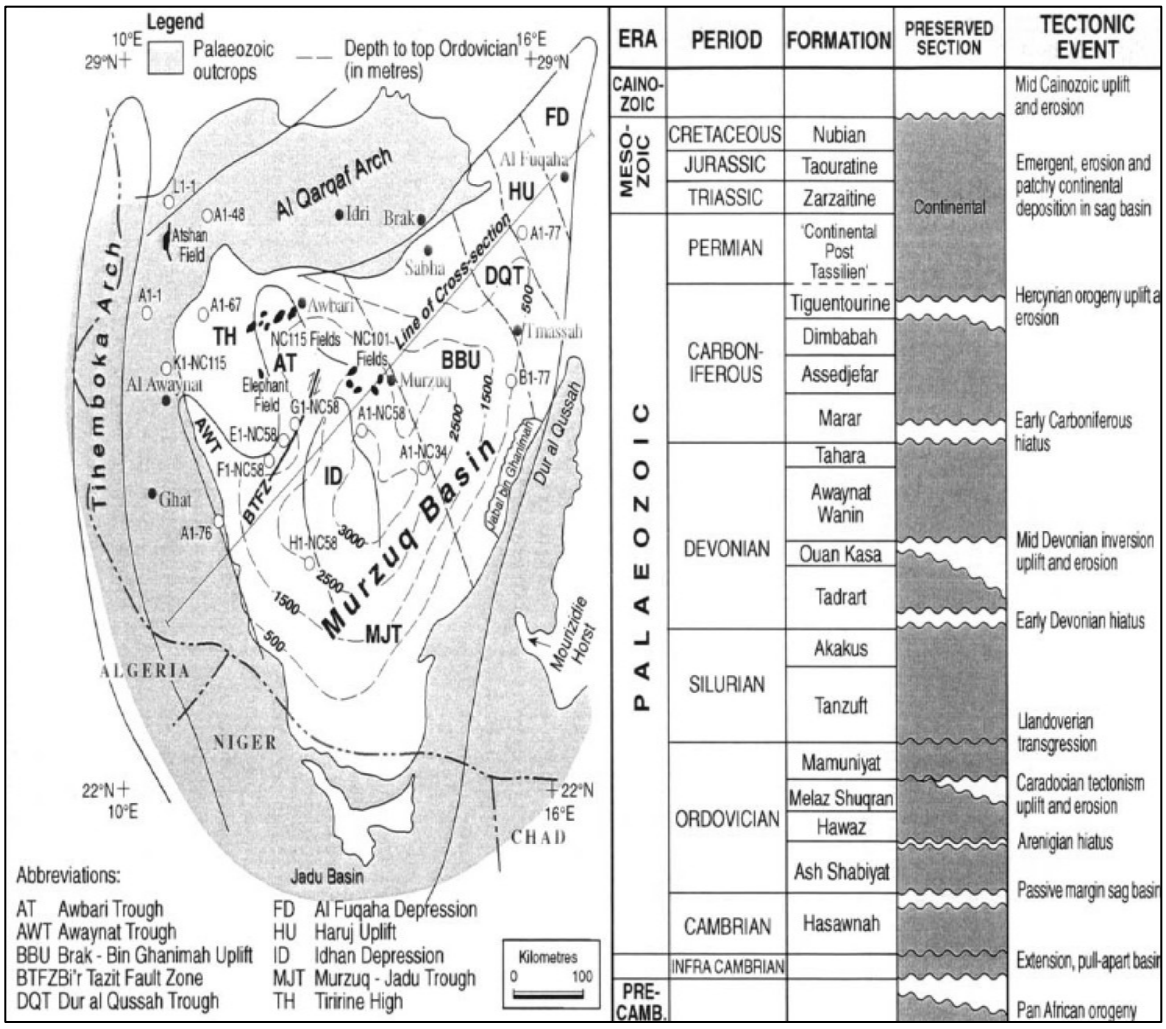

Figure 1.2. Shows tectonic elements map of the Murzuq Basin, Awbari Trough, and Idhan Depression, in which Tanezzuft Formation is characterized by mature source kitchens in Southwestern Libya.

The Murzuq Basin is a Palaeozoic sag basin, which underwent a major inversion during the mid-Devonian. The current SW-NE trend was imposed during the Hercynian Orogeny, but the basement structure retains indications of the earlier Pan-African trend. The Awaynat Trough and Idhan Depression are early Devonian depocentres, whilst the Tiririne High and Brak-Bin Ghanimah Uplift reflect the mid-Devonian uplift and erosion (Klituch. 1966; Pierobon. 1991; Meister et al., 1991; Echikh. 2000; Sutcliffe, et al., 2000; Hallett, 2002). (Contours modified from Echikh and Sola, 2000).

The basin is made up entirely of sedimentary rocks of Palaeozoic age, which cover a wide spectrum of depositional facies ranging from shallow water to fluvial sandstones.

1.3.2.1 Pre-Cambrian succession

The Pre-Cambrian unit that underlies the Cambrian Hasawnah Formation Sandstone is formed from the basement rocks and defined as the Mourizidie Formation (Figure 1.3), which is composed of high-grade metamorphic rocks associated with plutonic rocks, as well as low-grade metamorphic to unmetamorphic rocks of Precambrian era (Mourizidie Formation) (Jacqué, 1962; Ramos et al., 2006). The Mourizidie Formation occurs at the eastern rim of the basin as well as in some wells in the north part of the basin (Jacqué, 1962; Bellini and Massa, 1980; Hallett, 2002). It also consists of conglomeratic and shaly sandstone and siltstones. The basal 10m of the succession at the outcrop consists of large blocks of basement schist in a matrix of red sandstone (Bellini and Massa, 1980; Belaid et al., 2010). It overlies the basement with angular unconformity and also has been penetrated and cored by several wells in the block NC-115: Fields A1, D1, B31, and H27 at depth (2377–2378 m) reveals the presence of very hard quartzite with faint indications of folding (Aziz, 2000; Belaid et al., 2010).

1.3.2.2 Cambro-Ordovician succession

The Cambro-Ordovician succession of S.W. Libya was first defined in the area of the Al-Qarqaf Arch. Five formations have been recognized within the succession, four of

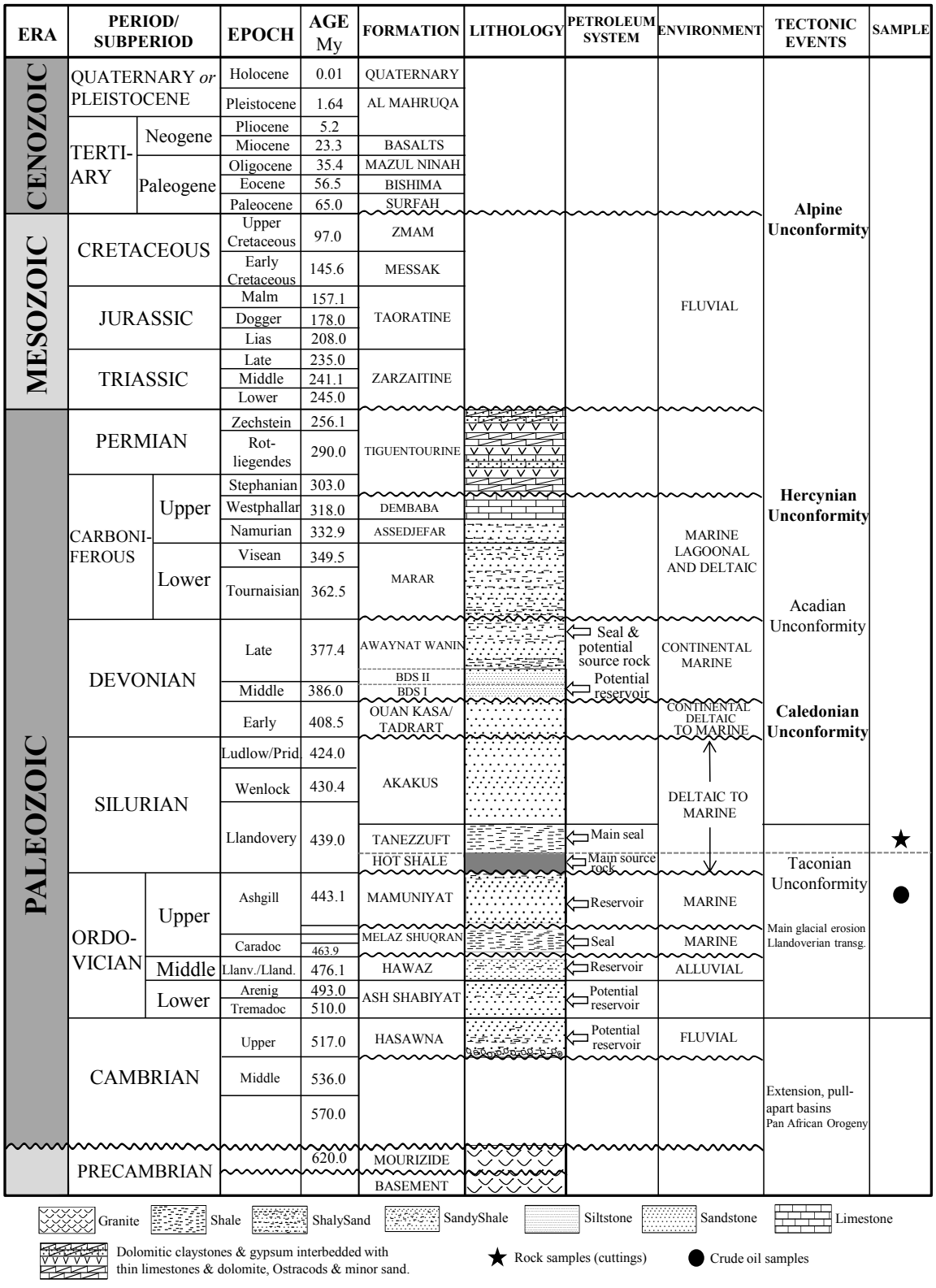

Figure 1.3. General stratigraphic column of the Murzuq Basin (NC-115), S.W. Libya. Modified and redrawn from Aziz, 2000; Yahia, 2000; Belaid et al., 2010.

them formally introduced by Massa and Collomb (1960). The first sediments to be deposited throughout the basin belong to the Cambrian Hasawnah Formation (Figure 1.3), which consists of several meters of basal conglomerate and coarse-grained, quartzitic sandstone (Davidson et al., 2000).

The overlying Ordovician Hawaz Formation is unconformably separated from the Hasawnah Formation. The unconformity was first defined by Massa and Collomb (1960). The type section of the Hawaz Formation on the Al-Qarqaf uplift consists of fine to medium-grained sandstone with minor intercalations of siltstone and shale. Vos (1981) suggested that the Hawaz Formation was deposited in a fan delta complex, which prograded across the Al-Qarqaf Arch (Figure 1.2). Massa and Collomb (1960) divided the Hawaz Formation into two new conformable formations, named Ash Shabiyat and Hawaz (Figure 1.3).

In the northwestern part of the basin, the Hawaz formation is overlain by shales of the upper Ordovician Melaz Shuqran Formation (Figures 1.3, 1.4 and 1.5). The shales were probably deposited in a relatively shallow marine environment, and the predominantly green color, which might indicate reducing conditions, suggests restricted marine circulation (Davidson et al., 2000). The Melaz Shuqran Formation is frequently absent in wells drilled in the center of the basin, and outcrops in the northwest of the Ghat area have a thickness of 5–7m (Aziz, 2000).

The uppermost Ordovician sediments of the Mamuniyat Formation form the main hydrocarbon reservoir in the basin. The Mamuniyat Formation consists primarily of sandstone with subordinate siltstone and shale beds. The sandstone is typically quartzitic, fine to medium-grained, and fairly well sorted (Aziz, 2000; Davidson et al., 2000). The

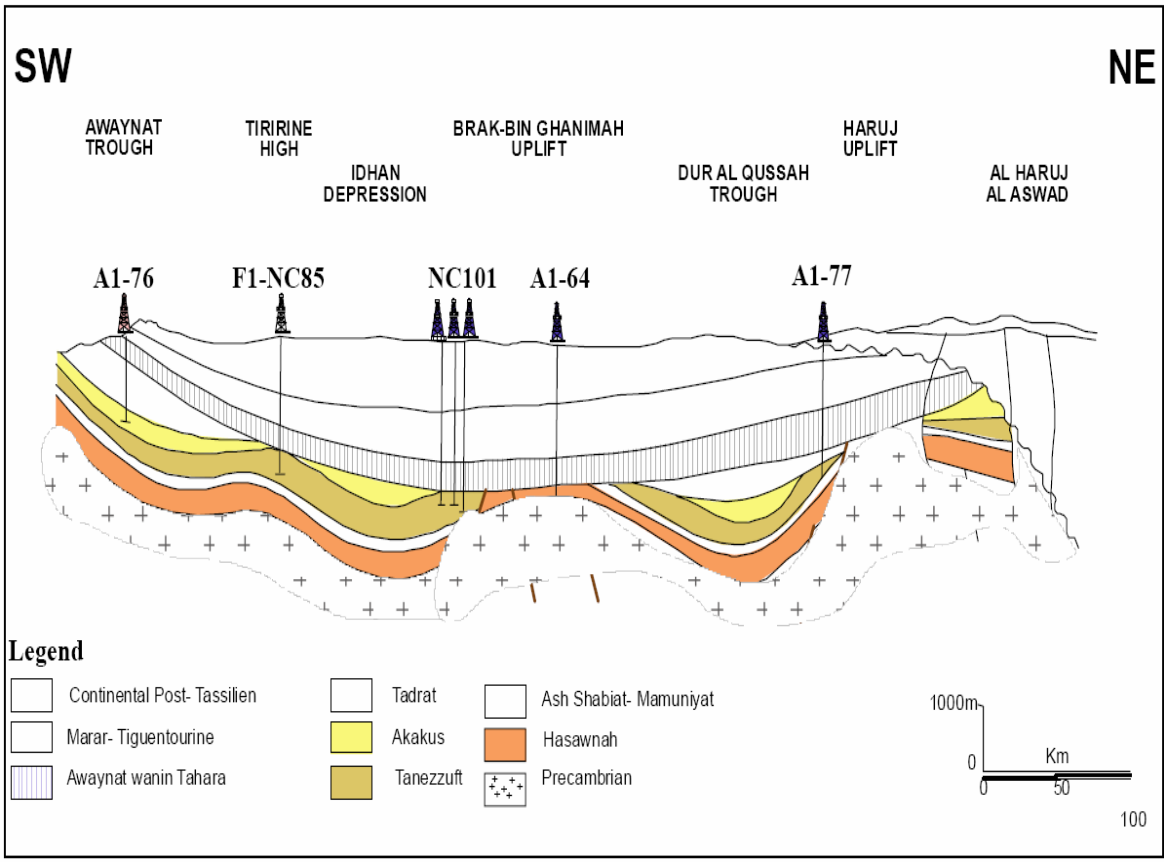

Figure 1.4. Diagrammatic Cross Section SW to NE of the Palaeozoic sequences within the Murzuq Basin, Libya (After Echikh, 2000; Suteliffe et al., 2000; Pierobon, 1991; Klitzch, 1971 and Hallett, 2002).

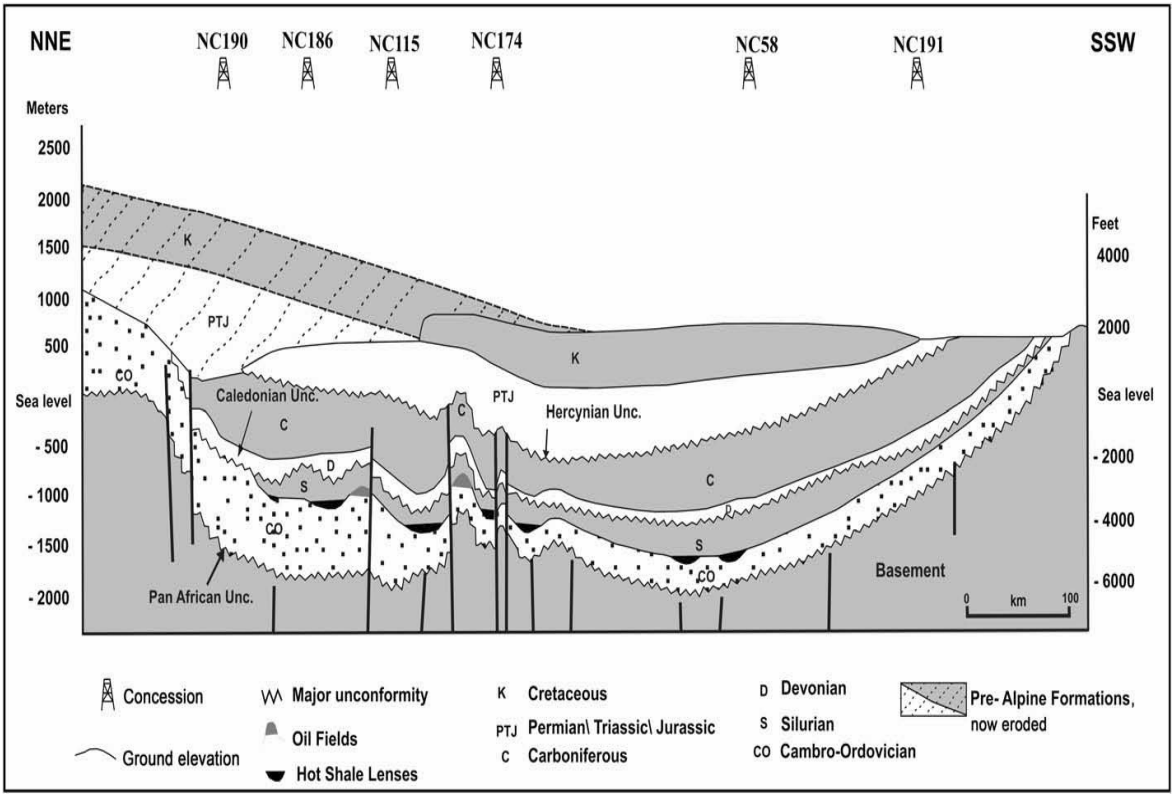

Figure 1.5. Schematic reconstructed cross-section showing major structures and three tectonic unconformities in the Murzuq Basin and eroded sedimentary sequences in the north (After Davidson et al., 2000).

Mamuniyat Formation and underlying Melaz Shuqran Formation were deposited at a time of glaciation over North Africa, which lay along the margin of Gondwanaland. It is likely that the ice sheet periodically extended as far north as the Murzuq Basin. There is some evidence for glaciation that has been observed on the western rim of the basin (Ghat area) by the presence of small dropstones in the Melaz Shuqran shale, and the occurrence of interpreted ice striations on bedding planes within the Mamuniyat Formation.

Echikh and Sola (2000) described the Bir Tlacsin Formation (Bi'r Tlakshin) as a transitional lithofacies between the Mamuniyat Formation sandstones and the Silurian Tanezzuft Shales. Hallett (2002) concluded that the Bir Tlacsin Formation unconformably overlies the Mamuniyat Formation, and it appears to infill topographic lows on the eroded and irregular Mamuniyat surface, and thins over topographic highs (Figure 1.6). It also has an unconformable relationship with the overlying Tanezzuft Formation, which truncates the Bir Tlacsin Formation. The Bir Tlacsin Formation consists of black mudstones containing abundant coarse sand grains, granules, and pebbles, which may have originated as a debris flow deposit. This formation is important from a petroleum system's point of view because it acts as a barrier between the Mamuniyat reservoir and the hot shale source rock (Echikh and Sola, 2000).

1.3.2.3 Silurian succession

The Silurian sediments are formally grouped into the Tanezzuft and Akakus Formations. Klitzsch (1963) observed the Silurian unconformably overlying older Cambro-Ordovician rocks. The transgressive Tanezzuft shale grades upward into the

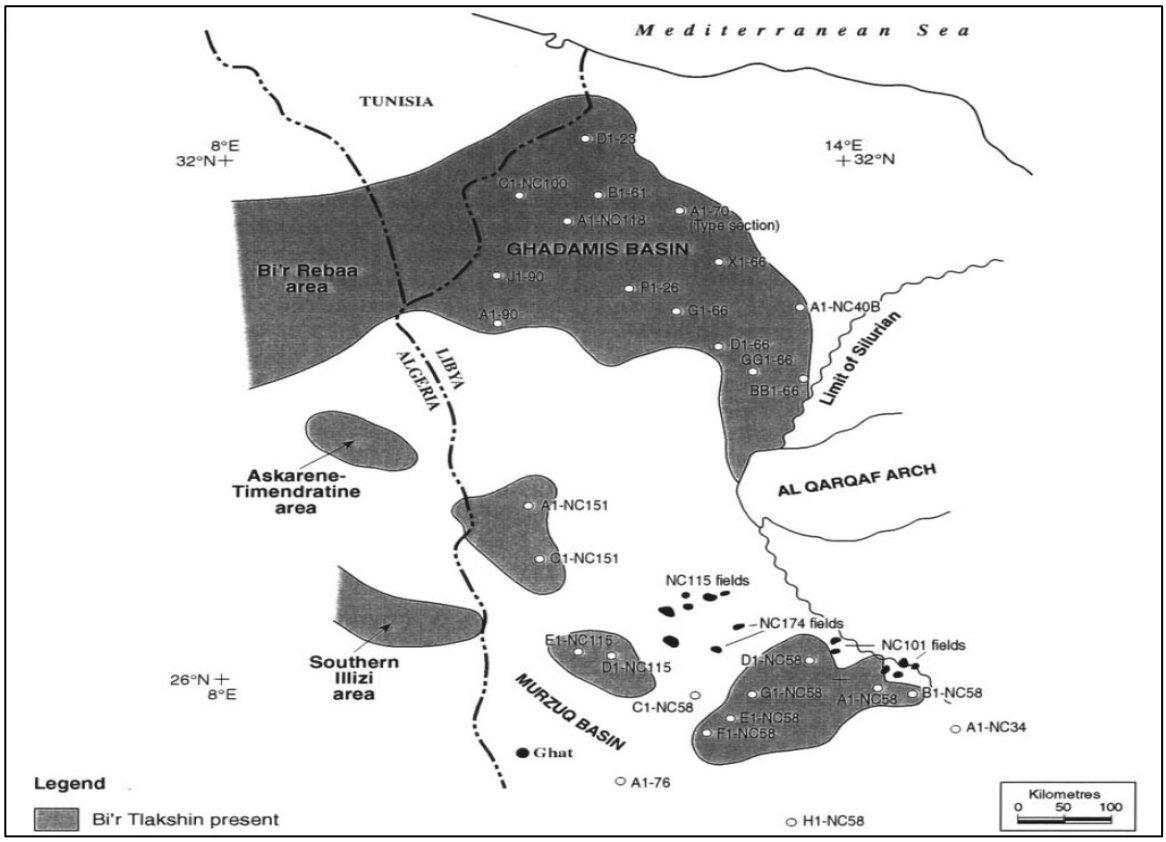

Figure 1.6. Bi’r Tlakshin (Bir Tlacsin) Formation, Distribution.

The informal Bi’r Tlakshin Formation of probable Rhuddanian age has a patchy development in western Libya, southern Tunisia and eastern Algeria. It unconformably overlies the Mamuniyat Formation and unconformably underlies the Tanezzuft Formation. The Bi’r Tlakshin Formation forms a barrier between the Mamuniyat reservoir and the Tanezzuft source rock. All of the Mamuniyat discoveries in the Murzuq Basin have been in areas where the Bi’r Tlakshin is absent. (After Echikh and Sola, 2000).

prograding Akakus sandstone and siltstone. Several authors showed that the contact of the marine Silurian formed a disconformity with the continental lower Devonian rocks (Massa and Collomb, 1960; Burollet, 1963; Banerjee, 1980). The Silurian sequence contains a complete sedimentary cycle ranging from deep marine shales to shallow marine and deltaic sediments. The main hydrocarbon source rock in the basin is the 'hot shale' Silurian Tanezzuft Formation (the lower part), which is characterized by a high content of uranium, organic material, and fossils such as graptolites. Melting of the late Ordovician ice cap of Gondwanaland led to a great eustatic sea level rise where the Tanezzuft shales were deposited. Later, a large deltaic system began its gradual NW-directed progradation over North Africa with deposition of a series of shallowing upward cycles (Akakus Formation; Figures 1.4 and 1.5; Bellini and Massa, 1980).

The Tanezzuft Formation (early-Llandoverian) was first introduced by Desio (1936b) and named after Wadi Tanezzuft, located between Ghat and Al Awaynat Cities (Figure 1.1). It consists of dark gray to black, graptolitic shales with intercalations of siltstone and fine grained sandstones often forming rhythmical alternation; it represents the broad marine transgression of the Silurian sea over the North African craton (Desio, 1936b). In southwestern Murzuq Basin, the Tanezzuft shale is about 475m thick, whereas in the subsurface, it ranges from 45 to 300m (Klitzsch, 1969). Over the northeastern part of the basin, an erosional pinch-out resulted from the uplifting of the Brak Bin-Ghanimah palaeohigh (Figures 1.2-1.5; Hallett, 2002).

The basal Tanezzuft Formation is recognized as radioactive hot shale and has a high gamma ray response (Figure 1.7). This is most probably due to the high content of uranium within the Tanezzuft shale (Lüning et al., 2000). The lower part of the Tanezzuft

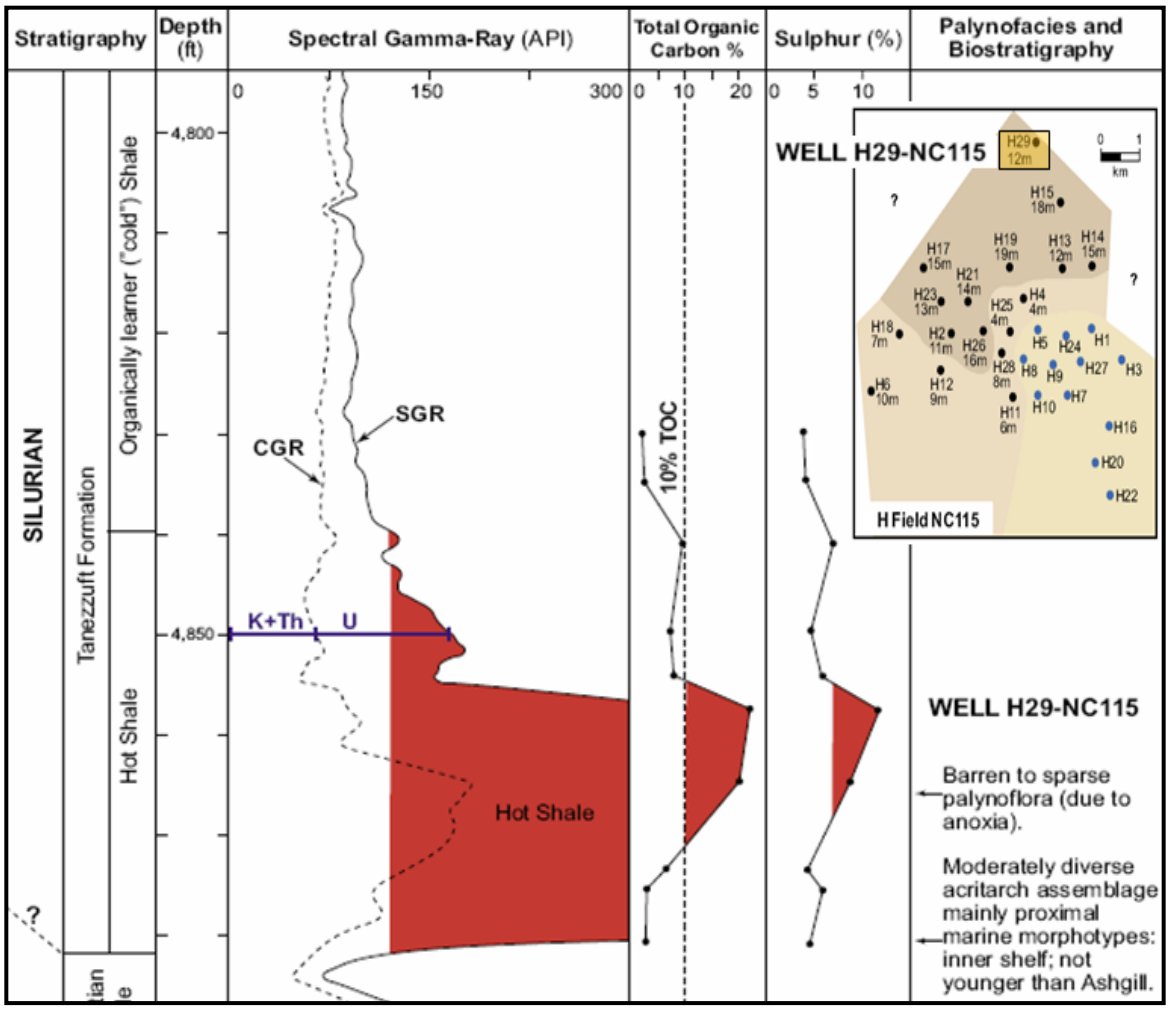

Figure 1.7. Spectral gamma-ray characteristics of the lower Silurian organic-rich shale in well H29-NC115. The high gamma-ray signal is almost entirely due to enrichment in uranium (note that values >300 API were not recorded) (After Fello et al., 2006).

Formation (hot shale) has been dated to be early Llandovery (Davidson et al., 2000). The transition between Tanezzuft Formation and overlying Akakus Formation is gradational and conformable. The upper part of the Silurian Akakus Formation is apparently absent in wells that are located at the present-day depocentres, which is possibly due to the Caledonian erosion event (Aziz, 2000; Davidson et al., 2000).

The Akakus Formation (middle-Llandoverian to Ludlorian) was first named by Desio (1936a) after Jabal 'Mountain' Akakus in the Ghat area. At the type locality, the Akakus Formation comprises 240m of fine to medium grained silty sandstone, thinly bedded, frequently cross-bedded, with ripple and flute marks (Desio, 1936a). The top is marked by a conspicuous horizon of ferruginous sandstone with convolute bedding and stromatolitic structures, which suggest a period of emergence. It contains the trace fossils *Arthrophycus alleghaniensis*, up to 40cms in length, plus *Corophiodes*, *Cruziana*, and *Tigillites dufrenoyi*, which are interbedded with dark gray graptolitic shale in the lower and middle parts (Hallett, 2002). The Akakus Formation has been interpreted as having been deposited in fluvial to shallow marine with tidal flat deposits. The lower contact is apparently conformable with the underlying Tanezzuft Formation (Figures 1.4 and 1.5), but the upper contact with the Tadrart Formation is distinctly unconformable (Hallett, 2002).

The Akakus Formation is also present in the subsurface of the Murzuq Basin where it reaches a thickness of 560m in the well F1-NC 58 (Figure 1.4 and 1.5). On the other hand, the formation outcrop thickness on the eastern margin of the basin varies greatly along the outcrop edge. In the Dura1 Qussah Trough, it reaches a thickness of 465m, but thins progressively to the south onto the Tripoli-Tibesti Uplift. South of the Mourizidie Horst, thickness ranges from 35 to 190m. The lithology in this area is principally thin

bedded sandstones, silty, and shaly in the lower part, but more massive, compact, cross-bedded, and ferruginous towards the top. The upper part of the Akakus Formation in the Dural Qussah Trough is characterized by psilophyte and lycophyte plant remains, which have been interpreted as deltaic or fluvial deposits (Hallett, 2002).

1.3.2.4 Lower Devonian succession

In early Devonian, the Murzuq Basin was situated on the northern margin of Gondwanaland and its shoreline began to migrate over southern Libya. This led to braided fluvial materials being deposited (Tadrart Formation). Sea level began to rise during the middle Devonian leading to shallow marine sedimentation. More deepening of the sea allowed the pro-deltaic shales to be deposited (Figure 1.8) (Lüning et al., 2007). However, the lower Devonian section is primarily characterized by Tadrart Sandstone and Ouan Kasa Sandstone with shale, grading upward into middle and upper Devonian Awaynat Wanin Sandstone and Shale (Figure 1.3). The Devonian successions show a typical seaward prograding and basinward thinning of clastic wedge exhibiting a classical interfering of facies patterns, which change from fluvial-continental to estuarine at the end of cycle to shallow marine neritic (Figure 1.8).

The Tadrart Formation (Early Devonian Siegenian) was first described by Burollet (1960). At the type locality, the Tadrart Formation forms a conspicuous scarp which weathers into large isolated pillars and blocks (Figure 1.9). In the western flank of the Murzuq Basin, the Tadrart Formation is made up of lenticular sandstone bodies

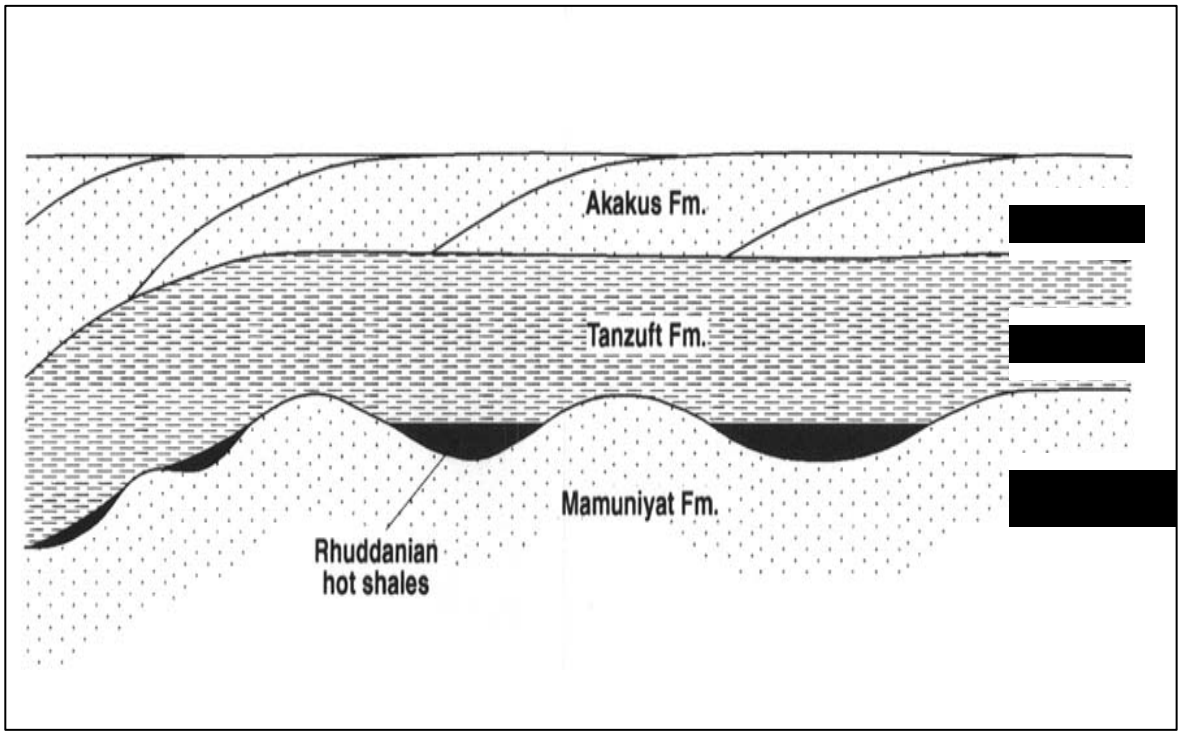

Figure 1.8. A model for Hot Shale Distribution of the Murzuq Basin, SW Libya.

The Silurian transgression introduced marine shales onto the irregular Ordovician post-glacial surface. The initial sediments deposited during the Rhuddanian stage were black anaerobic shales with a high content of uranium, which form excellent source rocks. As the transgression spread, the localized depressions were flooded by open marine shales with a much lower organic content. This explains the irregular distribution of the hot shales within the Murzuq Basin. (After Lüning et al., 1999).

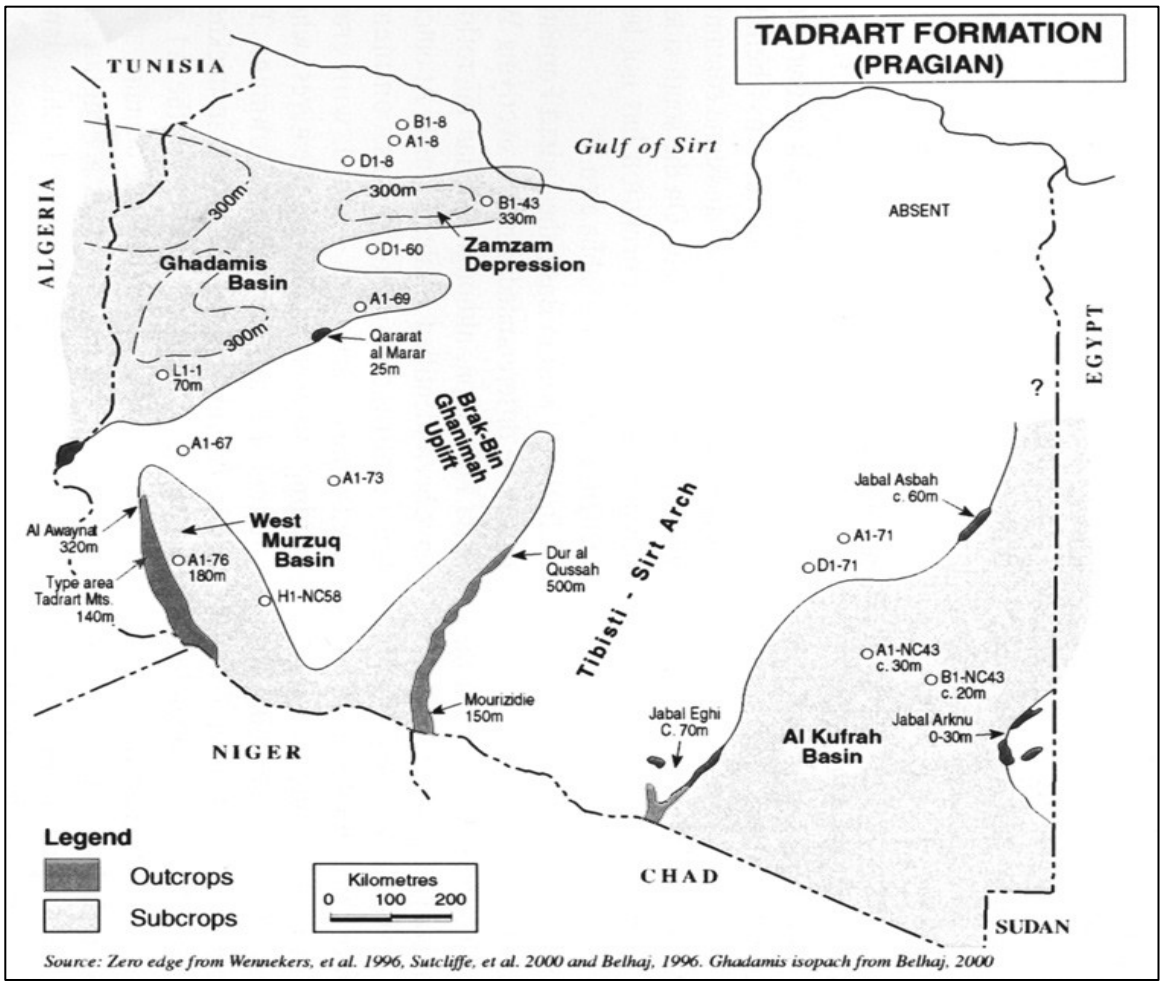

Figure 1.9. Showing Tadrart Formation Distribution, Murzuq Basin, S.W. Libya.

representing filled channels within a braided-river sequence. Grain size ranges from fine-grained to conglomeratic. The thickness reaches 320m at A1 Awaynat. The Tadrart Formation exhibits festoon cross bedding representing fluvial sandstones and herring-bone cross-bedding usually associated with tidal currents. The tidal current influence increases upwards. The Tadrart Sandstone represents excellent petroleum reservoir characteristics. It is dated to be Siegenian to Emsian in age (Klitzsch, 1969; Massa and Moreau-Benoit, 1976). Overlying the Tadrart Formation is the Ouan Kasa Formation.

The Ouan 'Wan' Kasa Formation is the second megacycle within the Devonian succession, and it has been interpreted as a marine transgressive sequence conformably overlying the much more massive sandstones of the Tadrart Formation. This sequence was first described by Borghi and Chiesa (1940) and was named after the Wadi Wan Kasa in the Jabal 'Mountain' Tadrart (Borghi and Chiesa, 1940). A formal type section was established by Klitzsch (1965) in the same area (Figure 1.10). It is composed of a series of alternating grey to reddish ferruginous siltstones and shales with thin layers of gypsum containing an abundant marine fauna of brachiopods, tentaculites, and trace fossils. A regional erosional event (early-middle Devonian unconformity) separates the lower from the middle-upper Devonian sequences (Bellini and Massa, 1980; Castro et al., 1985). The Devonian section lies between the two major unconformities in the Murzuq Basin: Caledonian and Hercynian (Figure 1.5).

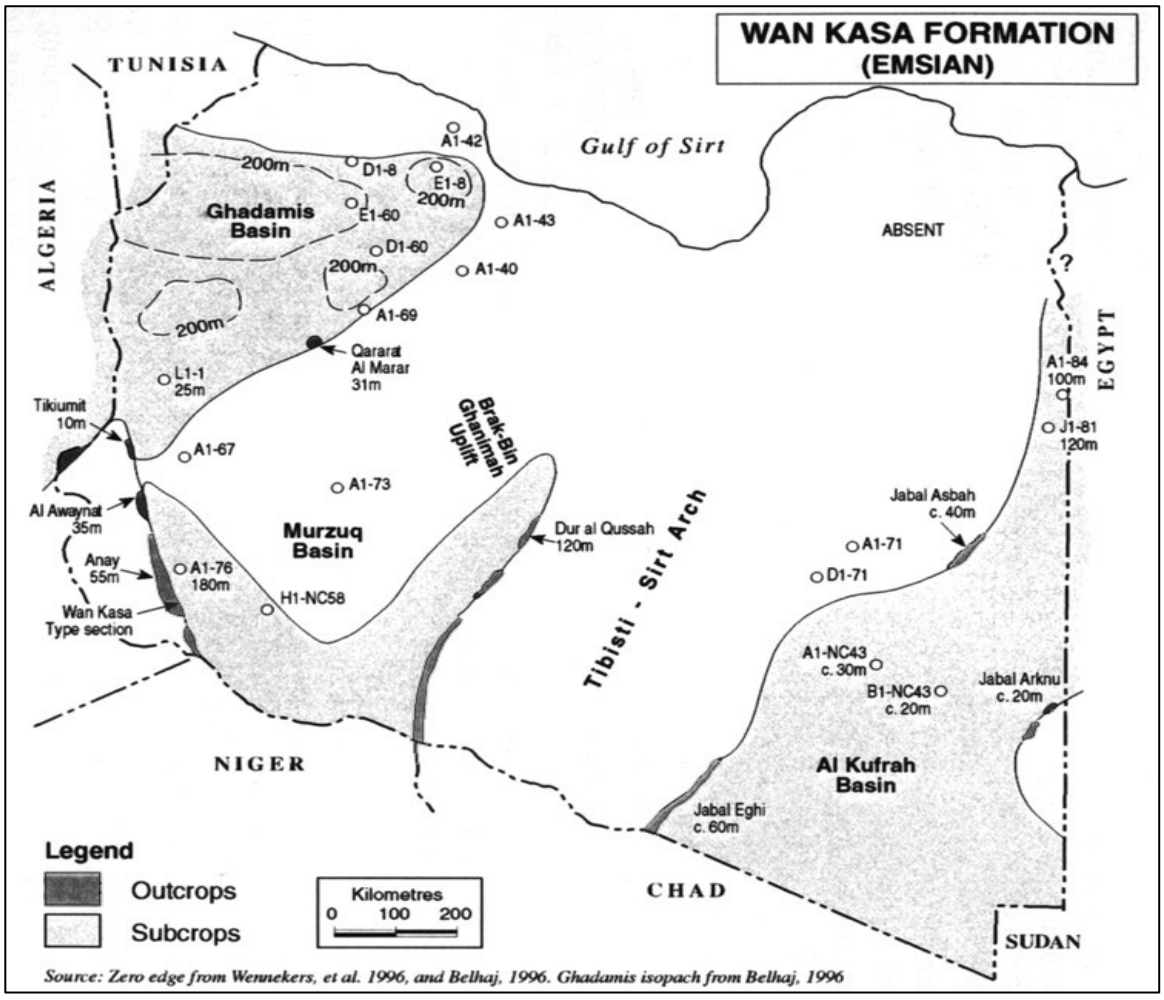

Figure 1.10. Distribution of the Ouan (Wan) Kasa Formation, Murzuq basin, S.W. Libya.

1.3.2.5 Middle-Upper Devonian succession

The age of Middle Devonian Rocks was first recognized by Borghi (1939) in the Awaynat Wanin area, but it was Lelubre (1946a) who first proposed the name Awaynat Wanin Formation, and Massa and Collomb (1960) who gave the first systematic description. The Middle-Upper formations can be attractive targets for hydrocarbon exploration as they exhibit fair quality reservoir and source beds (Borghi, 1939; Lelubre, 1946a; Massa and Collomb, 1960).

The Awaynat Wanin Formation (Middle-Late Devonian Couvinian to Strunian) comprises the entire sequence between the top of the Ouan Kasa Formation and the base of the Marar Formation. According to Vos (1981), it is marked by six repeated 'cyclothems' of claystones, sometimes ferruginous or gypsiferous, and of siltstones and sandstones, each cycle averaging 15-30m in thickness, with a total thickness of 162m (Vos, 1981). The sequence represents a deltaic environment ranging from delta front to fluvial-distributary channels, all reworked by tides and storm waves. The sandstones are repeatedly cross-bedded and contain various fauna of brachiopods. The lower part of the Awaynat Wanin Formation is apparently conformable with the underlying Ouan Kasa Formation and the top has a conformable contact with the overlying Marar Formation. Massa and Moreau-Benoit (1976) proposed upgrading the Awaynat Wanin to group status and dividing it into four units: Awaynat Wanin I to IV, corresponding to the Eifelian, Givetian, Frasnian, and Fammenian stages, which they were able to identify on the basis of faunal assemblages (Massa and Moreau-Benoit, 1976). The Awaynat Wanin Formation is conformably overlain by the Tahara Formation (Figure 1.3).

The Tahara Formation was established by Burollet and Manderscheid (1967), and was refined by Massa et al. (1974). It is a 60-70m shale sandstone cycle from a type section in the B 1-49 well in the southern Ghadamis Basin (Massa and Moreau-Benoit, 1976). It outcrops in a small area to the northwest of the Awaynat Wanin Formation, where two coarsening upwards cycles are exposed, separated by hard ground (Burollet and Manderscheid, 1967; Massa et al., 1974). The lower cycle represents typical tempestite features, and it shows thin bed sets with lenticular/wavy bedded shale and very fine sandstone at the base grading upwards in cyclic fashion into hummocky to cross-bedded sandstone; each cycle is no more than a few meters thick and is marked by intense bioturbation (Skolithos), the hard ground (middle unit) represents normal fair weather conditions, and the upper unit represents a tidally dominated facies. The middle and the upper units are fluvial deltaic deposits, whilst, the lower part represents marine conditions (Castro et al., 1985). Hassi (1998) recognized a sequence of sixteen shallowing-upwards sequences within the Tahara Formation representing a shelf-shoreface succession in a storm-dominated environment (Hassi, 1998).

1.3.2.6 Carboniferous-Permian succession

During the Carboniferous period, deposition in Libya was affected by tectonic events associated with the collision of western Gondwana with Laurasia to form Pangaea. These orogenic events resulted in compression, uplift, and the gradual emergence of a series of southwest–northeast intercratonic sags and arches, which increasingly affected sedimentation during the Carboniferous (Bishop, 1975). The type sections of

Carboniferous strata have been described by Klizsch (1963) and by Bellini and Massa (1980). The early Carboniferous sequence is dominated by deltaic and inner neritic facies. Late Namurian carbonate rocks reflect the last marine incursion of the Paleozoic, and the late Carboniferous is characterized by continental rocks. In general, the Carboniferous succession can be grouped into four formations (from the lower to the upper), namely the Mrar, Assedjefar, Dembaba, and Tiguentourine Formations.

The Marar Formation was first defined by Lelubre (1948) by referring to a type section at Qararat A1-Marar, northwest of the A1-Qarqaf Arch (Figure 1.1). It comprises about fifty stacked cycles of silty claystones, micaceous siltstones, and feldspathic quartz-sandstones (Lelubre, 1948). The claystones are greenish-grey, silty, and gypsiferous, and the sandstones and siltstones are ferruginous, flaggy, and often ripple-marked. The sandstones are sometimes conglomeratic at the base, frequently cross-bedded, and contain brachiopods and pelecypods. The fauna indicates an Upper Tournaisian-early Visean age (Massa et al., 1974).

The Assedjefar Formation was defined by Lelubre (1952) as a sequence of deltaic and shallow marine rocks conformably overlying the Marar Formation in the Hamadat Tanghirt area of west Libya (Figure 1.3). In the type area, there is a rapid transition from a dominantly sandy facies in the east, comprising coarse-grained, cross-bedded sandstones with fossil wood, to more shaly facies in the west. In both areas, the clastic sequence is overlain by marls and thin limestones (Lelubre, 1952).

The Dembaba Formation represents the last of the Carboniferous marine formations preserved in Libya, and generally, comprises shallow marine limestone and sandstone. In the Hamadat Tanghirt area, the lower unit comprises gypsiferous claystone, minor siltstones, and thin-bedded argillaceous limestones containing the stromatolitic alga

Collenia near the base. The algal horizon, which is distinguishable from that in the Marar Formation by its softness and lighter color, is patchily developed but very widespread and has been traced as far as Jadu Basin in Chad. The upper unit consists of dolomites and dolomitic limestones interbedded with claystones and siltstones. The Dembaba Formation has a thickness of 35 to 55m in the subsurface and rests unconformably upon older rocks (Lelubre, 1952; Hallett, 2002).

The Tiguentourine Formation represents the Upper Carboniferous and is comprised of red lacustrine mudstone. The formation may be found in parts of the Murzuq Basin, but it is often absent either due to non-deposition or as a result of uplift and erosion during the late Carboniferous, which produced the so-called Hercynian Unconformity (Figure 1.5; Davidson et al., 2000; Hallett, 2002).

Permian sediments are absent in the Murzuq Basin, most likely due to non-deposition following the late Carboniferous regional uplift (Davidson et al., 2000).

1.3.2.7 Mesozoic succession

The entire Triassic to Lower Cretaceous succession in the Murzuq Basin was deposited under continental conditions with fluvial sandstones and red mudstones of the Triassic to Jurassic Zarzaitine/Taouratine Formations and fluvial sandstones, conglomerates and mudstones of Jurassic/lower Cretaceous Mesak Formation (Figure 1.3). These formations seem to be conformable, but their contact may suggest a non-deposition period. Maximum thicknesses of over 1700m of Mesozoic sediments are found on the Idhan Depression (Figure 1.2), but in the northern part of the basin in block NC-

190, the entire Mesozoic section has been removed by erosion following the mid Cretaceous (Austrian) and early Tertiary (Alpine) uplifts as seen in Figure 1.5 (Davidson et al., 2000).

1.3.3 EXPLORATION HISTORY

Libya is one of the world's major hydrocarbon provinces with reserves on the order of some 17 BBO (billion barrels of oil) and with significant gas as well (Klett et al., 1997). The Murzuq Basin is considered one of the major hydrocarbon provinces in Libya with 238 MMBO (million barrels of oil) (Gumati et al., 1996). Exploration activity began in the Murzuq Basin in the 1950s and has been carried out sporadically since that time. Many companies have taken exploration licenses in the basin, such as Petrobras, Gulf Oil, Amoseas, British Petroleum, BOCO, RomPetrol, Lasmo, Total, and Wintershall.

BrasPetro drilled eight wells in NC-58 without encountering any commercial accumulations (Meister et al., 1991; Pierobon, 1991). BOCO made some oil discoveries in NC-101, and sixteen prospects have been drilled, resulting in the discovery of five oil accumulations in the Cambro-Ordovician reservoirs and two small oil accumulations in Devonian reservoirs. In the early 1980s, RomPetrol made a big discovery with three large fields 'A', 'B', and 'H' in block NC-115. Since then, Repsol (now Akakus) has initiated a development program for these fields with the first real production in 1997. The oil is transported through a pipeline to the oil terminal at al-Zawiyah City on the west coast of Tripoli. In 1992 and 1993, Lasmo Oil Company drilled four wildcats and discovered an oil field in the NC-174 Block (Elephant prospect), encountered excellent quality reservoir

sands of the Cambro-Ordovician Mamuniyat Formation. It has been estimated to contain over 500 million barrels of recoverable oil and at the time of drilling, was the largest oil discovery in Libya for fourteen years. In 2009, Repsol (Akakus) Oil Company, the operator of El-Sharara Oil Field in the Murzuq Basin, drilled several wells in the NC-115 and NC-174 Blocks and encountered excellent commercial accumulations. Nowadays, the Murzuq Basin has become an attractive area for further hydrocarbon exploration.

1.3.4 TANEZZUFT-MAMUNIYAT PETROLEUM SYSTEM

The Tanezzuft-Mamuniyat petroleum system is the only system so far discovered in the Murzuq Basin (Boote et al., 1998). Good quality source shales are present in both the Idhan Depression and Awbari Trough, and both of these areas are mature source kitchens. Hydrocarbon generation began in the Mesozoic but peaked in the Cenozoic (Echikh and Sola, 2000). Hydrocarbons reservoired in the Ordovician Mamuniyat Formation sandstones have been charged from the Silurian Tanezzuft Formation basal radioactive shales. Oil has not been found where the Tanezzuft seal is missing or where the Bi'r Tlakshin Formation intervenes between the source rock and the reservoir (Echikh and Sola, 2000; Hallett, 2002).

1.3.4.1 RESERVOIRS

Producing fields in the Murzuq Basin all have reservoirs in sandstones of Ordovician Mamuniyat and Hawaz Formations. However, reservoir quality in the Mamuniyat Formation fluctuates rapidly within a few hundred meters diagenetic sequence for the Mamuniyat sandstones in block NC-174, which showed a porosity reduction caused by quartz overgrowths and the growth of fibrous illite and porosity enhancement caused by dissolution of feldspars. Two distinct permeability groupings have been determined based on the content of clay in the reservoir (Echikh and Sola, 2000). The clean sandstones are characterized by high permeabilities between 100 and 1000mD, whilst the clay-rich sandstones showed very low permeabilities ranging from 0.1 and 1mD (Echikh and Sola, 2000). The Mamuniyat reservoirs in the Murzuq Basin have proven to be more prolific oil producers compared to that in Gadames Basin (NW Libya). Many oil fields within Murzuq basin have very good production rates. For instance, it is predicted that the Elephant Field (N1-NC174), one major discovery with estimated reserves of about 561MMB, can produce a maximum production rate of 150,000 BOPD. Another discovery was made in 2001 through the B1-NC-186 well drilled by Total, which tested 1300 barrels of oil per day with a gravity of 40API (Echikh and Sola, 2000). Repsol (the operator of El-Sharara Oil Field) discovered in 2001 through the A2-NC-186 well, flowed at 2670 b/d of 41API in the middle Ordovician sandstone of the Hawaz Formation.

1.3.4.2 SOURCE ROCK AND ITS QUALITY

The Silurian 'Tanezzuft Formation' and Devonian 'Awaynat Wanin' shales represent the most widespread source rocks in the Murzuq Basin, and genetically extends east- and westwards across northern Gondwana from Morocco to Oman (Lüning et al., 2000). Other local source rocks, such as the basal radioactive Melaz Shuqran shales likely represent Ordovician source rocks within the Murzuq Basin. However, the Tanezzuft Formation is limited in distribution due to several factors, such as clastic input, early Silurian marine transgression, mid-Devonian and post-Hercynian erosion (Echikh and Sola, 2000). Moreover, the basal hot shale is restricted to topographic depressions on the eroded Ordovician surface (Figure 1.8) in which the hot shales accumulated and where anoxic conditions prevailed (Echikh and Sola, 2000; Hallett, 2002). These factors could also affect the distribution of source richness and kerogen type. This is consistent with a dominance of amorphous kerogen in the central part of the basin whereas areas toward the southwest and south contain organic matter with more continental character and high coarse clastic contents. These features result in poor to non-source rock quality (Meister et al., 1991). In this study, the organically lean Tanezzuft Formation shales (the upper part) are defined as "cool" shales because the vast majority of shales are poor in organic content, low gamma values compared to the basal 'hot' shales (which is more organic rich, Lüning et al., 2000), and mostly have poor to fair oil potential (Lüning et al., 2000; Hall et al., 2010; Hodairi and Philp, 2011). However, the uppermost shales have been dated at the Ghat area of the Murzuq Basin, as early Aeronian (Klitzsch, 1969), and as ranging somewhere between late Rhuddanian–late Aeronian (Radulovic, 1984). The Tanezzuft Formation 'cool' shales have mostly less than 3% TOC and less than 10 mg

HC/g rock of S2 and type III or II/III kerogen (Hall et al., 2010; Hodairi and Philp, 2011) with the better quality kerogen often, but not always, at the base of the formation (Hall et al., 2010). Although, the Hot Shale is by far the dominant effective oil source rock, there are parts of the Tanezzuft Formation 'cool' shales with good potential. Hall et al. (2010) pointed out that in some areas there are thin horizons where shales are good oil prone source rocks, although not nearly as prolific as the basal 'hot' shales. The difference in kerogen composition of the Tanezzuft Formation 'cool' shale and the Tanezzuft Formation 'hot' shale appear to be mainly in quantity rather than composition (Hall et al., 2010).

The Tanezzuft Formation 'hot shale' (the lowermost part) extends in a belt from north to south with limited width and is missing both on the Tiririne High (Figure 1.2) and over much of the western part of the basin. The maximum thickness of the hot shales is about 45m in the southeastern parts of NC115 (Aziz, 2000). Hot shales are also absent in the southern and eastern parts of the basin where the sand content is high. In general, the thickness and quality of the hot shales decline southwards (Figure 1.11). The basal hot shales in the NC-174 area range in thickness from zero to more than 15m. Echikh and Sola (2000) published an isopach map, which demonstrates hot shale thicknesses of up to 30m, and extending as far south as well H1-NC 58 (Figure 1.11; Hallett, 2002).

Generally, the lower part of Tanezzuft Formation is a radioactive shale, which corresponds to a highly radioactive zone caused by high levels of uranium that is noticeable on wireline logs; spectral gamma-ray logs from well C1-NC174 and H29-NC115 show gamma-ray values up to 800 and 500 API units, respectively (Figure 1.7) (Hamyouni et al., 1984; Aziz, 2000; Echikh and Sola, 2000; Lüning et al., 2000). It is interesting that in the underlying Ordovician, thin high-radioactive zones are caused by

high levels of thorium and potassium rather than uranium (Lüning et al., 2000). In the Tanezzuft Formation shales are defined as "hot" if the gamma values exceed 150 API. The sediments enriched in authigenic uranium tend to be deposited under anoxic conditions that allow a large amount of organic matter to accumulate and uranium to be fixed (Wignall and Myers, 1988; Davidson et al., 2000). Meister et al. (1991), Aziz (2000), and Hallett (2002) concluded that the lower part of Tanezzuft Formation 'hot shale' in the northwestern and east central part of the basin is very rich in organic carbon with total organic content (TOC) ranging from 3 to 16.3%, hydrogen index (HI) from 197 to 393mg HC/g TOC with Type II kerogen (amorphous organic matter), and an average vitrinite reflectance (R_o) of 0.68%. On the contrary, the Tanezzuft 'cool' shale has a somewhat poorer source rock quality, with average TOC of 0.92% (Aziz, 2000; Hodairi and Philp, 2011). The shales with TOC values > 3% ('hot shale') usually contain marine organic matter and are thus oil-prone (Demaison and Moore, 1980; Tyson, 1995). These hot shales represent the source rock of the Tanezzuft Formation and correspond with the maximum flooding surface during the marine transgression (Davidson et al., 2000; Fello et al., 2006). Lüning et al. (2000) considered this lower part (Figure 1.8) as the source of 80–90% of all Paleozoic-sourced hydrocarbons in North Africa.

Based on vitrinite reflectance data, the hot shale is still at an early stage of maturity in wells D1-NC 58 and H1-NC 58 (Figures 1.11 and 1.12) in the depth range 2130 m to 2330 m, whilst in C1-NC 58 at a depth of only 1170m, the Tanezzuft shale is at a late stage of maturity (Meister et al., 1991; Aziz, 2000; Davidson et al., 2000; Echikh and Sola, 2000). It is mature to mid-mature in well H29-NC-115 (Figure 1.7). Maximum HI and S2 values were recorded for immature to early mature Hot Shale in F3-NC174

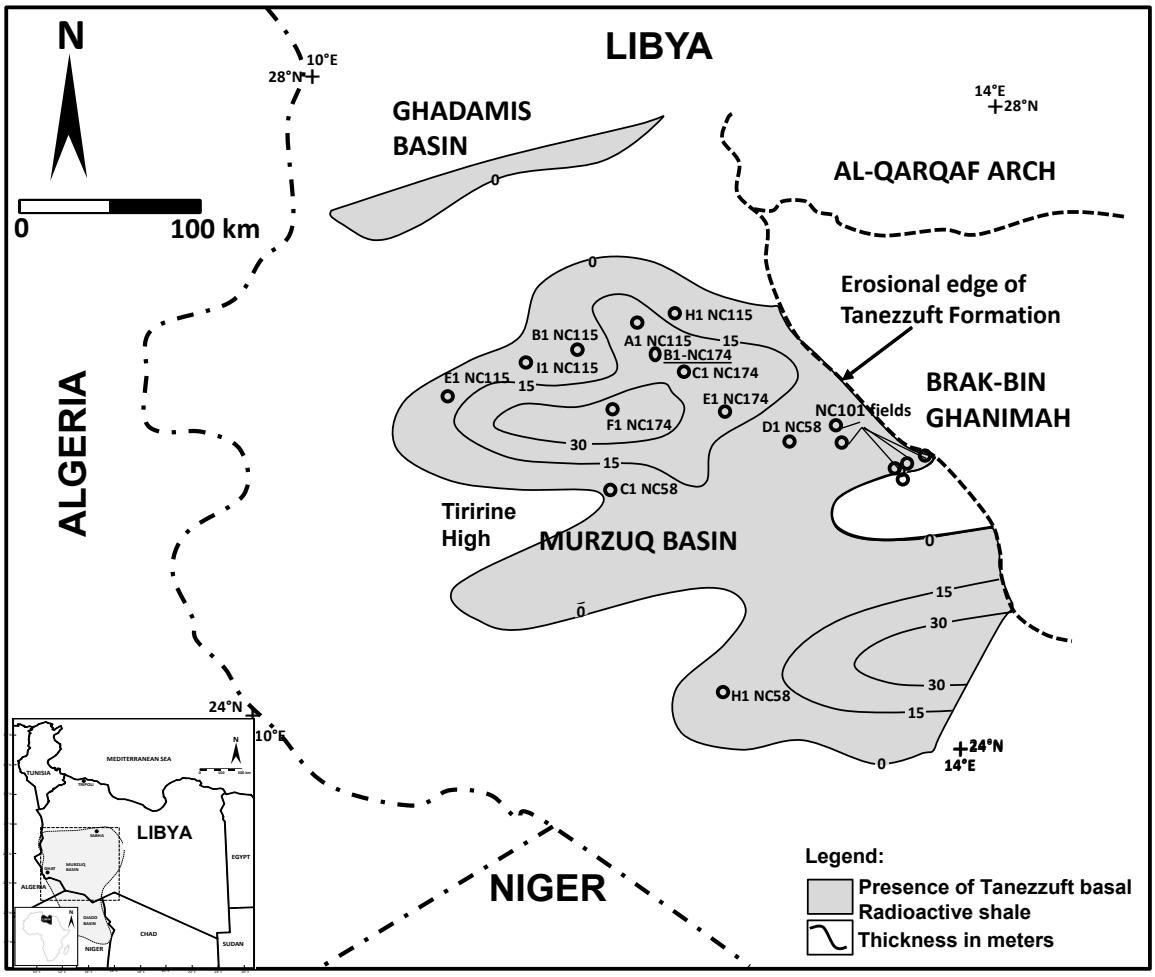

Figure 1.11. Showing the distribution and thickness of the basal Tanezzuft Formation 'hot' shale in the Murzuq Basin based on well data. Modified and redrawn from Echikh and Sola, (2000).

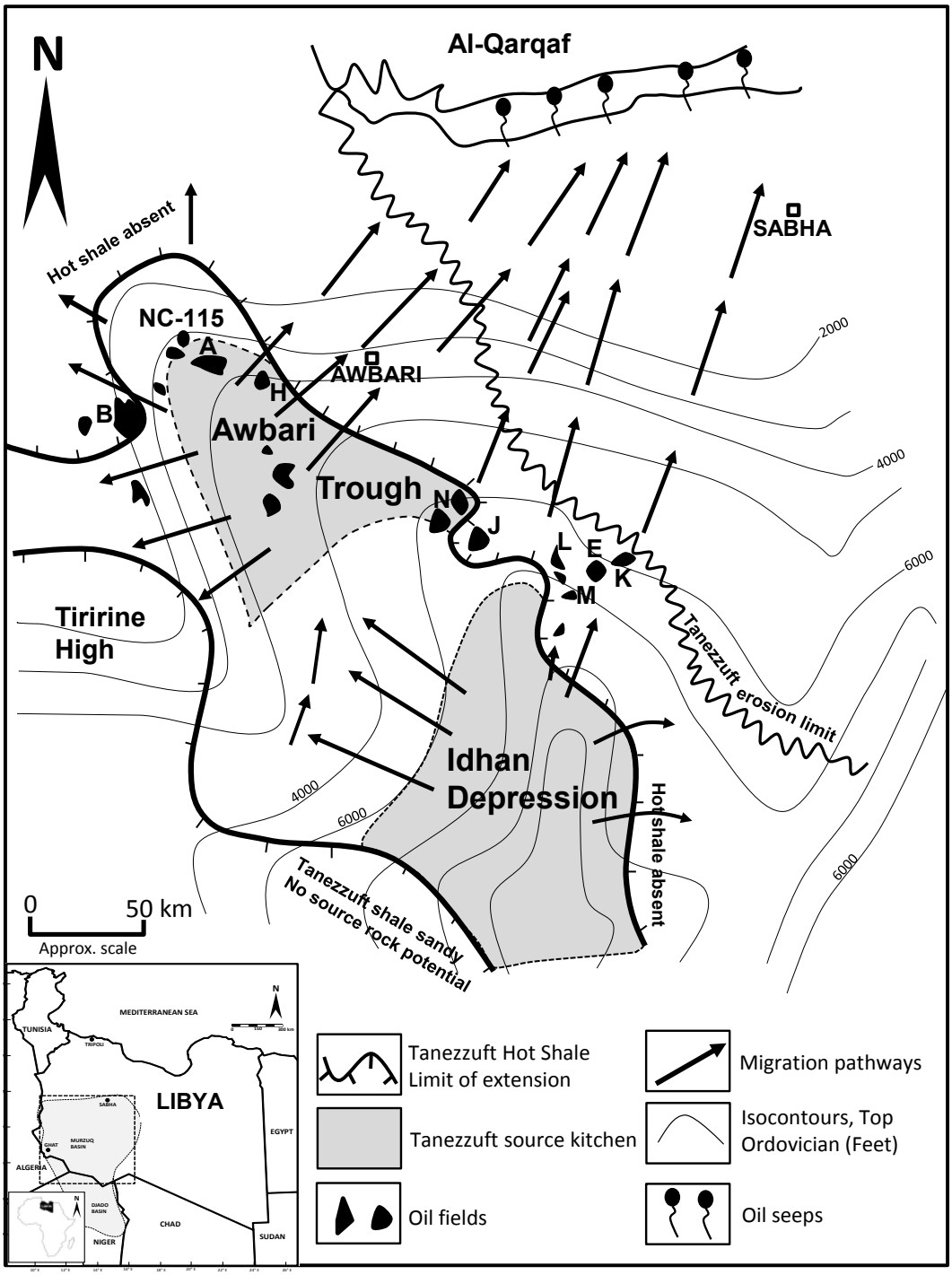

Figure 1.12. Tanezzuft-Mamuniyat Petroleum System in Murzuq Basin. Modified and redrawn from Echikh and Sola, (2000).

(Figures 1.11 and 1.12). Davidson et al. (2000) published results of maturity modeling on well B1-NC 174 (Figures 1.11 and 1.12), which suggest that the Tanezzuft source rock reached mid maturity (onset of oil generation) during the Cretaceous but was uplifted above the oil window during the Eocene (Figure 1.13). In block NC-115 the Tanezzuft source rock is currently at the late mature stage, although it may not have entered the oil window until the Cenozoic (Hallett, 2002). In the Awbari Trough (Figure 1.12) where NC-115 is located, the hot shale shows the highest level of maturity. Aziz (2000) concluded that the Awbari Trough can be thought of as the kitchen for the northern part of the Murzuq Basin. This is indicated by the occurrence of a major source rock with over 10m thick Hot Shale along the northern part of the Awbari Trough.

In general, maturity is related to deep burial (most probably during Late Jurassic/Early Cretaceous). As a result of Tertiary magmatic activity, heat flow is widespread in western Libya. Present day geothermal gradient is highest along an axis passing through the NC-115 fields and close to the NC-101 fields (Figure 1.12, Hallett, 2002).

Aziz (2000) suggested that migration took place by lateral diffusion from the source shales into adjacent Ordovician traps (e.g. Mamuniyat Formation; Figure 1.12), and there is no evidence of long-range migration. The oils found in these fields are light oils with almost no gas condensate and with gravities ranging from 34 to 45° API (Hallett, 2002).

1.3.4.3 SEALS

The Tanezzuft shales or Devonian shales provide a reliable seal throughout the area for the Mamuniyat Formation. The degree of lateral continuity of the sealing surface, in

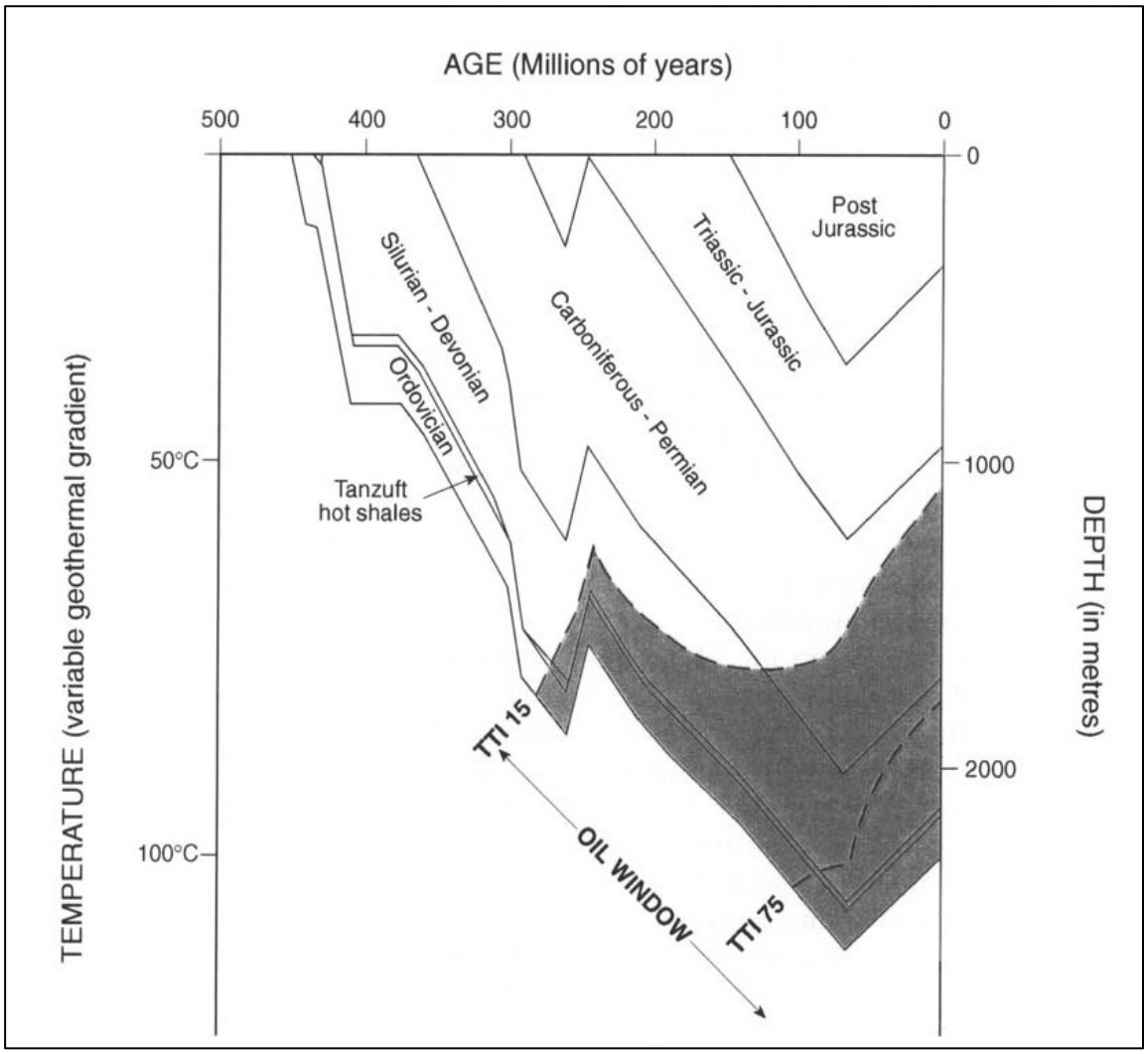

Figure 1.13. Burial History Plot for Well B1-NC 174 (See Figure 1.11 for location map).

Well B1-NC 174 is located in the northern Murzuq Basin, northeast of the Elephant field. It was drilled to a depth of 2293m. The modeling of this plot assumes uplift during the Hercynian orogeny and during the Cenozoic, and the geothermal gradient has been adjusted accordingly. The Silurian hot shales entered the oil window during the Permian, but did not reach peak maturity until the late Cretaceous and are still in the oil window at the present time. (After Davidson et al., 2000).

addition to other factors such as lateral permeability and fault barriers, presents the principal control on the distribution of migration pathway (Echikh and Sola, 2000). The sealing capacity of the Tanezzuft Formation is generally good, especially in areas where the lowermost Tanezzuft shales were deposited in deep marine environments (Echikh and Sola, 2000).

In the eastern part of the basin, where the Tanezzuft Formation is absent, the Mamuniyat reservoir is capped by Devonian units with variable sealing capacities (Echikh and Sola, 2000). Seeps in Devonian outcrops on the southern flank of the A1-Qarqaf Arch suggest that leakage has taken place in this area (Figure 1.14). The NC-101 fields are located very close to the pinchout limit of the Tanezzuft Shales and the seal in this area is not effective (Figure 1.14). However, in areas where reverse faulting has taken place (e.g. the H-NC 115 and Elephant structures), the oil pool is trapped against the fault which is clearly sealing (Echikh and Sola, 2000; Hallett, 2002).

1.3.4.4 TRAPS

Most of the oil discoveries in the Murzuq basin occur in structural traps, but palaeomorphological and stratigraphic traps are also present. The Elephant field (F-NC 174) is a large block faulted anticline with rollover into a steep reverse fault (Hallett, 2002). Pre-Hercynian simple anticlines are predominant in the blocks NC-101 and NC-58 (Figure 1.15A). Normal faulted anticlinal traps are also present in the same blocks (Figure 1.15B). Reverse thrust-faulted anticlines form the traps in the H- and C-NC 115 fields and on the Elephant fields, and in these cases the faults are sealing (Figure 1.15C).

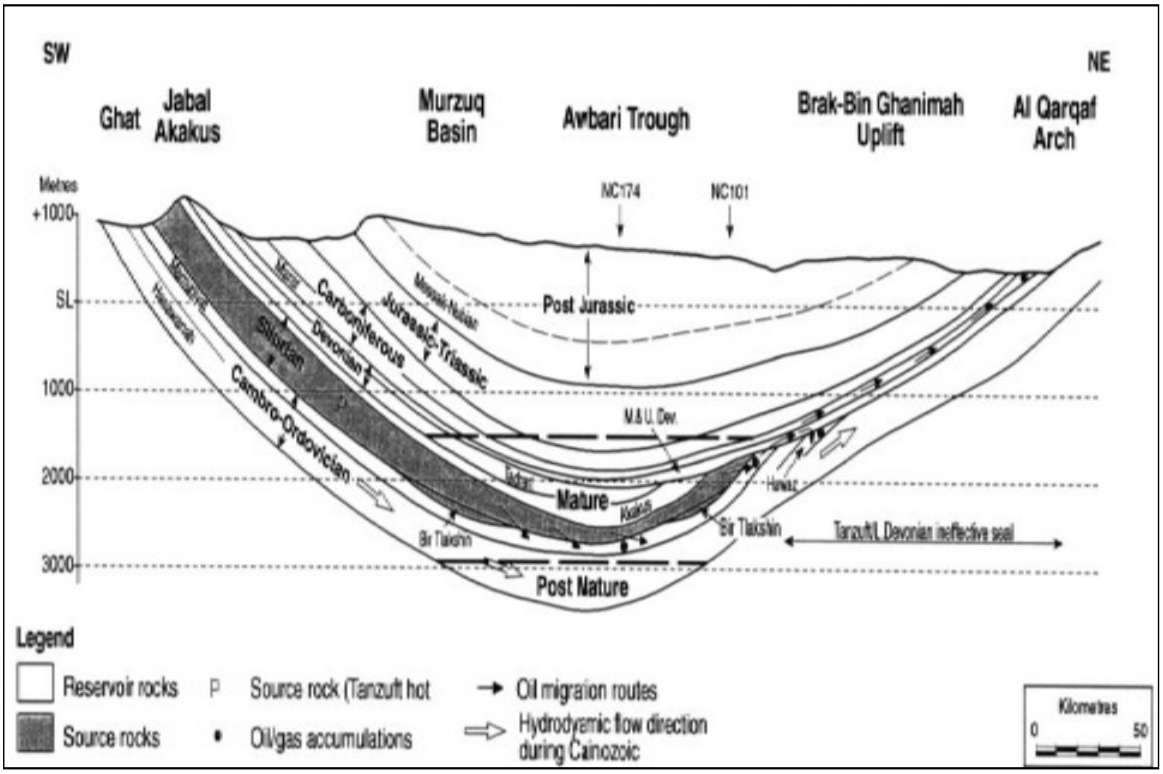

Figure 1.14. The Tanezzuft-Mamuniyat Petroleum System in Murzuq Basin, S.W. Libya.

Oil was generated from the Tanezzuft hot shale source kitchen and migrated into the underlying porous sandstones of the Mamuniyat Formation (Boote et al., 1998). The Mamuniyat does not appear to have been charged in areas where the Bi'r Tlakshin Formation is present. East of the NC 101 fields no effective seal is present, causing oil to leak into the Middle and Upper Devonian sandstones, which contain oil seeps on the flank of the A1-Qarqaf Arch. The direction of hydrodynamic flow during the Cainozoic was from southwest to northeast. (After Boote et al., 1998; Hallett, 2002).

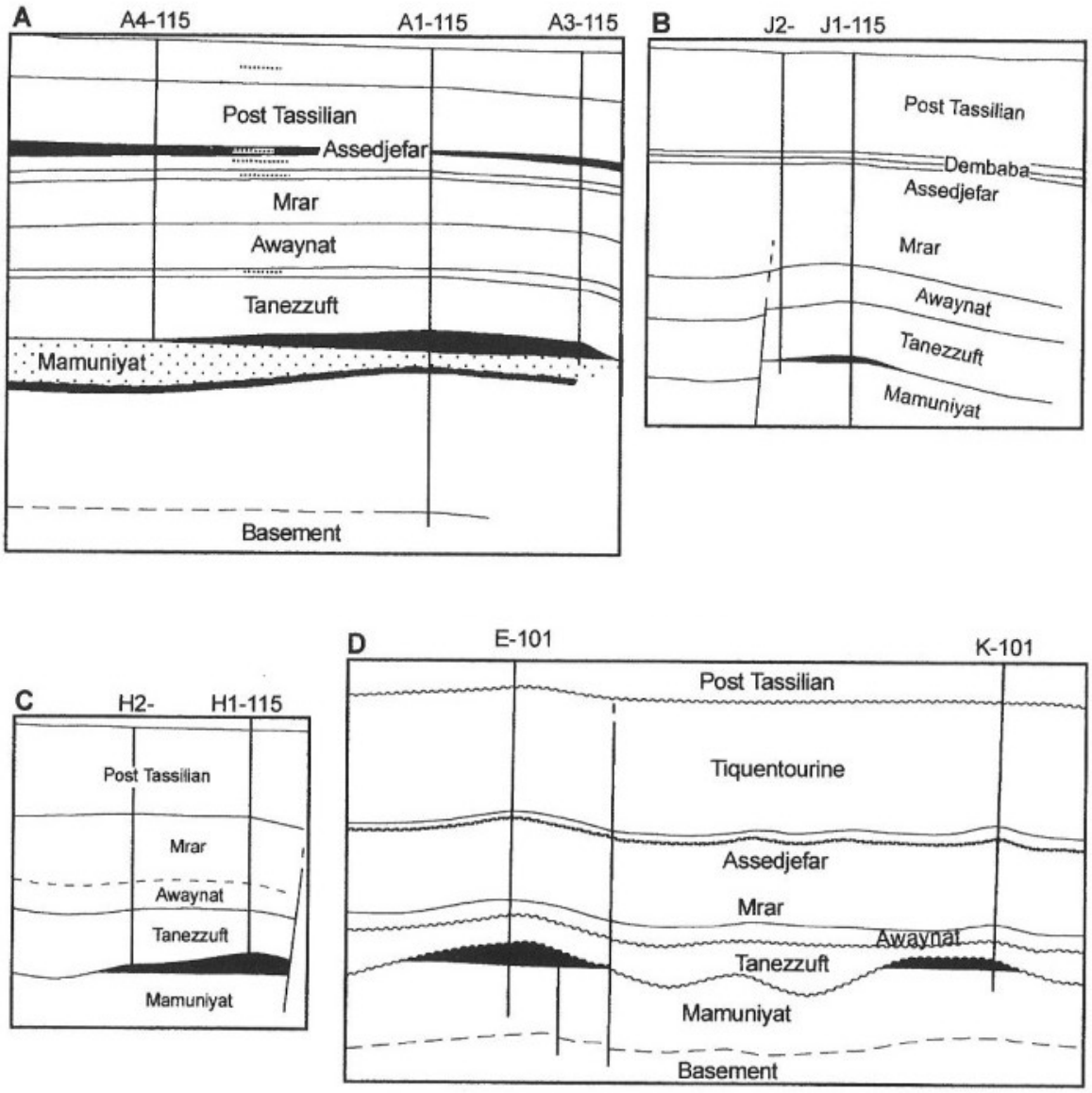

Figure 1.15. Trapping mechanisms in the Murzuq basin; A: Simple anticline, B: Normal-faulted anticline, C: Reverse-faulted anticline, D: Glacially related erosional palaeotopography (After Echikh and Sola, 2000).

Palaeotopographic features of possible glacial origin are present in the B-NC 115, E1-and K1-NC 101 structures (Figure 1.15D). This kind of trap represents a combination of structural and geomorphological features. In the Devonian, the complex nature of the mid-Devonian unconformity presents stratigraphic trap possibilities (Figure 1.14) (Echikh and Sola, 2000).

CHAPTER-II

2. BIOMARKER APPLICATIONS

2.1 INTRODUCTION

Biomarkers are organic constituents of sediments, sedimentary rocks and crude oil, which are derived from formerly living organisms. They are composed of carbon, hydrogen, and other elements (Eglinton et al., 1964; Eglinton and Calvin, 1967). Biomarkers are useful because they retain all or most of their original carbon skeleton from the original natural product and this structural similarity provides a record of environment in which they were deposited and diagenetic processes that have subsequently influenced and modified them (Engel and Macko, 1993). Moreover, biomarkers undergo systematic and sequential transformations during diagenesis and changes in their compositions can be used as indicators of the thermal history of sediments (Brassell, 1992). Figure 2.1 shows a general scheme of evolution of the organic matter from the time of deposition of sediment to the beginning of the metamorphism stage.

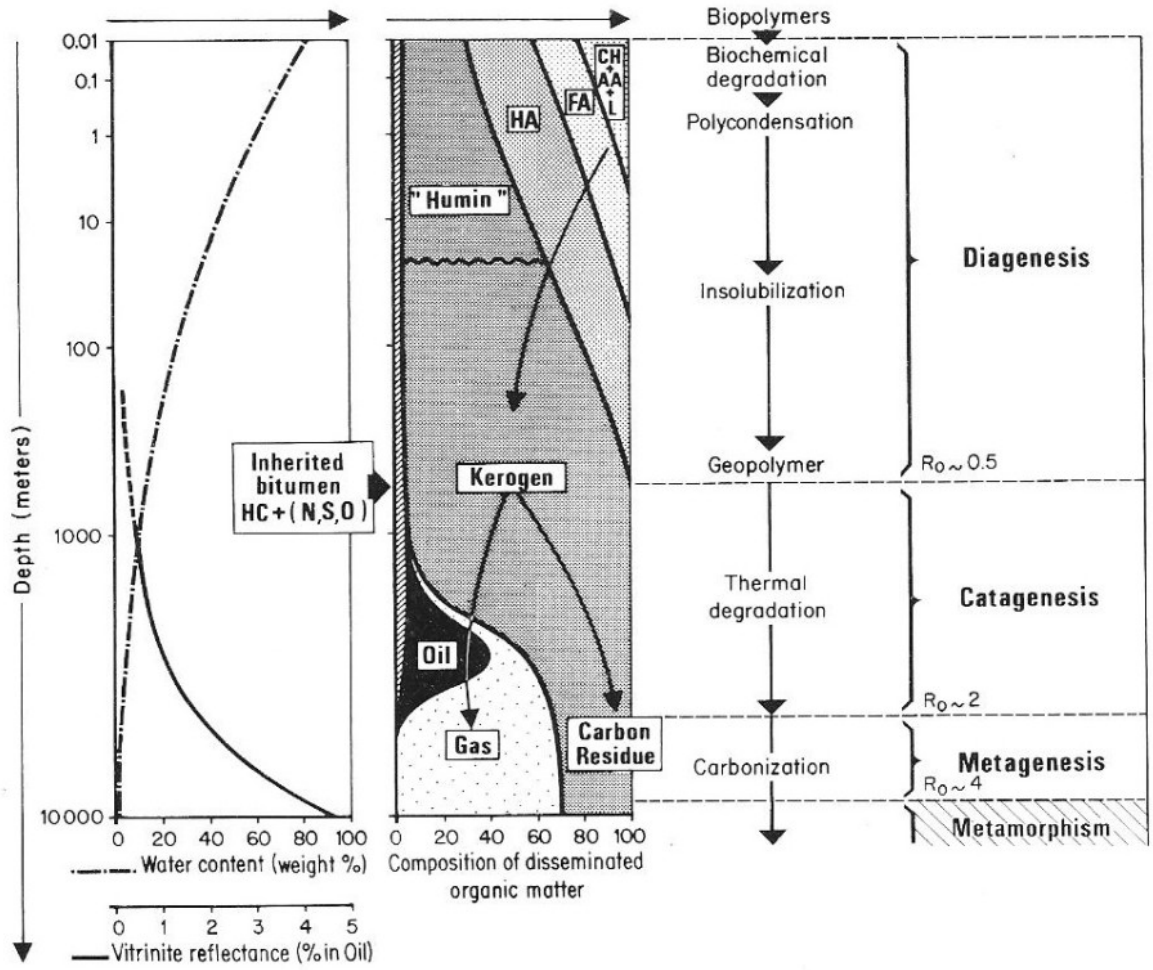

Figure 2.1. General scheme of evolution of the organic matter, from early deposited sediment to the metamorphic zone. CH: carbohydrates, AA: amino acids, FA: fluvic acids, HA: humic acids, L: lipids, HC: hydrocarbons, N, S, O: NSO compounds (After Tissot and Welte 1984).

2.2 TRANSFORMATION OF ORGANIC MATTER

2.2.1 DIAGENESIS

The term diagenesis refers to the biological, physical, and chemical alteration of organic matter in sediments prior to significant changes caused by heat. In sedimentary rocks that have undergone diagenesis, the organic matter consists of kerogen, bitumen, and minor amounts of hydrocarbon (Tissot and Welte, 1984).

During early diagenesis, one of the major factors of transformation is microbial activity. Aerobic organisms that live in the uppermost layer of sediments consume free oxygen, and anarobic organisms reduce sulfates to attain the needed oxygen. The conversion of organic matter into carbon dioxide, ammonia and water usually occurs in sands and partly in muds (Tissot and Welte, 1984). Microbial activity during sedimentation and early diagenesis destroys biogenic polymers (proteins and carbohydrates), and leaves new polycondensed structures that are percursors of kerogen (Figure 2.1). Methane is the most important hydrocarbon formed during diagenesis.

Organic matter preservation and formation of kerogen is typically attributed to selective preservation of resistant biomolecules, random polymerization of diagenetically degraded biomolecules (i.e. neogenesis) or in situ polymerisation of labile aliphatic components (Briggs, 1999). Organic matter preservation experiences biopolymer degradation, followed by random polycondensation, ending with non-biodegradable geopolymers (Nissenbaum and Kaplan, 1972; Welte, 1974) (Figure 2.1). Although its implication strictly depends on the occurrence of organisms containing resistant

biomacromolecules in the initial biomass, selective preservation may account in some cases for the major part of the constituents of a kerogen (Vandenbroucke and Largeau, 2007). Selective preservation may be important to ensure that macromolecular material survives the normal processes of rapid decay, but ultimately fossilization involves long-term diagenetic alteration, a process with important implications for the interpretation of fossil assemblages and for the origin of kerogen (Briggs, 1999). The most decay-resistant biomacromolecules are derived from algae and vascular plants; proteins and chitin are shown to have a very low preservation potential (Tegelaar et al., 1989; Van Bergen et al., 1995). Moreover, according to Vandenbrouche and Largeau, (2007), the selective preservation pathway is based on the production by some living organisms of insoluble biomacromolecules, which are extremely resistant to chemical and bacterial degradation. These biomacromolecules are generally highly aliphatic and remain almost unaffected by drastic basic and acid laboratory hydrolysis. Such macromolecular components also show a high resistance to attack by microbial hydrolytic enzymes. Thus, they can remain virtually unaffected during deposition while most of the other constituents of the initial biomass are heavily degraded and remineralized. As a result, selective preservation, and hence selective enrichment, of such biomacromolecules takes place during diagenesis. However, at later stages of diagenesis, organic matter forms CO_2, H_2O, and some heavy heteroatomic compounds. In addition, humic acids decrease at these stages, where most carboxyl groups have been removed (Tissot and Welte, 1984).

2.2.2 CATAGENESIS

Catagenesis is the process by which the organic matter in rocks is thermally altered by burial and heating at temperatures in the range of about 50 to 150°C under typical burial conditions requiring millions of years (Tissot and Welte, 1984). During catagenesis, biomarkers undergo structural changes that can be used to gauge the extent of heating of their host sediments or oils that have migrated from these sediments. Organic matter experiences major changes: through progressive evolution the kerogen produces first liquid crude oil; then in later stages wet gas and condensate, which are both associated with vast amounts of methane. The end of catagenesis is reached in the range where the disappearance of aliphatic carbon chains in kerogen is completed, and where the development of an ordering of basic kerogen units begins. This is equivalent to vitrinite reflectance of about 2.0 (Tissot and Welte, 1984).

2.2.3 METAGENESIS

Metagenesis is reached only at great depth. At temperatures in the range of about 150 to 200°C, prior to greenschist metamorphism, organic molecules are cracked to gas in a process called metagenesis. Biomarkers are severely reduced in concentration or absent because of their instability under these conditions (Tissot and Welte, 1984).

2.3 BIODEGRADATION

Aerobic bacteria are the primary factor in subsurface degradation of crude oil (Milner et al., 1977; Palmer, 1984). Anaerobic bacteria, such as sulfate reducers, can oxidize hydrocarbons, but probably do so much more slowly than aerobes. However, in terms of geologic time this difference in rate may not be critical. Anaerobes apparently require aerobes to initiate degradation of crude oil (Jobson et al., 1979). Peters and Moldowan (1993) stated that oil can be catabolized by aerobic bacteria only if several requirements are satisfied. These are: (i) access to surface recharge waters containing oxygen; (ii) temperatures no more than about 65 to 80°C; (iii) the crude oil must be free of H_2S, which poisons the bacteria (Peters and Moldowan, 1993).

Biodegradation is quasi-sequential because some of the more labile compounds in the more resistant compound classes can be attacked before complete destruction of less resistant classes (Peters and Moldowan, 1993). The general sequence of increasing resistance to biodegradation of biomarkers is: *n*-alkanes, isoprenoids, steranes, hopanes/diasteranes, aromatic steroids, and porphyrins (Chosson et al., 1992; Moldowan et al., 1992). Because of their differential resistance to biodegradation, comparisons of the amounts of biomarker types in crude oils can be used to rank these relative extents of biodegradation. Wenger et al. (2002) developed a scale based on Volkman et al. (1983) and Moldowan et al. (1992) to assess the extent of biodegradation based on the relative abundance of various hydrocarbon classes (Figure 2.2). According to Peters et al. (2005), the scaling concept was proposed initially by Alexander et al. (1983), Volkman et al., 1983a; 1983b; 1984, and later was modified by Moldowan et al. (1992). However,

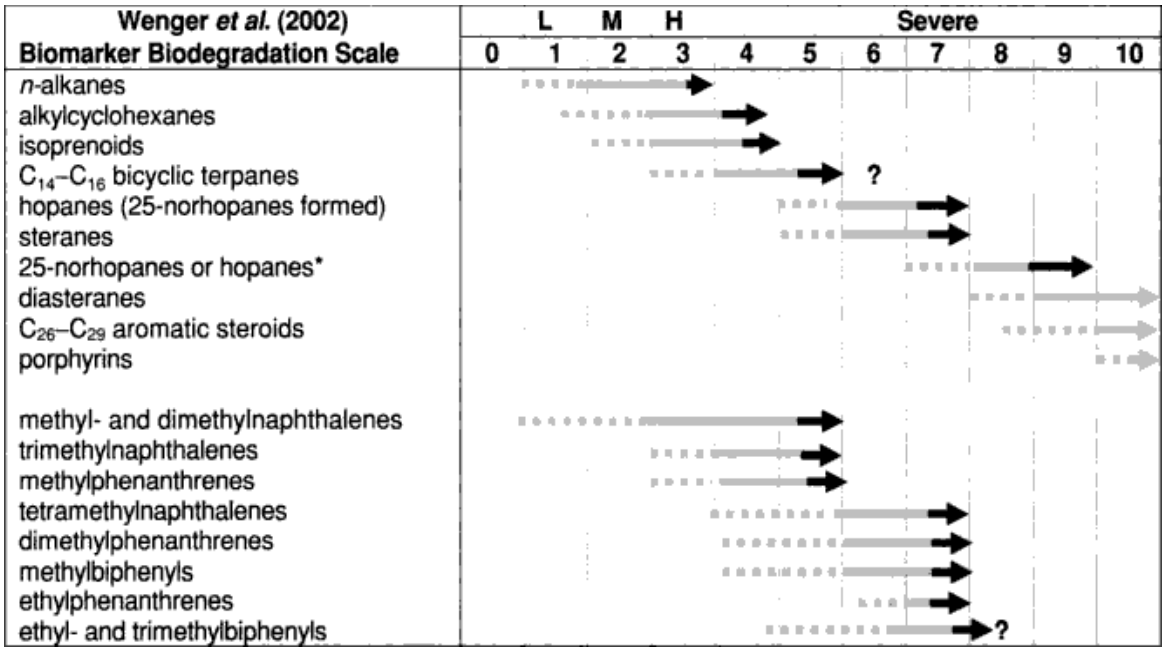

Figure 2.2. Shows the extent of biodegradation of mature crude oil can be ranked on a scale of 1-10 based on differing resistance of compound classes to microbial attack.
Arrows indicate where compound classes are first altered (dashed lines), substantially depleted (solid grey), and completely eliminated (black). Sequence of alteration of alkylated polyaromatic hydrocarbons is based on work by Fisher et al. (1996b; 1998) and Triolio et al. (1999). Degree of biodegradation from Wenger et al. (2002) reflects changes in oil quality (L: lightly biodegraded; M: moderately; H: heavily biodegraded). *Hopanes degraded without the formation of 25-norhopanes (The scaling concept was proposed initially by Alexander et al. (1983b) and later was modified by Moldowan et al. (1992).

biomarkers are powerful geochemical tools, partly because many are highly resistant to biodegradation. For example, biodegraded seep oils or asphalts commonly contain unaltered biomarkers that can be used for comparisons with nonbiodegraded oils (Alexander et al., 1983; Volkman et al., 1983a; Volkman et al., 1983b; Moldowan et al., 1992; Wenger et al., 2002; Peters et al., 2005).

2.4 SOURCE- AND DEPOSITIONAL ENVIRONMENT BIOMARKER PARAMETERS

The use of biomarkers as indicators for depositional environments arises from the fact that certain types of compounds are associated with organisms, or plants that grow in specific types of depositional environments (Philp, 2003). There are a number of biomarkers that are extremely useful for paleoreconstruction of depositional environments and as source indicators. For instance, gammacerane is widely used as an indicator of hypersalinity (de Leeuw and Sinnighe Damste, 1990). Botryococcane, an irregular C_{34} isoprenoid, is another good example of a compound associated with a specific algae, Botryococcous braunii, a green algae, which only grows in fresh/brackish water environments (Moldowan and Seifert, 1980).

2.4.1 *n*-Alkanes characteristics

The distribution of n-alkanes in crude oils and bitumens can be used to indicate sources of organic matter (Han and Calvin, 1969; Volkman et al., 1981). However,

interpretation of source input using the distribution of n-alkanes should be used with caution, because many marine and lacustrine sediments have a wide range of alkanes, typically from C_1-C_{45} in marine oils and upwards of C_{50} to C_{100}+ in oil shales (Peters et al., 2005). Moreover, n-alkanes are affected by several limitations, including biodegradation, maturation, and migration. For instance, the higher molecular weight n-alkanes are cracked into lighter products during maturation (Peters and Moldowan, 1993). In addition, it is known that low molecular weight n-alkanes are more susceptible to biodegradation than high molecular weight homologues, and n-alkanes are the first crude oil components to be biodegraded (Peters and Moldowan, 1991).

2.4.2 Pristane/ Phytane (Pr/Ph) ratio

The Pr/Ph ratio has had a long history in organic geochemistry. Pristane (C_{19}), phytane (C_{20}), and smaller isoprenoids are derived primarily from the phytyl side chain of chlorophyll in phototrophic organisms. Under anoxic conditions in sediments, the phytyl side chain is cleaved to yield phytol, which is reduced to dihydrophytol and then phytane (Figure 2.3). Under oxic conditions, phytol is oxidized to phytenic acid, decarboxylated to pristene and then reduced to pristane (Figure 2.3) (Peters and Moldowan, 1993).

Pristane/Phytane ratios of oils or bitumens have been used to indicate the redox potential of the source sediments (Brooks et al., 1969; Powell and McKirdy, 1973; Didyk et al., 1978). Pr/Ph ratios less than one have been reported to indicate an anoxic depositional environment and oxic environments are indicated by ratios greater than one

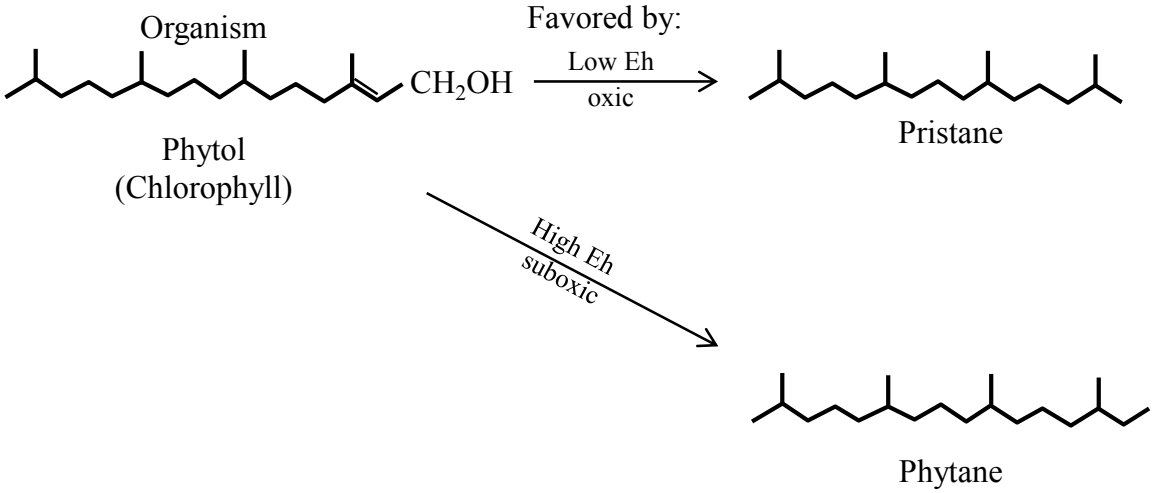

Figure 2.3. Diagenetic origin of pristane and phytane from phytol (derived from side chain of chlorophyll-a) (After Didyk et al., 1978).

(Peters and Moldowan, 1993). Volkman and Maxwell (1986) pointed out that for source rocks within the oil generative window, high Pr/Ph ratios (>3.0) indicate terrestrial organic matter input under oxic conditions, and low values (<0.8) indicate anoxic, commonly hypersaline environments. However, caution must be exercised when using Pr/Ph ratios as redox potential indicators because they are known to be possibly affected by maturation (Tissot and Welte, 1984) and more importantly by differences in possible precursors (Volkman, 1986; ten Haven et al., 1987).

2.4.3 Isoprenoids/n-alkanes

Pristane/nC_{17} and phytane/nC_{18} ratios are used to indicate the source of organic matter and are sometimes used in correlation studies (Lijmbach, 1975; Shanmugam, 1985). Caution should be exercised when using these ratios because both ratios decrease with increasing thermal maturity and increase with increasing biodegradation as a result of aerobic bacteria generally attacking the n-alkanes before the isoprenoids (Peters and Moldowan, 1993).

2.4.4 Terpanes *m/z* 191 fingerprint

2.4.4.1 Tricyclic terpanes and tricyclics/17α-hopanes

Tricyclic terpanes are used to correlate crude oils and source rock extracts, to predict source-rock characteristics, and to evaluate the extent of thermal maturity and

biodegradation (Seifert et al., 1980; Seifert and Moldowan, 1981; Zumberge, 1987; Peters and Moldowan, 1993). The widespread occurence of tricyclic terpanes is believed to result from precursors produced by algae and/or bacteria (Seifert and Moldowan, 1979; Philp and Gilbert, 1986; Philp et al., 1992) and are typically absent, or occur in small amounts, in oils from terrigenous source materials (Robinson, 1987; Peters et al., 2005). Philp et al. (1989) pointed out that tricyclic terpanes have also been reported in saline lacustrine oils from China, and suggested a salinity-controlled occurrence of these compounds. Tricyclic terpanes are generally more abundant in highly mature oils and/or source rocks because they are thermally more stable than other terpanes (Peters and Moldowan, 1993), and thus the ratio of tricyclic terpanes to 17α-hopanes will rise with increasing maturity (Waples and Machihara, 1990). For highly mature samples, pentacyclic hopanes may be preferentially removed and leave relatively high concentrations of tricyclic terpanes (Waples and Machihara, 1990; Peters and Moldowan, 1993). The high abundance of extended tricyclic terpanes relative to hopanes in oils and/or source rocks may also be related to maturity effects, and is also probably due to marine influenced depositional conditions (Seifert and Moldowan, 1979; Philp et al., 1992). Pentacyclic hopanes are related to specific bacteriohopanepolyols found in bacteria, such as bacteriohopanetetrol (Peters and Moldowan, 1991).

2.4.4.2 C_{24} Tetracyclic terpane

The contents of tricyclic and tetracyclic terpanes in crude oils are closely related to the nature of their organic matter (Seifert and Moldowan, 1978; Aquino Neto et al., 1983).

Connan et al. (1986) and Clark and Philp (1989) reported the occurrence of the C_{24} tetracyclic terpanes in samples from hypersaline environments. However, according to several authors, C_{24} tetracyclic terpanes are usually found in relatively high concentrations in oils from evaporite-carbonate sequences and typically dominate the terpane distribution (Palacas et al., 1984; Connan et al., 1986; Clark and Philp, 1989). The high preservation rate of organic matter in evaporitic environments is predominantly due to the decrease in solubility of oxygen with increasing salinity (Sammy, 1985). In addition, tetracyclic terpanes are more resistant to biodegradation than hopanes (Aquino Neto et al., 1983).

2.4.4.3 C_{30}-Diahopane/C_{29}Ts ratio

High ratios of C_{30}-diahopane/C_{29}Ts are found in oils derived from shales deposited under oxic-suboxic conditions, whereas shales deposited under anoxic conditions show lower values (Peters et al., 2005). Higher values have also been observed in oils derived from terrigenous source materials (Volkman et al., 1983a; Philp and Gilbert, 1986). Moreover, C_{30}-diahopane is characterized by high thermal stability (Kolaczkowska et al., 1990; Armanios et al., 1992; Huang et al., 1994). However, C_{30}-diahopane has virtually the same geochemical behavior as diasterane, where higher maturity is favorable for rearrangement of hopenoids, and formation of high C_{30}-diahopane content (Chang et al., 2007; Zhang et al., 2009). C_{30}-Diahopane (15α-methyl-17α(H)-27-norhopane) may be of a bacterial origin with arrangement occurring during diagenesis by clay-mediated acidic catalysis (Volkman et al., 1983a; Philp and Gilbert, 1986; Moldowan et al., 1991). Thus,

its occurrence in oils or rock extracts may indicate bacterial input to sediments containing clay deposited under oxic or suboxic conditions (Peters et al., 2005). However, Moldowan et al. (1991) stated that 17α-diahopane series are more stable than those of 18α-neohopane series, which in turn, are more stable than those of 17α-hopane series. Thus, increasing maturity should result in increased ratios of C_{30}-diahopane/C_{29}Ts, particularly in the late oil window (Kolaczkowska et al., 1990; Armanios et al., 1992; Huang et al., 1994).

2.4.4.4 C_{29}/C_{30} Hopane ratio

Hopanes are derived primarily from bacteria (Waples and Machihara, 1990). The C_{29} and C_{30} 17α(H)-hopanes, are the predominant triterpanes. The C_{29}/C_{30} hopane ratio is commonly used to distinguish the carbonate from clastic lithology (Palacas et al., 1984; Peters and Moldowan, 1993). Usually oils sourced from organic rich carbonates and evaporites are generally characterized by high values (>1) of C_{29}/C_{30} hopanes ratios (Zumberge, 1984; Connan et al., 1986; Price et al., 1987; Clark and Philp, 1989), while, low values of C_{29}/C_{30} hopanes ratios are characteristics of shales.

2.4.4.5 Homohopane Index (HI)

The homohopane index (HI) is used as an indicator of redox potential (Eh) in marine sediments during diagenesis (Moldowan et al., 1991). The homohopanes (C_{31} to C_{34}) are believed to be derived from bacteriopolyhopanol present in prokaryotic cell membranes

(Ourisson et al., 1979, 1984). According to Peters and Moldowan, (1993), low ratios of C_{35} to C_{34} homohopanes (0.38–0.65) suggest prevailing oxic to sub-oxic (high Eh) conditions during deposition and hence low quality organic matter (e.g. organic matter with low hydrogen index; Dahl et al., 1994). In order to avoid interference from co-eluting compounds, 22S epimer should be used rather than both 22S and 22R (Peters et al., 2005). Rangel et al. (2000) observed that high C_{35} hopane ratios are associated with high hydrogen indices in the source rocks due to better preservation of oil-prone organic matter. In addition, Moldowan et al. (1986) found that the low values of C_{35} homohopane indices are associated with high values of Pr/Ph and diasteranes/regular steranes ratios in sections of a sequence of Lower Toarcian shales where organic matter was exposed to higher levels of oxidation during deposition (Moldowan et al., 1986).

2.4.5 Steranes (*m/z* 217)

The distributions of C_{27}-, C_{28}-, and C_{29}-steranes on a ternary diagram are used extensively to show the relationship between oils and/or source rock extracts (Peters et al., 2000). The principal use of C_{27}-, C_{28}-, and C_{29}-sterane ternary diagrams is to discriminate groups of oils from different source rocks or different organic facies of the same source rock on the basis of source material (Huang and Meinschein, 1979; Peters et al., 2005). Steranes are derived from sterols that are widely dispersed in plants, animals, and organisms (Philp, 1985), with the C_{27} and C_{30} sterol precursors most abundant in marine organisms. Alternatively, high concentrations of C_{29} steranes indicate a contribution from higher land plants (Huang and Meinschein, 1979; Moldowan et al.,

1985). However, Fowler and Douglas, (1987) suggested that some C_{29} steranes come from cyanobacteria (blue-green algae), and Volkman (1986, 1988) has shown that algae can produce many types of sterols including C_{29} sterols (Volkman, 1986; Volkman and Maxwell, 1986; Fowler and Douglas, 1987; Volkman, 1988). Generally, oils generated from kerogens containing organic matter derived from marine phytoplankton display enhanced amounts of C_{27} relative to C_{29} steranes (Mackenzie et al., 1982; Czochanska et al., 1988; Waples and Machihara, 1991). High concentrations of C_{28} steranes may be related to lacustrine algae (Brassell and Eglinton, 1983; Philp, 1985; Peters and Moldowan, 1993).

Furthermore, the presence of C_{30} steranes (24-n-propylcholestanes) in oils and extracts is related to a marine source. It is thought to be related to pelagophyte algae, which indicates a contribution from marine and phytoplankton organic matter (Moldowan, 1984; Moldowan et al., 1990; Summons et al., 1992; Peters and Moldowan, 1993), with few exceptions (Moldowan et al., 1990). One possible exception exists for an Oligocene sample from a saline lake in the Bohai Basin, China (Moldowan et al., 1990). The algae that biosynthesize the precursors of these C_{30} compounds are believed to have appeared between Ordovician and Devonian times. The 24-n-propylcholestanes (C_{30} steranes) together with the regular steranes (C_{27}-C_{29}) provide evidence for a mixed source for steranes (Eglinton et al., 2006). However, any simplistic interpretation of C_{27} –C_{29} sterane ratios, especially in terms of paleoenvironment, is still risky. All interpretations of sterane distribution must be consistent with other geological evidence and with common-sense logic (Waples and Machihara, 1990).

2.4.6 Diasteranes (*m/z* 217)

Diasterane/sterane ratios are commonly used to discriminate carbonate from clay-rich source rocks. Low diasterane/sterane ratios indicate anoxic clay-poor or carbonate source rocks (Clark and Philp, 1989), whereas high ratios are usually a feature of oils, or source rocks, containing abundant clays (Mello et al., 1988b). During diagenesis, acidic sites on clays, catalyze the conversion of sterenes to diasteranes (Kirk and Shaw, 1975; Rubinstein et al., 1975; Sieskind et al., 1979; Grantham and Wakefield, 1988). However, the proportion of diasteranes compared with regular steranes is known to be dependent upon maturity as well, because the original steranes are converted gradually to mixture of diasteranes and steranes (Hughes et al., 1985; Goodarzi et al., 1989a). Seifert and Moldowan (1979) also suggested that high proportions of diasteranes compared with regular steranes in oil is consistent with heavy biodegradation, resulting in elimination of steranes relative to diasteranes.

2.4.7 Pregnane and homopregnane (*m/z* 217)

The precursors of pregnane ($C_{21}H_{36}$) and homopregnane ($C_{22}H_{38}$) are pregnol and homopregnol which exist in protozoans (Yang, 1991). However, pregnane and homopregnane are also related to hypersaline environments (ten Haven et al., 1985) and could also result from thermal cracking of C_{27}-C_{29} steranes (Mueller et al., 1995).

2.5 MATURITY PARAMETERS

2.5.1 Organic petrography

Graptolites are an extinct class of colonial marine vertebrates found in clastic and carbonate rocks of Cambrian to Pennsylvanian age (Bulman, 1970). Graptolite reflectance was assumed by earliest workers to follow the same maturation trend as vitrinite reflectance. Graptolite reflectance can be used as a qualitative measure of thermal maturation in interpretation of the thermal history of pre-Devonian strata. Graptolites occur mainly in Lower Ordovician to Lower Devonian marine sediments, and sediments of these ages normally lack vitrinite (Robert, 1980; Goodarzi, 1982, 1986). Goodarzi and Norford (1989b) stated that for immature rocks ($\%R_o$ =0.2-0.5, CAI: 1.5), graptolite reflectance (%Rg) ranges from 0.6 to 1.2%; rocks in the oil generation zone ($\%R_o$ =0.5-1.30, CAI: 1.5-2.5) have graptolite reflectance ranging from 1.2 to 2.2%. Moreover, the presence of solid hydrocarbon (bitumens) is indicative of mature and post-mature rocks, and can be found in shales and siltstones (Landis and Castaño, 1995). Like crude oil, solid hydrocarbons are generated by the thermal conversion of kerogen. Reflectance measurements obtained from solid hydrocarbon can be converted into vitrinite reflectance values using the formula of Landis and Castaño, (1994): vitrinite reflectance = $(BR_o+0.41)/1.09$, whereas BR_o is the reflectance of solid bitumen.

2.5.2 MATURITY-RELATED BIOMARKER PARAMETERS

Biomarkers are transformed by thermal reactions, whose rates are governed by subsurface temperatures and the length of time exposed to those temperatures (Waples and Machihara, 1990). Therefore, biomarkers in oils are valuable for determining the level of maturity at which the oils were actually generated. Assessment of the level of thermal maturity of bitumens and oils assists in correlation studies. For instance, migrated oil in a reservoir that is more mature than indigenous bitumen from surrounding shales clearly could not have originated from the shales (Peters et al., 2005). However, some of the more reliable biomarkers such as C_{29} sterane isomerization ratios are not useful for highly mature samples because the reactions they represent have surpassed the equilibrium values. Selected biomarker ratios can be used to assess highly mature samples including side-chain cleavage ratios for the mono- and triaromatic steroids (Peters et al., 2005), together with the methylphenanthrene index, steranes, hopanes, tricyclics/17α-hopanes, diasteranes/steranes, and Ts/(Ts+Tm) ratios (van Graas, 1990; Philp, 2003).

2.5.2.1 Homohopane isomerization

Transformation of the biologically produced 22R epimer of the C_{31}–C_{35} extended 17α(H)-hopanes to the 22S epimer (Figure 2.4) occurs in the same manner as the 20R-20S conversion for the steranes, but at a faster rate (Waples and Machihara, 1990). 22S/(22S+22R) Homohopane isomerization ratios are typically used as maturity

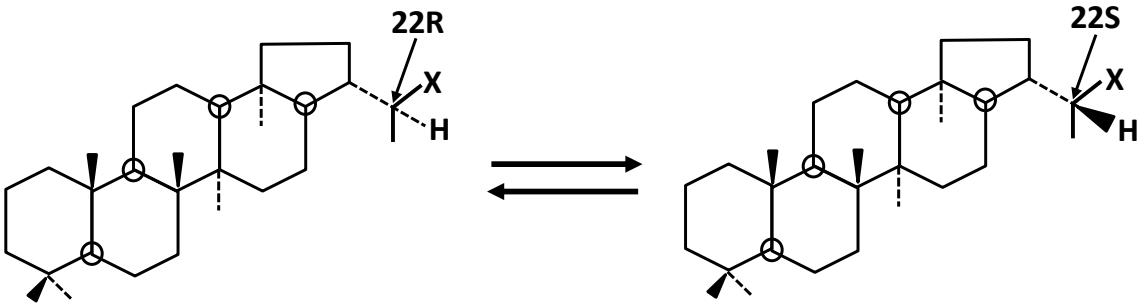

X = n-C_2H_5, n-C_3H_7, n-C_4H_9, n-C_5H_{11}, n-C_6H_{13}

Figure 2.4. Equilibration between 22R (biological epimer) and 22S (geologicalepimer) for the C_{31} to C_{35} homohopanes (After Peters and Moldowan, 1993).

indicators for immature to early mature source rocks (Peters et al., 2005). Samples with values in the range of (0.5–0.54) have barely entered the oil generation window, while those in the range of (0.57–0.62) indicate that the main phase of oil generation has been reached or surpassed (Peters et al., 2005). When the 22S/(22S+22R) ratio remains constant, no futher maturity information is available after reaching equilibrium at an early oil-generative stage. However, the inflection point in a plot of 22S/(22S+22R) versus vitrinite reflectance or other maturity generation parameters can be used to calibrate the parameters for the onset of oil generation for a given source rock in a basin (Peters and Moldowan, 1993).

Zumberge (1987) found that the 22S/(22S+22R) ratios for the C_{31} to C_{35} 17α (H)-homohopane may differ slightly. Typically, the C-22 epimer (Figure 2.4) ratios increase slightly for the higher homologs from C_{31} to C_{35}. He calculated the average equilibrium 22S/(22S+22R) ratios for 27 low maturity oils at C_{31}, C_{32}, C_{33}, C_{34}, and C_{35} as 0.55, 0.58, 0.60, 0.62, and 0.59, respectively. In some cases interference by coeluting peaks can invalidate certain ratios. However certain factors, such as lithology, may affect the rate of 17α-homohopane isomerization. For instance, Moldowan et al. (1992) found fully isomerized homohopanes in very immature carbonate rocks from the Adriatic Basin. Furthermore, ten Haven et al. (1986) noted that many bitumens from immature rocks deposited under hypersaline conditions show mature hopane patterns. These bitumens contain hop-17(21)-enes and extended 17α(H), 21β(H)-homohopanes fully isomerized at C-22 (50–60% 22S) typical of immature and mature samples, respectively (Peters et al., 2005). Apparently unusual diagenetic pathways for the hopanes (and steranes) in hypersaline environments may be account for this discrepancy (ten Haven et al., 1986).

On the contrary, Rullkötter et al. (1984a) explained this discrepancy by the variation in composition of precursores in source organisms (Rullkötter et al., 1984a).

2.5.2.2 Tricyclics/17α(H)-hopanes

The tricyclics/17α(H)-hopanes ratio has been used by some workers as a qualitative indicator of maturity (van Graas, 1989). The ratio increases systematically with increasing thermal maturity (Seifert and Moldowan, 1978) because proportionally more tricyclic terpanes than hopanes are released from the kerogen at higher levels of maturity (Aquino Neto et al., 1983). Tricyclic terpanes and hopanes originated from diagenesis of different biological precursors (Ourisson et al., 1982). The tricyclics/17α(H)-hopanes ratio can differ considerably between crude oils from different source rocks or different facies of the same source rock (Peters et al., 2005).

2.5.2.3 C_{30}-Moretane/ C_{30}-hopane ratio

The 17β,21α(H)-moretanes are thermally less stable than 17α,21β(H)-hopanes, and thus the C_{30}-moretane/C_{30}-hopane ($C_{30}\beta\alpha/C_{30}\alpha\beta$) ratios decrease with increasing thermal maturity from ~0.8 in immature source rock to values of less than 0.15 in mature stage (Mackenzie et al., 1980; Waples and Machihara, 1990; Peters and Moldowan, 1993; Arfaoui and Montacer, 2007). This ratio also depends on source input or nature of the depositional environment. Rullkötter and Marzi (1988) noted higher moretane/hopane ratios in bitumens from hypersaline rocks compared with the adjacent shales. Moreover, it

has been observed that relatively high concentrations of C_{30} moretane can also be associated with samples characterized by higher-plant input (Isaksen and Bohacs, 1995).

2.5.2.4 Ts/(Ts+Tm) ratios

The C_{27} pentacyclic triterpane ratio, 18α(H)-22,29,30-trisnorhopane(Ts) vs. 17α(H)-22,29,30-trisnorhopane(Tm), has been used extensively as an indicator of maturity in samples containing similar source materials (Seifert and Moldowan, 1978). Peters et al. (2005) stated that the Ts/(Ts+Tm) ratio is more reliable than the Ts/Tm ratio as a maturity indicator when evaluating samples from a common source of consistent organic facies, yet it should be used with caution. The Ts/Tm ratio is dependent on the depositional environment and the source of organic material (Philp et al., 1992). The ratio is also affected by lithology and oxicity of the depositional environment, where bitumens from many hypersaline source rocks show high Ts/(Ts+Tm) ratios (Fan Pu et al., 1987; Rullkötter and Marzi, 1988). Furthermore, it was observed that the ratio increases at lower Eh and decreases at higher pH for the depositional environment of a series of Lower Toarcian marine shales from southwestern Germany (Moldowan et al., 1986), and it also decreases in an anoxic (low Eh) carbonate section (Peters et al., 2005). It has also been observed that oils from carbonate source rocks were shown to have unusually low Ts/(Ts+Tm) ratios compared with those from shales (McKirdy et al., 1983; McKirdy et al., 1984; Rullkötter et al., 1985; Price et al., 1987).

2.5.2.5 Steranes

The two most commonly used sterane maturity parameters are the C_{29} 14α(H),17α(H)(20S/ (20S + 20R)) ratio and the C_{29} 14α(H),17α(H) (20S + 20R)/14α (H),17α(H)(20S + 20R) + 14β(H)17β(H)(20S + 20R) ratio (Seifert and Moldowan, 1986). Both ββ/(ββ+αα) and 20S/(20S+20R) isomerization ratios increase with increasing maturity (Mackenzie et al., 1980). As maturity increases, the αα epimer, which is produced biologically, is gradually converted into a mixture of αα and ββ epimers. The conversion of ααC_{29} 20R to 20S steranes causes the ratio of 20S/(20S+20R) to increase with increasing maturity, usually reaching an equilibrium value of ~0.55 near the main oil generation window (Mackenzie et al., 1980). Because the ββ/(ββ+αα) ratio is slower to reach an equilibrium value of ~0.70 around peak oil generation, it is more effective at higher levels of maturity (Mackenzie et al., 1980; Peters and Moldowan, 1993; Ramón and Dzou, 1999). However, Peters and Moldowan (1993) indicated that this ratio is also independent of source organic matter input. There are many factors that can affect the sterane maturity parameters and produce anomalously low or high values. For instance, ββ/(ββ+αα) ratio can be strongly affected by diagenetic conditions as well as maturity (ten Haven et al., 1986; Peakman and Maxwell, 1988; Peakman et al., 1989). In particular, under hypersaline conditions the ββ/(ββ+αα) ratio may be abnormally high (Rullkötter and Marzi, 1988). Furthermore, destruction of steranes at high maturities may lead to changes in the 20S/(20S+20R) ratio through preferential destruction of the 20S epimer (Marzi and Rullkötter, 1989). Peters and Moldowan (1993) reported that both ratios of ββ/(ββ+αα) and 20S/(20S+20R) are also sensitive to the availability of clay minerals. The influence of the mineral matrix on the epimerisation of steranes have also been reported

by several authors (Strachan et al., 1989; Peters et al., 1990). Thus, both of the sterane maturity parameters could be affected by these potentially serious weaknesses.

2.5.2.6 Methylphenanthrene index (MPI)

Several ratios based on phenanthrene distributions have been proposed as indicators of thermal maturity (e.g. MPI-1, MPI-2, MPI-3, and MPR). The methylphenanthrene index 2 (MPl-2) was used in the present study. This ratio was calculated as proposed by Radke and Welte, (1983) from the peak areas of phenanthrene (P) and methylphenanthrene (MP) components in the *m/z* 178 and 192 mass chromatograms, respectively, as follows:

$$\text{MPI 2} = 3 \text{ X } \frac{[2\text{-MP}]}{[\text{P} + 1\text{-MP} + 9\text{-MP}]}$$

Although the methylphenanthrene index 1 (MPl-1) is more frequently used as a maturity indicator than MPI-2; in the present study, MPI-2 index was found to be more consistent with the other aromatic maturity parameters (e.g. MA(I)/MA(I+II) and TA(I)/TA(I+II)) than MPI-1 index. Based on MPI-2 index, the following classification of crude oils was proposed: high maturity crude oils MPI-2 > 1.00, medium maturity MPI-2 = 0.80–1.00, and immature crude oils MPI-2 > 0.80 (Angelin et al., 1983; Radke, 1987; Ivanov and Golovko, 1992).

Radke et al., (1982a and b; 1983) observed an increase in the relative amounts of 2- and 3-methylphenanthrenes compared to 1- and 9-methylphenanthrenes with increasing burial depth and temperature. This can be explained in terms of rearrangement of monomethylphenanthrenes, favoring, at higher temperatures, the more

thermodynamically stable 2- and 3- positions (Radke et al., 1982a; Radke and Welte, 1983). Steroids and triterpenoids have been proposed as biological precursors for the phenanthrenes found in fossil material (Kvalheim et al., 1987). Partial de-alkylation of these precursors gives rise only to 1- and 2-methylphenanthrenes (Tissot and Welte, 1984). The presence of 3- and 9-methylphenanthrenes in sediment extracts and crude oils has been ascribed to methylation of phenanthrene and rearrangement of mono-methylphenanthrenes (Radke et al., 1982b).

2.5.2.7 Aromatic steroid hydrocarbons

The distributions of aromatic steroids have been increasingly used as fingerprints for the study of the maturation of the organic matter of sediments, as well as for correlation of crude oils and source rocks (Peters and Moldowan, 1993). Ratios of short- to long-side chain mono- and triaromatic steroids and tri- to monoaromatic steroids have been used for maturity assessment of both crude oils and source rocks (Mackenzie et al., 1981). The conversion of C-ring monoaromatic (MA) steroids to ABC-ring triaromatic (TA) steroids involves the loss of both the methyl group at the A/B ring juncture and the asymmetric center at C-5 (Peters et al., 2005). Although the mechanism of these transformations is not clear, clay minerals may play an important role as a catalyst (Rubinstein et al., 1975). The ratio of TA/(MA+TA) increases with increasing levels of thermal maturity from 0 to 100% (Mackenzie et al., 1981).

The mono- and triaromatic steroid hydrocarbon ratios [MA(I)/MA(I+II) and TA(I)/TA(I+II), respectively] incorporates the sum of all major C_{27}–C_{29} monoaromatic

steroids as MA(II) and C_{21} plus C_{22} as MA(I) and the sum of C_{26}–C_{28} (20S+20R) triaromatic steroids as TA(II) and the sum of C_{20} and C_{21} triaromatic steroids as TA(I), respectively in order to reduce the source input effect (Peters et al., 2005). Both ratios increase with increasing maturity as a result of preferential thermal degradation of the long- versus short-chain components, and conversion of long-chain to short-chain aromatic steroids or both (Beach et al., 1989; Peters and Moldowan, 1993).

CHAPTER-III

3. SAMPLE SELECTION AND EXPERIMENTAL METHODS

3.1 Samples Collection and Preparation

A total of 20 crude oil samples and 55 cuttings (Silurian shale) were collected from wells selected from the NC-115 and NC-186 Blocks, the El-Sharara Oil Field particularly from A-, I-, & R-Fields, in the Murzuq Basin, S.W. Libya (Table 3.1, Figures 3.1 & 1.3). Only twenty prospective good quality shale samples identified during the screening stage were selected for further detailed evaluation of their source and maturity characteristics. All shale samples were taken from the upper part of the Silurian Tanezzuft Formation (Figure 1.3).

A schematic flow chart of the experimental methods applied in this study is shown in Figure 3.2. In order to remove any contamination (e.g. drilling mud, dust, and handling), all shale samples were washed and treated with distilled water and 1:1 mixture of dichloromethane (CH_2Cl_2) and methanol (CH_3OH). After the samples were totally dried, they were crushed to finely ground powder using a porcelain mortar and pestle for Rock-Eval pyrolysis and TOC along with soxhlet extraction.

Table 3.1. List of Tanezzuft Shale and crude oil samples analyzed in this study.

Well Name	Median Depth (ft)	Sample ID	Lithology	Sample Type	Tanezzuft Formation	Basin	Block	Reservoir
A3	4,213	**A3**	Shale	Cutting	Cool shale	Murzuq	NC-115	–
A5	4,315	**A5**	Shale	Cutting	Cool shale	Murzuq	NC-115	–
A6	4,500	**A6a**	Shale	Cutting	Cool shale	Murzuq	NC-115	–
A6	4,610	**A6b**	Shale	Cutting	Cool shale	Murzuq	NC-115	–
A10	4,659	**A10**	Shale	Cutting	Cool shale	Murzuq	NC-115	–
A17	4,370	**A17a**	Shale	Cutting	Cool shale	Murzuq	NC-115	–
A17	4,190	**A17b**	Shale	Cutting	Cool shale	Murzuq	NC-115	–
A18	4,200	**A18**	Shale	Cutting	Cool shale	Murzuq	NC-115	–
A19	4,200	**A19a**	Shale	Cutting	Cool shale	Murzuq	NC-115	–
A19	4,200	**A19b**	Shale	Cutting	Cool shale	Murzuq	NC-115	–
A20	4,545	**A20a**	Shale	Cutting	Cool shale	Murzuq	NC-115	–
A20	4,530	**A20b**	Shale	Cutting	Cool shale	Murzuq	NC-115	–
A21	4,600	**A21**	Shale	Cutting	Cool shale	Murzuq	NC-115	–
A22	4,600	**A22**	Shale	Cutting	Cool shale	Murzuq	NC-115	–
A23	4,150	**A23**	Shale	Cutting	Cool shale	Murzuq	NC-115	–
A34	4,730	**A34**	Shale	Cutting	Cool shale	Murzuq	NC-115	–
A35	4,840	**A35a**	Shale	Cutting	Cool shale	Murzuq	NC-115	–
A35	4,000	**A35b**	Shale	Cutting	Cool shale	Murzuq	NC-115	–
A37	5,010	**A37a**	Shale	Cutting	Cool shale	Murzuq	NC-115	–
A1	–	**A1**	–	Oil	–	Murzuq	NC-115	Mamuniyat
A7	–	**A7**	–	Oil	–	Murzuq	NC-115	Mamuniyat
A10	–	**A10**	–	Oil	–	Murzuq	NC-115	Mamuniyat
A11	–	**A11**	–	Oil	–	Murzuq	NC-115	Mamuniyat
A12	–	**A12**	–	Oil	–	Murzuq	NC-115	Mamuniyat
A14	–	**A14**	–	Oil	–	Murzuq	NC-115	Mamuniyat
A15	–	**A15**	–	Oil	–	Murzuq	NC-115	Mamuniyat
A16	–	**A16**	–	Oil	–	Murzuq	NC-115	Mamuniyat
A24	–	**A24**	–	Oil	–	Murzuq	NC-115	Mamuniyat
A25	–	**A25**	–	Oil	–	Murzuq	NC-115	Mamuniyat
A26	–	**A26**	–	Oil	–	Murzuq	NC-115	Mamuniyat
A27	–	**A27**	–	Oil	–	Murzuq	NC-115	Mamuniyat
A28	–	**A28**	–	Oil	–	Murzuq	NC-115	Mamuniyat
A30	–	**A30**	–	Oil	–	Murzuq	NC-115	Mamuniyat
A31	–	**A31**	–	Oil	–	Murzuq	NC-115	Mamuniyat
A32	–	**A32**	–	Oil	–	Murzuq	NC-115	Mamuniyat
R-1	–	**R-1**	–	Oil	–	Murzuq	NC-186	Mamuniyat
R-7	–	**R-7**	–	Oil	–	Murzuq	NC-186	Mamuniyat
I-2	–	**I-2**	–	Oil	–	Murzuq	NC-186	Mamuniyat
I-11	–	**I-11**	–	Oil	–	Murzuq	NC-186	Mamuniyat

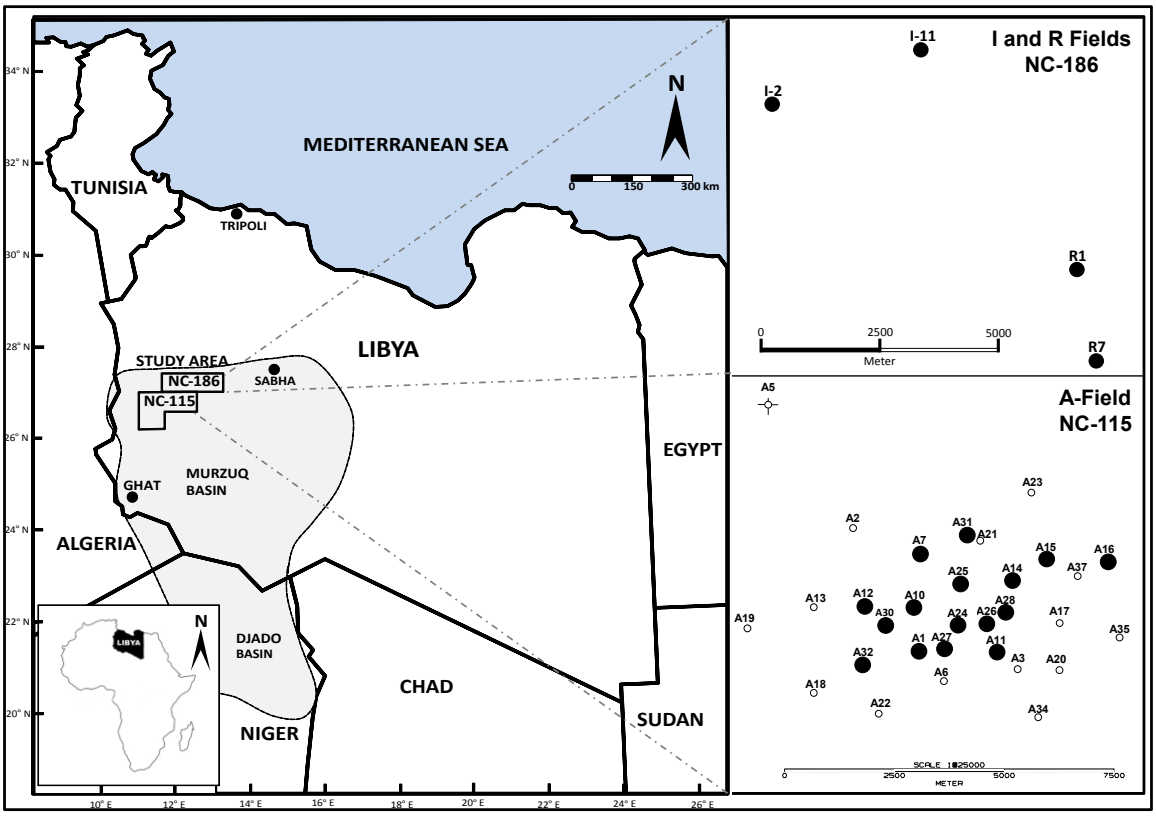

Figure 3.1. Location map of the Murzuq Basin, S.W. Libya with position of the study area where Blocks NC-115 and NC-186 are located. It also shows the location of wells from which rock and crude oil samples were collected. Block NC-115 contains A Field from which rock and crude oil samples were collected. Block NC-115 contains A Field from which 16 oil samples and 20 rock samples were taken. Block NC-186 comprises R- and I-Fields, where two oil samples were taken from each.

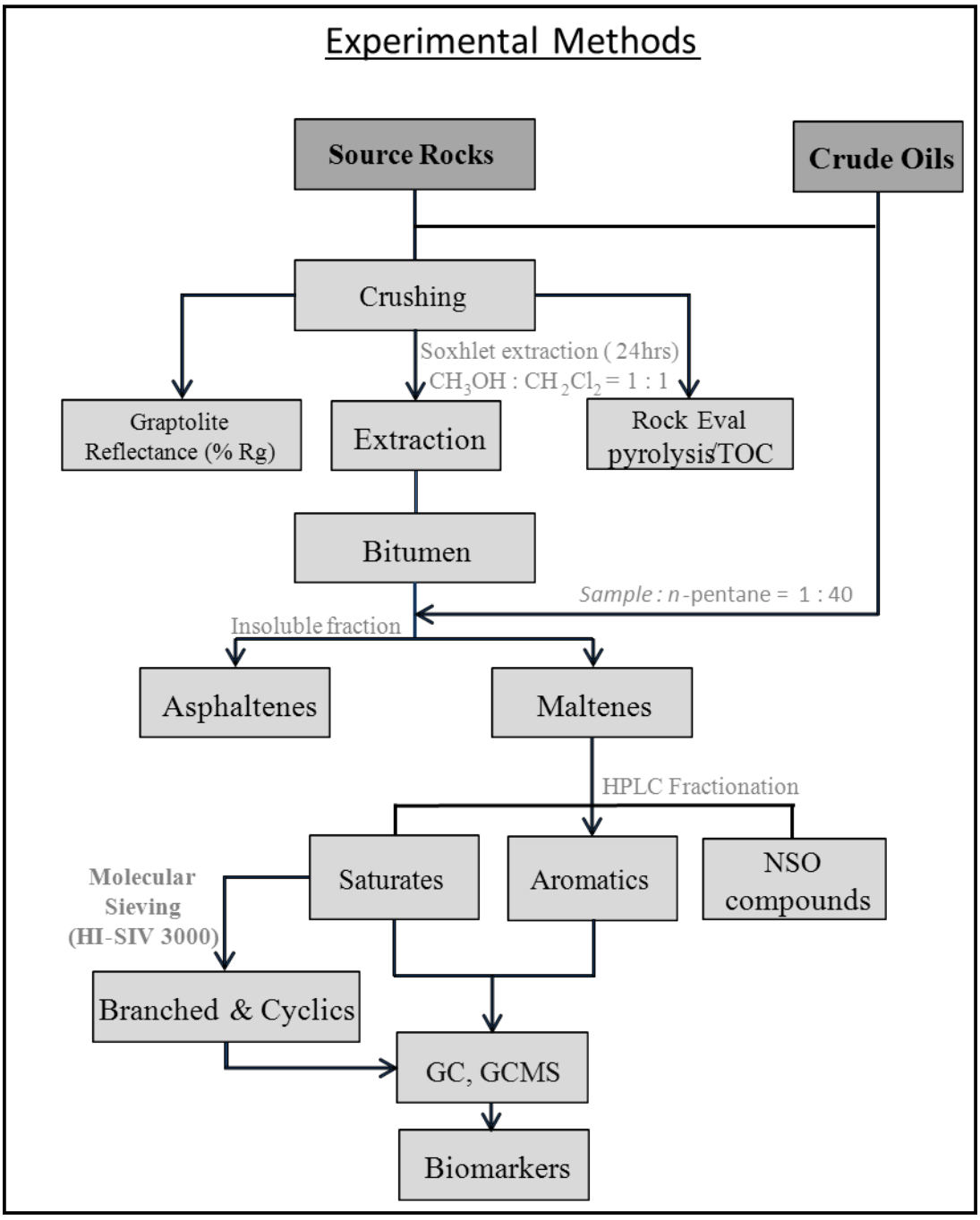

Figure 3.2. Schematic workflow of the experimental methods used in this study.

3.1.1 Rock-Eval pyrolysis and TOC

Shale samples (1-2 grams) were characterized by Rock-Eval analyses at GEOMARK RESEARCH, LTD in Humble, Texas in order to determine TOC (wt%), S1 (mg HC/g rock), S2 (mg HC/g rock), S3 (mg CO_2/g rock), Tmax (ºC), HI (Hydrogen index, S2/TOC), OI (Oxygen index, S3/TOC), and PI (Production index, S1/(S1+S2). Prospective good quality samples identified during the screening stage above were selected for further detailed evaluation of their source and maturity characteristics.

3.1.2 Source Rock Extraction

Approximately 20-50 grams of each sample was finely crushed, and Soxhlet extracted using a mixture (50:50 v/v) of dichloromethane (CH_2Cl_2) and methanol (CH_3OH). In Soxhlet extraction, (Figure 3.3) solvent is vaporized from a flask, passes upward through the side arm of the apparatus, condenses and drips down into a cellulose thimble containing the powdered sample within the Soxhlet. The hot solvent extracts the soluble organic matter from the sample and is periodically recycled into the solvent reservoir flask via a siphon. Several cycles of this process are required to ensure exhaustive extraction; hence the apparatus is typically operated for 24 hours, depending on sample size and richness. Extraction is typically complete when the solvent surrounding the thimble becomes clear, rather than some variant shade of black, brown, red or yellow.

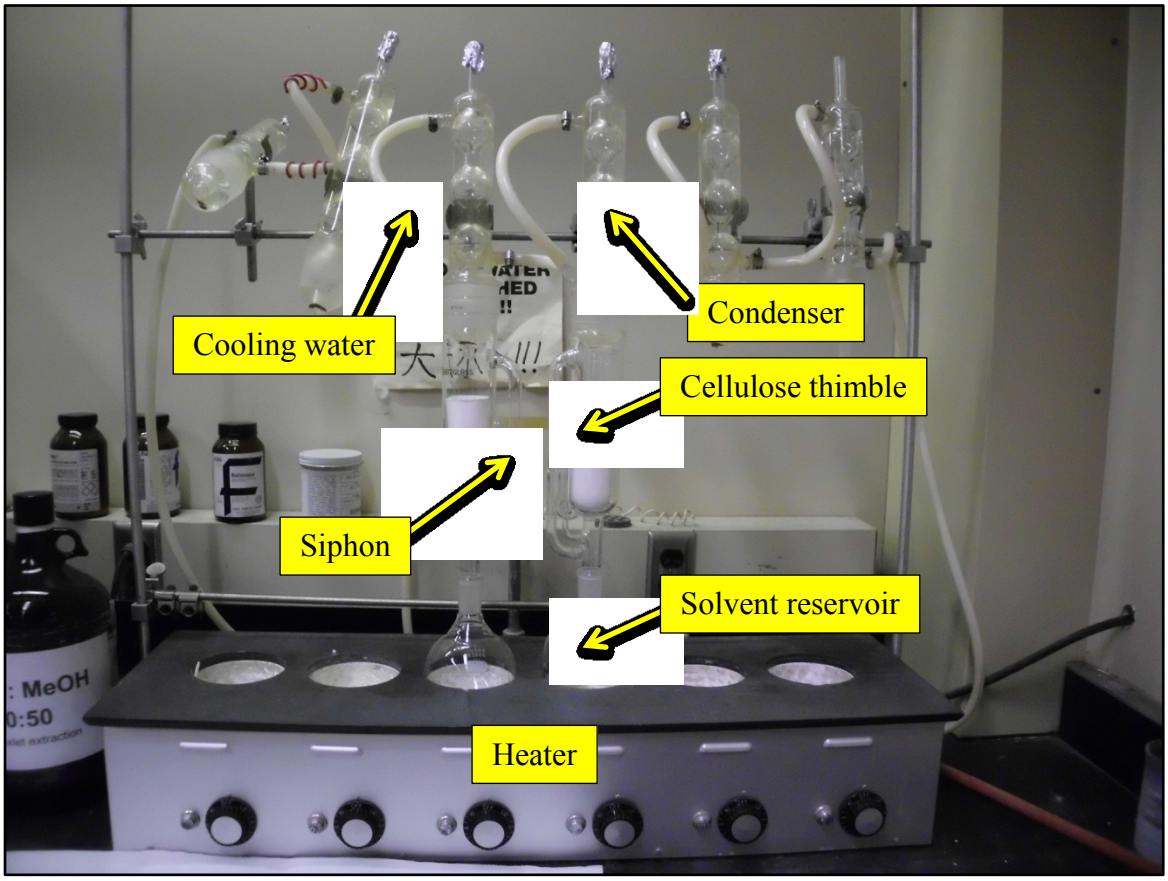

Figure 3.3. Illustration of a Soxhlet extraction in progress. Organic Geochemistry Laboratories, University of Oklahoma.

3.1.3 Asphaltene Precipitation and Fractionation of Rock Extracts and Oils

Source rock extracts and oils were treated in the same manner for asphaltene removal and fractionation, and are described together. *n*-Pentane (40mL) and sample (50 mg for bitumens and 10 ml for oils) were placed into glass centrifuge tubes. The centrifuge tubes were shaken and kept in a freezer for 1hr to precipitate the asphaltenes. The tubes were then centrifuged for 20 minutes at 1000 RPM. After centrifugation, the *n*-pentane containing maltenes was decanted from the sample. Asphaltenes, which precipitated were washed with *n*-pentane to recover maltenes adsorbed to the asphaltenes. The *n*-pentane solution was evaporated and the remaining maltenes transferred into a pre-weighed glass vial and quantified.

Fractionation of the maltenes into saturates, aromatics, and NSO compounds (polars) was performed using a Hewlett Packard 1050 series HPLC (high performance liquid chromatography) for which sample aliquots were dissolved in hexane in a ratio of 20mg maltene per 50µL hexane and then 50µL of maltene solution was injected into the HPLC. Saturate, aromatic and polar fractions were eluted according to a modified gradient program adapted from McDonald and Kennicutt (1992) using hexane, DCM and ethyl acetate as eluents. Saturate, aromatic and polar fractions were collected in three 100 ml round bottom flasks according to the following times: saturates (0-5.50 minutes); aromatics: (5.50-10.33 minutes); polars: (10.33-16.91 minutes). The excess solvents were then evaporated, and the fractions quantified (McDonald and Kennicutt, 1992). For more information on the extraction and fractionation data of crude oils and source rocks from the Murzuq Basin, see Appendix I.

The saturate fractions were sieved for *n*-alkane removal prior to GC-MS analyses using a pasteur pipette packed with 2g of HI-SIV 3000. In order to remove any impurities, three bed volumes of hexane were added to the pipette, and then the sample was placed into the pipette. Three additional bed volumes of hexane were then added above the sample. The *n*-alkanes were retained in the sieve whereas the branched and cyclic (B/C) compounds eluted from the pipette were collected in a pre-weighed glass vial and to be dried and quantified. The concentration of branched and cyclic fraction used in the analysis of biomarkers in GCMS was 1.5 mg of B/C : 1ml of DCM (dichloromethane). Analytical techniques including gas chromatography (GC) and gas chromatography-mass spectrometry (GCMS) were applied to the analyses of both saturate and aromatic fractions.

3.1.4 Petrography

3.1.4.1 Polished Pellets

A total of 24 polished pellets were prepared for petrographic study at the Oklahoma Geological Survey Organic Petrography Labratories, University of Oklahoma. Dispersed organic pellets were prepared from the same shale samples used in extraction (finely crushed), where a certain amount of each sample was placed in plastic ring forms. Epoxide epoxy resin mixture (epoxy : hardener = 5:1) was poured into a plastic centrifuge tube, and placed in the centrifuge for 3 minutes to remove air bubbles from epoxy. Bubble-free epoxide mixture was poured into each plastic ring form until about half full.

Each sample was slowly sprinkled into its designated ring form (less than the volume of the epoxy). Using a stirring stick, the sample and epoxy were slowly stirred until the entire crushed sample was thoroughly mixed and coated with epoxy and spread evenly across the bottom of the ring form. More bubble-free epoxy was poured in each ring form up to the rim. They were then left to harden.

The pellets were then ground using Buehler Ecomet III Grinding and Polishing Apparatus (Figure 3.4) until the surface became flat and free of irregularities. The samples were ground using water as a lubricant; initially with 320 grit paper, followed by 400 and finally on 600 grit paper (1-3 minutes on each grit paper). The pellets were rinsed off with distilled water and placed into an ultrasonic bath (distilled water mixed with a few drops of Kodak Photo-Flo 200 Solution) for 1-2 minutes. The pellets were polished on Buehler Texmet polishing cloth with Wendt Dunnington 0.3 micron alumina slurry and distilled water was used as a lubricant. Total polishing time was four minutes. The pellets were placed in the ultrasonic bath again for 1-2 minutes, then rinsed off with distilled water. The pellets were polished with Wendt Dunnington 0.05 micron alumina slurry using the same conditions as in the 0.3 micron step. Finally, the polished pellets were rinsed under running water to get rid of the slurry residue, blown off with filtered air, and wiped with paper towel.

3.1.4.2 Microscopic Examination and Graptolite Reflectance (%Rg)

The petrographic examination was done at the Oklahoma Geological Survey Organic Petrography Labratories, University of Oklahoma. Petrographic examination of polished

Figure 3.4. Buehler Ecomet III Grinding and Polishing Apparatus used for polishing dispersed organic pellets. Organic Petrology Laboratory, Oklahoma Geological Survey, University of Oklahoma.

shale pellets was performed on a Vickers M17-Photomicroscope with ×50/0.85 objective under oil immersion and reflected white light (Figure 3.5). The microscope was fitted with a DR-2 Digital Radiometer and a D-47A Photomultiplier Detector that were used to measure the amount of light reflected from the surface of a highly polished rock sample. Graptolite reflectance (%Rg) measurements were performed in plane-polarized reflected 'white' light. However, the quality of samples in this study was not good enough to be used for maturity evaluation without further support by other maturity parameters (e.g. Rock-Eval and biomarkers). All samples were finely ground making it very difficult to obtain many measurements on different particles for most of the samples, and there were not sufficient measurements to evaluate the thermal maturity of the source rock. Moreover, reflectance measurements on some samples could not be taken because of the size of particles, which were smaller than the measurement spot. Hence, data should be supported further by other geochemical evidence, including Rock-Eval data and biomarker maturity parameters.

3.1.5 Gas Chromatography (GC)

The saturate hydrocarbon fractions were analyzed by gas chromatography (GC-FID) using a Hewlett-Packard 35141 gas chromatography (Figure 3.6). A fused silica capillary column used was coated with DB-PETRO (100m × 0.25mm i.d.; 0.25μm film thickness) and a temperature program from 40 to 300°C at rate of 4°C/min was used. The injector and flame ionization detector (FID) temperatures were set at 300°C and 310°C,

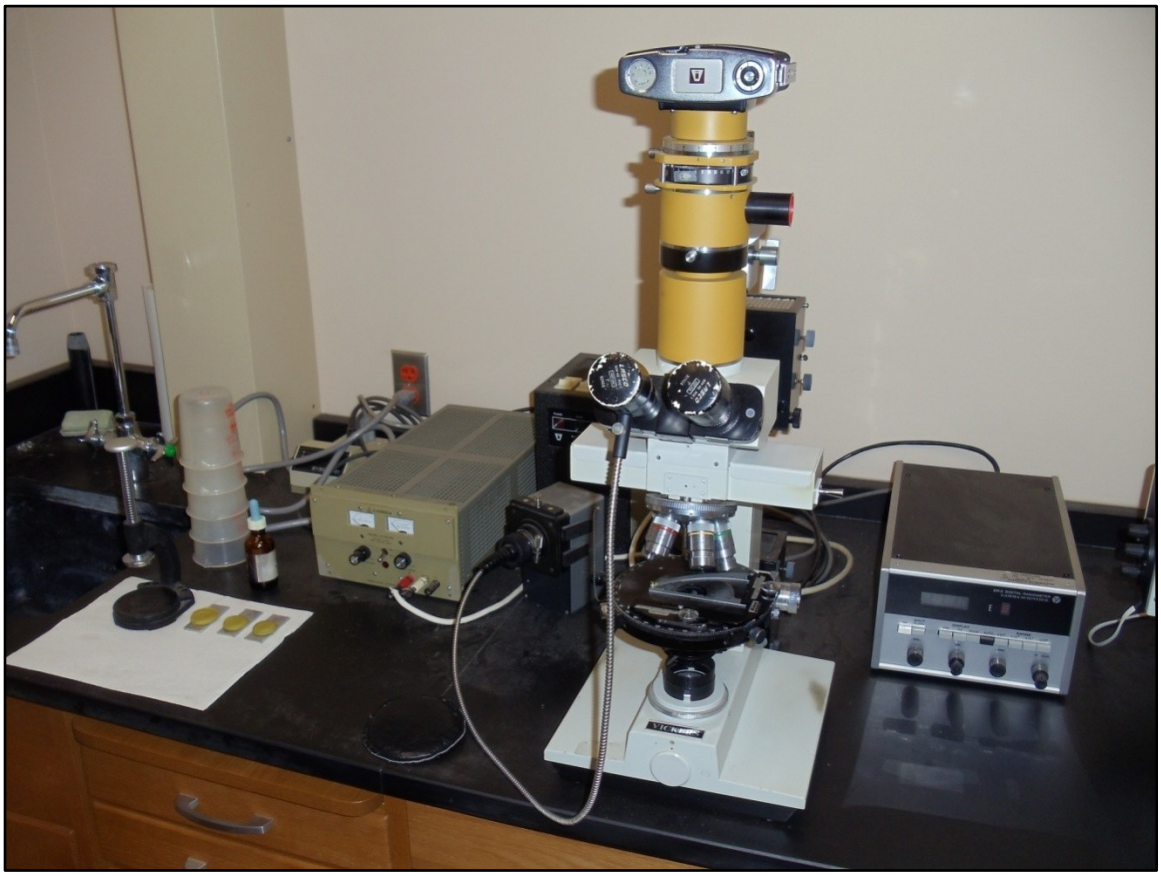

Figure 3.5. A Vickers M17-Photomicroscope used for graptolite reflectance study. Organic Petrology Laboratory, Oklahoma Geological Survey, University of Oklahoma.

Figure 3.6. Gas chromatography (GC-FID) (Hewlett-Packard 35141) used in the study. Organic Geochemistry Laboratories, University of Oklahoma.

respectively. Injection was performed in the splitless mode using helium (He) as the carrier gas and a flow rate of 0.5mL/min.

3.1.6 Gas Chromatography-Mass Spectrometry (GCMS)

GC-MS analyses were performed using Agilent 7890A (Figure 3.7). A fused silica capillary column coated with DB-5MS (60m × 0.25mm i.d.; 0.25µm film thickness) was temperature programmed from 40°–300°C at 4°C/min. The ion source, injector, and transfer line temperatures were maintained at 200°C, 300°C and 310°C, respectively. Helium was used as the carrier gas. The GC-MS analysis was based on fragmentograms at *m/z* 183, 191, and 217 in order to determine the distribution of long-chain isoprenoids, triterpanes, and steranes, respectively. The relative concentrations of particular compounds were calculated from peak areas. Biomarkers were identified by comparison with previously published accounts (Philp, 1985; Jones and Philp, 1990; Peters and Moldowan, 1993).

3.1.7 Quantitative Biomarker Analysis

Quantitation was accomplished using deuterated *n*-tetracosane ($C_{24}D_{50}$) as an internal standard (*m/z* 66). The saturate fractions of each crude oil sample and extract were quantitatively spiked with deuterated *n*-tetracosane prior to GCMS analysis. The relative concentrations of the steranes and triterpanes (ppm) were calculated by comparing the peak area of the appropriate biomarker relative to that of the co-injected deuterated *n*-

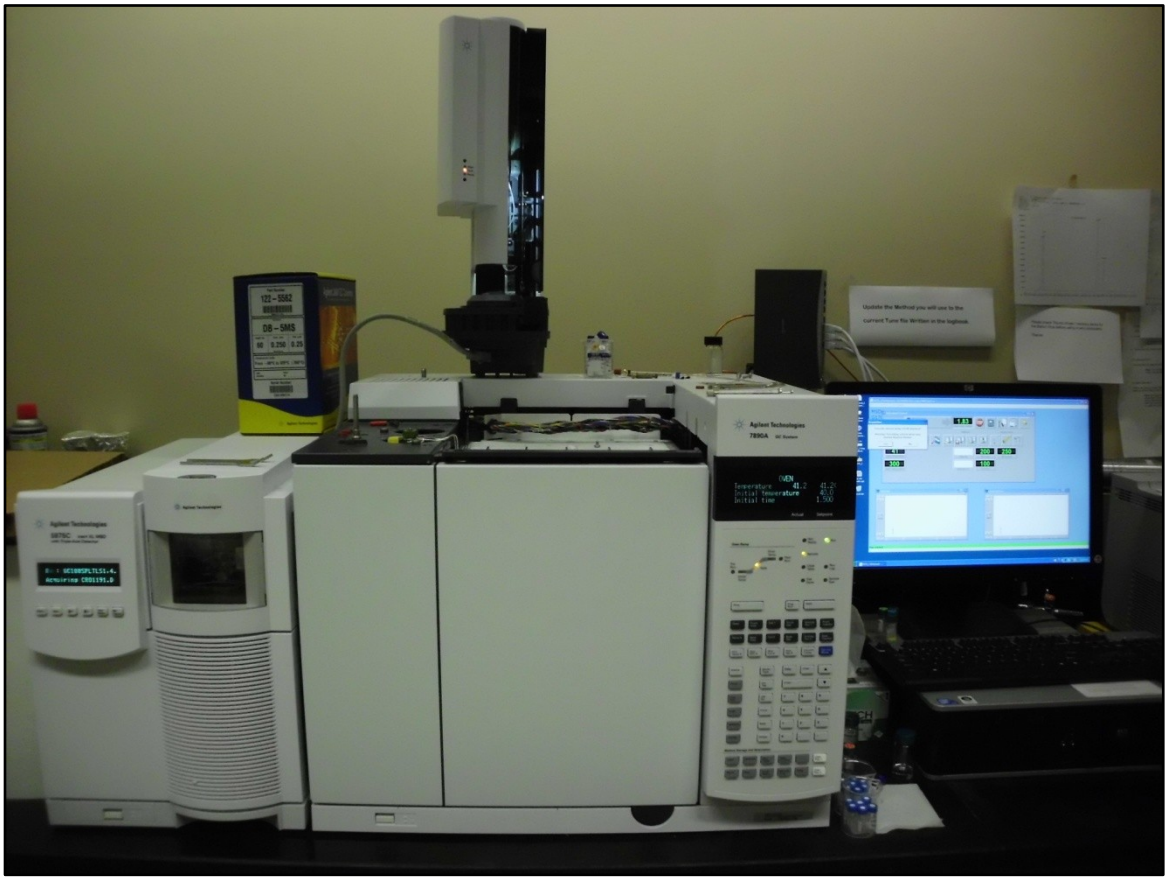

Figure 3.7. Gas chromatography-mass spectrometry (GC-MS) (Agilent 7890A) used in the study. Organic Geochemistry Laboratories, University of Oklahoma.

tetracosane ($C_{24}D_{50}$). The response factor of individual compounds relative to the standard was assumed to be one. The relative biomarker concentrations of crude oils were calculated by normalization to the saturate fractions, expressed as micrograms of biomarkers per gram of saturate fraction (µg/g Sat). This allows the comparison of the concentrations between oils and source rocks in terms of biomarker content and distribution. The calculation was based on the following equation:

$$\text{Relative concentration of biomarkers } (C_{ABC}) = \frac{(C_{BIO} \times V_{B/C} \times 1{,}000{,}000)}{(\%SAT_{TOTAL}\,(\%SAT) \times Wt_{SAMPLE} \times \%S_{SAT} \times \%MLT)} \quad (\mu g/g\ SAT)$$

C_{BIO} is the relative concentration of biomarker expressed in a unit of µg biomarker per ml solvent and can be calculated as the following: $C_{BIO} = (C_{ISTD} \times A_{BIO})/A_{ISTD}$ (µg/ml), Where C_{ISTD} is the known concentration of internal standard ($C_{24}D_{50}$); A_{ISTD} is the integrated peak area of that internal standard; A_{BIO} is the integrated peak area of biomarker.

$V_{B/C}$ is the volume of branched and cyclic fractions expressed in a unit of ml and can be calculated by the following equation: $V_{B/C} = W_{B/C} \div 1.5$ (mg/ml), where $W_{B/C}$ is the weight of the branched and cyclic fractions and 1.5 (mg/ml) is the concentration utilized in the analysis of biomarkers (1.5mg of B/C : 1ml of DCM);

1,000,000 is the number used to cancel the three percentages in the denominator of the equation;

$\%SAT_{TOTAL}$ is the total saturated fraction of the oil/extract expressed in a unit of percent;

Wt_{SAMPLE} is the weight of the oil/rock sample used for analysis, and expressed in gram;

$\%S_{SAT}$ is the percentage of the saturate fraction used for preparing branched and cyclic saturate fractions by high molecular sieve (HI-SIV 3000);

% MLT is the percentage of maltene used for fractionation analysis by HPLC.

However, errors may occur while quantifying the data. For instance, errors could happen in the sample weighing or taking accurate amounts of the internal standard. Errors may occur in fractionation as well, where the percentages of *n*-alkane and branched and cyclic biomarkers removed are unknown. Moreover, error could also result from response factors of the standard and biomarkers. The differences in response factors between the internal standard and other compounds (e.g. tricyclic terpanes and steranes) are unknown (Wang, 1993; Wang and Philp, 1997). In this study, since standards were not available for each biomarker, the response factor of each compound used in GC/MS analysis was considered as one. Therefore, the concentrations of biomarkers in this study are considered to be relative concentrations.

3.1.8 Bulk Isotopes Analysis

Bulk carbon isotope values of the crude oils were determined by sealed tube combustion (Sofer, 1980; Engel and Maynard, 1989). Approximately 1mg of sample material was loaded into pyrex glass tubes along with 3g of fired cupric oxide, sealed under vacuum, and combusted at 550 °C for 2½ hours. The resulting CO_2 gas was isolated and purified cryogenically on a vacuum line and analyzed by dual inlet mode with a Finnigan Mat Delta E isotope ratio mass spectrometer. The results are reported in standard delta notation (δ) in part per thousand (‰) using the following equation:

$$\delta^{13}C = \left[\frac{C^{13}/C^{12}_{sample}}{C^{13}/C^{12}_{standard}} - 1\right] \times 10^3 \ (‰)$$

CHAPTER-IV

4. RESULTS AND DISCUSSION

4.1 SOURCE ROCK

4.1.1 Origin of Organic Matter and Depositional Conditions

4.1.1.1 Rock-Eval Pyrolysis/TOC

Rock-Eval pyrolysis is used as a screening tool in evaluating the quantity, quality, and thermal maturity of rock samples (Espitalié et al., 1977). TOC is the quantity of organic carbon expressed as weight percentage (wt %) of the rock (Ronov, 1958). When using TOC, the hydrocarbon generating potential is commonly interpreted through a semi-quantitative scale such as shown in Table 4.1 (Jarvie, 1991; Peters and Moldowan, 1993). According to Tissot et al. (1974), not all organic matter in a source rock with a high content of TOC, has the same generation potential; some organic matter will generate oil, some gas, and some will not generate anything. Thus, TOC by itself is not necessarily a good indicator for how much hydrocarbon can be generated (Tissot et al., 1974). The presence of hydrogen associated with the carbon is more reliable for hydrocarbon generation. The more hydrogen associated with the carbon, the more hydrocarbons it can generate. Hydrogen content can be measured directly with elemental analysis

Table 4.1. (a) Generative potential (quantity) of immature source rock, (b) kerogen type and expelled products (quality), and (c) thermal maturity (Peters and Cassa, 1994).

(a) Potential (quantity)	Poor	Fair	Good	Very good	Excellent
TOC (Total organic carbon) (wt %)	<0.5	0.5–1.0	1.0–2.0	2.0–4.0	>4.0
S1 pyrolysis yield (mg of HC/g of rock)	<0.5	0.5–1.0	1.0–2.0	2.0–4.0	>4.0
S2 pyrolysis yield (mg of HC/g of rock)	<2.5	2.5–5.0	5.0–10	10–20	>20

(b) Kerogen (quality)	Inert	Gas-prone	Oil/gas	Oil-prone	Very oil-prone
HI (Hydrogen Index) (mg of HC/g of TOC)	<50	50–200	200–300	300–600	>600

(c) Maturation & Generation	Immature	Early mature	Oil-expulsion	Late mature	Postmature
Tmax (°C) Maximum temperature at top of S2 peak	<435	435–445	445–450	450–470	>470
PI (Production index) (S1/(S1+S2))	<0.10	0.10–0.15	0.25–0.40	>0.40	–

(Durand and Monin, 1978). Rock-Eval estimates the organic matter's hydrogen content from the S2 value, remaining hydrocarbon potential, which decreases with increasing thermal maturity (Espitalié et al., 1977; Jarvie, 1991; Peters et al., 2005). By determining HI, we can assess how much organic matter is present and how much hydrogen is associated with it (Peters et al., 2005; Dembicki, 2009). S1 corresponds to hydrocarbons that can be thermally distilled from the rock (mg HC/g rock). Tissot and Welte (1984) proposed that low TOC may be indicative of the relative oxicity of the depositional environment, which affects the amount and elemental composition of the preserved organic matter. On the contrary, less oxic environments promotes better organic preservation in the depositional environment. Thus, low values of TOC in samples could be attributed to the oxicity of the depositional environment conditions and/or the hydrocarbons had already been generated and migrated away from the source rock (Espitalié et al., 1977; Tissot and Welte, 1984; Jarvie, 1991; Peters and Moldowan, 1993). In the present study, samples investigated generally show poor to fair TOC with values ranging from 0.40% to 0.68% (Figure 4.1; Tables 4.1 and 4.2), only three samples (A6b, A23, and A37a) show good values of 1.28%, 1.03%, and 1.27%, respectively, and A6a shows an excellent value of 4.54% (Tables 4.1 and 4.2). The relatively low values of TOC may be interpreted as these samples have been deposited in relatively suboxic depositional conditions as strongly suggested by the values of Pr/Ph ratios (1.14–2.32), the presence of C_{30}-diahopane, and the low ratios of C_{35} to C_{34} homohopanes, all of which are indicative of suboxic depositional conditions. Moreover, maturity effect here could be excluded since most of the samples were shown to be at early-intermediate stages of thermal maturity as indicated by Rock-Eval Tmax data, ratios of 22S/(22S+22R), ββ/(ββ+αα), 20S/(20S+20R) and C_{30}-moretanes/C_{30}-hopanes(C_{30}βα/C_{30}αβ) ratios as well

Table 4.2. Result of Rock-Eval analyses of selected rock samples from the Tanezzuft Formation "cool" shale, NC-115, A-Field, Murzuq Basin.

Sample	Depth (ft)	TOC (wt % HC)	S1 (mg HC/g)	S2 (mg HC/g)	HI (S2x100/TOC)	PI (S1/(S1+S2))	Tmax (°C)
A3	4,213	0.74	0.3	0.45	62	0.4	432
A5	4,315	0.59	0.62	1.07	181	0.37	438
A6a	4,500	4.54	58.55	4.82	106	0.92	432
A6b	4,610	1.28	10.59	2.55	199	0.81	432
A10	4,659	0.50	0.93	0.38	75	0.71	438
A17a	4,370	0.53	0.47	0.78	147	0.38	435
A17b	4,190	0.52	0.41	0.53	102	0.44	436
A18	4,200	0.45	0.53	0.57	126	0.48	435
A19b	4,200	0.68	0.38	0.96	142	0.28	436
A20a	4,545	0.66	0.46	1.25	190	0.27	437
A21	4,600	0.52	0.21	0.21	41	0.50	433
A22	4,600	0.58	0.50	0.75	129	0.40	437
A23	4,150	1.03	0.59	0.67	65	0.47	432
A34	4,730	0.56	1.03	1.08	192	0.49	439
A35a	4,840	0.50	0.62	0.97	195	0.39	443
A35b	4,000	0.63	0.23	1.41	224	0.14	439
A37a	5,010	1.17	1.27	1.82	156	0.41	438
A37b	4,570	0.44	0.51	0.85	195	0.38	440

TOC: total organic carbon (%); HI: hydrogen index; PI: production index; Tmax: maximum pyrolysis temperature.

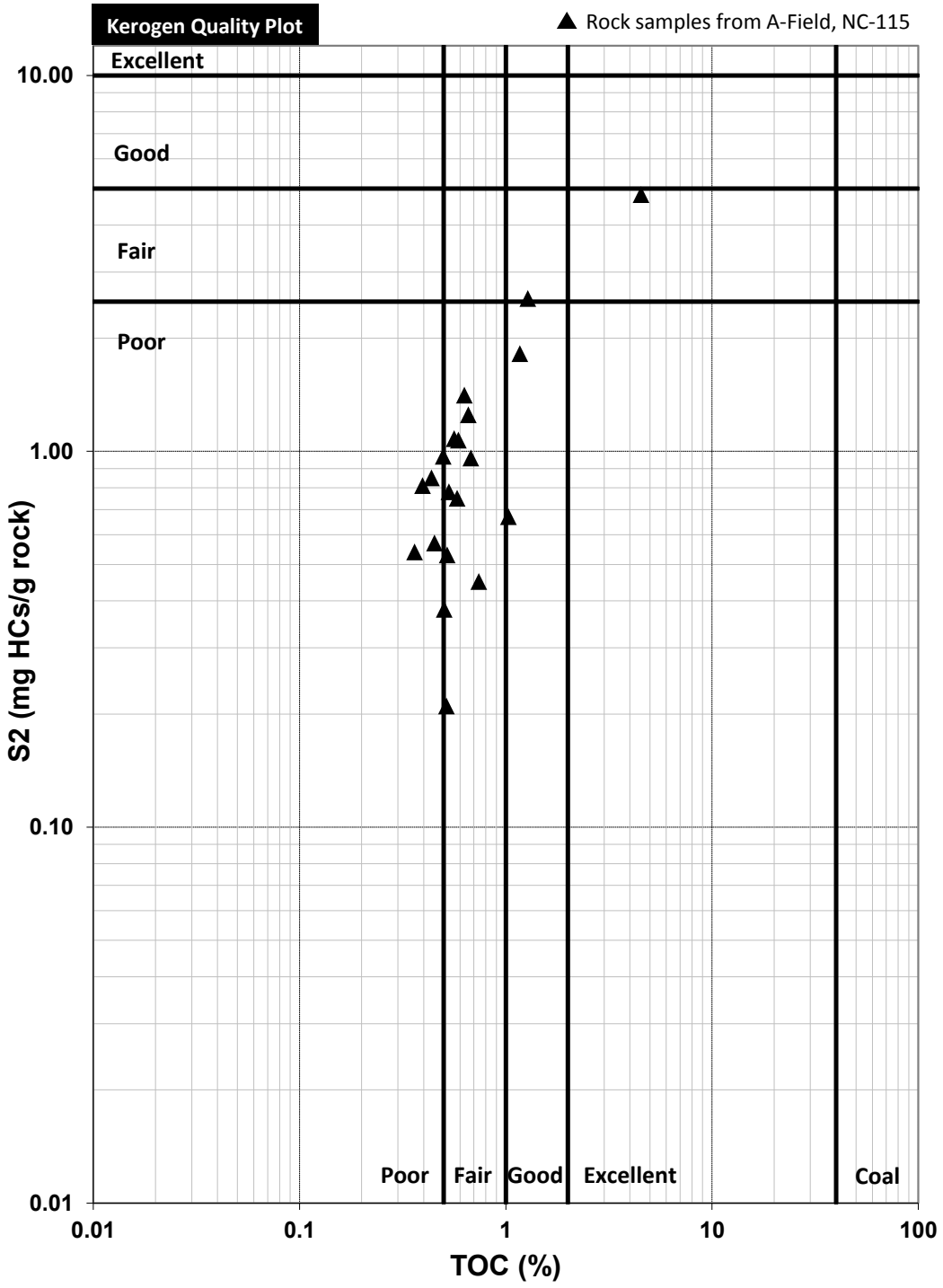

Figure 4.1. Crossplot showing the organic matter quantity with generally low S2 values for the Tanezzuft Formation "cool" shales. Modified from Espitalié et al., (1985).

as by the graptolite reflectance (discussed in Section 4.1.2.3). However, samples with high values of TOC may represent a more reducing depositional environment as indicated by low values of Pr/Ph ratios (0.83–0.96). S1 values are also shown to be generally poor to fair values ranging from 0.21 to 0.93 mg of HC/g, samples A34 and A37a show good to very good values of 1.03 and 1.27 mg of HC/g, respectively (Tables 4.1 and 4.2). In contrast, only two samples (A6a and A6b) show excellent values of 10.59 and 58.55 mg of HC/g, respectively (Tables 4.1 and 4.2). These anomalous high values may be resulted by contamination of migration and/or drilling mud additives. However, the low S1 values may indicate that insufficient amounts of hydrocarbon were generated. Generally, S2 values for most of the samples are low and range from 0.38 to 1.82 mg of HC/g of rock (Tables 4.1 and 4.2), suggesting that the remaining hydrocarbon potential of these samples is very low (fair potential).

To better characterize the source rock quality, a crossplot S2 vs. TOC (Figure 4.1) was used to determine the hydrocarbon potential for the samples in this study. As observed herein, most of the samples were plotted in the poor and fair zones, suggesting low quality and potential source rock. Such variation (poor-fair) in samples may be due to variability and heterogeneity of kerogen in the different organic facies. The other crossplots of hydrogen index vs. oxygen index (HI vs. OI) (Figure 4.2) were used in order to have a better understanding of the type of kerogen and consequently the product type. As can be observed in this crossplot, most of the samples are shown to be Type III kerogens, which are characterized by low HI and relatively high OI derived from terrestrial plant debris and/or aquatic organic matter deposited in an oxidizing environment that produces mainly gas (Tissot et al., 1974). A small contribution of mixed type II and III kerogens (gas/oil prone) is also observed. Hydrocarbon proneness and

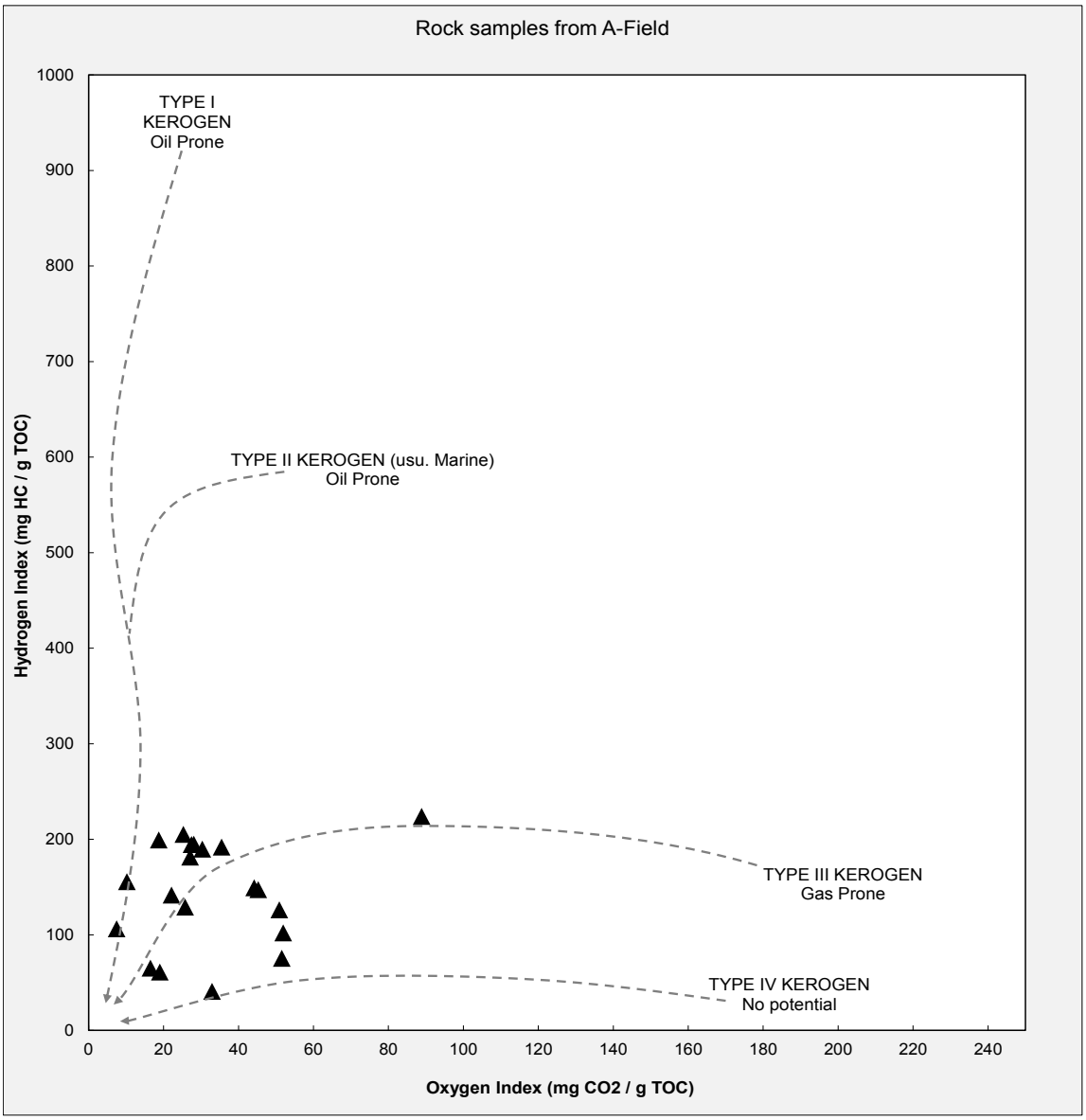

Figure 4.2. Pseudo van Krevelen diagram showing kerogen type and respective hydrocarbon proneness of Tanezzuft Formation "cool" shales, Murzuq Basin, S.W. Libya. Modified from Espitalié et al., (1977).

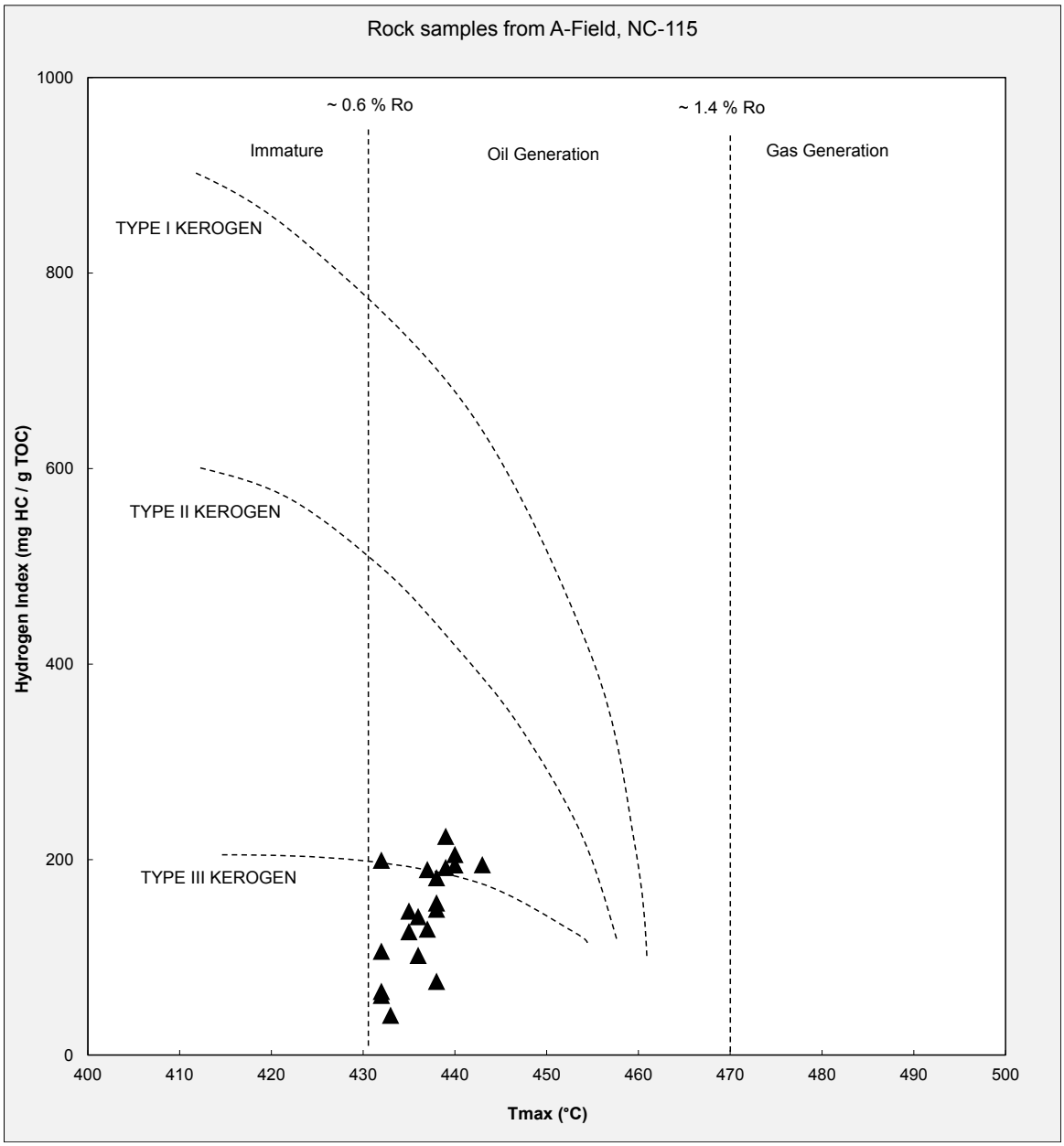

Figure 4.3. Tmax vs. HI plot showing the respective hydrocarbon proneness and the kerogen type of the source rock as well as the maturity of Tanezzuft Formation "cool" shale samples. (Modified from Espitalié et al., 1977; Tissot and Welte, 1984). Oil window definition for different kerogen types according to Espitalité (1986) is represented by dashed lines.

kerogen type of the source rock can also be determined from Figure 4.3 (Pepper and Corvi, 1995). The hydrogen index values of samples range from 65 to 224 mg of HC/g TOC (Table 4.2). Samples in the range of 50-200 are mainly indicative of gas-prone source rock and samples characterized as oil/gas-prone kerogens fall in the 200-400 HI trend (Figure 4.3; Tables 4.1 and 4.2).

4.1.1.2 *n*-Alkanes distributions and acyclic isoprenoids

The aliphatic hydrocarbon chromatograms were dominated by *n*-alkanes in C_{13}-C_{27} range (Table 4.3; Figure 4.4). Most of the GC traces have a unimodal profile of *n*-alkanes (Figure 4.4-A3, A6b, A17b, A20a, A35a) although some samples have a bimodal profile (e.g. Figure 4.4-A34), which may indicate an influence of marine organic matter along with some contribution from terrestrially-derived organic matter (Eglinton and Hamilton, 1969; Philp, 1985; Wakeham, 1990; Huang et al., 1999). The *n*-alkanes typically maximize at *n*-C_{16} or *n*-C_{17} (Table 4.3; Figure 4.4). However, a crossplot of $Pr/_nC_{17}$ vs. $Ph/_nC_{18}$ (Figure 4.5) was used in order to infer the organic matter source (Lijmbach, 1975; Shanmugam, 1985). Most of the samples appear in the region of mixed marine/terrigenous sources with slightly higher contributions of marine organic matter. This conclusion is consistent with the interpretation of Rock-Eval data (Figure 4.3), n-alkane distributions (Figure 4.4), the presence of C_{30} steranes, and the predominance of C_{27} and C_{29} steranes in most of the samples (Figures 4.6 and 4.7). Moreover, this interpretation is also in agreement with the crossplot of stable carbon isotopic

Table 4.3. Gas chromatogram data of n-alkanes and acyclic isoprenoids from Tanezzuft Formation "cool" shale, NC-115, A-Field, Murzuq Basin.

Sample ID	Lithology	Range	n-alkane Maximum	Pr/Ph	Pr/nC_{17}	Ph/nC_{18}	nC_{17}/nC_{25}	Pr+nC_{17}/Ph+nC_{18}	CPI
A3	Shale	nC_{13}-nC_{27}	nC_{16}	1.56	0.53	0.50	28.45	1.49	1.25
A5	Shale	nC_{13}-nC_{27}	nC_{14}	1.71	0.48	0.39	43.10	1.47	1.39
A6a	Shale	nC_{16}-nC_{27}	nC_{19}	0.83	0.57	0.42	2.51	0.67	1.86
A6b	Shale	nC_{15}-nC_{26}	nC_{19}	0.96	0.58	0.44	8.69	0.80	1.61
A10	Shale	nC_{14}-nC_{24}	nC_{17}	1.69	0.59	0.46	–	1.43	–
A17a	Shale	nC_{13}-nC_{26}	nC_{16}	2.27	0.63	0.46	58.72	1.86	1.42
A17b	Shale	nC_{13}-nC_{24}	nC_{16}	1.98	0.52	0.44	93.74	1.77	–
A18	Shale	nC_{13}-nC_{26}	nC_{16}	2.21	0.67	0.48	72.44	1.77	1.15
A19a	Shale	nC_{13}-nC_{27}	nC_{16}	1.93	0.56	0.45	52.91	1.68	1.56
A19b	Shale	nC_{13}-nC_{27}	nC_{16}	1.58	0.44	0.38	34.26	1.41	1.48
A20a	Shale	nC_{13}-nC_{27}	nC_{16}	2.32	0.70	0.49	29.91	1.85	1.15
A20b	Shale	nC_{13}-nC_{27}	nC_{17}	1.85	0.61	0.48	41.17	1.59	1.24
A21	Shale	nC_{13}-nC_{27}	nC_{16}	2.10	0.44	0.34	67.43	1.73	1.19
A22	Shale	nC_{12}-nC_{27}	nC_{16}	2.15	0.47	0.31	16.43	1.58	1.13
A23	Shale	nC_{12}-nC_{27}	nC_{17}	1.79	0.51	0.41	29.05	1.55	1.19
A34	Shale	nC_{13}-nC_{31}	nC_{16}	1.23	0.48	0.53	6.01	1.32	1.25
A35a	Shale	nC_{13}-nC_{30}	nC_{17}	1.84	0.55	0.43	19.21	1.55	1.17
A35b	Shale	nC_{12}-nC_{32}	nC_{17}	1.94	0.46	0.34	5.94	1.55	1.12
A37a	Shale	nC_{13}-nC_{25}	nC_{15}	2.23	0.61	0.43	39.70	1.76	–
A37b	Shale	nC_{12}-nC_{31}	nC_{15}	1.14	0.83	0.97	6.55	1.24	1.28

Pr: pristane; Ph: phytane; CPI: Carbon Preference Index was calculated based on Bray and Evans, (1961) Formula:

$$\textbf{CPI} = 1/2 \left[\frac{C_{25}+C_{27}+C_{29}+C_{31}+C_{33}}{C_{26}+C_{28}+C_{30}+C_{32}+C_{34}} + \frac{C_{25}+C_{27}+C_{29}+C_{31}+C_{33}}{C_{24}+C_{26}+C_{28}+C_{30}+C_{32}} \right]$$

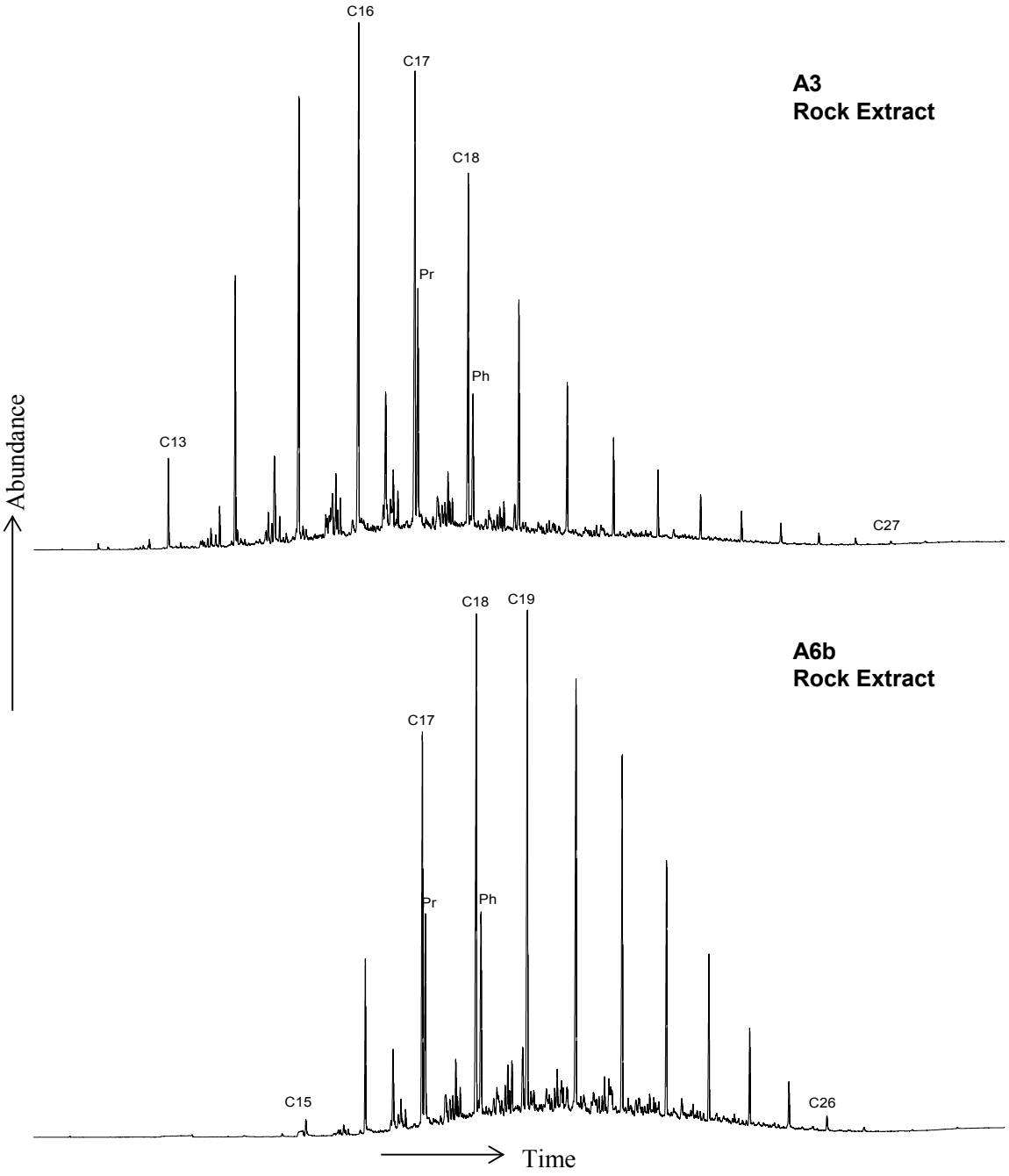

Figure 4.4. Gas chromatograms of aliphatic fractions showing the n-alkanes and acyclic isoprenoids for selected rock samples from 'cool' shale Tanezzuft Formation, Murzuq Basin, NC-115, A-Field. For more gas chromatograms of rock samples see Appendix II.

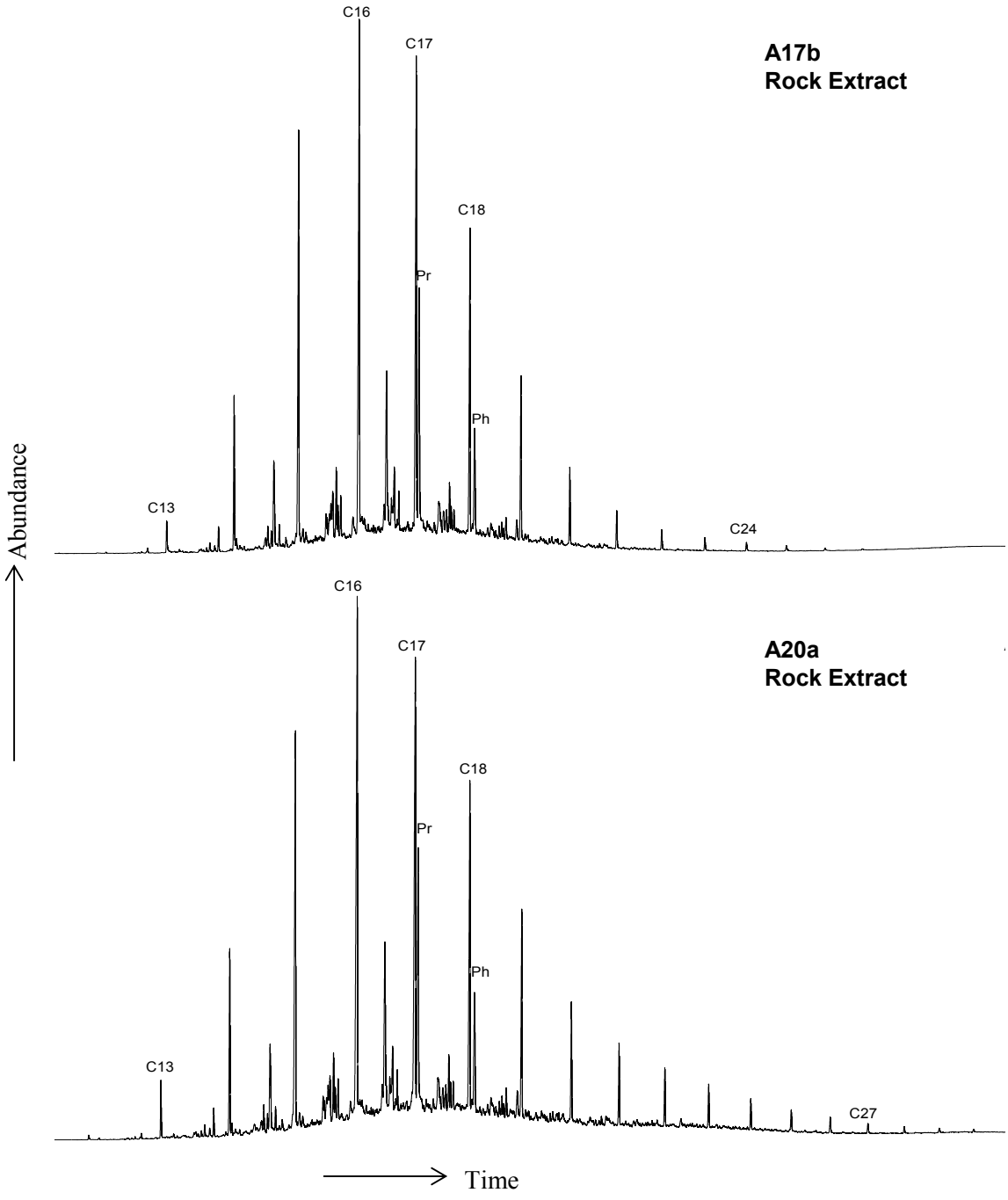

Figure 4.4. (cont.)

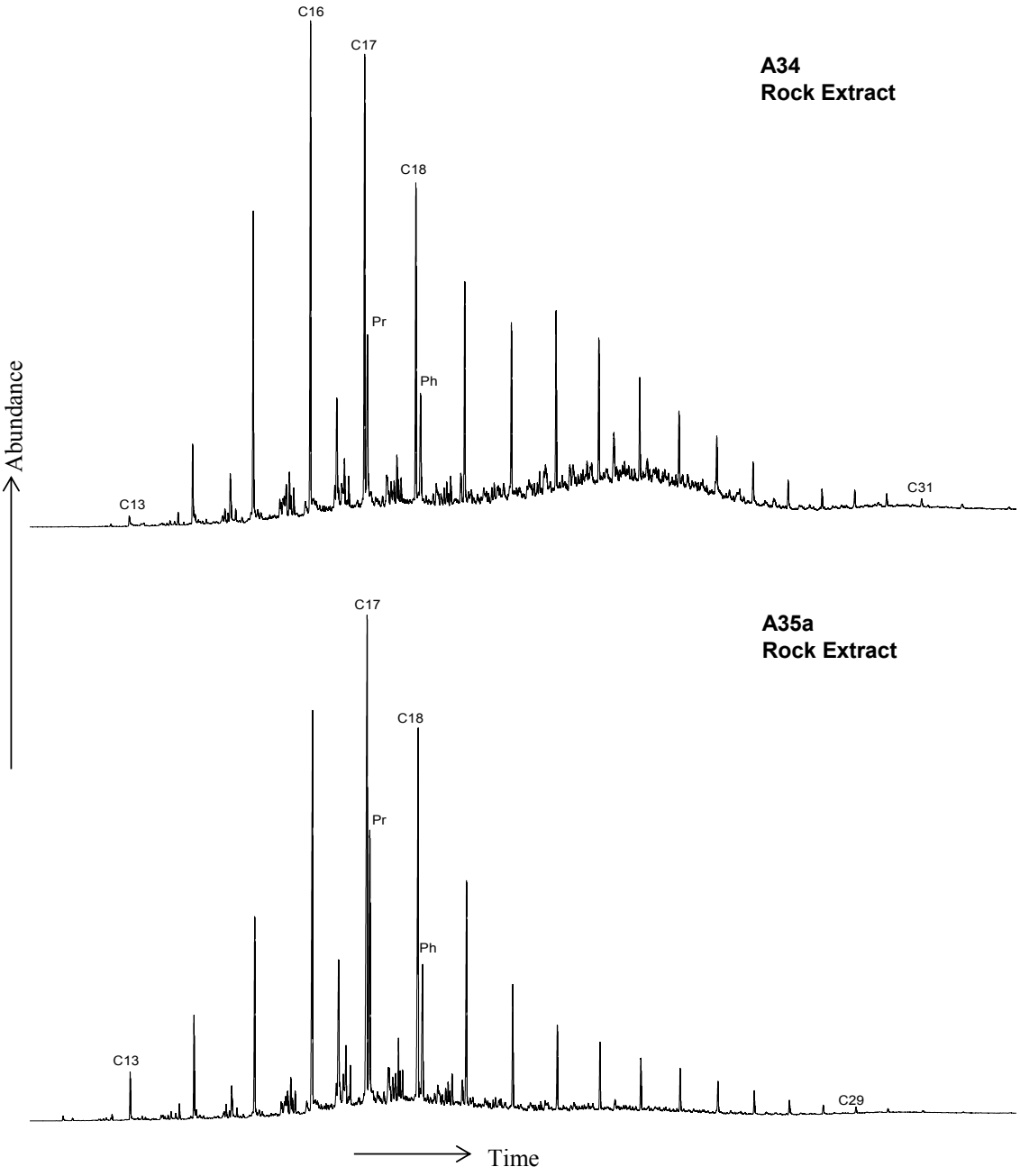

Figure 4.4. (cont.)

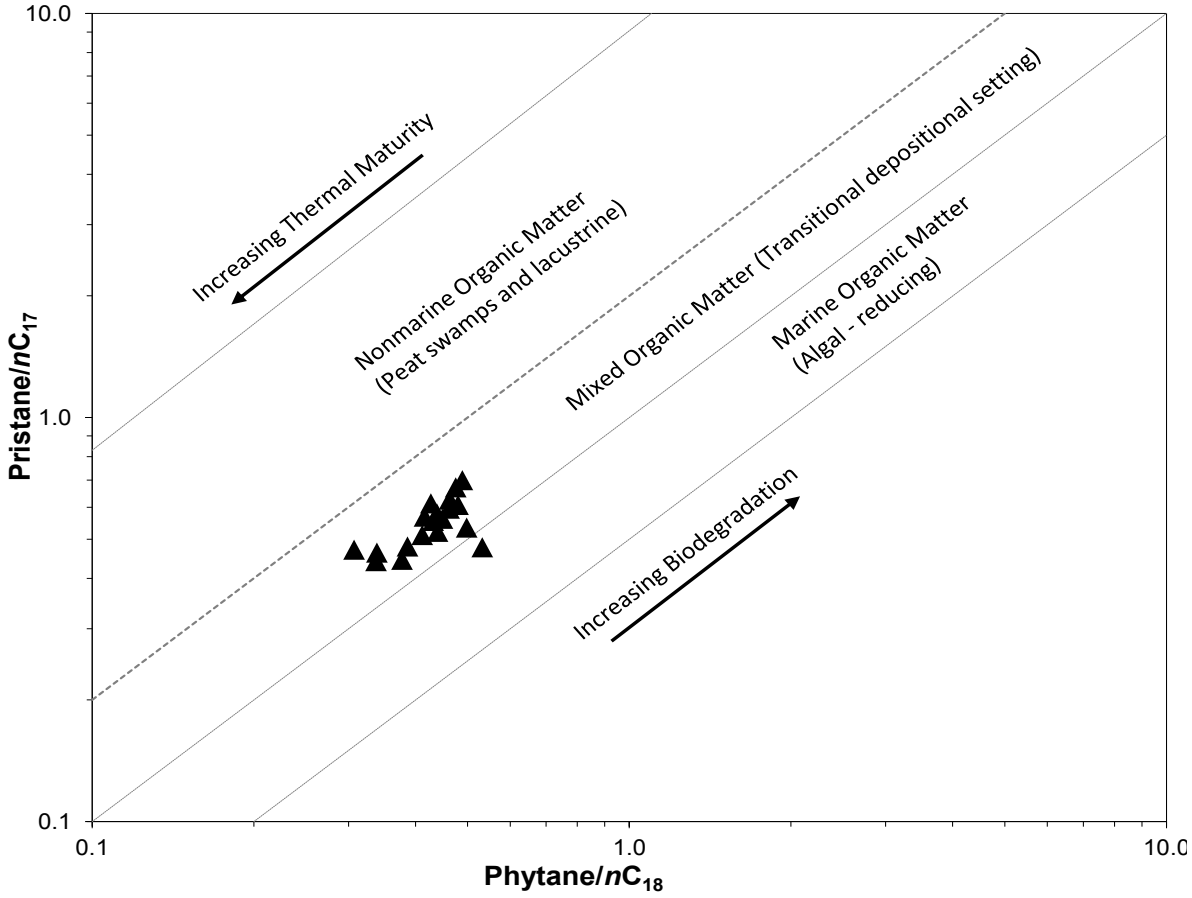

Figure 4.5. Isoprenoids plot of pristane/nC_{17} vs. phytane/nC_{18} showing redox conditions and depositional environments (Shanmugam, 1985) for samples of shales from the Tanezzuft Formation "cool" shale, NC-115, Murzuq Basin.

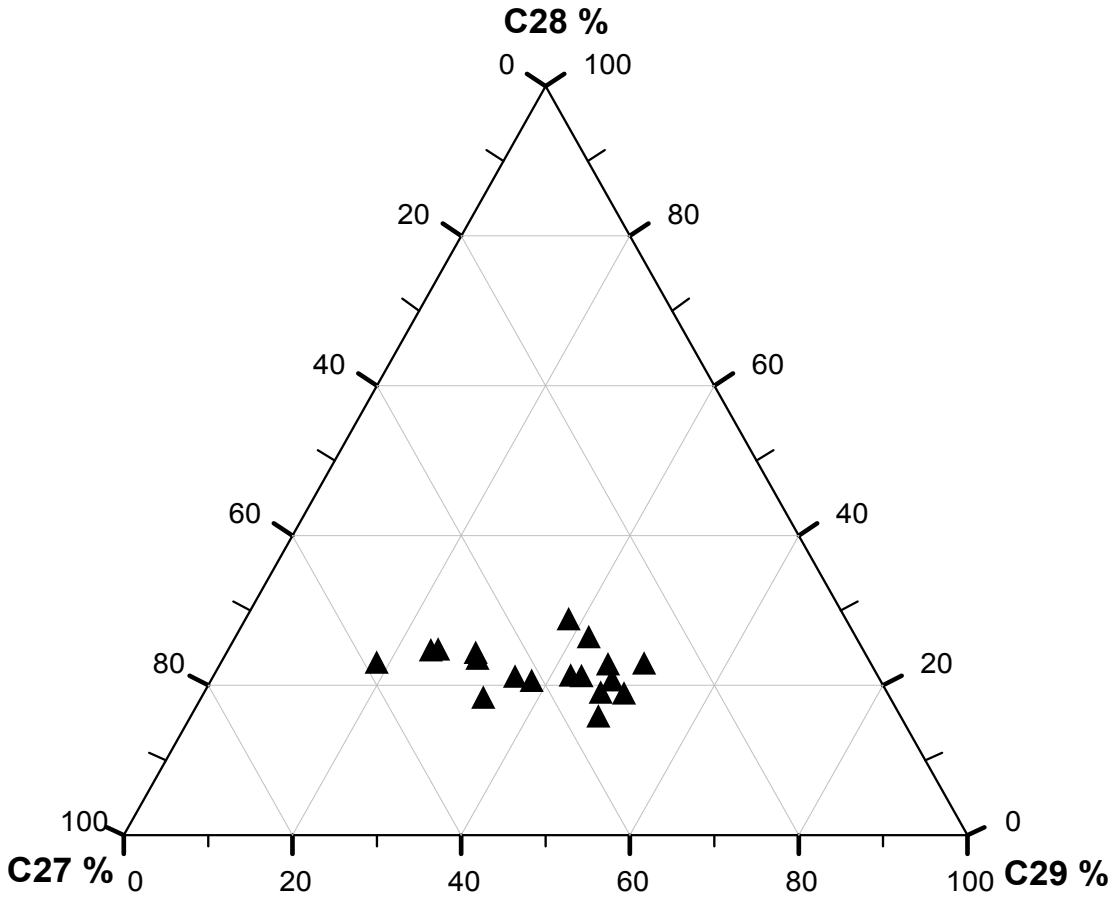

Figure 4.6. Ternary diagram indicating relative distributions of C27, C28, and C29 regular steranes of rock samples from the Tanezzuft Formation "cool" shale, NC-115, Murzuq Basin.

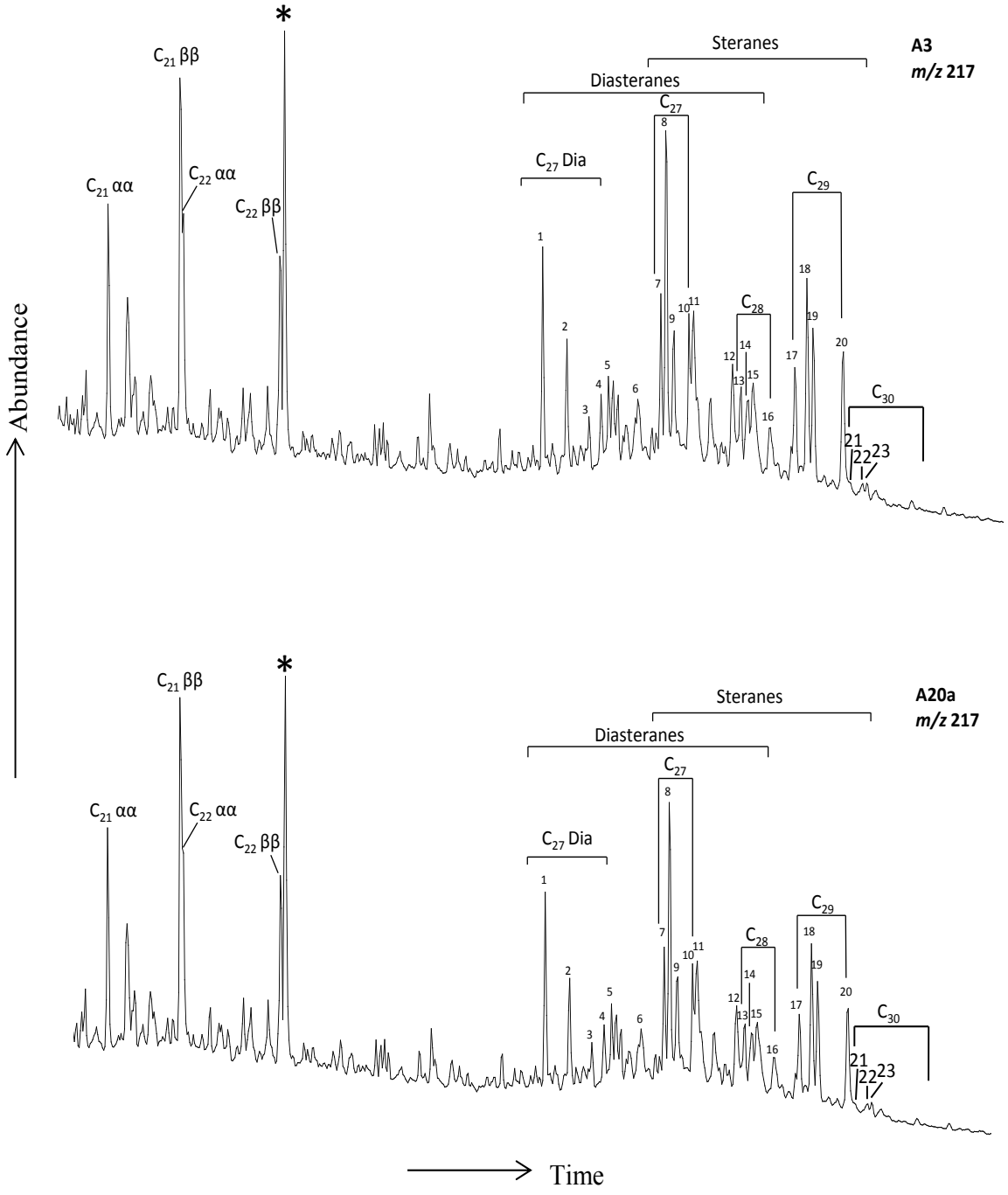

Figure 4.7. Mass chromatograms showing the distribution of steranes (*m/z* 217) of selected samples from the Tanezzuft Formation "cool" shale, A-Field, NC-115 in the Murzuq Basin, S.W. Libya. (*) Deuterated Internal Standard ($C_{24}D_{50}$). See Table 4.6 for peak identifications. For more mass chromatograms of rock samples see Appendix III.

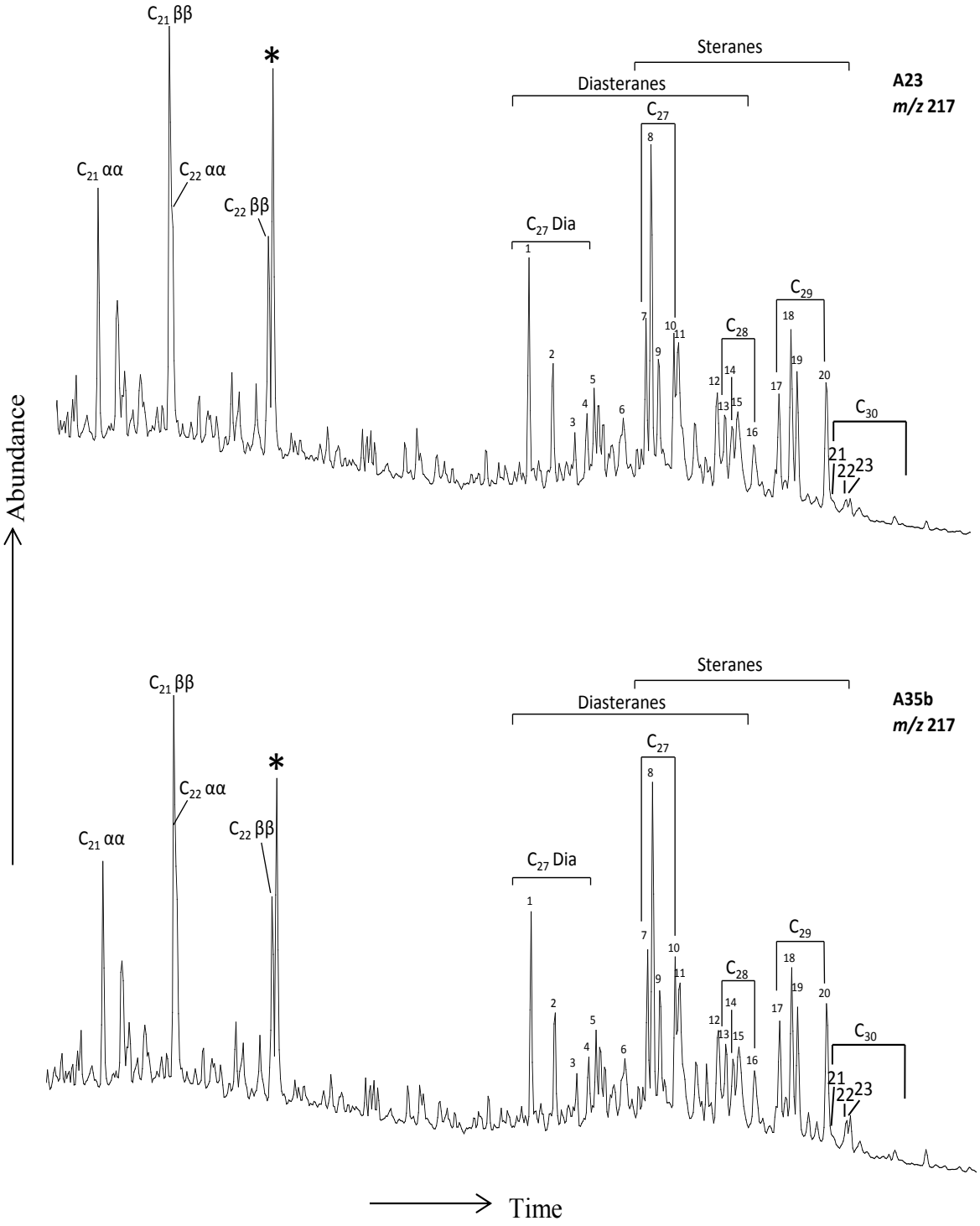

Figure 4.7. (cont.)

composition for saturate and aromatic hydrocarbons of selected extracts shown in Figure 4.8, where the rock samples plotted suggest mixed marine to terrigenous organic matter.

Pristane (Pr) and phytane (Ph) are the dominant isoprenoids present in all of the samples. Most of the samples have Pr/Ph ratios less than 3 (> 3), ranging between 1.23 and 2.32, except for samples A6a-b, which show values of 0.83 and 0.96, respectively (Table 4.3). This may be due to variations in depositional conditions of source material, since pristane/phytane (Pr/Ph) ratios have been used to assess the redox potential of the depositional environment (Didyk et al., 1978). However, it can be concluded that samples in this study, which have Pr/Ph ratios between 1.14 and 2.32, were deposited in sub-oxic conditions. Nevertheless, Peters and Moldowan (1993) proposed that for samples showing Pr/Ph ratios in the range between 0.8 and 2.5, Pr/Ph ratios should not be used as an indicator of palaeoenvironment without corroborating data since these ratios are also known to be affected by maturation (Tissot and Welte, 1984) and differences in possible precursors (Volkman and Maxwell, 1986; ten Haven et al., 1987).

4.1.1.3 Sterane distributions (*m/z* 217)

Sterane identifications in this study were based on previously published data (e.g. Philp, 1985). The identities of the steranes present in the *m/z* 217 chromatograms in Figure 4.7 are listed in Table 4.4. The distribution of C_{27}, C_{28} and C_{29} regular steranes for Tanezzuft Formation "cool" shale samples are scattered over a wide area between C_{27} and C_{29} of the ternary diagram (Figure 4.6), the most abundant are the C_{27} and C_{29} steranes ranging from 27–58% and 18–50%, respectively (Table 4.5). The predominance of C_{27}

Table 4.4. Sterane (*m/z* 217) identification in chromatograms of Figures 4.7 and 4.15, based on Philp (1985).

Peak I.D.	Steranes
21αα	Diapregnane
21ββ	5α(H),14β(H),17β(H)- pregnane
22αα	Diahomopregnane
22ββ	5α(H),14β(H),17β(H)-homopregnane
1	13β(H),17α(H),20(S)-cholestane (diasterane)
2	13β(H),17α(H),20(R)-cholestane (diasterane)
3	13α(H),17β(H),20(S)-cholestane (diasterane)
4	13α(H),17β(H),20(R)-cholestane (diasterane)
5	24-methyl-13β(H),17α(H),20(S)-cholestane (diasterane)
6	24-methyl-13β(H),17α(H),20(R)-cholestane (diasterane)
7	5α(H),14α(H),17α(H),20(S)-cholestane + 24-methyl-13α(H),17β(H),20(S)-cholestane (diasterane)
8	5α(H),14β(H),17β(H),20(R)-cholestane + 24-ethyl-13β(H),17α(H),20(S)-cholestane (diasterane)
9	5α(H),14β(H),17β(H),20(S)-cholestane + 24-methyl-13α(H),17β(H),20(R)-cholestane (diasterane)
10	5α(H),14α(H),17α(H),20(R)-cholestane
11	24-ethyl-13β(H),17α(H),20(R)-cholestane (diasterane)
12	24-ethyl-13α(H),17β(H),20(S)-cholestane (diasterane)
13	24-methyl-5α(H),14α(H),17α(H),20(S)-cholestane
14	24-methyl-5α(H),14β(H),17β(H),20(R)-cholestane + 24-ethyl-13α(H),17β(H),20(R)-cholestane (diasterane)
15	24-methyl-5α(H),14β(H),17β(H),20(S)-cholestane
16	24-methyl-5α(H),14α(H),17α(H),20(R)-cholestane
17	24-ethyl-5α(H),14α(H),17α(H),20(S)-cholestane
18	24-ethyl-5α(H),14β(H),17β(H),20(R)-cholestane
19	24-ethyl-5α(H),14β(H),17β(H),20(S)-cholestane
20	24-ethyl-5α(H),14α(H),17α(H),20(R)-cholestane
21	24-propyl-5α(H),14α(H),17α(H),20(S)-cholestane
22	24-propyl-5α(H),14β(H),17β(H),20(R)-cholestane
23	24-propyl-5α(H),14β(H),17β(H),20(S)-cholestane
24	24-propyl-5α(H),14α(H),17α(H),20(R)-cholestane

Table 4.5. Sterane parameters (*m/z* 217 chromatograms) of Tanezzuft Formation "cool" shale samples from A-Field, NC-115, Murzuq Basin.

Sample	Steranes [a]				Diasteranes/steranes[b]	C_{29}[c]	C_{29}[d]	C_{27}/C_{29}[e]	Preg/(preg+ster+dias)[f]
	C_{27} %	C_{28} %	C_{29} %	C_{30}%		ββ/(ββ+αα)	20S/(20S+20R)		
A3	34	21	42	4	0.6	0.43	0.41	0.8	0.6
A5	33	19	46	2	1	0.47	0.39	0.72	0.64
A6a	50	25	25	–	3.3	0.55	0.49	2.02	0.35
A6b	44	23	28	5	2.2	0.57	0.47	1.56	0.85
A10	45	23	30	2	1.3	0.49	0.44	1.53	0.82
A17a	27	23	50	–	1.5	0.55	0.43	0.53	0.63
A17b	30	18	48	3	1.6	0.45	0.42	0.62	0.73
A18	40	20	37	2	1.1	0.45	0.4	1.08	0.76
A19a	40	22	34	4	0.9	0.55	0.44	1.17	0.79
A19b	31	20	46	4	1.5	0.51	0.33	0.66	0.73
A20a	35	21	41	4	1.5	0.52	0.41	0.85	0.67
A20b	41	21	35	2	0.8	0.51	0.4	1.17	0.72
A21	30	22	45	3	2	0.51	0.37	0.67	0.67
A22	35	16	48	1	1.8	0.54	0.4	0.74	0.47
A23	31	26	41	2	0.8	0.44	0.45	0.75	0.58
A34	50	24	24	2	0.6	0.52	0.49	2.13	0.72
A35a	47	18	33	2	0.8	0.53	0.37	1.44	0.64
A35b	32	28	37	2	0.5	0.44	0.44	0.85	0.51
A37a	58	23	18	–	0.6	0.54	0.52	3.17	0.73
A37b	43	21	36	–	1.4	0.54	0.41	1.2	0.72

[a] 5α(H),14α(H),17α(H)-20R-Steranes, [b] 13β(H),17α(H),20(R)-cholestane (C_{27}-diasterane)/5α(H),14α(H),17α(H),20(R)-cholestane (C_{27}-Regular sterane), [C] 5α(H),14β(H),17β(H)/[5α(H),14β(H),17β(H) + 5α(H),14α(H),17α(H)] for C29-Steranes, [d] calculated for C_{29}-5α (H),14α(H),17α(H)-Steranes, [e] 5α (H),14α(H),17α(H)-20R-Steranes, [f] [5α (H),14β (H),17β(H) –Pregnane + 5α(H),14β(H),17β(H) – Homopregnane]/ [5α(H),14β(H),17β(H),20(R)-cholestane + pregnane + homopregnane +13β(H),17α(H),20(S)-diacholestane].

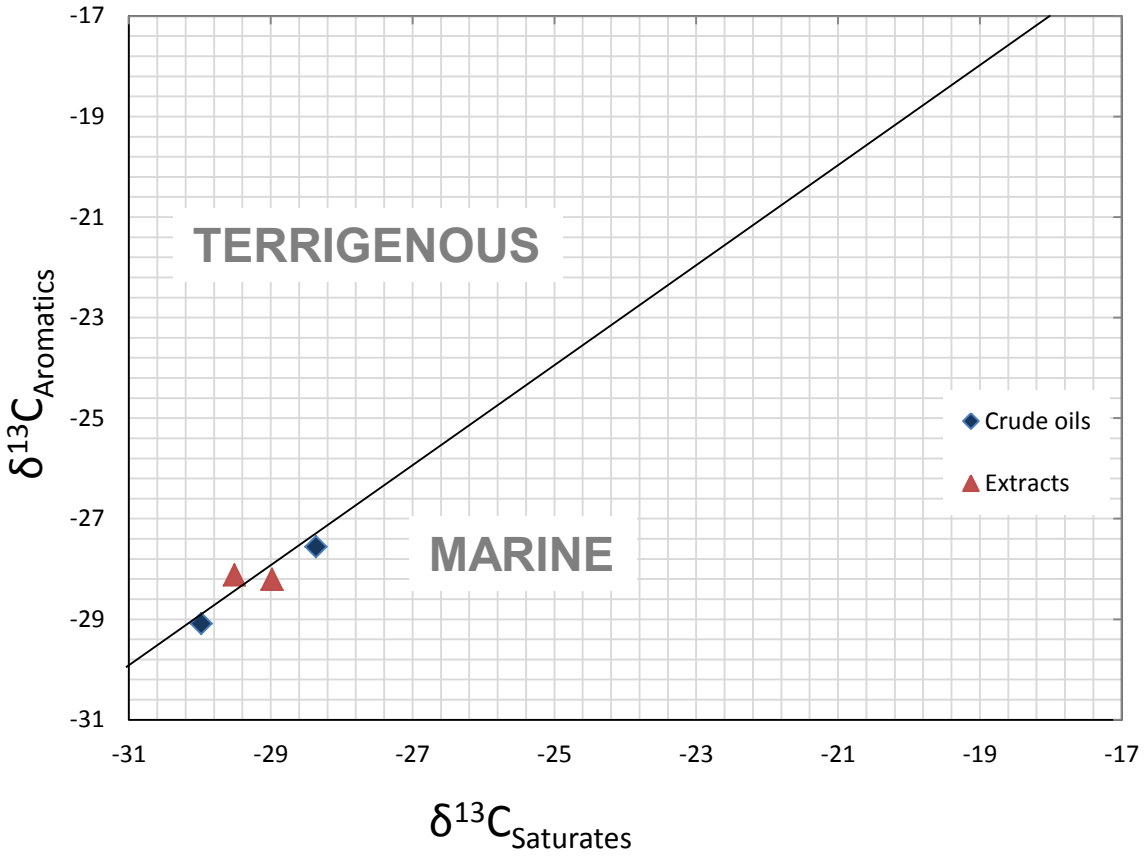

Figure 4.8. Stable carbon isotopic composition (‰ relative to the VPDB scale) for saturate and aromatic hydrocarbons of selected crude oils and extracts. The samples plotted suggest mixed marine to terrigenous organic matter. Modified from Sofer (1984).

and C_{29} steranes in most of the samples is interpreted to indicate a marine phytoplankton and terrestrial input, respectively (Brassell and Eglinton, 1983; Philp, 1985). The presence of C_{30} steranes in low concentrations ranging from 1–5% (Table 4.5) in most of samples may indicate a slight influence of marine input (Moldowan, 1984; Moldowan et al., 1990; Summons et al., 1992; Peters and Moldowan, 1993). This conclusion is consistent with the interpretation of Rock-Eval data, n-alkane distributions (Figure 4.4), and the high abundance of tricyclic terpanes in most of the samples along with the crossplot of Pr/nC_{17} and Ph/nC_{18} ratios shown in Figure 4.5 and the stable carbon isotopic composition for saturate and aromatic hydrocarbons of selected extracts (Figure 4.8).

Table 4.5 illustrates a wide range of diasterane/sterane ratios from 0.5 to 2.2. High values of this ratio could be interpreted as a result of samples having been deposited under highly oxic conditions and/or due to clay catalysis (Mello et al., 1988b; Moldowan et al., 1992), and/or high maturity (Hughes et al., 1985; Goodarzi et al., 1989a; Peters et al., 1990). The latter could be excluded in this study since the majority of samples are at the early mature stage with some intermediate maturity samples (for more detail see section 4.1.2.). Several parameters such as the Pr/Ph ratios (0.83–2.32), the presence of C_{30}-diahopane, low ratios of C_{35} to C_{34} homohopanes as well as Rock-Eval data (e.g. low quality organic matter, S2 vs. TOC and HI vs OI crossplots) support this interpretation.

As mentioned above in section 2.4.7, the presence of pregnane and homopregnane is related to hypersaline sedimentation conditions (ten Haven et al., 1988) or can result from thermal cracking of C_{27}-C_{29} steranes (Mueller et al., 1995). In the present study, the latter was ruled out because the samples are at early to intermediate levels of thermal maturity. Thus, the presence of pregnane and homopregnane in most of the samples (Figure 4.7),

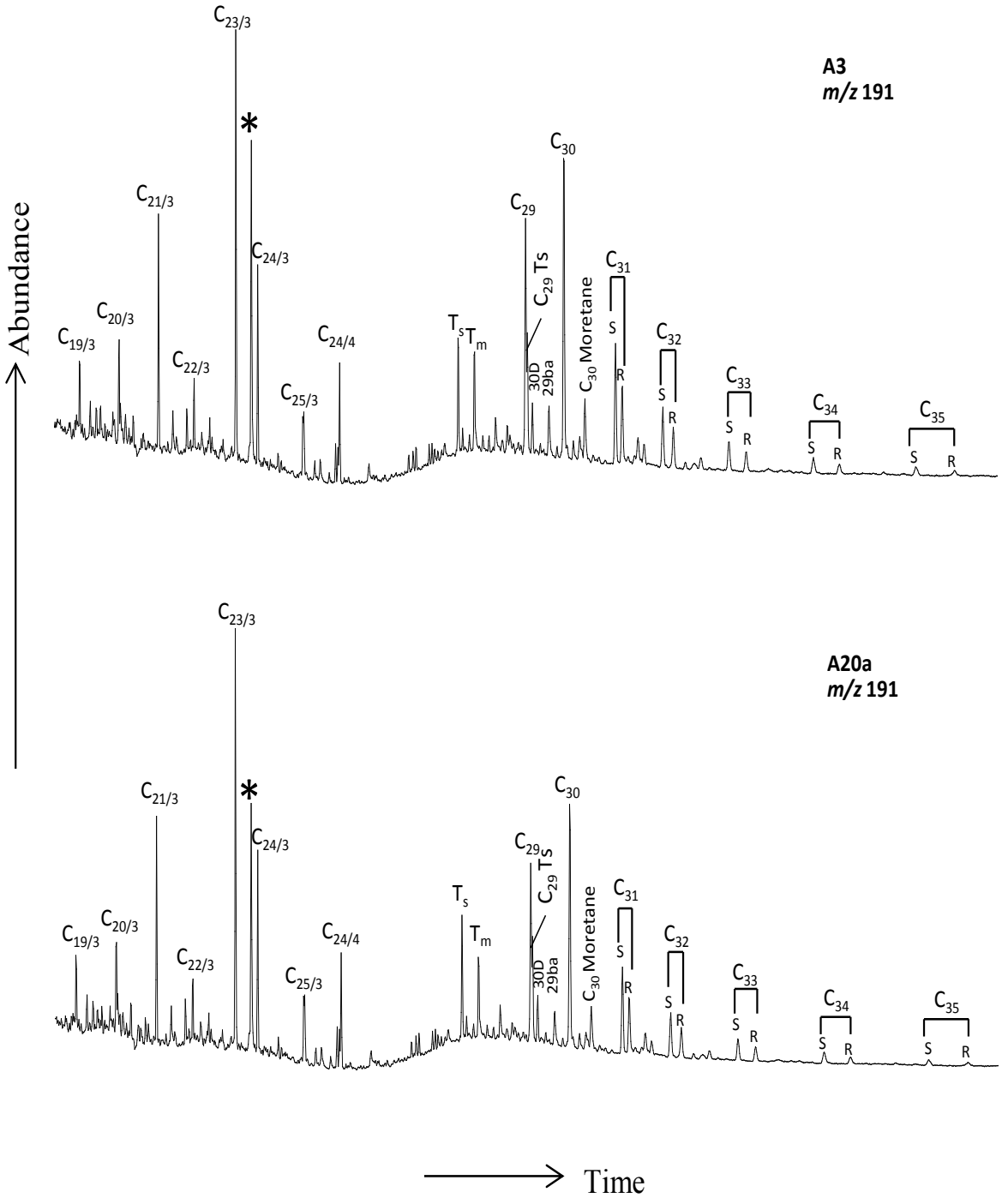

Figure 4.9. Mass chromatograms showing the distribution of hopanes (m/z 191) of selected rock samples from the Tanezzuft Formation "cool" shale, A-Field, NC115 in the Murzuq Basin, S.W. Libya. (*) Deuterated Internal Standard (C24D50). See Table 4.6 for peak identifications. For more mass chromatograms of rock samples see Appendix IV.

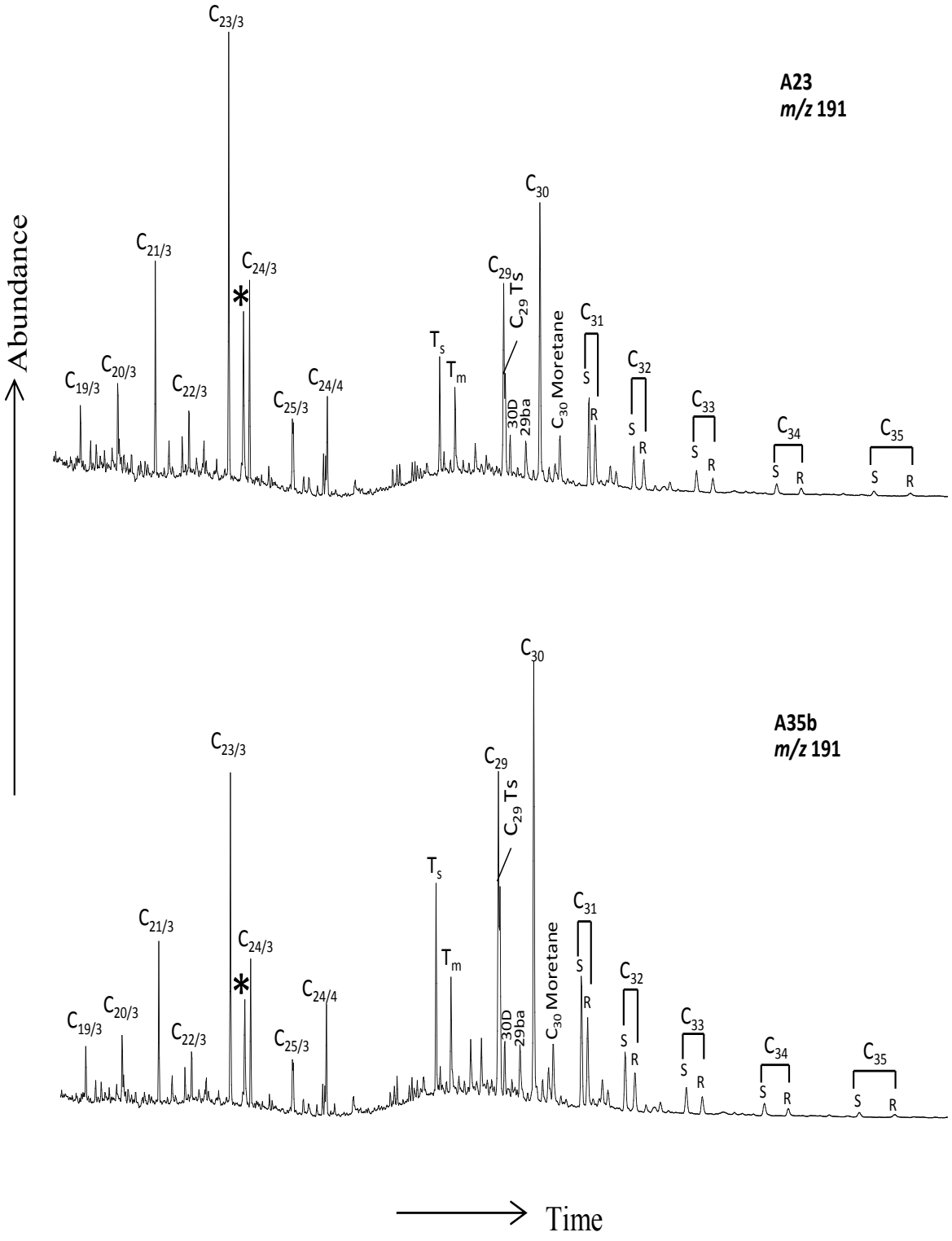

Figure 4.9. (cont.)

may be related to hypersaline conditions although gammacerane could not be detected in any samples (Figure 4.9).

4.1.1.4 Terpane biomarker distributions (*m/z* 191)

The identity of the terpanes present in the *m/z* 191 chromatograms in Figure 4.9 are listed in Table 4.6. In the present study, most of the samples are characterized by high values of the tricyclic terpane/17α-hopane ratios ranging from 1.29 to 7.45. Samples A3, A5, A17a, A19b, A22, A23, and A35b show low values of 0.66, 0.64, 0.84, 0.83, 0.97, 0.75, and 0.22, respectively (Table 4.7; Figure 4.9). The high abundance of extended tricyclic terpanes relative to hopanes in oils and source rocks can be related to maturity effects, but also to marine influenced depositional conditions (Seifert and Moldowan, 1979; Philp et al., 1992). Due to the presence of C_{30} steranes (marine indicator) in many samples, it can be concluded that samples with a high abundance of tricyclic terpanes may be related to marine influenced depositional conditions (Peters et al., 2005) rather than a maturity effect (Waples and Machihara, 1990) since these samples are at early to intermediate maturity levels (e.g. Section 4.1.2). This conclusion is further supported by the distribution of n-alkanes and the presence of C_{30} steranes. However, samples with low values of tricyclic terpane/17α-hopane ratios may reflect a lack of marine-influenced depositional conditions.

The C_{23} tricyclic/C_{24} tetracyclic ratios of samples range broadly from 1.58 to 16.32 (Table 4.7; Figure 4.9). The relatively low concentration of the C_{24} tetracyclic terpane in most of the samples may indicate suboxic depositional environment conditions

Table 4.6. Tricyclic, tetracyclic and pentacyclic terpanes (*m/z* 191) identified in chromatograms of Figures 4.9 and 4.18, based on Philp (1985) and Peters and Moldowan, (1993).

PEAK IDENTIFICATION	COMPOUND
C_{19}/3	C_{19} Tricyclic Terpane
C_{20}/3	C_{20} Tricyclic Terpane
C_{21}/3	C_{21} Tricyclic Terpane
C_{23}/3	C_{23} Tricyclic Terpane
C_{24}/3	C_{24} Tricyclic Terpane
C_{25}/3	C_{25} Tricyclic Terpane
C_{24}/4	C_{24} Tetracyclic Terpane
Ts	C_{27} 18a (H)-22,29,30-trisnorneohopane (Ts)
Tm	C_{27} 17a (H)-22,29,30-trisnorhopane (Tm)
$C_{29}\alpha\beta$	C_{29} 17a (H),21β(H)-30-norhopane
C_{29} Ts	C_{29} Ts 18α(H)-30-norneohopane
30D	15α-methyl-17α(H)-27-norhopane (diahopane)
29βα	17β (H), 21α (H)-30-norhopane (normoretane)
$C_{30}\alpha\beta$	C_{30} 17a (H),21β(H)-hopane
C_{30}M	C_{30} 17β (H),21α (H)-moretane
$C_{31}\alpha\beta$S	C_{31} 17a (H),21β(H)-30-homohopane (22S & 22R)
$C_{32}\alpha\beta$S	C_{32} 17a (H),21 β (H)-30-bishomohopane (22S & 22R)
$C_{33}\alpha\beta$S	C_{33} 17a (H),21 β (H)-30-trishomohopane (22S & 22R)
$C_{34}\alpha\beta$S	C_{34} 17a (H),21 β (H)-30-tetrakishomohopane (22S & 22R)
$C_{35}\alpha\beta$S	C_{35} 17a (H),21 β (H)-30-pentakishomohopane (22S & 22R)

Table 4.7. Hopane indices of Tanezzuft Formation "cool" shale samples measured on the *m/z* 191, Tanezzuft Formation, NC-115, A-Field, Murzuq Basin.

Samples	Ts/(Ts+Tm)[a]	C_{29}Ts/(C_{29}Ts+C_{29})[b]	C_{19}/C_{23}[c]	22S/(22S+22R)[d]	HHI[e]	C_{29}/C_{30}[f]	C_{23}/C_{24}[g]	$C_{30}\beta\alpha/C_{30}\alpha\beta$[h]	C_{24}/C_{30}[i]	C_{23}/C_{30}[j]	C_{23}/C_{29}[k]	Tris/17α-hop[l]	C_{30}d/C_{29}Ts[m]
A3	0.45	0.29	0.2	0.56	0.65	0.66	3.67	0.23	0.2	0.76	1.14	0.66	0.58
A5	0.6	0.36	0.36	0.57	0.58	0.66	2.55	0.35	0.27	0.7	1.05	0.64	0.53
A6a	–	–	0.06	–	–	–	34.6	–	–	–	–	–	–
A6b	0.51	0.2	0.2	0.53	–	0.72	16.32	0.13	0.46	7.59	10.48	7.45	0.67
A10	0.52	0.2	0.27	0.51	–	1.14	4.62	0.29	1.42	6.57	5.72	5.27	0.93
A17a	0.65	0.35	0.55	0.55	0.6	0.59	2.81	0.18	0.22	0.64	1.09	0.84	0.68
A17b	0.65	0.32	0.44	0.54	–	0.73	2.48	0.21	0.41	1.02	1.39	1.29	0.22
A18	0.53	0.3	0.41	0.6	–	0.72	3.33	0.22	0.39	1.32	1.83	1.54	0.54
A19a	0.54	0.27	0.24	0.63	–	0.78	4.05	0.16	0.52	2.13	2.7	2.11	0.53
A19b	0.57	0.45	0.32	0.58	0.39	0.61	2.64	0.16	0.26	0.7	1.14	0.83	0.39
A20a	0.53	0.45	0.19	0.57	0.42	0.54	3.51	0.13	0.4	1.41	2.61	1.32	0.54
A20b	0.44	0.18	0.14	0.57	0.57	0.95	3.99	0.17	0.47	1.88	1.98	1.36	0.83
A21	0.56	0.23	0.28	0.6	–	0.8	3.69	0.13	0.49	1.81	2.25	1.95	0.63
A22	0.6	0.46	0.29	0.59	0.51	0.55	2.93	0.23	0.34	1	1.78	0.97	0.76
A23	0.47	0.19	0.11	0.57	0.5	0.87	5.37	0.21	0.17	0.95	1.09	0.75	0.53
A34	0.42	0.16	0.04	0.58	–	0.95	5.63	0.11	0.75	4.25	4.46	3.22	0.49
A35a	0.61	0.2	0.13	0.48	0.93	0.87	5.25	0.19	0.57	3.028	3.47	2.38	1.49
A35b	0.57	0.4	0.21	0.57	0.34	0.68	1.58	0.2	0.14	0.22	0.33	0.22	0.24
A37a	0.56	0.17	0.06	0.66	–	1.28	4.96	0.21	1.77	8.8	6.83	4.94	0.99
A37b	0.7	0.4	0.1	0.61	–	0.6	5.41	0.18	0.73	3.9	6.56	3.27	1.17

[a] 18α (H)-22,29,30-trisnorneohopane/(18α (H)-22,29,30-trisnorneohopane + 17α (H)-22,29,30-trisnorhopane), [b] 18α(H)-30-norneohopane/(18α(H)-30-norneohopane + 17α(H), 21β(H)-30-norhopane), [c] $C_{19}H_{34}$ tricyclic terpane/ $C_{23}H_{42}$ tricyclic terpane, [d] 17α(H), 21β(H), 22(S)-bishomohopane/(17α(H), 21β(H), 22(S) bishomohopane+17α(H), 21β(H), 22(R)-bishomohopane): for C_{32}homohopane, [e] Homohopane Index; 17α(H), 21β(H), 22(S+R)-pentakishomohopane/(17α(H) 21β(H), 22(S+R)- tetrakishomohopane (C35/C34 homohopanes), [f] 17α(H), 21β(H)-30-norhopane / 17α(H), 21β(H)-hopane, [g] $C_{23}H_{42}$ tricyclic terpane /$C_{24}H_4$ tetracyclic terpane, [h] 17β (H), 21α (H)-hopane (moretane)/ 17α(H), 21β(H)-hopane, [i] $C_{24}H_{44}$ tetracyclic terpane/17α(H), 21β(H)-hopane, [j] $C_{23}H_{42}$ tricyclic terpane/17α(H), 21β(H)-hopane, [k] $C_{23}H_{42}$ tricyclic terpane/17α(H), 21β(H)-30-norhopane, [l] tricyclic terpanes/17α -hopanes [C_{19}+C_{20}+C_{21}+C_{22}+C_{23}+C_{24}+C_{25}]/[17α (H)-22,29,30-trisnorhopane + 17α(H), 21β(H)-30-norhopane + 17α(H), 21β(H)-hopane + 17α(H), 21β(H), 22(S+R) homohopane + 17α(H), 21β(H), 22(S+R)-bishomohopane + 17α(H), 21β(H), 22(S+R)-trishomohopane + 17α(H), 21β(H), 22(S+R)- tetrakishomohopane + 17α(H) 21β(H), 22(S+R)-pentakishomohopane], [m] 15α-methyl-17α(H)-27-norhopane/18α (H)-30-norneohopane.

(Sammy, 1985; Connan et al., 1986; Philp and Gilbert, 1986; Connan and Dessort, 1987). This conclusion is further suggested by the values of Pr/Ph and diasterane/sterane ratios as well as the presence of C_{30}-diahopanes along with low ratios of C_{35} to C_{34} homohopanes and low quality organic matter manifested by low hydrogen indicies for the majority of samples.

The C_{30}-diahopane was present in relatively low amounts in most of the samples (Figure 4.9). Only two samples (e.g. A35a and A37b) show high values of C_{30}-diahopane/C_{29}Ts ratios of 1.49 and 1.17, respectively (Table 4.7). The relative low concentration of C_{30}-diahopane in most of the samples may indicate the suboxicity of depositional environment conditions and/or probably the low maturity for these samples, since most of the samples are at low levels of thermal maturity. Samples with high concentrations of this compound may reflect more oxic depositional conditions with more terrigenous source materials (Volkman et al., 1983a; Philp and Gilbert, 1986; Peters et al., 2005).

As mentioned in Chapter II, Section 2.4.4.4, the C_{29}/C_{30} hopane ratio is commonly used to distinguish the carbonate from clastic lithology (Palacas et al., 1984; Peters and Moldowan, 1993). The majority of the samples in the present study show lower values of C_{29} hopane/C_{30} hopane ranging from (0.55-0.95), except for samples A10 and A37a that have values of 1.14 and 1.28, respectively (Table 4.7). C_{29}/C_{30} ratios lower than 1.0 suggests a stronger clastic shaly nature of the source, while the higher values (A10 and A37a) are characteristic of samples contain a greater carbonate component (Zumberge, 1984; Connan et al., 1986; Price et al., 1987; Clark and Philp, 1989).

The low values of the C_{35} to C_{34} homohopane ratio (HI; 0.34–0.93) in samples (Table 4.7) suggest prevailing oxic to sub-oxic (high Eh) conditions during deposition (Peters

and Moldowan, 1991; Peters and Moldowan, 1993) and low hydrogen index values as well as low quality organic matter (Tables 4.1 and 4.2; Figures 4.1 and 4.2) (Dahl et al., 1994).

4.1.2 Evaluation of Thermal Maturity

4.1.2.1 Maximum pyrolysis temperature (Tmax) and hydrogen index (HI)

Tmax is the temperature at which the S2 peak maximizes during Rock-Eval pyrolysis (Espitalié et al., 1984; Peters, 1986; Tissot et al., 1987) and is widely used as a maturity indicator (Table 4.1). In the present study, the majority of samples have Tmax values in the range of 435 to 445°C (Table 4.2) indicating that the organic matter has reached the early to intermediate stages of thermal maturity (Figure 4.10). This is further supported by the HI vs. Tmax crossplot shown in Figure 4.3, where most of the samples fall in the beginning of oil generation zone. A number of samples show intermediate levels of thermal maturity.

4.1.2.2 Biomarker Maturity Parameters

4.1.2.2.1 Terpanes

As mentioned in Section 2.5.2.1, samples with 22S/(22S+22R) homohopane isomerization values in the range of (0.5–0.54) have barely entered the oil generation

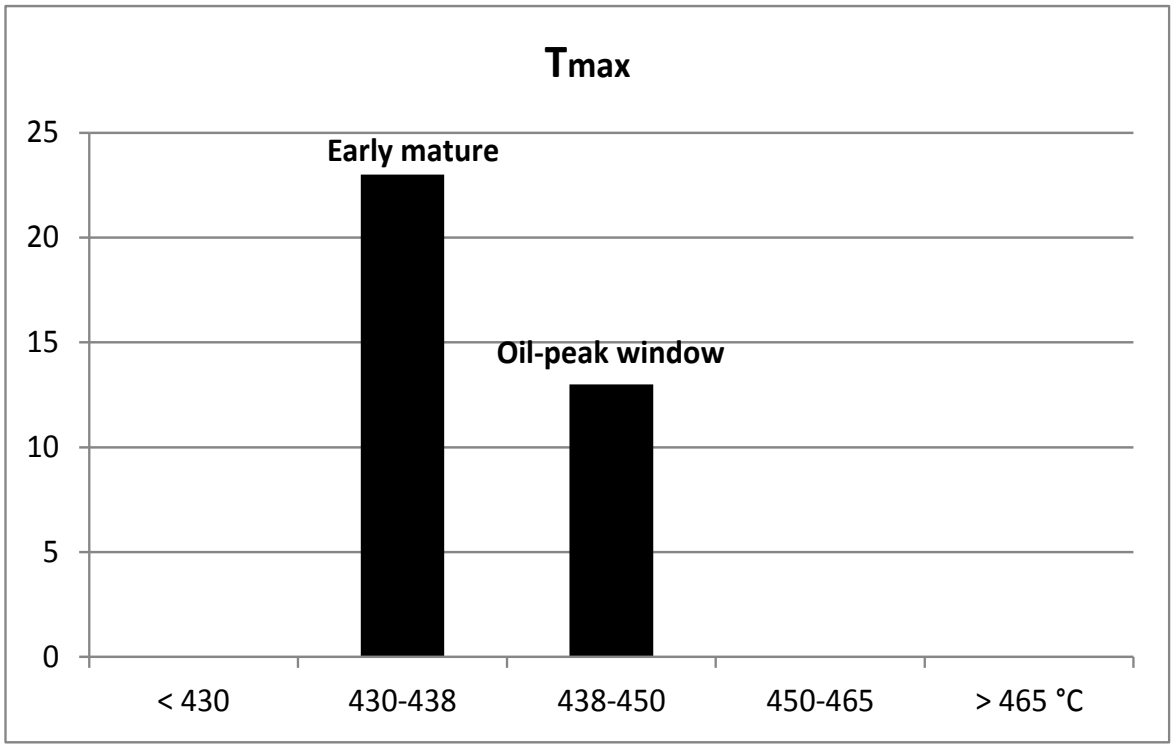

Figure 4.10. Tmax distribution of Tanezzuft Formation “cool” shale samples in Block NC-115, A Field, Murzuq Basin, S.W. Libya.

window, while those in the range of (0.57–0.62) indicate that the main phase of oil generation has been reached (Peters and Moldowan, 1993). In the present study, most of the samples show values of 22S/(22S+22R) ranging from 0.48–0.66 for the C_{32} homohopane (Table 4.7, Figure 4.9), suggesting early to intermediate levels of thermal maturity as supported by HI vs. Tmax crossplot (Figure 4.3) and Tmax distribution (Figure 4.10). This interpretation is further supported by the low values of the C_{30}-moretane/C_{30}-hopane ($C_{30}\beta\alpha/C_{30}\alpha\beta$) ratios (0.11–0.35) for all samples (Table 4.7, Figure 4.9). The ratio of $C_{30}\beta\alpha/C_{30}\alpha\beta$ typically decreases with increasing thermal maturity from 0.8 in immature source rocks to values of less than 0.15 in mature stages (Rullkötter and Marzi, 1988; Peters and Moldowan, 1993; see Section 2.5.2.3 in Chapter II).

The Ts/(Ts+Tm) ratios in all samples show a wide range of low values (Table 4.7) ranging from 0.42 to 0.7, and do not show any consistency with other maturity parameters [e.g. Rock-Eval data, 22S/(22S+22R) homohopane isomerization, ββ/(ββ+αα) and 20S/(20S+20R) sterane isomerization ratios, as well as C_{30}-moretane/C_{30}-hopane ratios] and therefore may reflect the nature of the depositional environment (Moldowan et al., 1986; Philp et al., 1992; Peters et al., 2005).

4.1.2.2.2 Steranes

The ratios of ββ/(ββ+αα) and 20S/(20S+20R) range from 0.43–0.57 and 0.33–0.52, respectively (Table 4.5). These relatively low values may indicate that the majority of the samples have not reached the main oil generation window (Mackenzie et al., 1980; Peters and Moldowan, 1993; Ramón and Dzou, 1999), which is further supported by the Rock-

Eval data (e.g. Tmax values and hydrogen index vs. Tmax crossplot) together with biomarkers (e.g. 22S/(22S+22R), C_{30}-moretane/C_{30}-hopane).

4.1.2.3 Organic petrography

As mentioned above in Section 2.5.1, for immature rocks (%R_o =0.2-0.5, CAI: 1.5), graptolite reflectance values (%Rg) range from 0.6 to 1.2%; rocks in the oil generation zone (%R_o =0.5-1.30, CAI: 1.5-2.5) have graptolite reflectance ranging from 1.2 to 2.2% (Goodarzi and Norford, 1989b). The presence of solid hydrocarbon (bitumens) is indicative of mature and post-mature rocks, and can be found in shales and siltstones (Landis and Castaño, 1995). In the present study, graptolite reflectance (%Rg) for most of the samples ranges from 1.03% to 1.49% suggesting early to intermediate stages of thermal maturity (Figure 4.11), consistent with the results of Rock-Eval data and biomarkers. However, solid bitumens (SB) were also found in some samples (e.g. A6b and A35b) with reflectance values of 2.34% and 2.23%, respectively (Figure 4.12) suggesting post-maturity for these samples. These two high values do not show any consistency with the conclusion that samples A6b and A35b are at intermediate and early maturity levels, respectively as indicated by Rock-Eval data, 22S/(22S+22R), C_{30}-moretanes/C_{30}-hopanes, ββ/(ββ+αα), and 20S/(20S+20R) ratios. Therefore, the presence of solid hydrocarbon in these samples may reflect residues of oils (migrated from elsewhere) in the migration pathways.

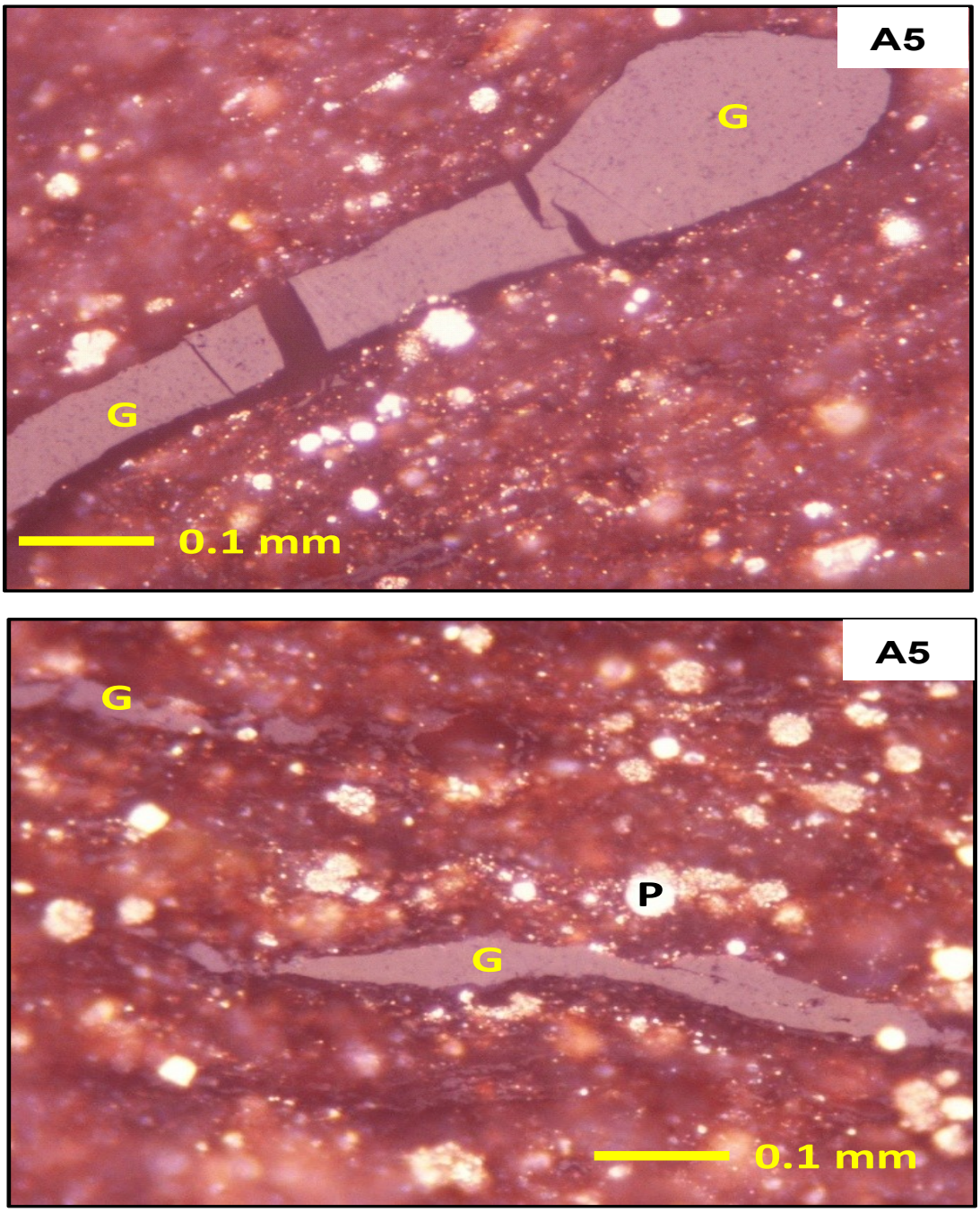

Figure 4.11. Photomicrograph showing elongated and parallel walls of the graptolite periderm (G), under white light, oil immersion. (P) represents pyrite. Silurian Tanezzuft Formation "cool" shale, Murzuq Basin. 50x.

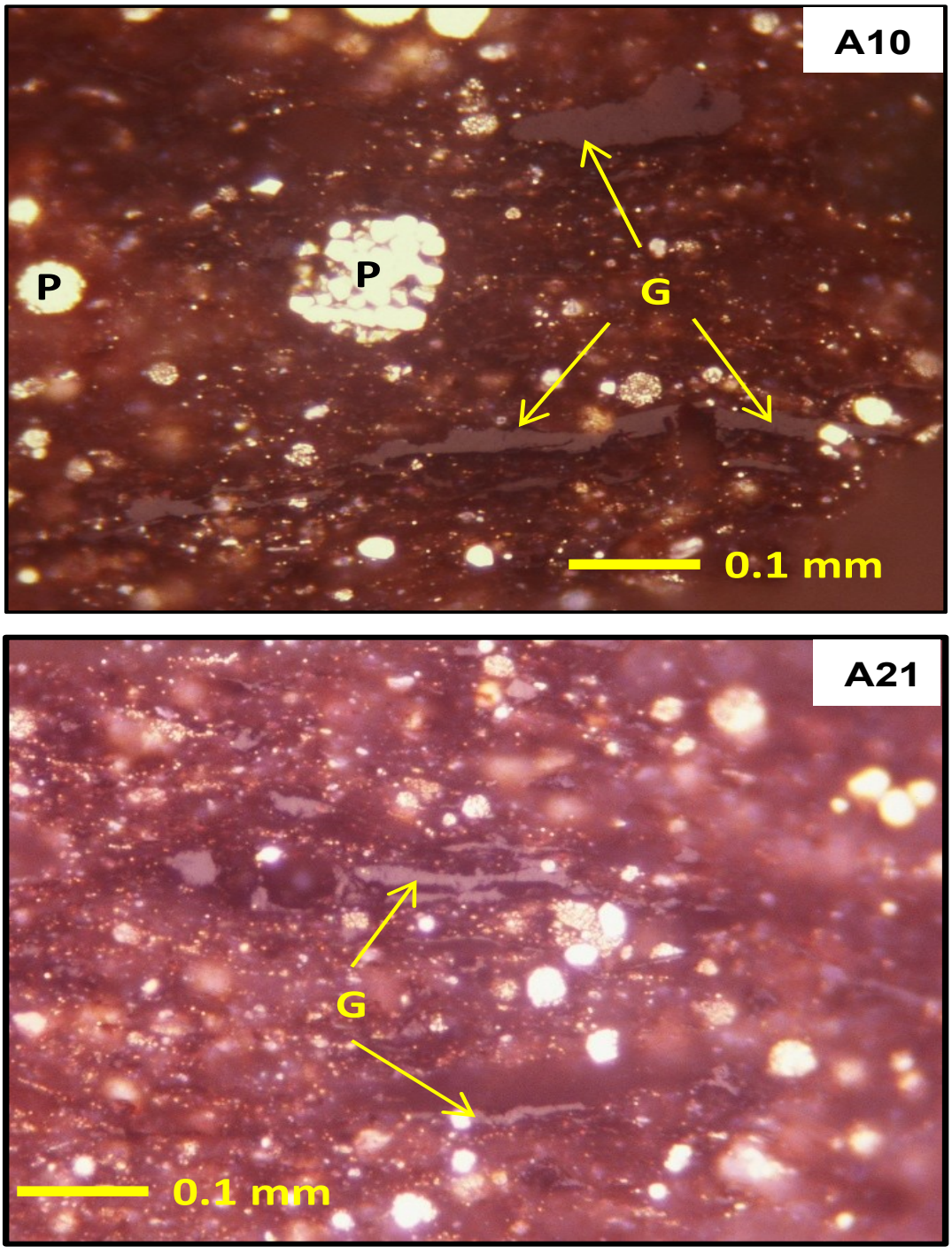

Figure 4.11. (cont.)

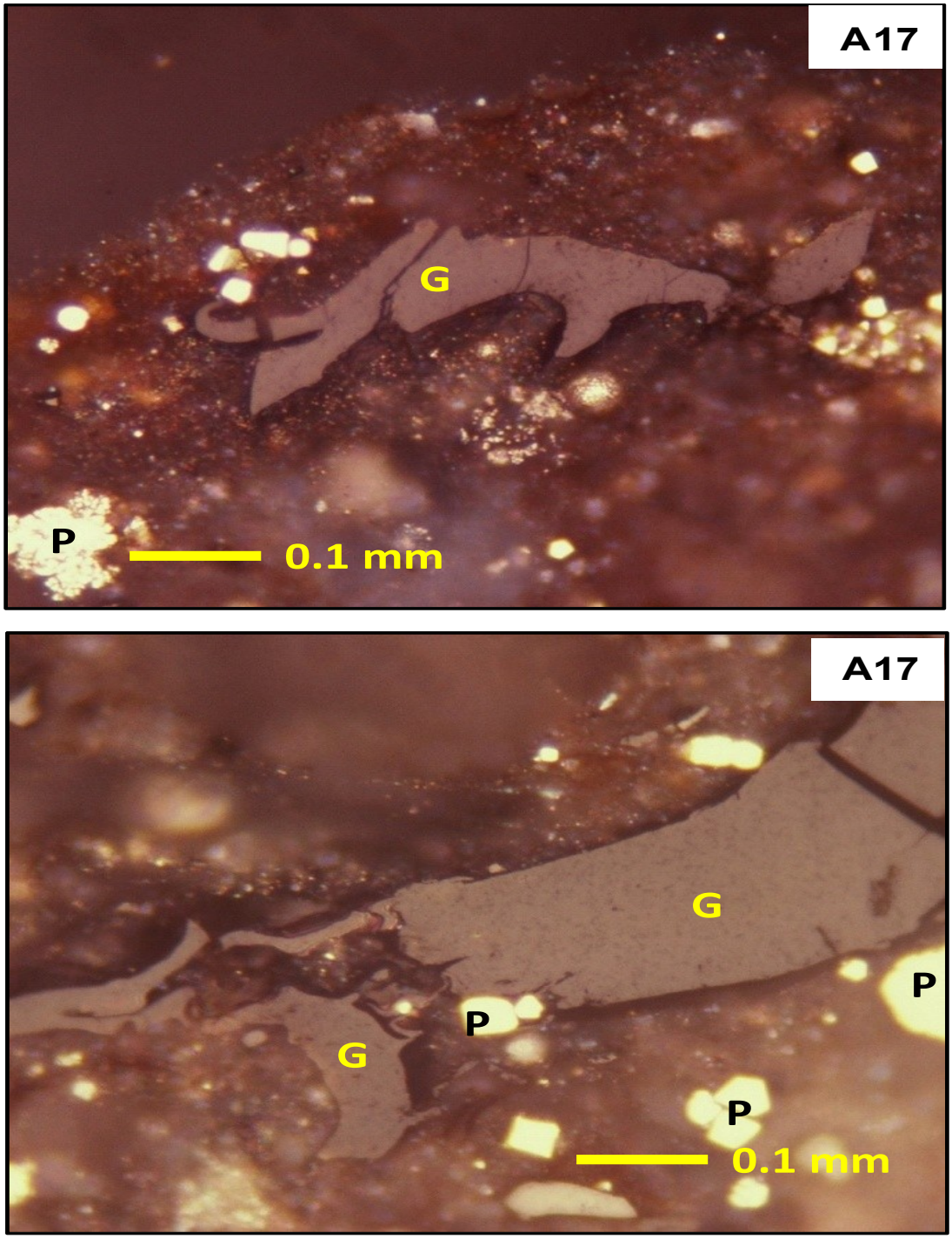

Figure 4.11. (cont.)

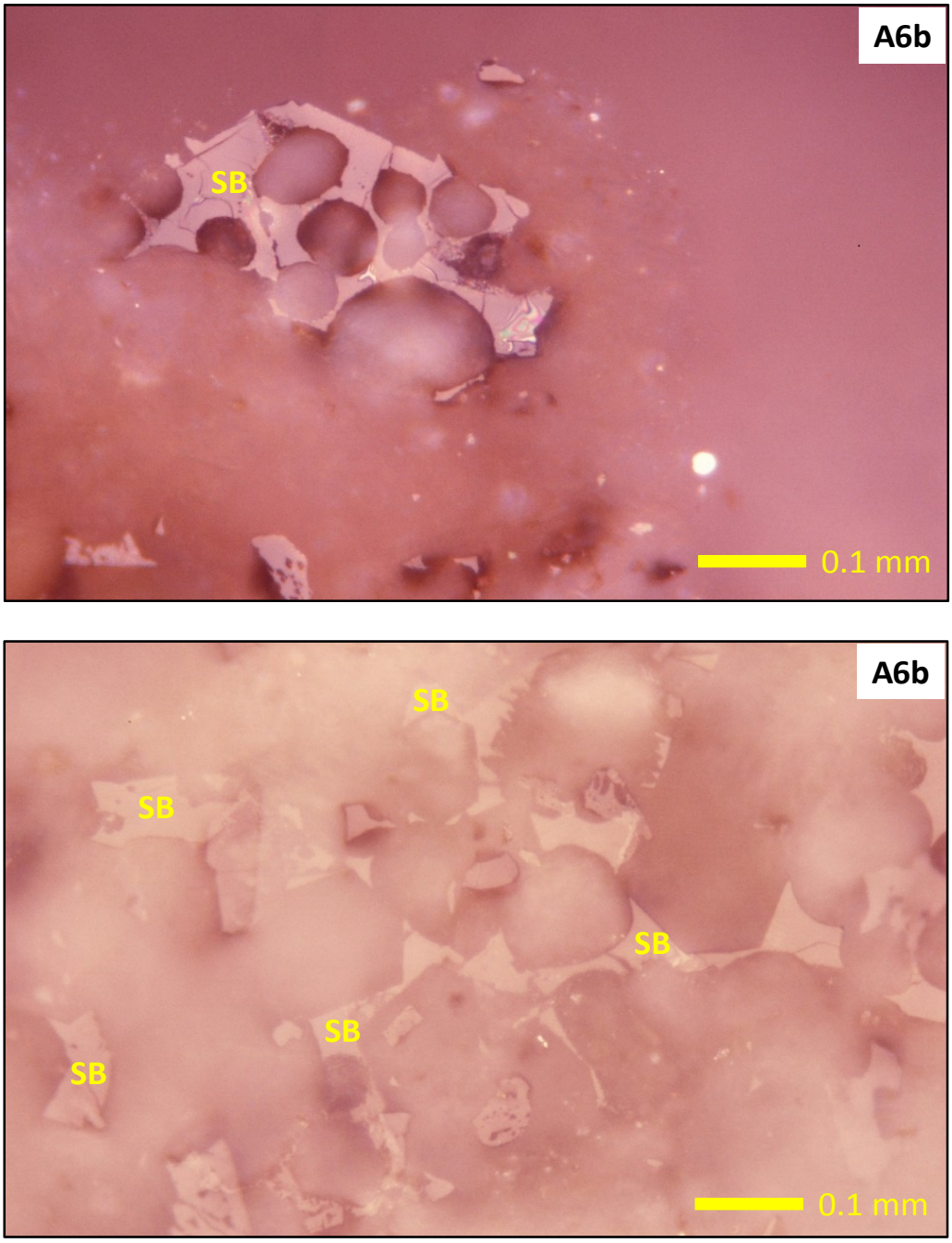

Figure 4.12. Photomicrograph showing solid hydrocarbon (SB) filling the pore spaces in shale, reflected white light, under oil immersion. Silurian Tanezzuft Formation "cool" shale, Murzuq Basin. 50x.

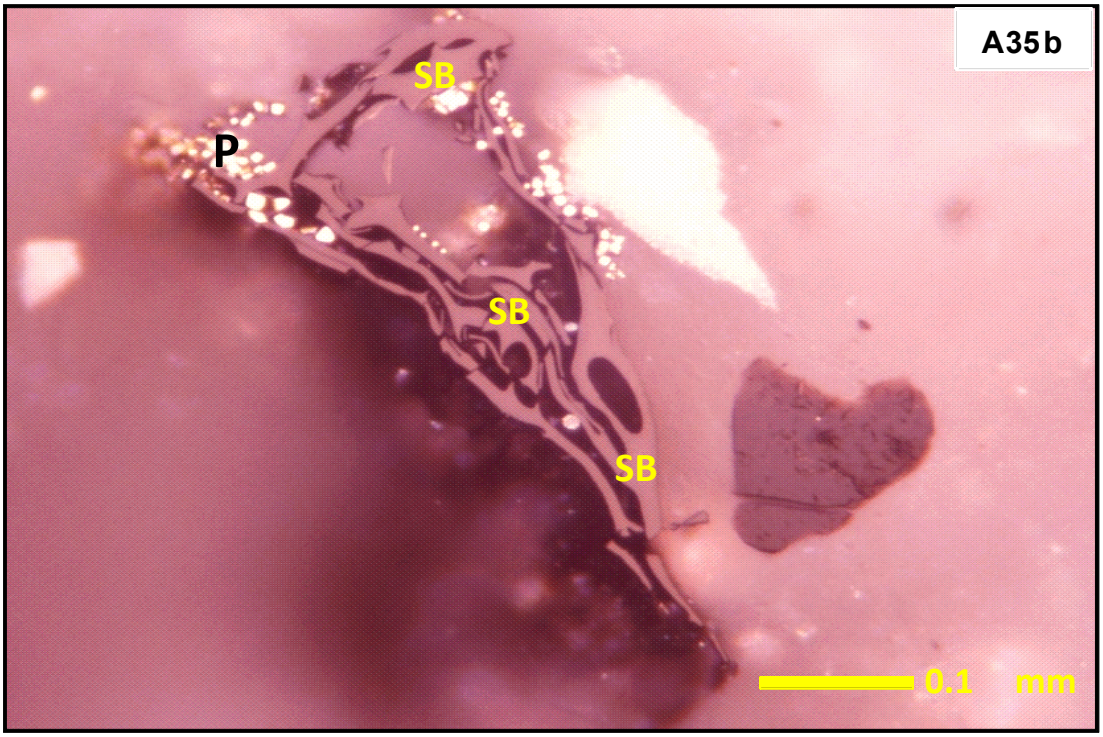

Figure 4.12. (cont.)

4.2 CRUDE OILS

4.2.1 Origin of Organic Matter and Depositional Conditions

4.2.1.1 *n*-Alkane distributions and acyclic isoprenoids

Gas chromatographic data of *n*-alkanes and acyclic isoprenoids are reported in Table 4.8 and the chromatograms are shown in Figure 4.13. The *n*-alkanes are the most abundant components in the saturate hydrocarbon fractions in all oils. The *n*-alkane distributions in all of the oils have a unimodal profile and are generally in the C_{11}-C_{32} range, and typically maximize at *n*-C_{13} or *n*-C_{15} (Table 4.8; Figure 4.13). The n-alkane distributions of the all oils in this study may indicate mainly marine-derived organic matter (Eglinton and Hamilton, 1969; Philp, 1985; Peters and Moldowan, 1993). However, based on the crossplot of Pr/nC_{17} vs. Ph/nC_{18}, all plotted samples fall in the zone of mixed marine/terrigenous organic matter (Figure 4.14). This conclusion is further supported by the distribution of steranes (Figure 4.15) as well as the crossplot of stable carbon isotopic composition for saturate and aromatic hydrocarbons of selected crude oils, where the oil samples plotted fall on the margin line between terrigenous and marine suggesting a mixture of organic matter input (Figure 4.8).

Pristane (Pr) and phytane (Ph) are the predominant isoprenoids in all of the samples. Generally, Pr/Ph ratios of oil samples from A-Field show a small variation from 1.36 to 1.82, except for sample A30, which shows a relatively higher value of 2.10 (Table 4.8).

Table 4.8. Gas chromatogram data of n-alkanes and acyclic isoprenoids for crude oils from the Murzuq Basin.

Sample No.	Range	n-alkane Maximum	Pr/Ph	Pr/nC_{17}	Ph/nC_{18}	nC_{17}/nC_{25}	$Pr+nC_{17}/Ph+nC_{18}$	CPI	long-/short-chain n-alkanes $\sum(nC_{21}-nC_{31})/\sum(nC_{15}-nC_{21})$
A1	nC_{11}-nC_{32}	nC_{13}	1.82	0.54	0.39	4.49	1.47	1.13	0.39
A7	nC_{11}-nC_{32}	nC_{15}	1.74	0.54	0.36	4.04	1.32	0.99	0.39
A10	nC_{12}-nC_{32}	nC_{15}	1.76	0.67	0.40	2.13	1.25	0.97	0.62
A11	nC_{11}-nC_{32}	nC_{13}	1.72	0.68	0.41	2.23	1.24	1.01	0.63
A12	nC_{12}-nC_{32}	nC_{15}	1.71	0.67	0.41	1.94	1.24	1.19	0.77
A14	nC_{11}-nC_{32}	nC_{14}	1.80	0.67	0.40	2.08	1.28	1.05	0.62
A15	nC_{10}-nC_{32}	nC_{13}	1.80	0.56	0.37	4.45	1.36	1.07	0.38
A16	nC_{10}-nC_{32}	nC_{13}	1.77	0.55	0.37	3.73	1.34	1.05	0.43
A24	nC_{14}-nC_{32}	nC_{17}	1.45	0.69	0.41	1.50	1.04	1.06	0.95
A25	nC_{10}-nC_{32}	nC_{13}	1.74	0.55	0.37	3.65	1.32	1.06	0.49
A26	nC_{14}-nC_{32}	nC_{17}	1.49	0.67	0.40	1.57	1.07	0.93	1.00
A27	nC_{10}-nC_{32}	nC_{13}	1.76	0.55	0.37	3.62	1.33	1.07	0.43
A28	nC_{14}-nC_{32}	nC_{17}	1.42	0.69	0.41	1.47	1.02	1.00	1.00
A30	nC_{11}-nC_{32}	nC_{15}	2.10	0.65	0.37	4.54	1.45	1.20	0.32
A31	nC_{14}-nC_{32}	nC_{18}	1.36	0.48	0.34	2.42	1.07	1.04	0.66
A32	nC_{14}-nC_{32}	nC_{17}	1.54	0.70	0.41	1.63	1.10	0.79	1.02
R-1	nC_{11}-nC_{32}	nC_{15}	1.90	0.80	0.46	2.00	1.34	0.71	0.73
R-7	nC_{12}-nC_{32}	nC_{15}	1.83	0.81	0.46	1.89	1.29	1.00	0.76
I-2	nC_{12}-nC_{32}	nC_{15}	1.86	0.80	0.45	1.74	1.30	1.00	0.83
I-11	nC_{11}-nC_{32}	nC_{15}	1.87	0.79	0.45	1.81	1.31	1.05	0.83

Pr: pristane; Ph: phytane; CPI: Carbon Preference Index was calculated based on Bray and Evans, (1961)

Formula:

$$\mathbf{CPI} = 1/2 \left[\frac{C_{25}+C_{27}+C_{29}+C_{31}+C_{33}}{C_{26}+C_{28}+C_{30}+C_{32}+C_{34}} + \frac{C_{25}+C_{27}+C_{29}+C_{31}+C_{33}}{C_{24}+C_{26}+C_{28}+C_{30}+C_{32}} \right]$$

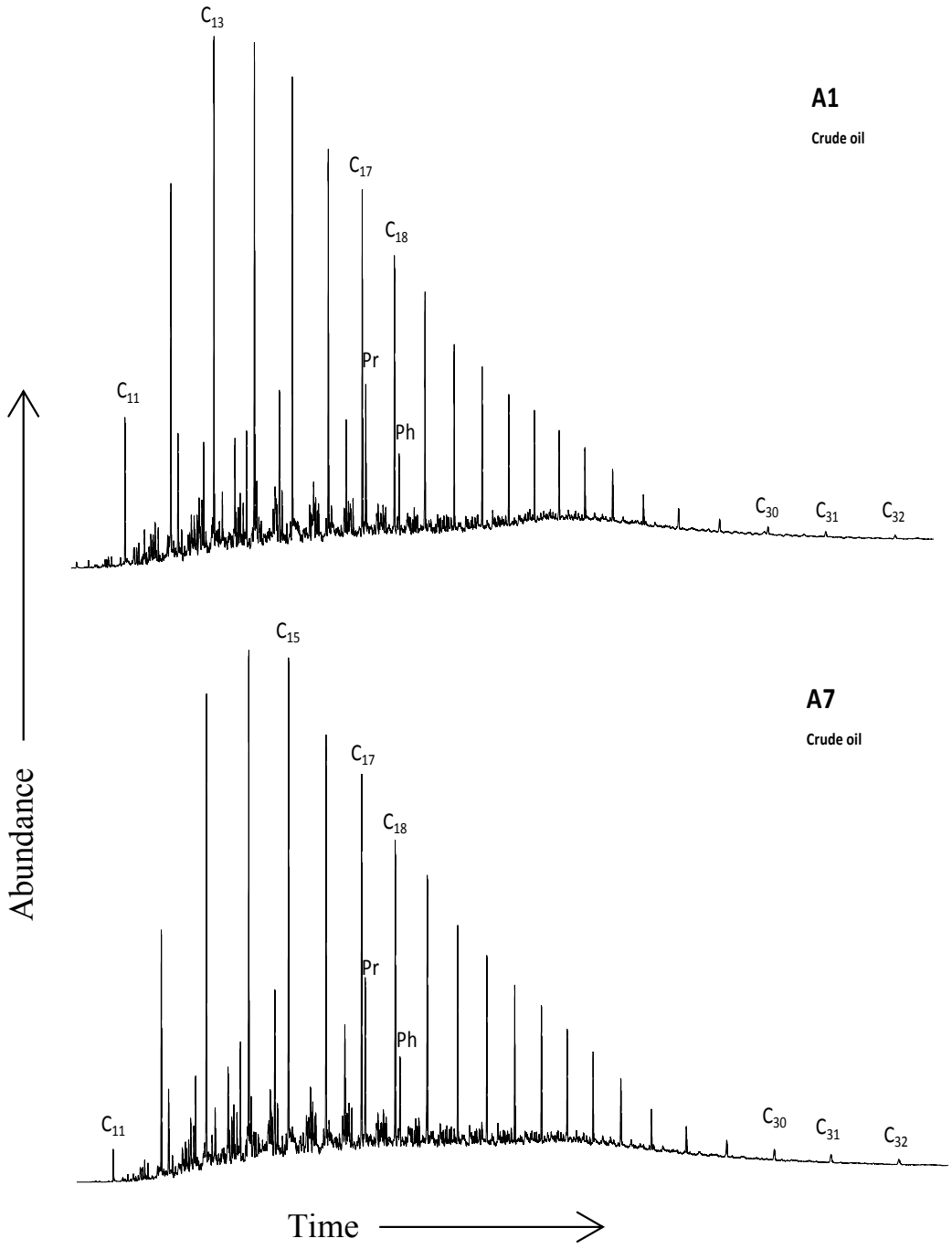

Figure 4.13. Gas chromatograms of aliphatic fractions showing the n-alkanes and acyclic isoprenoids for selected crude oils from Murzuq Basin, NC-115, A Field and NC186, I and R Fields. For more gas chromatograms of rock samples see Appendix V.

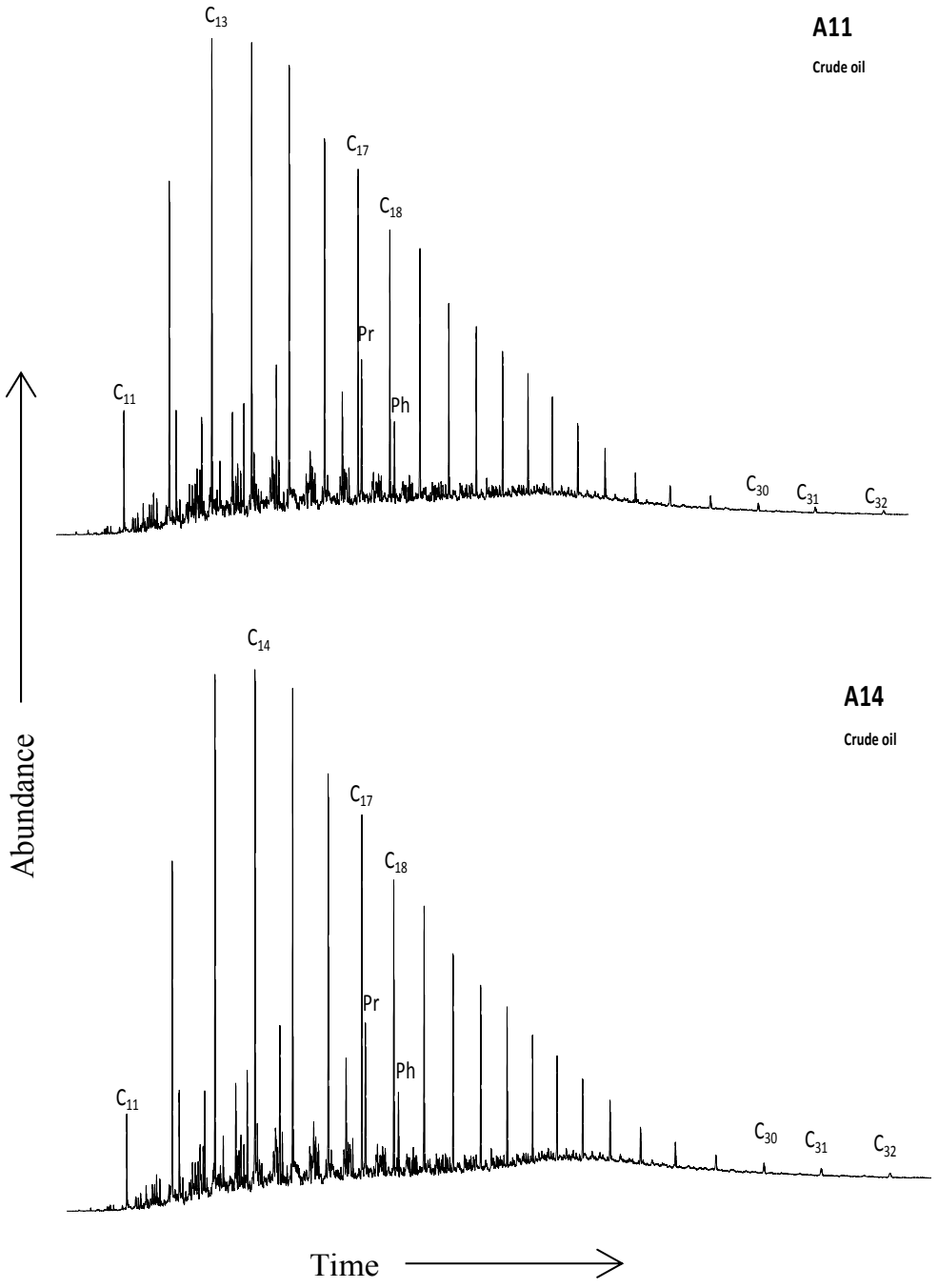

Figure 4.13 (cont.)

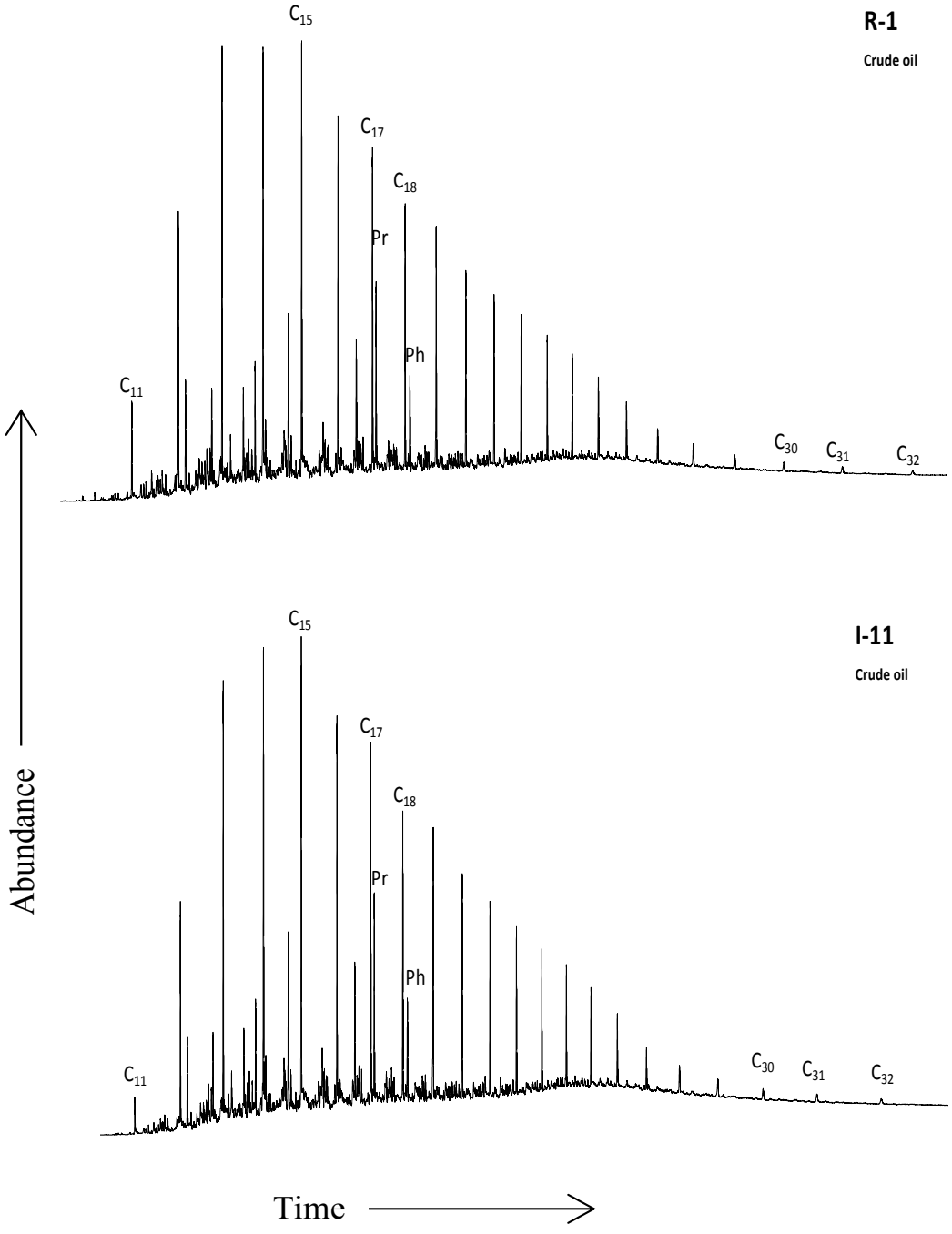

Figure 4.13 (cont.)

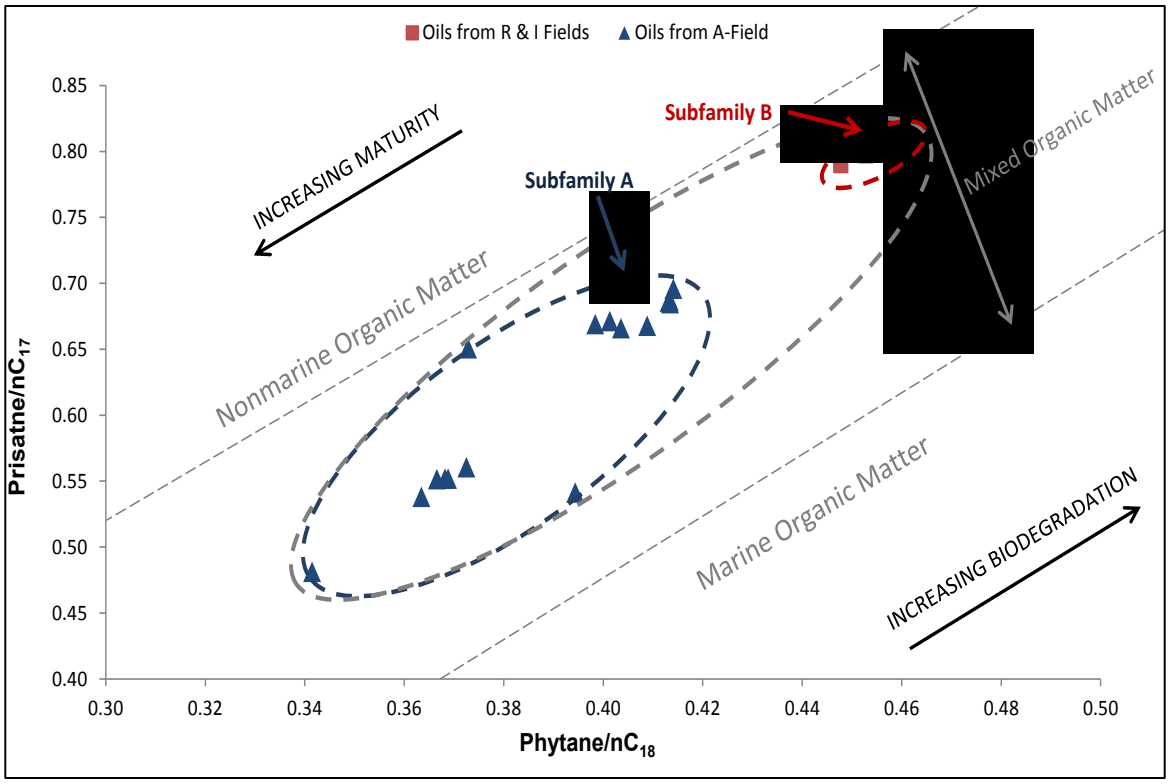

Figure 4.14. Pristane/nC_{17} vs. phytane/nC_{18} showing redox conditions and depositional environments, and its use for the classification of crude oils. It appears that these oils are one genetic family that can be grouped into two subfamilies. Subfamily A represents highly mature oils from A-Field, and Subfamily B represents middle mature oils from R- and I-Fields. (Adopted from Shanmugam, 1985).

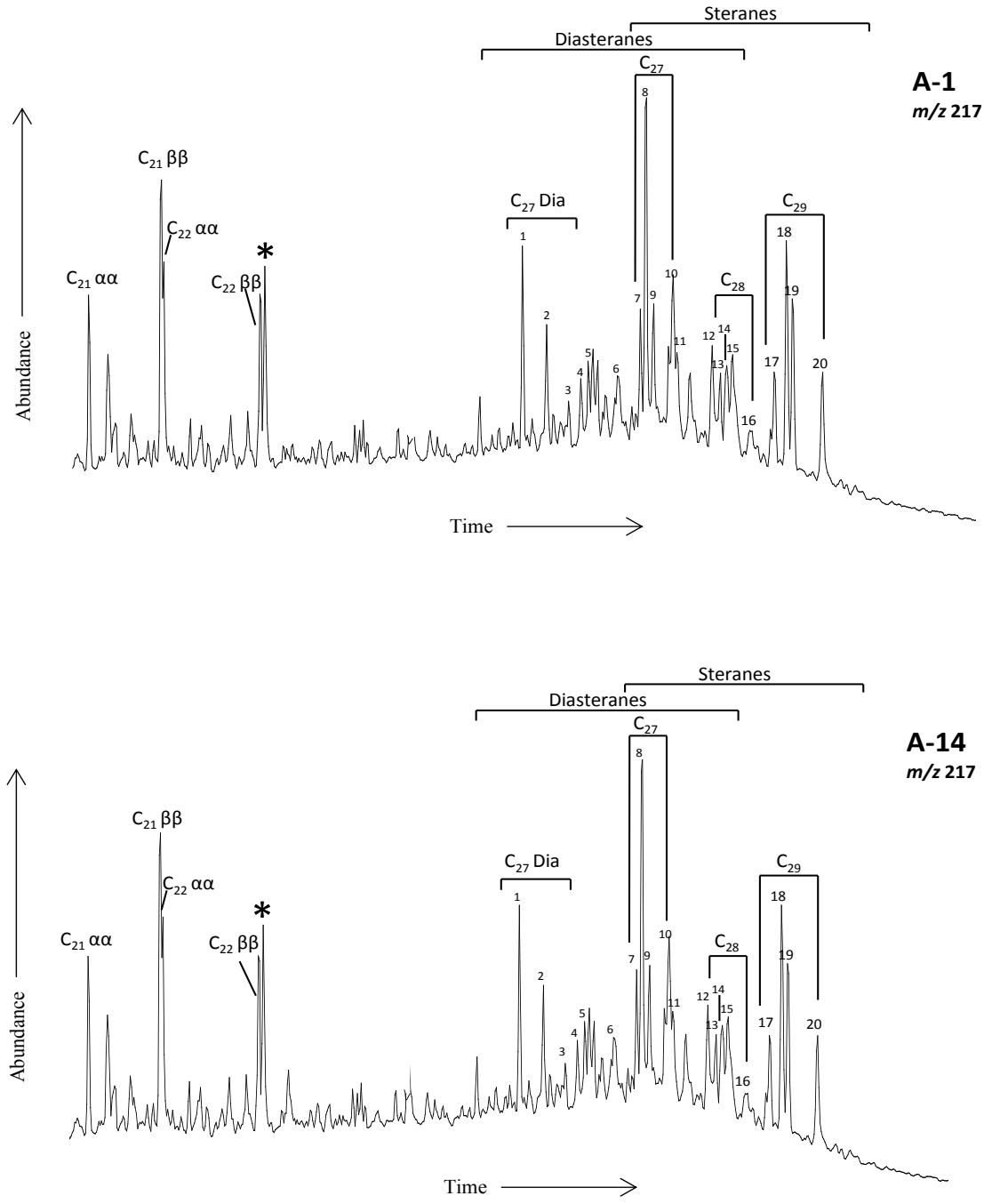

Figure 4.15. Mass chromatograms showing the distribution of steranes (*m/z* 217) of selected crude oil samples from Murzuq Basin. (*): deuterated internal standard ($C_{24}D_{50}$). See Table 4.4 for peak identifications. For more mass chromatograms of rock samples see Appendix VI.

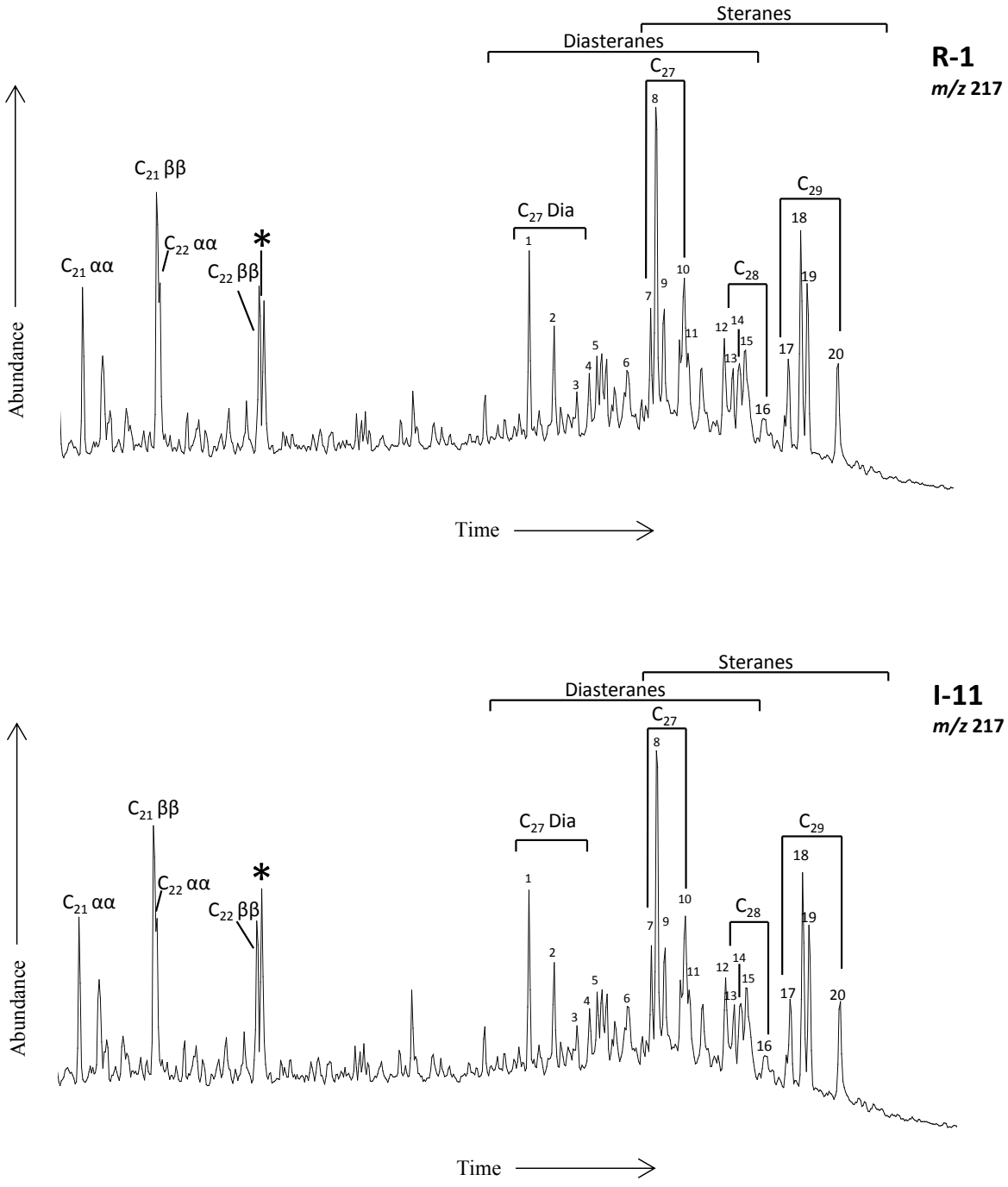

Figure 4.15 (cont.)

Similarly, oils from R- and I-Fields have slightly higher values relative to oils from A-Field ranging from 1.83 to 1.90 (Table 4.8). As mentioned in Section 2.4.2, high Pr/Ph ratios (>3.0) indicate terrigenous organic matter input deposited under oxic conditions, while the low values (<0.8) suggest anoxic conditions, commonly, hypersaline environments (Lijmbach, 1975; Didyk et al., 1978; Peters and Moldowan, 1991; Hughes et al., 1995). Consequently, the values of Pr/Ph ratios (1.36–2.10) may suggest that these oil samples were sourced from sediments deposited under sub-oxic conditions. A crossplot of the dibenzothiophene/phenanthrene ratio (DBT/P) vs. the pristane/phytane (Pr/Ph) ratio (Figure 4.16) was used to determine the crude oil source rock depositional environments and lithologies (Hughes et al., 1995). All the oil samples plotted appear to be derived from marine shale source rocks. Generally, all oils in present study are characterized by very low DBT/P ratios, which may be the result of the very high phenanthrene concentrations in these oils (Hughes et al., 1995).

4.2.1.2 Steranes (*m/z* 217)

The *m/z* 217 mass chromatograms (steranes) from the B/C fractions of selected oils are shown in Figure 4.17, and their identities are listed in Table 4.4. Peak identification of C_{27}-cholestane, C_{28}-ergostane and C_{29}-stigmastane with their 20S and 20R epimers was determined based on previously published data (e.g. Philp, 1985). The most abundant sterane among all oils is the C_{29} sterane with 44–54% of the total C_{27}–C_{29} regular steranes. C_{27} and C_{28} steranes comprise 24–31% and 18–28%, respectively of the total C_{27}–C_{29} regular steranes (Table 4.9). C_{30} steranes have not been detected in any of the

Table 4.9. Sterane parameters (*m/z* 217 chromatograms) for crude oils from the Murzuq Basin.

	Steranes [a]			Diasteranes/steranes[b]	C_{29}[c]	C_{29}[d]	C_{27}/C_{29}[e]	Preg/(preg+ster+dias)[f]
	C_{27} %	C_{28} %	C_{29} %		ββ/(ββ+αα)	20S/(20S+20R)		
A1	29	20	51	1.4	0.57	0.41	0.55	0.49
A7	27	21	52	1.5	0.56	0.42	0.51	0.52
A10	32	26	42	1	0.56	0.44	0.75	0.52
A11	27	23	50	1.5	0.58	0.38	0.54	0.54
A12	32	18	50	1.8	0.55	0.45	0.64	0.6
A14	30	19	51	1.3	0.56	0.43	0.58	0.51
A15	31	20	49	1.2	0.56	0.42	0.63	0.49
A16	27	28	45	1.3	0.55	0.44	0.59	0.49
A24	30	21	49	1.3	0.56	0.41	0.59	0.5
A25	30	21	49	1.2	0.56	0.42	0.61	0.5
A26	26	28	46	1.4	0.57	0.43	0.57	0.5
A27	28	20	52	1.4	0.56	0.43	0.54	0.5
A28	30	21	50	1.2	0.56	0.42	0.61	0.5
A30	28	18	54	1.5	0.55	0.45	0.51	0.5
A31	31	20	49	1.2	0.56	0.44	0.62	0.51
A32	31	20	49	1.3	0.56	0.42	0.61	0.51
I-2	29	27	44	1.1	0.57	0.45	0.65	0.45
I-11	26	28	46	1.3	0.57	0.47	0.55	0.47
R-1	24	27	49	1.4	0.57	0.45	0.49	0.45
R-7	24	24	52	1.7	0.58	0.46	0.45	0.46

[a]5α(H),14α(H),17α(H)-20R-Steranes, [b]13β(H),17α(H),20(R)-cholestane (C27-diasterane)/5α(H),14α(H),17α(H),20(R)-cholestane (C27-Regular sterane), [c]5α(H),14β(H),17β(H)/[5α(H),14β(H),17β(H) + 5α(H),14α(H),17α(H)] for C29-Steranes, [d]calculated for C29-5α (H),14α(H),17α(H)-Steranes, [e]5α (H),14α(H),17α(H)-20R-Steranes, [f][5α (H),14β (H),17β(H) –Pregnane + 5α(H),14β(H),17β(H) –Homopregnane]/ [5α(H),14β(H),17β(H),20(R)-cholestane + pregnane + homopregnane +13β(H),17α(H),20(S)-diacholestane].

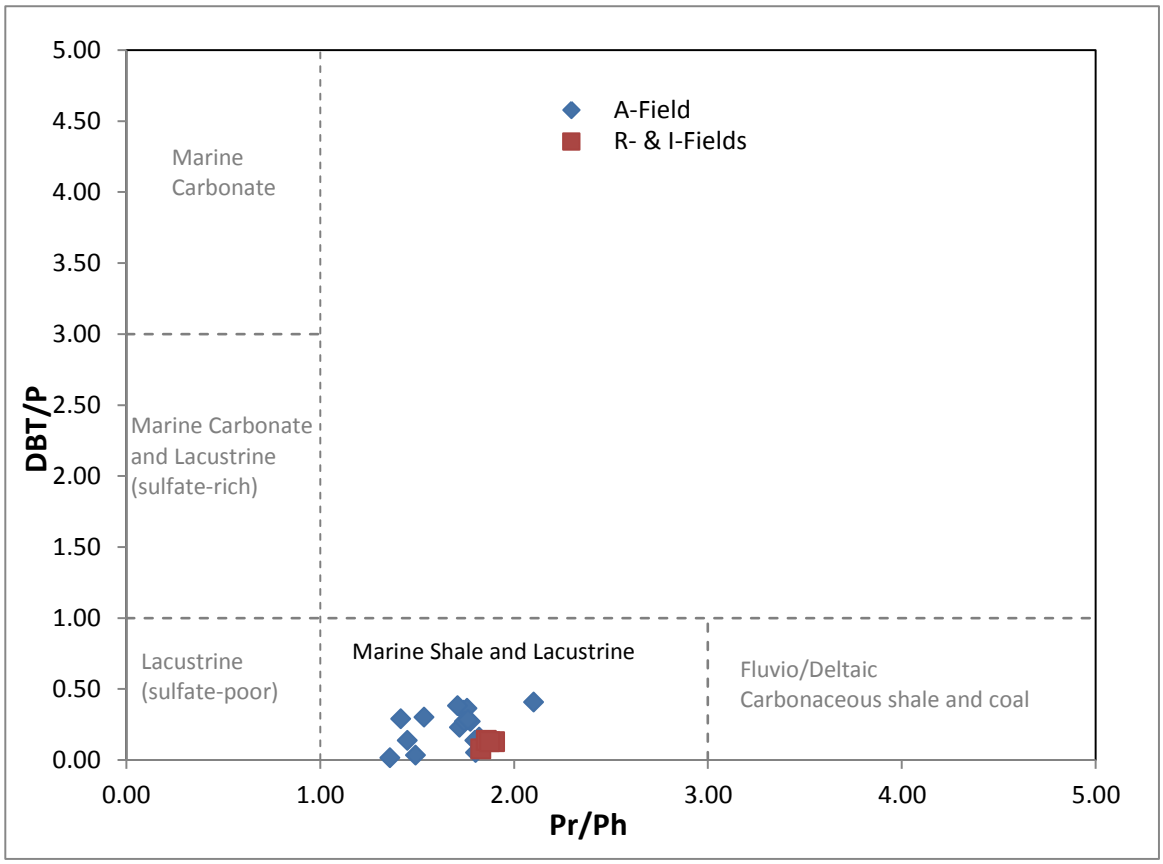

Figure 4.16. Crossplot of dibenzothiophene/phenanthrene ratio (DBT/P) vs. pristane/phytane (Pr/Ph) ratio indicating crude oil source rock depositional environments and lithologies. Murzuq Basin, S.W. Libya. Redrawn after Hughes et al. (1995).

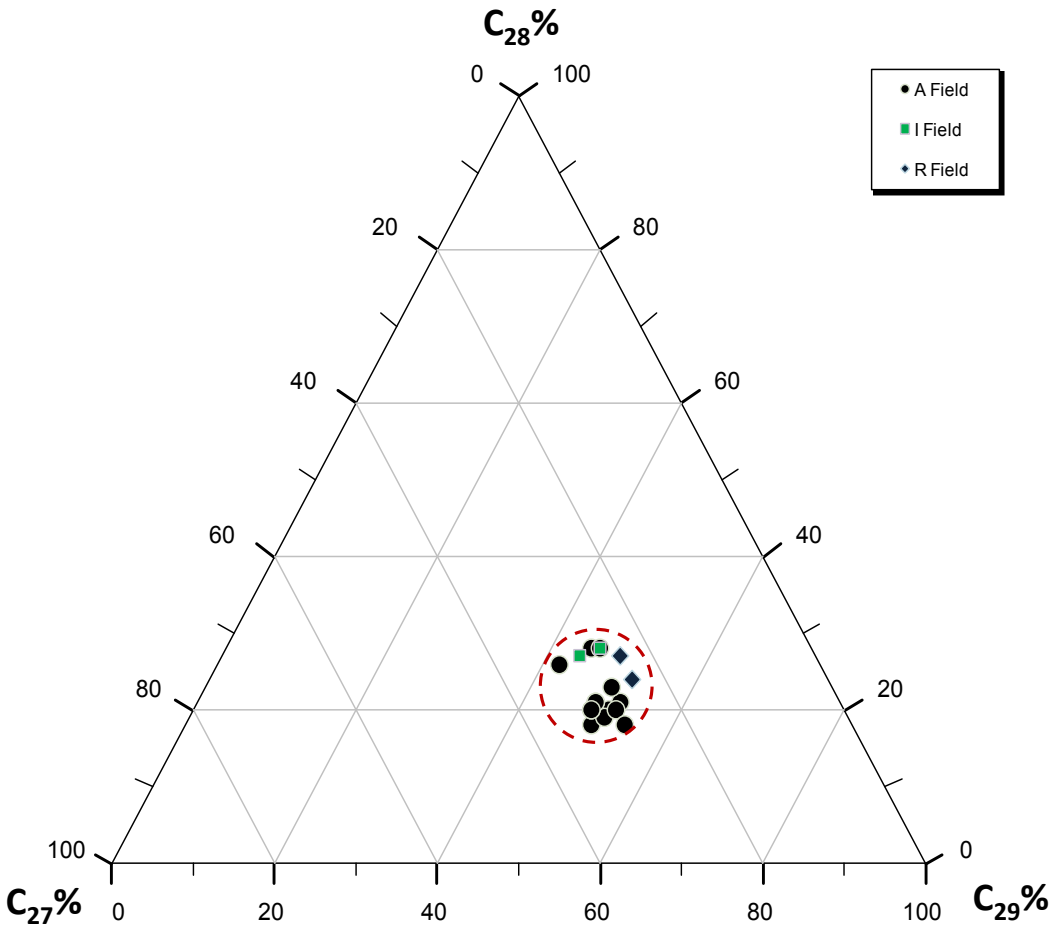

Figure 4.17. Ternary diagram indicating relative distributions of the concentration of C_{27}, C_{28}, and C_{29} regular steranes for crude oil samples from the Murzuq Basin.

samples (Figure 4.15). However, it has been proposed that the absence of C_{30} steranes is a feature of non-marine oils from Australia, Sudan, Chad, China, Brazil and U.S.A. (Moldowan et al., 1985; McKirdy et al., 1986; Mello et al., 1988a). Moldowan et al. (1985) proposed that C_{30} steranes are absent in crude oil or rocks older than ~500 Ma due to the evolutionary lag in the appearance of C_{30} sterols in marine organisms or domination of the marine biota by a few species that did not contain C_{30} sterols, although the specific period in the past at which the C_{30} steranes evolved is also unknown (Waples and Machihara, 1991). However, the absence of C_{30} steranes in all oils in this investigation could not be explained at the present time. Nevertheless, the distribution of C_{27}, C_{28} and C_{29} regular steranes for oil samples are illustrated in the ternary diagram (Figure 4.17), where samples plotted fall over a small area between C_{27} and C_{29} steranes, with slightly higher concentrations of C_{29} steranes (44–54%) compared to C_{27} steranes (24–31%), suggesting a mixed input of marine and terrestrial organic matter (Huang and Meinschein, 1979; Moldowan et al., 1985; Philp, 1985) as previously indicated by the distribution of n-alkanes (Figure 4.13), the crossplot of Pr/nC_{17} vs. Ph/nC_{18} (Figure 4.14) as well as the stable carbon isotopic composition for saturate and aromatic hydrocarbons of selected crude oils (Figure 4.8). The suggestion of the C_{29} steranes in this investigation as partially originating from higher plants is further consistent with several studies carried out on the Tanezzuft Formation in the Murzuq Basin. Conclusive proof for the presence of land plants in the lower part of the Tanezzuft Formation has been proposed to be found in the form of trilete spores belonging to the genus *Ambitisporites* in the southwest of the Al-Qarqaf Arch, which could be as old as Llandoverian (Hoffmeister, 1959; Richardson and Ioannides, 1973; Hallett, 2002). This conclusion is further consistent with a recent study done by Elkelani et al. (2011) on the early Silurian from western Libya, where it was

confirmed that organic microfossils (spores and phytodebris) in the Tanezzuft Formation, which is thought to be the source rock for the oils in this study, provided evidence for the occurrence of higher plants on the North African shore during the early Silurian (Elkelani et al., 2011).

4.2.1.3 Diasteranes and pregnane (*m/z* 217)

The diasterane/sterane ratios for the oils are reported in Table 4.9. Generally, all of the oils in this study are characterized by a small variation in the high values of this ratio ranging from 1.0 to 1.8 (Table 4.9; Figure 4.15). The relatively high diasterane/sterane ratios for all oils (1.0 to 1.8) indicate that oils were sourced from clay-rich source rock, deposited under suboxic conditions (Mello et al., 1988b; Clark and Philp, 1989). The latter is further suggested by the values of Pr/Ph ratios (1.36–2.10) and the relatively high concentration of C_{30}-diahopane for all oils. Since all oils are at advanced levels of maturity, the relatively high diasterane/sterane ratios could be also related to maturity (Hughes et al., 1985; Goodarzi et al., 1989a).

Pregnane ($C_{21}H_{36}$) is present in all oils with values for the pregnane/sterane ratio ranging from 0.49-0.51 for oils from A-Field and from 0.45 to 0.47 for oils from R- and I-Fields (Table 4.9; Figure 4.15). Due to the advanced thermal maturity levels of all oils (intermediate to high levels), the relatively high abundance of pregnane and homopregnane in the oils (Figure 4.15) may be attributed more to thermal maturity (Mueller et al., 1995) rather than to depositional conditions, in particular since gammacerane (hypersaline indicator) is absent in all oils.

4.2.1.4 Terpanes (*m/z* 191)

Hopane indices of the crude oils measured on the *m/z* 191 mass chromatograms of the B/C fractions are reported in Table 4.10 and Figure 4.18, and their peak identities are listed in Table 4.6. Peak identification of all terpanes are based on their retention times and comparison with the previously published values (Philp, 1985). Generally, all oils from A-Field display a wide variation of tricyclic terpane/hopane ratios ranging from 1.71 to 6.77. On the contrary, oils from R- and I-Fields are characterized by low values of tricyclic/hopane ratios averaging 0.6 and 0.59, respectively (Table 4.10). The high abundance of tricyclic terpanes relative to hopanes in oil samples from A-Field (Table 4.6; Figure 4.18) is probably due to the high maturity for these oils (Waples and Machihara, 1990; Peters and Moldowan, 1993) rather than source material. On the contrary, the low values of tricyclic/hopane ratios in oils from R- and I-Fields are probably due to their lower level of maturity compared to A-Field oils.

A C_{24} tetracyclic terpane is identified in all samples, and the C_{23} tricyclic/C_{24} tetracyclic ratios range from 5.8 to 11.93 (Table 4.10). The relatively low concentrations of the C_{24} tetracyclic terpane in all of the oil samples may indicate that the environments might have been slightly affected by salinity (suboxic depositional conditions) as suggested by the ratios of Pr/Ph (1.36–2.10) and diasteranes/steranes along with the presence of C_{30}-diahopanes. According to several authors, C_{24} tetracyclic terpanes are usually found in relatively high concentrations in oils from evaporite-carbonate sequences, and typically dominate the terpane distribution (Palacas et al., 1984; Connan et al., 1986; Clark and Philp, 1989). The occurrence of the C_{24} tetracyclic terpane has also

Table 4.10. Hopane indices (*m/z* 191 chromatograms) of crude oil samples from Murzuq Basin.

	Ts/(Ts+Tm)[a]	C_{29}Ts/(C_{29}Ts+C_{29})[b]	C_{19}/C_{23}[c]	22S/(22S+22R)[d]	HHI[e]	C_{29}/C_{30}[f]	C_{23}/C_{24}[g]	C30βα/C30αβ[h]	C_{24}/C_{30}[i]	C_{23}/C_{30}[j]	C_{23}/C_{29}[k]	Tris/17α-hop[l]	C_{30}d/C_{29}Ts[m]
A1	0.71	0.41	0.47	—	—	0.66	9.07	0.21	0.19	1.73	2.64	2.15	0.98
A7	0.75	0.27	0.41	—	—	0.58	9.34	0.15	0.21	2	3.46	2.72	2.41
A10	0.69	0.38	0.57	—	—	0.47	7.99	0.19	0.18	1.45	3.07	2.37	1.09
A11	0.71	0.43	0.39	—	—	0.72	5.8	0	0.25	1.45	2.01	3.04	0.91
A12	0.72	0.41	0.37	—	—	0.46	11.93	0.22	0.31	3.8	8.35	6.77	1.71
A14	0.68	0.37	0.41	—	—	0.48	7.12	0.26	0.16	1.16	2.44	1.72	1.54
A15	0.76	0.37	0.43	—	—	0.60	7.76	0.19	0.19	1.51	2.51	2.11	0.99
A16	0.63	0.36	0.51	—	—	0.55	7.18	0.27	0.17	1.23	2.25	1.99	1.61
A24	0.71	0.36	0.48	—	—	0.58	8.37	0.19	0.16	1.36	2.36	1.87	1.23
A25	0.77	0.33	0.5	—	—	0.65	6.37	0.22	0.23	1.5	2.3	2	1.67
A26	0.59	0.35	0.34	—	—	0.57	8.67	0.15	0.14	1.26	2.21	1.71	1.15
A27	0.69	0.37	0.34	—	—	0.62	7.11	0.29	0.19	1.35	2.18	1.9	1.6
A28	0.79	0.38	0.41	—	—	0.51	6.3	0.16	0.19	1.24	2.43	1.77	1.44
A30	0.76	0.37	0.39	—	—	0.57	5.83	0.3	0.24	1.41	2.49	1.95	1.08
A31	0.69	0.33	0.36	—	—	0.53	6.28	0.23	0.2	1.27	2.42	1.84	1.19
A32	0.71	0.32	0.37	—	—	0.64	7.4	0.25	0.18	1.37	2.13	2.13	1.92
R-1	0.57	0.28	0.38	0.62	0.77	0.51	6.51	0.12	0.07	0.5	0.99	0.59	0.81
R-7	0.57	0.29	0.37	0.60	0.66	0.51	7.03	0.11	0.07	0.5	0.99	0.59	0.99
I-2	0.55	0.23	0.42	0.55	0.6	0.50	6.08	0.13	0.08	0.49	0.98	0.6	1.36
I-11	0.61	0.26	0.35	0.60	0.62	0.50	6.49	0.15	0.08	0.52	1.04	0.6	0.92

[a]18α (H)-22,29,30-trisnorneohopane/(18α (H)-22,29,30-trisnorneohopane + 17α (H)-22,29,30-trisnorhopane), [b]18α(H)-30-norneohopane/(18α(H)-30-norneohopane + 17α(H), 21β(H)-30-norhopane), [c]$C_{19}H_{34}$ tricyclic terpane/ $C_{23}H_{42}$ tricyclic terpane, [d]17α(H), 21β(H), 22(S)-bishomohopane/(17α(H), 21β(H), 22(S)-bishomohopane+17α(H), 21β(H), 22(R)-bishomohopane): for C_{32}homohopane, [e]Homohopane Index; 17α(H), 21β(H), 22(S+R)-pentakishomohopane/(17α(H), 21β(H), 22(S+R)-tetrakishomohopane (C35/C34 homohopanes), [f]17α(H), 21β(H)-30-norhopane / 17α(H), 21β(H)-hopane, [g]$C_{23}H_{42}$ tricyclic terpane /$C_{24}H_{42}$ tetracyclic terpane, [h]17β (H), 21α (H)-hopane (moretane)/ 17α(H), 21β(H)-hopane, [i]$C_{24}H_{44}$ tetracyclic terpane/17α(H), 21β(H)-hopane, [j]$C_{23}H_{42}$ tricyclic terpane/17α(H), 21β(H)-hopane, [k]$C_{23}H_{42}$ tricyclic terpane/17α(H), 21β(H)-30-norhopane, [l]tricyclic terpanes/17α -hopanes: [C19+C20+C21+C22+C23+C24+C25]/[17α (H)-22,29,30-trisnorhopane + 17α(H), 21β(H)-30-norhopane + 17α(H), 21β(H)-hopane + 17α(H), 21β(H), 22(S+R)-homohopane + 17α(H), 21β(H), 22(S+R)-bishomohopane + 17α(H), 21β(H), 22(S+R)-trishomohopane + 17α(H), 21β(H), 22(S+R)- tetrakishomohopane + 17α(H), 21β(H), 22(S+R)-pentakishomohopane], [m]15α-methyl-17α(H)-27-norhopane/18α (H)-30-norneohopane.

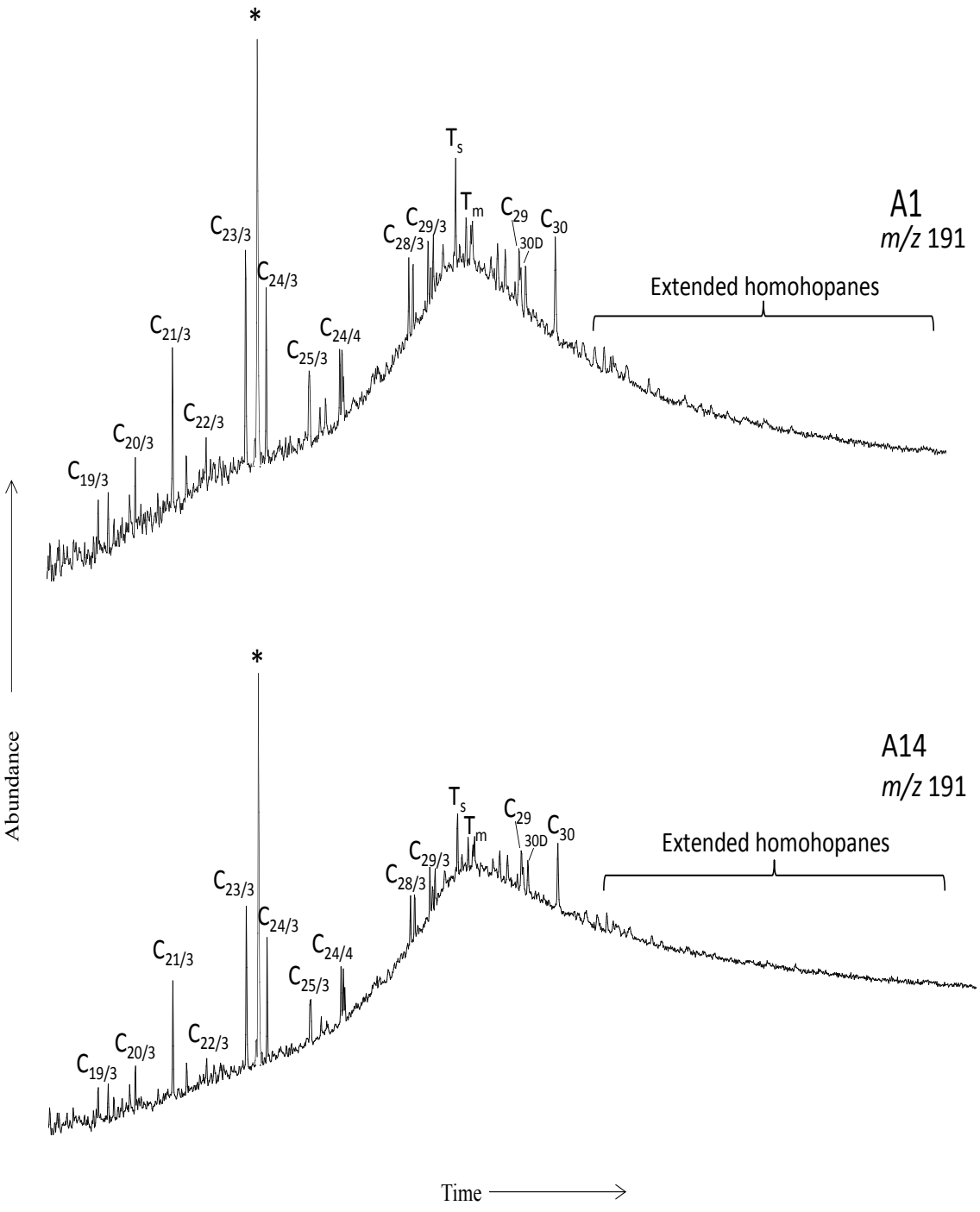

Figure 4.18. Mass chromatograms showing: (I) the distribution of hopanes (*m/z* 191) and (II) the absence of 25-norhopanes (*m/z* 177) of selected crude oils from Murzuq Basin, S.W. Libya. (*): deuterated internal standard ($C_{24}D_{50}$). See Table 4.6 for peak identifications. For more mass chromatograms of rock samples see Appendix VII.

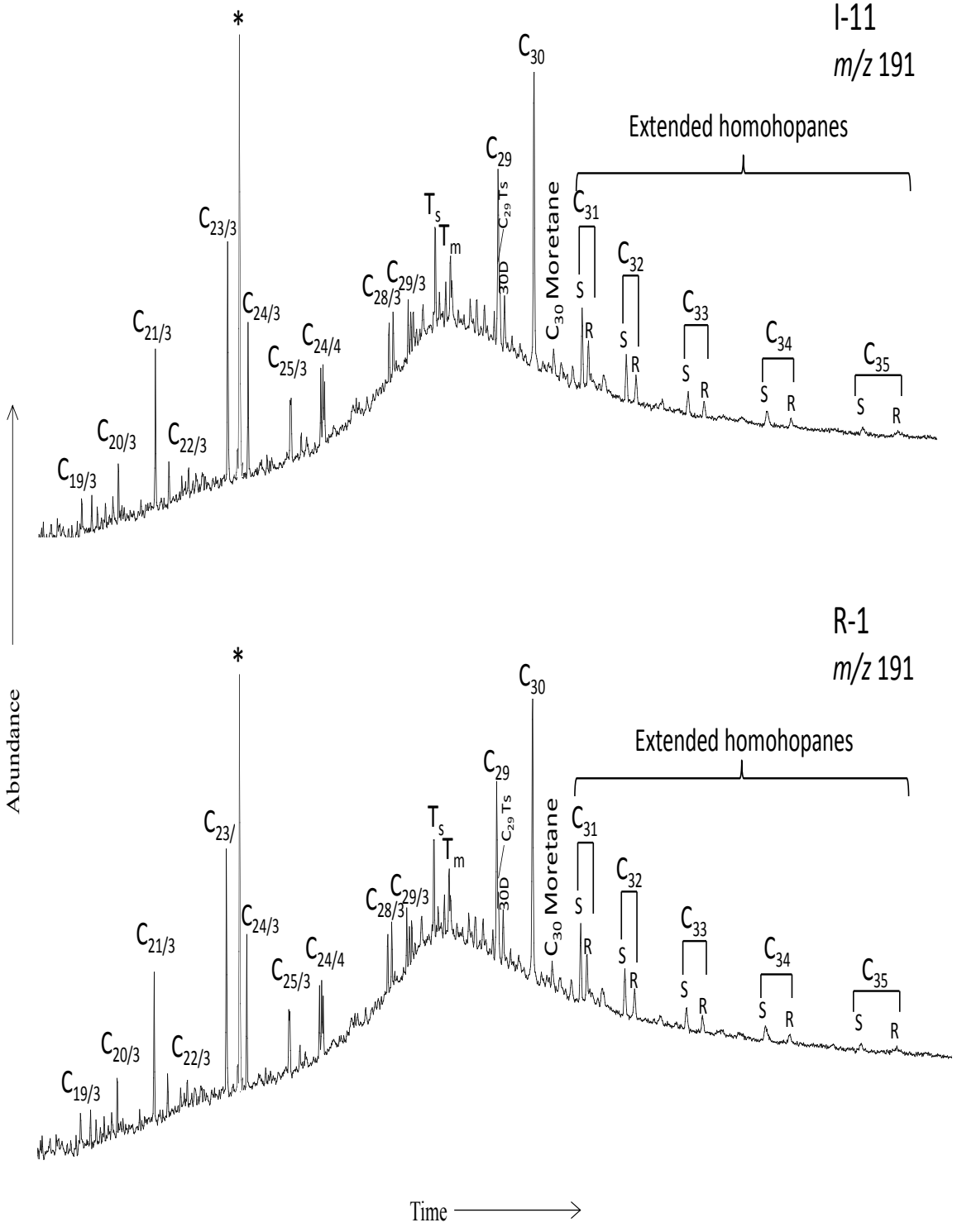

Figure 4.18. (cont.)

been reported in samples from hypersaline environments (Connan et al., 1986), although the absence of gammacerane indicates that the depositional environment for the samples in the present study is not hypersaline.

The C_{30}-diahopane is also present in the majority of oils in relatively high concentrations compared to C_{29}Ts ranging from 1.08 to 2.41 (Table 4.10). On the contrary, only a few oil samples (A1, A11, A15, R-1, R-7, & I-11) have relatively lower values ranging from 0.81 to 0.99 (Table 4.10). The relatively high concentrations of C_{30}-diahopane relative to C_{29}Ts in the majority of oils (Table 4.10) may suggest that these oils originated from sediments characterized by high clastic content, deposited under sub-oxic conditions. Samples with lower values (0.81–0.99) may represent more reducing depositional conditions. According to Peters et al. (2005), high ratios of C_{30}-diahopane/C_{29}Ts are found in oils derived from shales deposited under oxic-suboxic conditions, whereas shales deposited under anoxic conditions show lower values. However, C_{30}-diahopane is characterized by similar geochemical behavior as diasteranes, and thus the ratio of C_{30}-diahopane/C_{29}Ts increases with increasing maturity (Moldowan et al., 1991; Peters and Moldowan, 1993).

All the oils generally show relatively low values for the C_{29}/C_{30}-hopane ratio ranging from 0.47–0.72 (Table 4.10) confirming, along with other parameters (e.g. high values of C_{30}-diahopane/C_{29}Ts and diasterane/sterane ratios), that the oils have been sourced from clay-rich source rocks. C_{29}/C_{30}-Hopane ratios are generally high (>1) in oils generated from organic rich carbonates and evaporites (Price et al., 1987; Zumberge, 1987; Clark and Philp, 1989), and are low (<1) in oils sourced from clay-rich source rocks (Connan et al., 1986).

The ratios of C_{35} to C_{34} homohopanes (homohopane index) could not be calculated for oils from A-Field due to the absence/very low concentrations of extended homohopanes. It is important to note that the C_{35} homohopanes decrease at higher maturity levels, due to preferential generation of shorter-chain hopanes compared to long-chain ones (Peters and Moldowan, 1991). Accordingly, this ratio could not be calculated for oils from A-Field due to the absence/very low concentrations of extended homohopanes as a result of high maturity. However, oils from R- and I-Fields display relatively low values of this ratio ranging from 0.66 to 0.77 and from 0.6 to 0.62, respectively (Table 4.10). The relatively low values in these oils may suggest that the oils were sourced from sediments deposited under sub-oxic conditions.

4.2.2 Assessment of thermal maturation

The maturation of crude oils is an important parameter for understanding their thermal history and is generally determined by several biomarker parameters (Seifert and Moldowan, 1978; Mackenzie and Mackenzie, 1983; Mackenzie, 1984; Philp, 1985; Peters et al., 1999; Philp, 2003). Many of these ratios are based on phenanthrenes, and aromatic steroid hydrocarbons (e.g. mono- and triaromatic steranes), together with tricyclic terpane/17α hopane ratios and diasterane/sterane ratios.

4.2.2.1 Terpanes (*m/z* 191)

Because of the high maturity levels of all A-Field oils as suggested by various aromatic maturity parameters (e.g. monoaromatic steroids: MA(I)/MA(I+II), triaromatic steroids: TA(I)/TA(I+II), and methylphenanthrene index: MPI), the relatively high concentrations of tricyclic terpanes relative to hopanes in A-Field crude oils (Table 4.10; Figure 4.18) are most likely related to maturity rather than to source material. Oils of lower maturity from R-and I-Fields compared to A-Field oils, show low values of the tricyclic terpane/hopane ratios (Table 4.10; Figure 4.18). According to the values of the 22S/(22S+22R) ratio for the C_{32} homohopanes obtained for oils from the R- and I-Fields (0.55–0.62), these oils have attained the so-called "equilibrium value" of 58% proposed by Mackenzie et al. (1982) (Table 4.10; Figure 4.18). As mentioned above, we could not calculate this ratio for oils fom A-Field due to the absence/low concentrations of extended homohopanes as a result of maturity. The Ts/(Ts+Tm) ratio is particularly useful in the oil window, where it responds sensitively to maturity increments before reaching unity in zones of higher maturity (Murray and Boreham, 1992). In the present study, no distinct differentiation could be made between oils from A-, R-, and I-Fields based on the Ts/(Ts+Tm) ratios, where all oils are generally characterized by relatively low values ranging from 0.55 to 0.79 (Table 4.10). These relatively low values of Ts/(Ts+Tm) ratios do not show any correlation with the other maturity parameters such as tricyclic/hopane ratios, diasterane/sterane ratios, and the aromatic maturity parameters [e.g. MPI, MA(I)/MA(I+II) and TA(I)/TA(I+II)]. Therefore, it is not appropriate to use the Ts/(Ts+Tm) ratio for quantitative estimation of maturity, because facies and depositional environments can also effect this ratio (Cornford et al., 1983; Schou et al., 1985).

However, Seifert and Moldowan, (1978) recommended the C_{27} Ts/Tm ratio to be used as an indicator of maturity in samples containing similar source materials. The ratio is also dependent upon the depositional environment and the source of organic material (Philp et al., 1992). However, redox potential is more important than lithology, with lower Ts/(Ts+Tm) ratios in anoxic sediments than in oxic ones (Moldowan et al., 1986). Thus, the relatively low values of Ts/(Ts+Tm) ratios for all oils may be assumed to reflect the nature of the depositional environment.

4.2.2.2 Steranes (*m/z* 217)

Both ratios of ββ/(ββ+αα) and 20S/(20S+20R) for C_{29} steranes display relatively low values ranging from 0.55–0.58 and 0.38–0.47, respectively (Table 4.9). These relatively low values do not show any relationship with the other maturity parameters such as aromatic maturity parameters [e.g. MPI, MA(I)/MA(I+II) and TA(I)/TA(I+II)] or tricyclic/hopane and diasterane/sterane ratios. Thus, it is not appropriate to use ββ/(ββ+αα) and 20S/(20S+20R) ratios for quantitative estimation of maturity.

The proportion of diasteranes compared to the regular steranes is known to be dependent upon maturity as well as oxicity and lithology. The original steranes are gradually converted to a mixture of diasteranes and steranes (Hughes et al., 1985; Goodarzi et al., 1989a). In the present study, the high diasterane/sterane ratios (1.0 to 1.8) (Table 4.9) in all oils could be related to maturity since all oils are at advanced levels of thermal maturity (intermediate to highly mature) suggested by aromatic maturity parameters (e.g. MA(I)/MA(I+II), TA(I)/TA(I+II), and MPI), and/or related to oxicity as

suggested by the values of Pr/Ph ratio (1.36–2.10), and/or related to lithology as indicated by the high ratios of C_{30}-diahopane/C_{29}Ts and low ratios of C_{29}/C_{30}-hopane.

4.2.2.3 Methylphenanthrene index (MPI)

The *m/z* 178+192+206 mass chromatograms of the aromatic hydrocarbon fractions (phenanthrene compounds) for selected crude oils are displayed in Figure 4.19. MPI-2 data for the oils are shown in Table 4.11. For more detailed information about these parameters, see Section 2.5.2.6 in Chapter II. All crude oils from A-Field show relatively higher values of MPI-2 index ranging from 1.02 to 1.5, whereas oils from R- and I-Fields display slightly lower values of (0.84–0.86) and (0.86–0.89), respectively (Table 4.11; Figure 4.19). Based on the proposal of classification of crude oils according to the MPI-2 index, high maturity crude oils are characterized by MPI-2 > 1.00, whereas medium maturity oils usually have MPI-2 = 0.80–1.00, and low maturity crude oils have MPI-2 <0.80 (Angelin et al., 1983; Radke, 1987; Ivanov and Golovko, 1992). Thus, it can be concluded that all crude oils from A-Field possessed values greater than one, are at higher levels of thermal maturity than oils from R- and I-Fields (0.84–0.89), which showed intermediate levels of thermal maturity. This is further supported by values of mono-and triaromatic steroids (Table 4.11; Figures 4.20 and 4.21) as well as by the Pr/C_{17} vs. Ph/C_{18} crossplot (Figure 4.14).

Table 4.11. Aromatic hydrocarbon maturity parameters calculated on the basis of the distribution of methylphenanthrene isomers as well as mono- and triaromatic steroids.

Sample ID:	A1	A7	A10	A11	A12	A14	A15	A16	A24	A25	A26	A27	A28	A30	A31	A32	R-1	R-7	I-2	I-11
MPI-1	1.10	1.11	1.12	1.15	1.18	0.83	1.03	1.01	1.10	1.11	0.82	1.09	1.28	0.95	0.84	1.17	0.93	0.62	0.97	0.91
MPI-2	1.17	1.18	1.10	1.18	1.19	1.09	1.50	1.09	1.19	1.09	1.04	1.16	1.41	1.22	1.02	1.17	0.86	0.84	0.89	0.86
MA(I)/MA(I+II)	0.62	0.64	0.68	0.65	0.68	0.62	0.64	0.62	0.63	0.61	0.61	0.62	0.65	0.61	0.67	0.62	0.46	0.45	0.46	0.45
TA(I)/TA(I+II)	0.87	0.86	0.83	0.84	0.86	0.80	0.90	0.90	0.86	0.89	0.80	0.87	0.84	0.85	0.80	0.88	0.62	0.60	0.66	0.65

$$\text{MPI 1} = 1.5 \times \frac{[\text{2-MP} + \text{3-MP}]}{[\text{P} + \text{1-MP} + \text{9-MP}]}$$ (Radke et al., 1982a)

$$\text{MPI 2} = 3 \times \frac{[\text{2-MP}]}{[\text{P} + \text{1-MP} + \text{9-MP}]}$$ (Radke and Welte, 1983)

MA(I)/MA(I+II): MA(II) is the sum of C_{27}–C_{29} monoaromatic steroids and MA(I) is the sum of C_{21} and C_{22} monoaromatic steroids.

TA(I)/TA(I+II): TA(II) is the sum of C_{26}–C_{28} (20S+20R) triaromatic steroids, and TA(I) is the sum of C_{20} and C_{21} triaromatic steroids.

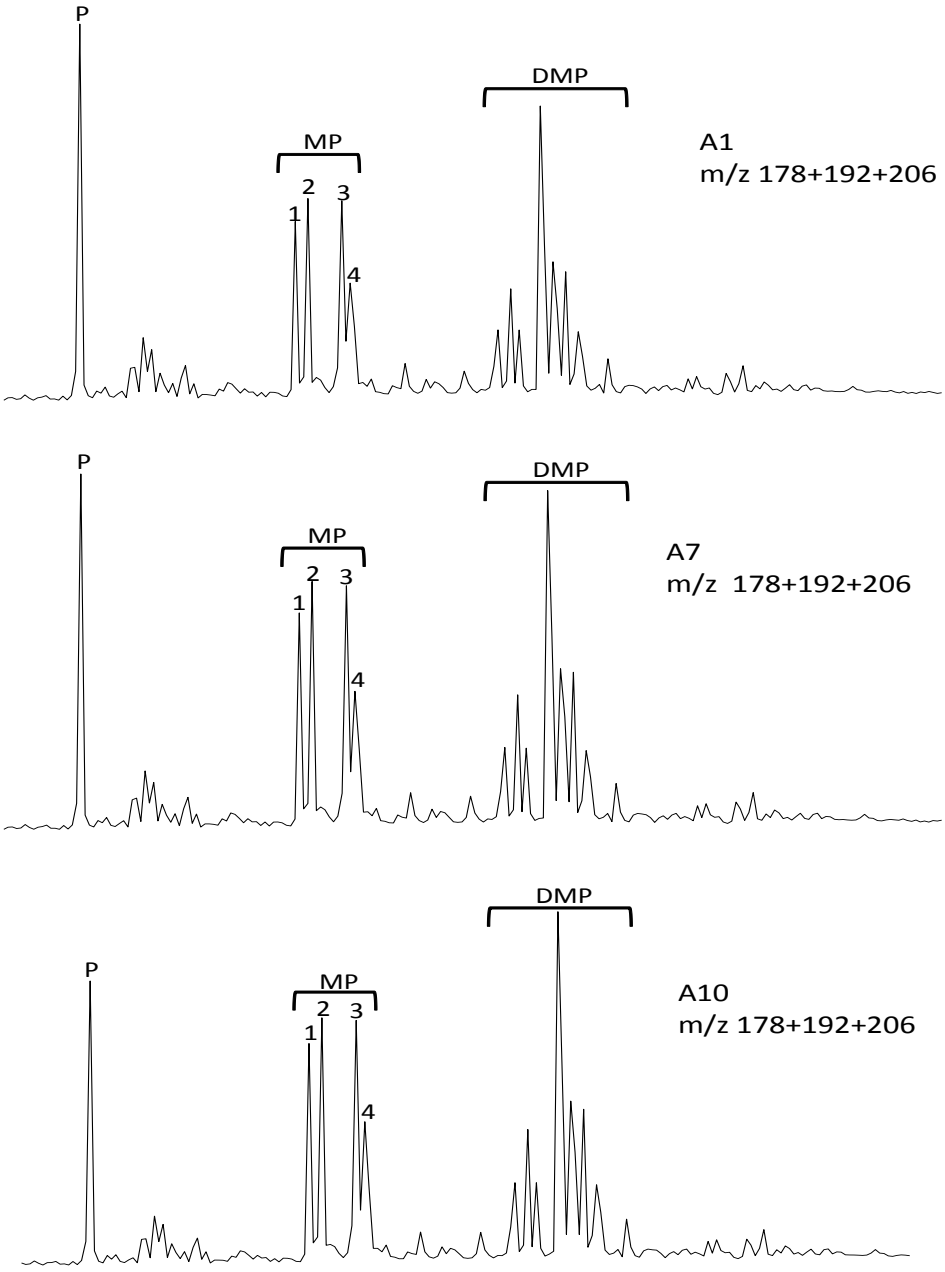

Figure 4.19. Mass chromatograms (*m/z* 178+192+206) showing the phenanthrene compounds in the aromatic fractions of Murzuq Basin crude oils. (I) crude oils from A-Fields are at high levels of maturity, (II) crude oils from R- and I-Fields are at intermediate levels of maturity.Peak identification: (P) Phenanthrene, (1) 3-methylphenanthrene, (2) 2-methylphenanthrene, (3) 9-methylphenanthrene, (4) 1-methylphenanthrene, MP: methylphenanthrene, DMP: dimethylphenanthrene. For more mass chromatograms of rock samples see Appendix VIII.

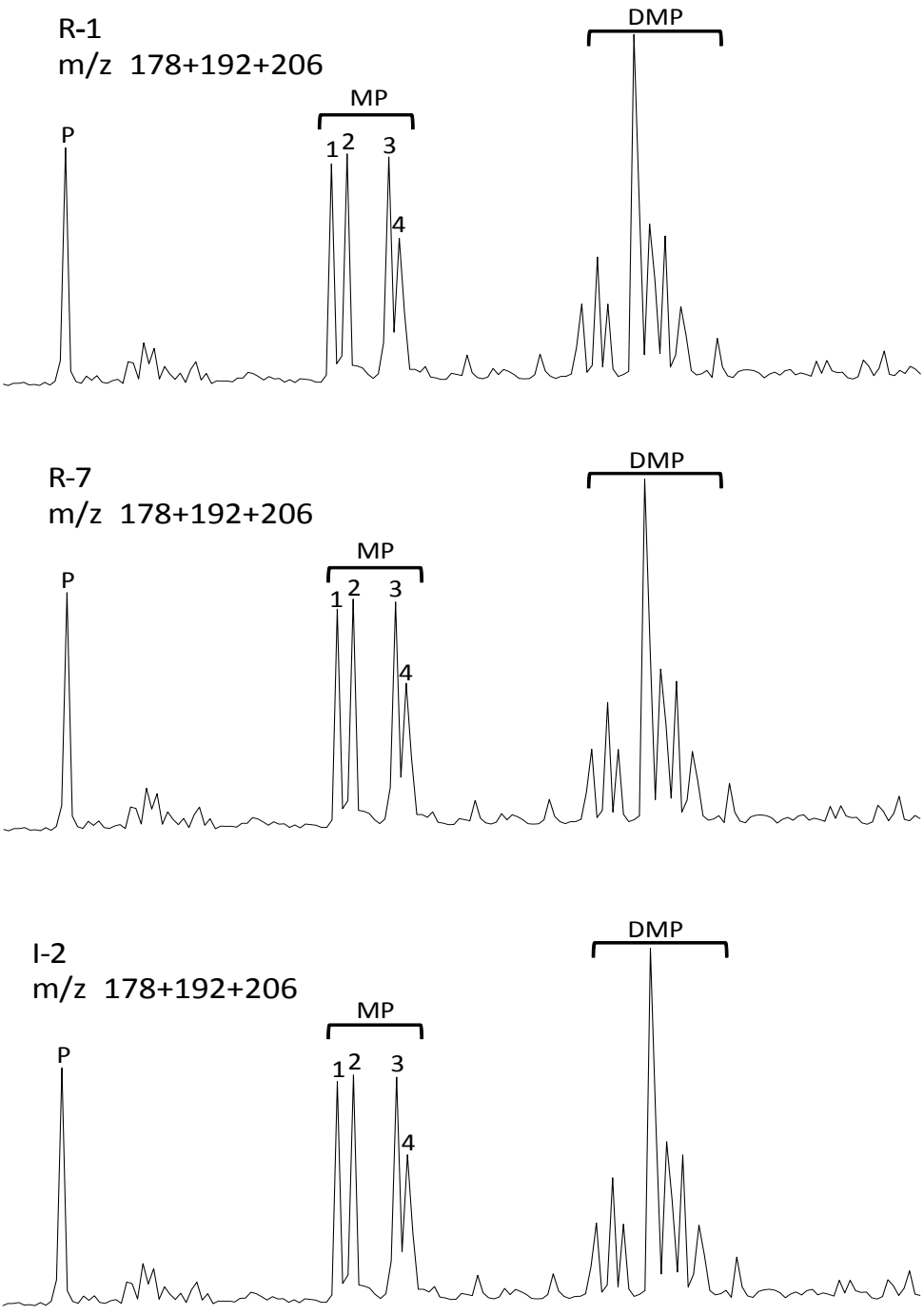

Figure 4.19. (cont.)

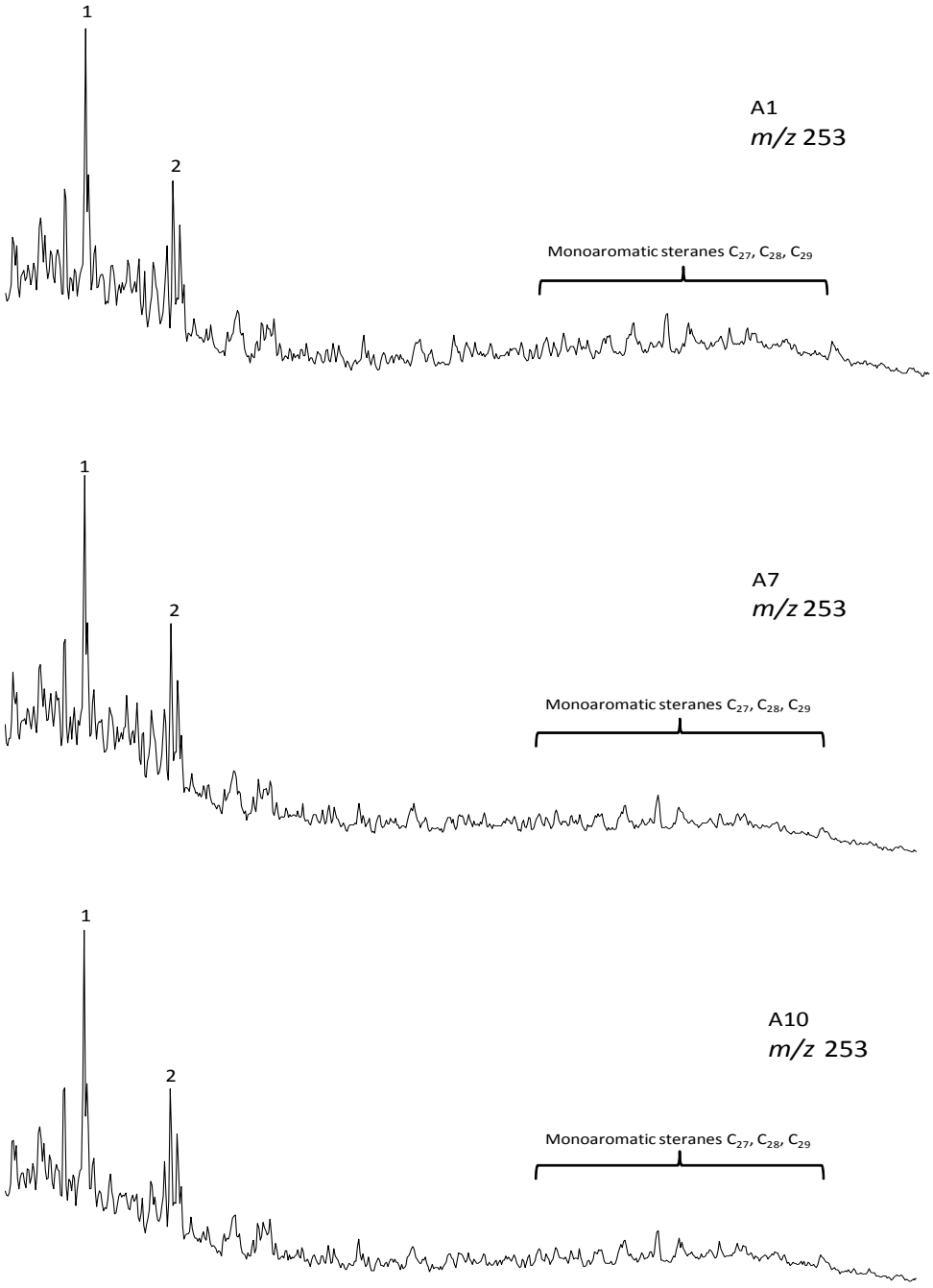

Figure 4.20. Mass chromatograms of *m/z* 253 showing the distribution of the monoaromatic steroid hydrocarbons in the aromatic fractions of crude oil samples: (I) crude oils from A-Field are at high levels of maturity, (II) crude oils from R-and I-Fields are at intermediate levels of maturity. Labeled peaks are identified in Table 4.12. For more mass chromatograms of rock samples see Appendix IX.

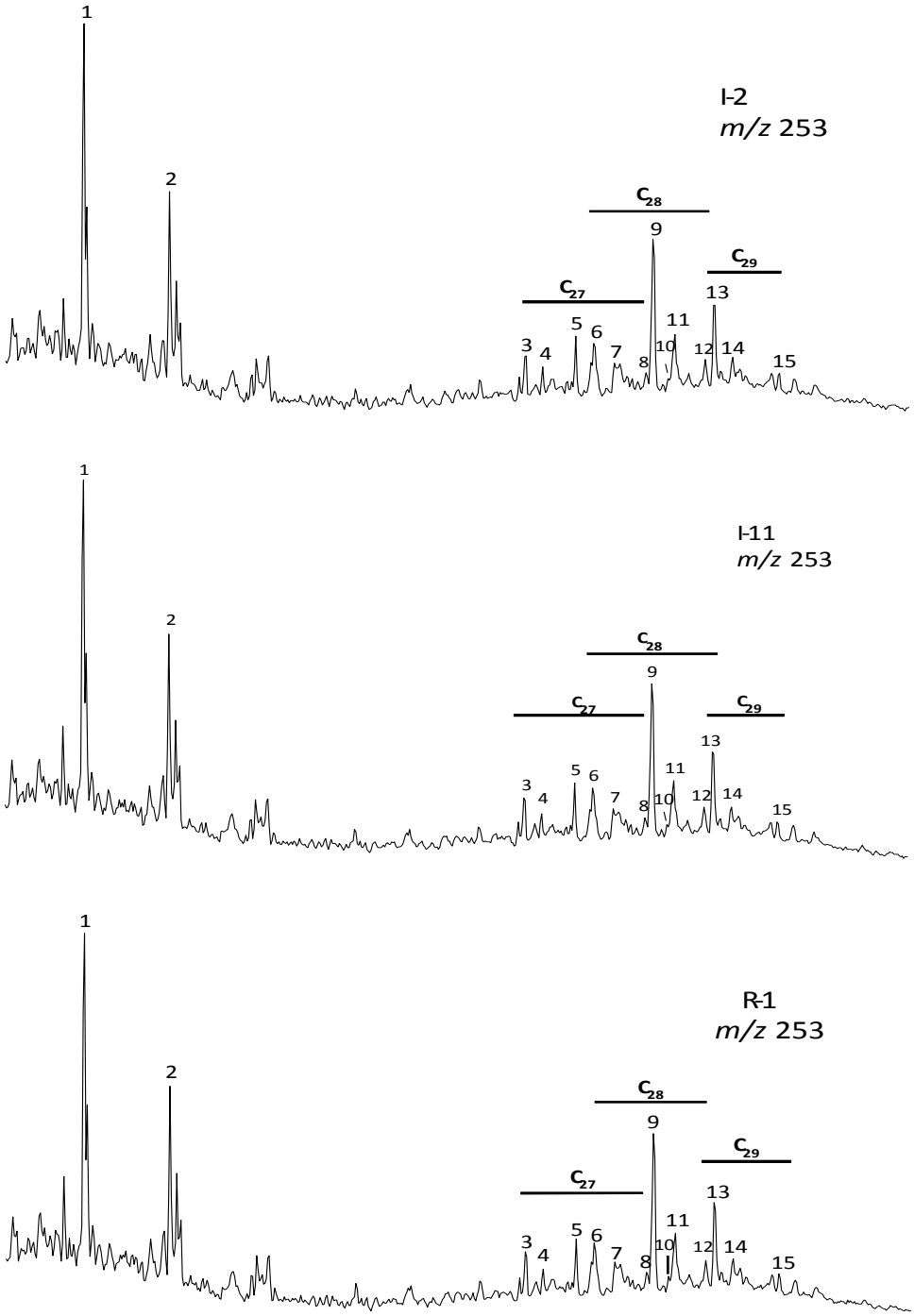

Figure 4.20. (cont.)

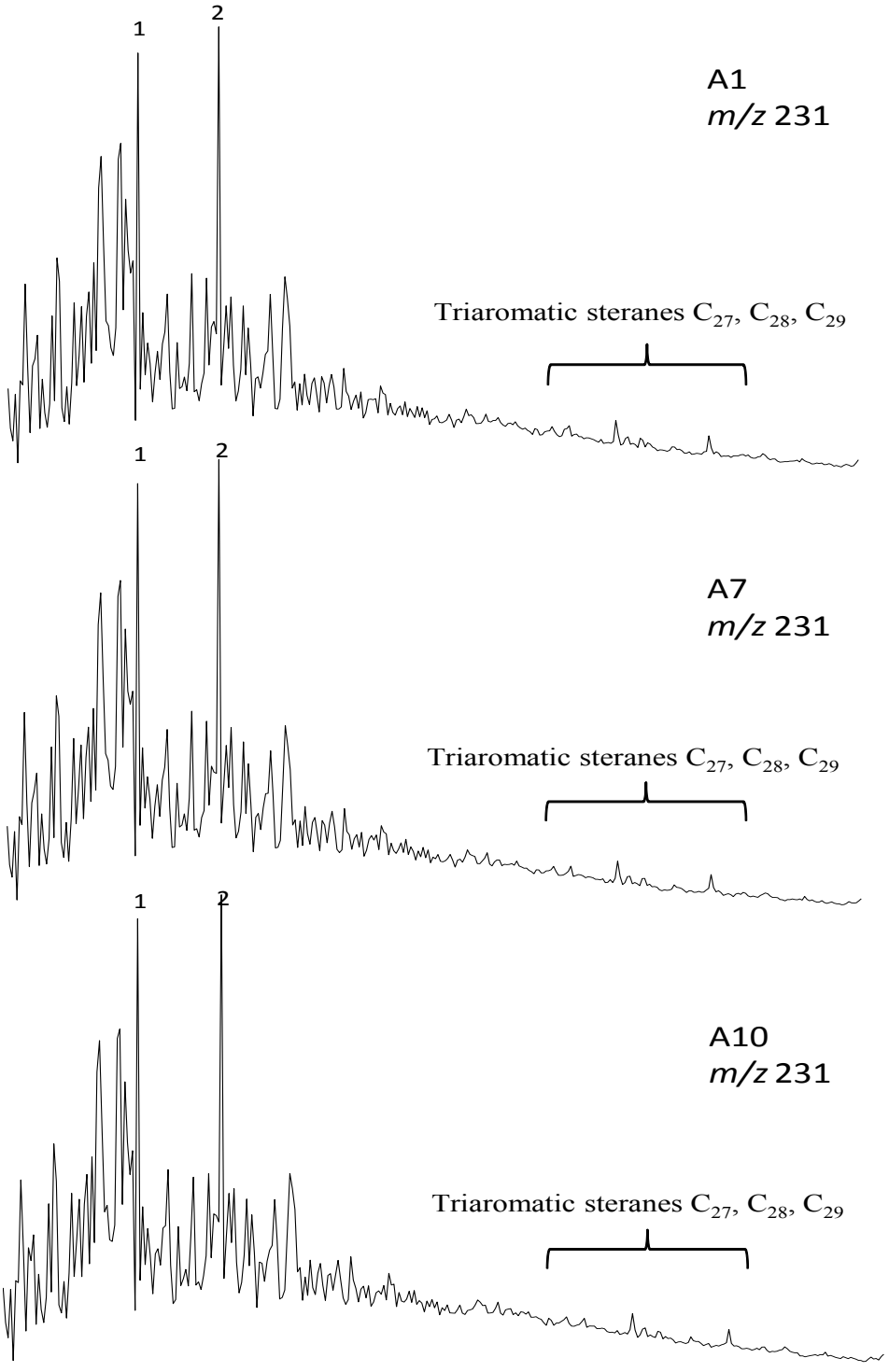

Figure 4.21. Mass chromatograms of *m/z* 231 showing the distribution of the triaromatic steroid hydrocarbons in the oil samples from A-Field, which are at high levels of maturity. Labeled peaks are identified in Table 4.12. For more mass chromatograms of rock samples see Appendix X.

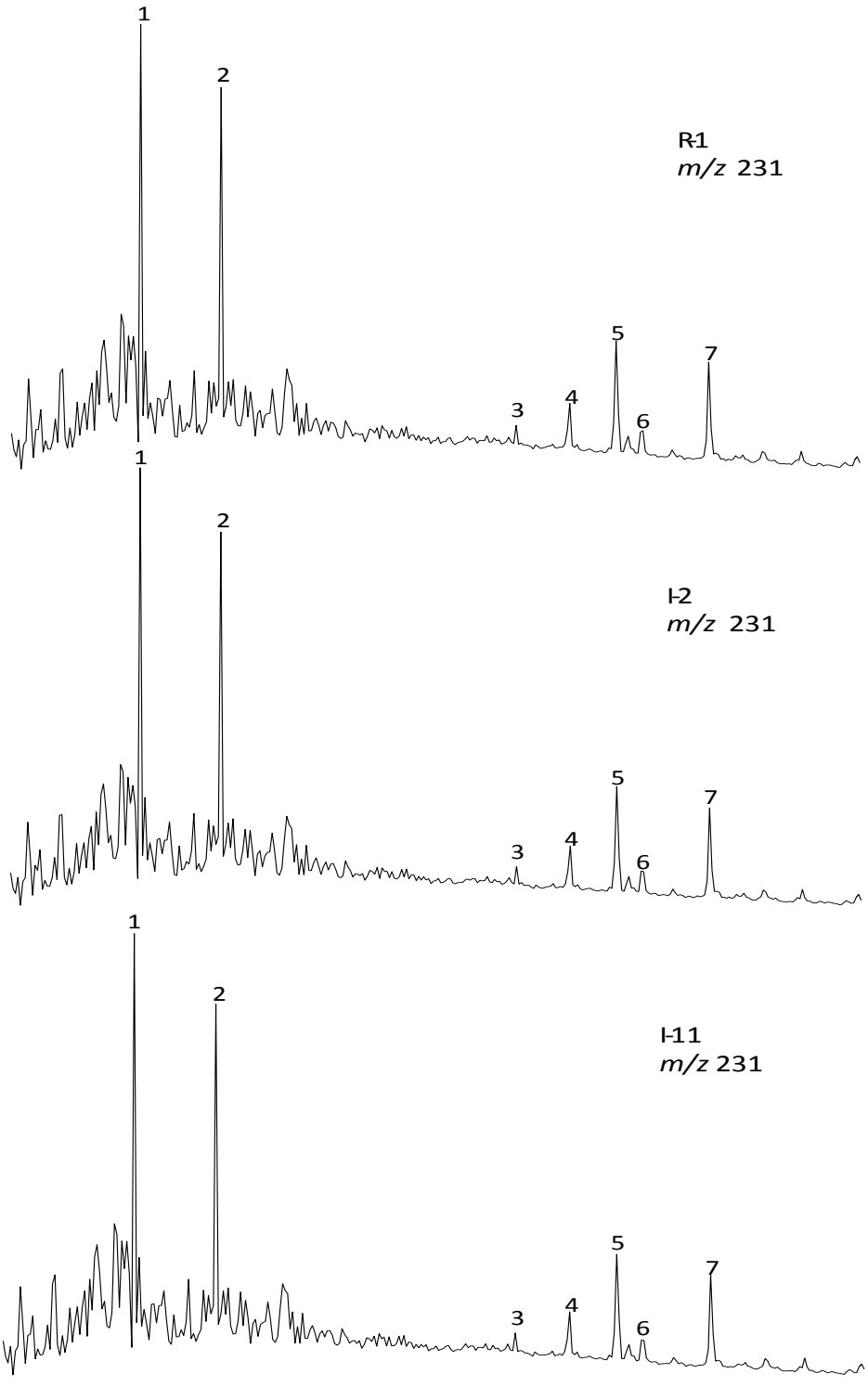

Figure 4.21. (cont.)

4.2.2.4 Mono- and triaromatic steroid hydrocarbons

The distribution of mono- and triaromatic steroid hydrocarbons in the aromatic fractions of the oil samples as determined from their *m/z* 253 and *m/z* 231 chromatograms are shown in Figures 4.20 and 4.21. Values of mono- and triaromatic steroid hydrocarbon ratios calculated from the peak areas of the *m/z* 253 and *m/z* 231 mass chromatograms are listed in Table 4.11, and their peak identities are shown in Table 4.12. For more detailed information about these two parameters, see Section 2.5.2.7 in Chapter II. Oils from A-Field show high values of MA(I)/MA(I+II) and TA(I)/TA(I+II) ratios in the range of 0.61–0.68 and 0.8–0.9, respectively (Table 4.11), indicating higher levels of thermal maturity for these oils (Figures 4.20, 4.21, and 4.22). Whereas, both oils from R- and I Fields display lower values ranging from 0.45–0.46 and 0.60–0.66, respectively (Table 4.11), suggesting intermediate levels of thermal maturity (Figures 4.20, 4.21, and 4.22; Table 4.11). This suggestion is further supported by the values of MPI-2 (Table 4.11; Figure 4.22).

4.2.3 Extent of Biodegradation

The normal distribution of *n*-alkanes in oils showing relatively abundant 25-norhopanes is usually taken as an indicator of mixing of fresh oils with biodegraded oil residues (Philp, 1982), and such mixing may be common in biodegraded oil reservoirs (Koopmans et al., 2002). The 25-norhopanes result from the bacterial removal of methyl group at C-10 from regular hopanes during biodegradation (Peters and Moldowan, 1993).

Table 4.12. Monoaromatic (*m/z* 253) and triaromatic steroid hydrocarbons (*m/z* 231) identified in chromatograms of Figures 4.20 and 4.21.

Monoaromatic steroids		Triaromatic steroids		
Peak I.D.	Compounds	Peak I.D.	Elemental composition	compound
1	Pregnane (X = ethyl)	1	$C_{20}H_{20}$	C_{20}-triaromatic sterane
2	20-Methylpregnane (X = 2-propyl)	2	$C_{21}H_{22}$	C_{21}-triaromatic sterane
3	Monoaromatic sterane C27	3	$C_{26}H_{32}$	C_{26}-triaromatic sterane (20S)
4	Monoaromatic sterane C27	4	$C_{26}H_{32}$ + $C_{27}H_{34}$	C_{26}-triaromatic sterane (20R) + C_{27}-triaromatic sterane (20S)
5	Monoaromatic sterane C27	5	$C_{28}H_{36}$	C_{28}-triaromatic sterane (20S)
6	Monoaromatic sterane C27+C28	6	$C_{27}H_{34}$	C_{27}-triaromatic sterane (20R)
7	Monoaromatic sterane C27+C28	7	$C_{28}H_{36}$	C_{28}-triaromatic sterane (20R)
8+9	Monoaromatic sterane C27+C28			
10	Monoaromatic sterane C27+C28			
11	Monoaromatic sterane C27+C28			
12	Monoaromatic sterane C28+C29			
13	Monoaromatic sterane C28+C29			
14	Monoaromatic sterane C29			
15	Monoaromatic sterane C29			

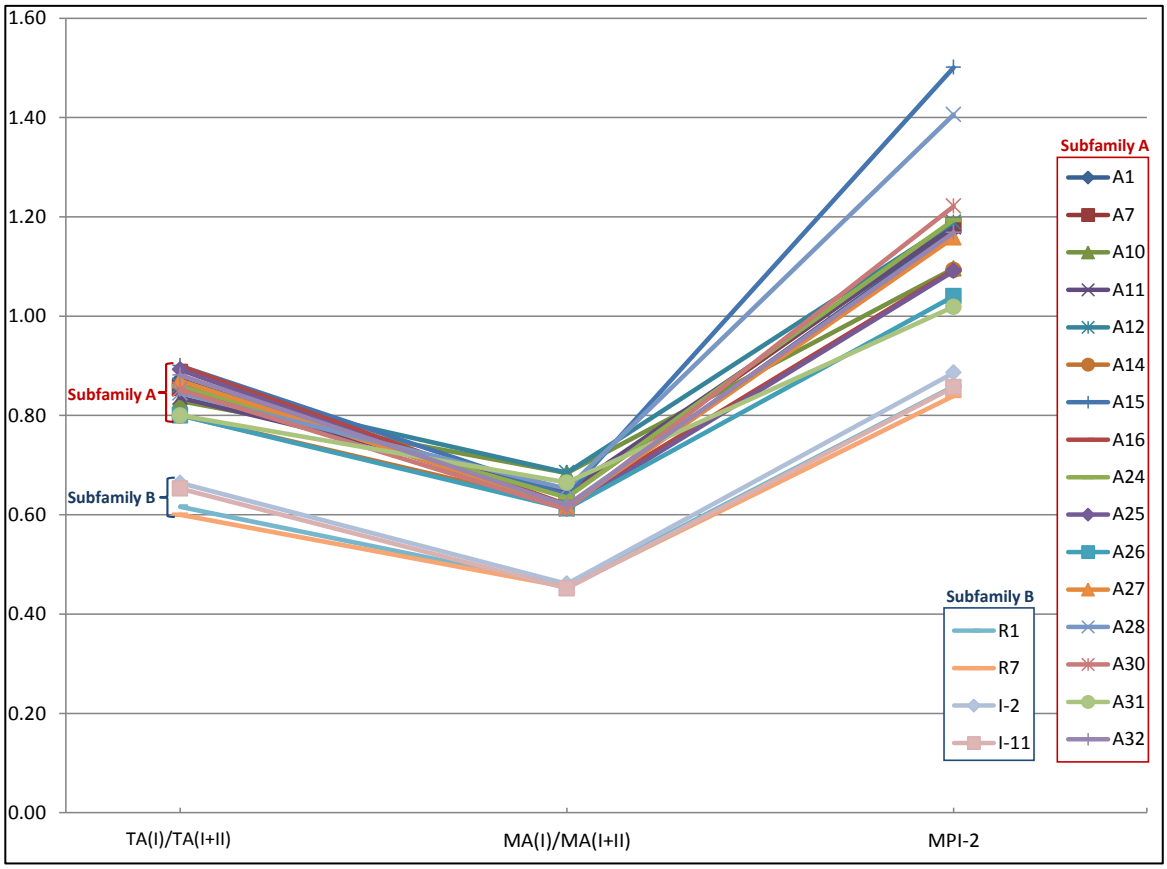

Figure 4.22. Showing the two subfamilies (A&B) of oils based on the aromatic maturity parameters.

In these oils, the distribution of *n*-alkanes range from *n*-C_{11} to *n*-C_{32} (Figure 4.13), suggest that the oils have not been biodegraded. This conclusion is further supported by GC-MS analysis for the B/C of saturate hydrocarbons (*m/z* 177), where no 25-norhopanes were detected in any of the oils (Figure 4.23).

4.2.4 Relative biomarker concentrations and correlations

To better understand and characterize the biomarker distributions in crude oils, a quantitative analysis was undertaken on both rock extracts and crude oils from the A-, R-, and I-Fields in the El-Sharara Oil Field, Murzuq Basin (Figure 1.1). A quantitative approach is helpful in establishing a comparison of biomarker concentrations in oils and source rocks (Eglinton and Douglas, 1988). The diversity in biomarker concentrations illustrates differences in sources, depositional environments and quality of the source rocks and oils (Wang, 1993; Wang and Philp, 1997). The concentration of biomarkers decreases with increasing maturity levels of the source rock (Fu et al., 1985; Requejo, 1992), and increases with biodegradation relative to unaltered samples (Seifert and Moldowan, 1979; Requejo et al., 1989). Rullkötter et al., (1984) used biomarker concentrations together with other molecular characteristics to classify families of oils and to recognize mixing of oils of different maturities (Rullkötter et al., 1984b). Quantitative analysis has also been used in classification of depositional environments (Mello et al., 1988a), and assessment of the relative contributions of biomarkers originating from bitumen and kerogen during simulated maturation of source rocks (Eglinton and Douglas, 1988).

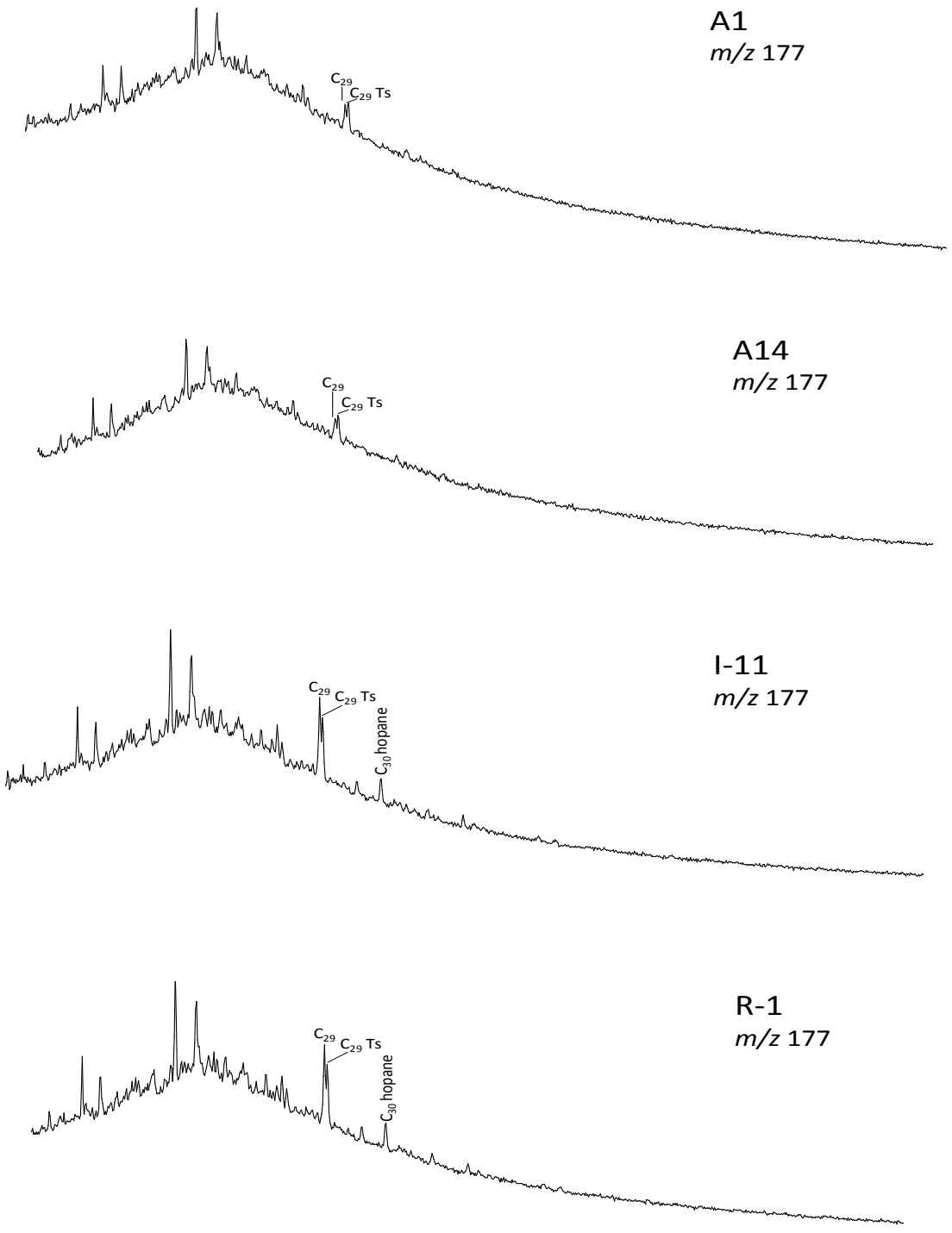

Figure 4.23. Mass chromatograms showing: the absence of 25-norhopanes (*m/z* 177) of selected crude oils from A-, I-, & R-Fields within Murzuq Basin, S.W. Libya. For more mass chromatograms of rock samples see Appendix XI.

The relative biomarker concentrations of both Tanezzuft 'cool' shale samples and crude oils normalized to saturate fractions and expressed by the unit of micrograms of biomarkers per gram of saturate fraction (μg/g Sat) or ppm are shown in Tables 4.13 and 4.14, respectively. The relative concentrations of various steranes and hopanes for crude oils are plotted in Figures 4.24 and 4.25. Based on the distribution of relative concentrations of C_{27}, C_{28}, and C_{29} regular steranes (Figure 4.24), all crude oils are genetically related as indicated by the ternary diagram of these compounds (Figure 4.17). This conclusion is further supported by the similar carbon isotope values for these oil samples, as will be mentioned later and the distribution of triterpanes (Figure 4.25), where the majority of oils show a similar distribution trend, even though there are two samples (A27 and A30) that show higher concentrations of C_{21} and C_{23} tricyclic terpanes. This may be related to maturity since it has been confirmed that all oils have a similar origin. The relative concentrations of various triterpanes and steranes of the Tanezzuft 'cool' shales are plotted in Figures 4.26 and 4.27, respectively. Based on the distribution of relative triterpane concentrations (Figure 4.26), only one sample (A3) displays relatively high concentrations of triterpanes relative to the rest of the rock samples. This is most probably due to the variation in organic facies in the Tanezzuft "cool" shale rather than maturity since all samples show a small range of thermal maturity levels (early–intermediate) according to several maturity parameters [e.g. Rock-Eval data, 22S/(22S+22R) homohopane isomerization, ββ/(ββ+αα) and 20S/(20S+20R) sterane isomerization ratios, as well as C_{30}-moretane/C_{30}-hopane ratios]. However, the majority of samples in Figure 4.26 are dominated by the C_{30} hopane, C_{23} tricyclic terpane, and C_{29} norhopane, respectively. The trend of the extended homohopane distributions shows a gradual decrease in abundance of homohopane epimers (C_{31}S+R homologues dominated)

Table 4.13. The relative biomarker concentration of Tanezzuft 'cool' shale samples (µg/g Sat) normalized to saturate fractions- *m/z* 191 and 217 biomarker distributions.

	Depth	C_{19}/3	C_{20}/3	C_{21}/3	C_{22}/3	C_{23}/3	C_{24}/3	C_{25}/3	C_{24}/4	Ts	Tm	C_{29}	C_{29}Ts	C_{30}d	C_{30} Hop.	C_{30} Mor.	C_{31}abS	C_{31}abR	C_{32}abS	C_{32}abR	C_{33}abS	C_{33}abR	C_{34}abS	C_{34}abR	C_{35}abS	C_{35}abR
Sample ID	(ft)	(ppm)	(ppm)	(ppm)	(ppm)	(ppm)	(ppm)	(ppm)	(ppm)	(ppm)	(ppm)	(ppm)	(ppm)	(ppm)	(ppm)	(ppm)	(ppm)	(ppm)	(ppm)	(ppm)	(ppm)	(ppm)	(ppm)	(ppm)	(ppm)	(ppm)
A3	4213	4.68	8.47	12.45	4.82	22.71	10.11	7.07	6.19	8.51	10.40	19.84	8.39	4.94	29.79	6.92	11.03	8.32	6.60	4.98	3.89	2.98	2.40	1.90	1.69	1.40
A5	4315	0.13	0.18	0.27	0.08	0.36	0.18	0.11	0.14	0.23	0.15	0.34	0.19	0.10	0.51	0.18	0.19	0.39	0.11	0.18	0.07	0.05	0.06	0.03	0.03	0.03
A6a	4500	0.03	0.04	0.12	0.08	0.47	0.38	0.40	0.01	0.00	0.00	0.00	0.00	0.00	0.00	0.00	0.00	0.00	0.00	0.00	0.00	0.00	0.00	0.00	0.00	0.00
A6b	4610	1.77	3.53	5.99	1.52	7.89	4.66	2.97	0.48	0.42	0.40	0.75	0.20	0.13	1.04	0.14	0.51	0.32	0.31	0.18	0.18	0.12	0.04	0.08	0.00	0.00
A10	4659	0.13	0.22	0.32	0.09	0.47	0.22	0.15	0.10	0.07	0.06	0.08	0.02	0.02	0.07	0.02	0.04	0.02	0.02	0.01	0.01	0.01	0.01	0.00	0.00	0.00
A17a	4370	0.21	0.28	0.36	0.08	0.38	0.18	0.13	0.13	0.28	0.15	0.35	0.19	0.13	0.59	0.11	0.17	0.14	0.12	0.10	0.08	0.06	0.06	0.04	0.03	0.03
A17b	4190	0.03	0.05	0.06	0.02	0.06	0.03	0.02	0.03	0.03	0.02	0.04	0.02	0.00	0.06	0.01	0.02	0.01	0.01	0.01	0.01	0.00	0.00	0.00	0.00	0.00
A18	4200	0.01	0.02	0.03	0.01	0.03	0.02	0.01	0.01	0.01	0.01	0.02	0.01	0.00	0.03	0.01	0.01	0.01	0.00	0.00	0.00	0.00	0.00	0.00	0.00	0.00
A19a	4565	0.15	0.29	0.38	0.12	0.62	0.28	0.18	0.15	0.15	0.13	0.23	0.08	0.04	0.29	0.05	0.09	0.07	0.05	0.03	0.03	0.02	0.01	0.01	0.00	0.00
A19b	4200	0.15	0.29	0.38	0.12	0.62	0.28	0.18	0.15	0.15	0.13	0.23	0.08	0.04	0.29	0.05	0.09	0.07	0.05	0.03	0.03	0.02	0.01	0.01	0.00	0.00
A20a	4545	0.07	0.12	0.17	0.05	0.22	0.09	0.06	0.08	0.15	0.11	0.19	0.16	0.06	0.31	0.05	0.09	0.07	0.05	0.04	0.02	0.02	0.01	0.01	0.01	0.00
A20b	4295	0.05	0.09	0.16	0.07	0.39	0.20	0.16	0.10	0.09	0.11	0.20	0.04	0.04	0.21	0.04	0.08	0.06	0.05	0.03	0.03	0.02	0.02	0.01	0.01	0.01
A21	4600	0.05	0.08	0.12	0.04	0.24	0.12	0.09	0.07	0.09	0.08	0.09	0.08	0.04	0.17	0.02	0.05	0.04	0.04	0.03	0.02	0.01	0.01	0.01	0.01	0.00
A22	4600	0.05	0.09	0.16	0.07	0.39	0.20	0.16	0.10	0.09	0.11	0.20	0.04	0.04	0.21	0.04	0.08	0.06	0.05	0.03	0.03	0.02	0.02	0.01	0.01	0.01
A23	4150	0.41	0.71	1.04	0.30	1.47	0.69	0.44	0.40	0.52	0.40	0.65	0.20	0.13	0.81	0.11	0.19	0.14	0.13	0.08	0.07	0.04	0.04	0.03	0.00	0.00
A34	4730	0.05	0.07	0.12	0.04	0.18	0.09	0.07	0.06	0.12	0.08	0.10	0.09	0.07	0.18	0.04	0.06	0.05	0.04	0.03	0.02	0.02	0.02	0.01	0.01	0.01
A35a	4840	0.02	0.03	0.06	0.03	0.13	0.06	0.04	0.02	0.03	0.04	0.12	0.03	0.02	0.14	0.03	0.05	0.04	0.03	0.02	0.02	0.01	0.01	0.01	0.00	0.00
A35b	4000	0.48	1.30	3.30	2.40	9.54	4.95	3.48	1.69	1.06	1.42	2.14	0.42	0.21	2.24	0.25	0.64	0.50	0.32	0.23	0.12	0.10	0.14	0.05	0.00	0.00
A37a	5010	0.07	0.11	0.20	0.10	0.53	0.27	0.23	0.10	0.10	0.06	0.15	0.04	0.06	0.18	0.04	0.05	0.05	0.03	0.03	0.02	0.02	0.02	0.01	0.01	0.01
A37b	4570	0.39	0.55	0.91	0.61	1.82	0.81	0.60	1.15	2.82	2.09	5.45	3.68	0.90	7.93	1.60	2.95	2.00	1.48	1.10	0.63	0.48	0.42	0.27	0.15	0.09

***m/z* 217**

	Depth	I	Preg.	III	Homprg.	1	2	3	4	5	6	7	8	9	10	11	12	13	14	15	16	17	18	19	20
	(ft)	21aa	21bb	22aa	22bb	27dβS	27dβR	27dαS	27dαR	28dβS	28dβR	αα 20(S)	ββ 20(R)	ββ 20(S)	αα 20(R)	29dβR	29dβS	αα 20(S)	ββ 20(R)	ββ 20(S)	αα 20(R)	αα 20(S)	ββ 20(R)	ββ 20(S)	αα 20(R)
A3	4213	5.38	10.13	4.14	4.93	3.78	2.50	1.19	1.94	3.25	2.36	3.21	5.95	2.77	3.89	4.31	2.88	2.00	1.64	2.80	2.37	3.43	3.64	2.64	4.84
A5	4315	0.13	0.20	0.08	0.09	0.07	0.05	0.02	0.03	0.05	0.03	0.05	0.09	0.06	0.05	0.06	0.04	0.03	0.03	0.04	0.03	0.04	0.05	0.04	0.06
A6a	4500	0.07	0.12	0.06	0.08	0.27	0.17	0.05	0.06	0.13	0.09	0.05	0.10	0.09	0.05	0.08	0.02	0.03	0.02	0.03	0.03	0.02	0.03	0.03	0.03
A6b	4610	3.70	7.79	2.42	2.42	1.18	0.68	0.24	0.27	0.58	0.33	0.35	0.62	0.37	0.30	0.44	0.20	0.24	0.23	0.22	0.16	0.18	0.29	0.21	0.19
A10	4659	0.15	0.33	0.00	0.10	0.05	0.04	0.01	0.02	0.03	0.02	0.02	0.05	0.03	0.03	0.03	0.02	0.01	0.01	0.02	0.01	0.01	0.02	0.01	0.02
A17a	4370	0.18	0.39	0.00	0.12	0.11	0.09	0.03	0.05	0.10	0.08	0.06	0.18	0.10	0.05	0.13	0.08	0.05	0.05	0.11	0.05	0.08	0.12	0.10	0.10
A17b	4190	0.03	0.06	0.00	0.02	0.01	0.01	0.00	0.00	0.01	0.01	0.01	0.02	0.01	0.01	0.01	0.01	0.00	0.00	0.01	0.00	0.01	0.01	0.01	0.01
A18	4200	0.01	0.03	0.00	0.01	0.01	0.00	0.00	0.00	0.00	0.00	0.00	0.01	0.00	0.00	0.00	0.00	0.00	0.00	0.00	0.00	0.00	0.00	0.00	0.00
A19a	4565	0.16	0.43	0.00	0.14	0.07	0.05	0.05	0.02	0.04	0.03	0.04	0.08	0.05	0.05	0.06	0.04	0.03	0.03	0.03	0.03	0.03	0.06	0.03	0.04
A19b	4200	0.16	0.43	0.00	0.14	0.07	0.05	0.02	0.02	0.04	0.03	0.04	0.08	0.05	0.05	0.06	0.04	0.03	0.03	0.03	0.03	0.03	0.06	0.03	0.04
A20a	4545	0.08	0.17	0.00	0.05	0.04	0.03	0.01	0.02	0.03	0.02	0.02	0.04	0.02	0.02	0.04	0.02	0.01	0.01	0.02	0.01	0.01	0.02	0.02	0.03
A20b	4295	0.07	0.20	0.00	0.08	0.04	0.03	0.03	0.02	0.03	0.02	0.04	0.06	0.05	0.04	0.04	0.02	0.03	0.02	0.02	0.02	0.02	0.04	0.02	0.03
A21	4600	0.06	0.16	0.00	0.07	0.05	0.03	0.01	0.02	0.04	0.02	0.03	0.06	0.04	0.02	0.05	0.02	0.02	0.02	0.03	0.01	0.02	0.03	0.02	0.03
A22	4600	0.07	0.20	0.00	0.08	0.04	0.03	0.01	0.02	0.03	0.02	0.04	0.06	0.05	0.04	0.04	0.02	0.03	0.02	0.02	0.02	0.02	0.04	0.02	0.03
A23	4150	0.53	0.67	0.48	0.42	0.26	0.18	0.08	0.10	0.19	0.12	0.13	0.27	0.13	0.09	0.24	0.11	0.09	0.08	0.14	0.06	0.08	0.12	0.09	0.13
A34	4730	0.06	0.08	0.05	0.05	0.07	0.05	0.02	0.03	0.05	0.05	0.03	0.09	0.04	0.03	0.07	0.04	0.02	0.02	0.04	0.01	0.02	0.04	0.03	0.03
A35a	4840	0.02	0.06	0.00	0.02	0.02	0.02	0.01	0.01	0.02	0.02	0.02	0.04	0.03	0.02	0.03	0.02	0.01	0.01	0.02	0.02	0.02	0.02	0.01	0.02
A35b	4000	0.84	3.44	0.00	1.48	0.79	0.57	0.19	0.27	0.71	0.38	0.76	1.13	1.05	0.89	0.58	0.41	0.60	0.45	0.34	0.43	0.41	0.55	0.37	0.42
A37a	5010	0.09	0.26	0.00	0.10	0.09	0.06	0.02	0.04	0.07	0.04	0.07	0.11	0.10	0.07	0.08	0.04	0.05	0.04	0.05	0.03	0.03	0.05	0.04	0.05
A37b	4570	0.27	0.80	0.00	0.31	0.36	0.27	0.14	0.21	0.43	0.40	0.54	0.67	0.44	0.52	0.63	0.47	0.36	0.27	0.54	0.46	0.48	0.50	0.39	0.61

Table 4.14. Relative biomarker concentrations of crude oils (µg/g Sat) normalized to the saturate fractions-*m/z* 191 and 217 biomarker distributions.

***m/z* 191**

Sample ID	C_{19}/3 (ppm)	C_{20}/3 (ppm)	C_{21}/3 (ppm)	C_{22}/3 (ppm)	C_{23}/3 (ppm)	C_{24}/3 (ppm)	C_{25}/3 (ppm)	C_{24}/4 (ppm)	Ts (ppm)	Tm (ppm)	C_{29} (ppm)	C_{29}Ts (ppm)	C_{30}d (ppm)	C_{30} Hop. (ppm)	C_{30} Mor. (ppm)	C_{31}abS (ppm)	C_{31}abR (ppm)	C_{32}abS (ppm)	C_{32}abR (ppm)	C_{33}abS (ppm)	C_{33}abR (ppm)	C_{34}abS (ppm)	C_{34}abR (ppm)	C_{35}abS (ppm)	C_{35}abR (ppm)
A1	9.56	10.80	18.57	8.57	26.48	21.58	14.73	10.04	13.39	7.83	12.68	7.61	10.48	18.66	2.34	–	–	–	–	–	–	–	–	–	–
A7	6.59	10.61	15.19	6.62	25.66	16.14	13.83	9.28	16.33	6.11	10.88	4.90	7.65	18.14	3.00	–	–	–	–	–	–	–	–	–	–
A10	0.80	0.52	0.63	0.92	1.21	2.74	2.14	0.56	1.45	0.82	1.66	0.61	0.99	2.73	0.73	–	–	–	–	–	–	–	–	–	–
A11	2.72	6.04	10.11	3.36	14.02	11.23	7.41	4.21	6.14	3.82	6.66	3.24	4.26	10.62	1.06	–	–	–	–	–	–	–	–	–	–
A12	2.69	2.73	5.47	2.55	7.18	5.02	2.07	0.60	1.40	0.54	0.86	0.60	1.02	1.89	0.43	–	–	–	–	–	–	–	–	–	–
A14	3.35	3.09	5.53	1.66	8.16	5.30	4.08	1.15	5.16	2.40	3.34	2.01	3.11	7.00	1.83	–	–	–	–	–	–	–	–	–	–
A15	3.89	5.44	10.00	2.42	14.12	11.79	7.83	4.43	6.99	3.80	6.64	2.81	3.70	10.00	1.70	–	–	–	–	–	–	–	–	–	–
A16	6.12	4.90	8.01	2.68	11.83	8.82	6.09	1.65	5.24	3.04	5.24	2.99	4.83	9.61	2.61	–	–	–	–	–	–	–	–	–	–
A24	4.32	3.00	6.04	1.72	8.91	6.29	4.56	1.06	3.89	1.56	3.76	2.14	2.63	6.54	1.25	–	–	–	–	–	–	–	–	–	–
A25	5.58	4.18	8.14	2.31	11.06	7.32	6.53	1.74	9.89	2.89	4.73	2.42	4.05	7.34	1.61	–	–	–	–	–	–	–	–	–	–
A26	2.91	4.54	8.56	2.71	12.77	9.18	6.65	4.48	5.38	2.83	5.27	1.85	4.34	9.20	0.58	–	–	–	–	–	–	–	–	–	–
A27	13.36	17.88	38.88	12.99	60.57	43.37	32.67	22.42	34.31	16.29	25.17	9.97	19.14	40.11	3.50	–	–	–	–	–	–	–	–	–	–
A28	7.74	6.74	14.01	3.75	18.72	12.89	9.11	2.97	18.83	4.77	7.69	4.75	6.85	15.01	2.40	–	–	–	–	–	–	–	–	–	–
A30	15.62	17.01	33.86	13.39	56.60	38.54	29.27	18.20	21.61	11.99	22.83	10.62	13.26	35.88	4.68	–	–	–	–	–	–	–	–	–	–
A31	7.01	6.65	14.65	4.16	19.07	14.91	9.54	3.04	9.96	4.29	7.87	4.04	4.83	14.91	3.46	–	–	–	–	–	–	–	–	–	–
A32	3.11	5.57	10.68	4.16	16.42	10.89	9.51	5.29	6.28	4.31	6.74	2.64	5.82	9.28	1.15	–	–	–	–	–	–	–	–	–	–
I-2	10.05	8.20	14.62	3.66	23.65	15.12	11.35	3.89	13.20	10.43	24.00	7.21	9.85	48.04	6.61	12.95	8.40	7.96	6.54	6.06	4.09	5.76	3.54	3.24	2.40
I-11	5.14	5.46	10.74	2.39	19.53	10.95	8.85	3.56	11.32	4.53	19.45	4.52	6.48	36.58	4.01	9.29	6.29	7.08	4.74	4.15	2.96	4.04	2.04	1.78	1.27
R-1	11.28	8.55	18.63	4.12	29.13	16.78	15.36	4.47	15.38	11.39	29.22	11.37	9.32	57.21	7.31	14.81	10.56	11.89	7.35	7.51	4.08	7.42	3.82	3.08	2.63
R-7	5.17	9.47	12.48	2.53	20.17	13.22	6.93	4.56	13.33	4.96	22.26	5.97	8.39	41.77	4.67	10.56	7.19	8.91	6.03	4.59	3.47	5.05	2.94	2.66	1.26

***m/z* 217**

Sample ID	21αα	Preg. 21ββ	22αα	Homprg. 22ββ	1 27dβS	2 27dβR	3 27dαS	4 27dαR	5 28dβS	6 28dβR	7 αα 20(S)	8 ββ 20(R)	9 ββ 20(S)	10 αα 20(R)	11 29dβR	12 29dβS	13 αα 20(S)	14 ββ 20(R)	15 ββ 20(S)	16 αα 20(R)	17 αα 20(S)	18 ββ 20(R)	19 ββ 20(S)	20 αα 20(R)
A1	24.7	43.8	24.0	26.1	25.9	19.3	19.3	11.5	38.9	23.4	13.6	47.2	16.4	13.0	28.6	15.6	11.0	19.4	25.5	9.0	16.8	30.6	23.9	23.4
A7	13.3	22.0	15.5	13.9	11.2	8.1	8.1	5.0	17.4	10.3	6.0	20.9	7.6	5.2	13.3	7.0	4.2	7.6	11.5	4.1	7.4	12.8	9.5	10.0
A10	4.5	8.3	4.6	4.7	3.8	2.9	2.9	1.8	6.6	3.8	2.4	8.0	3.2	2.7	4.2	2.5	2.0	3.8	4.4	2.2	2.9	4.8	3.6	3.6
A11	13.0	24.0	15.6	14.3	13.7	9.0	2.4	4.2	6.1	9.1	7.8	29.9	11.0	17.3	8.8	10.2	6.3	12.6	13.8	5.2	8.8	18.1	13.6	13.6
A12	4.4	8.1	4.6	4.5	3.2	2.4	2.4	1.2	4.5	2.5	1.4	4.9	1.6	1.3	2.8	1.7	1.0	1.8	2.4	0.7	1.7	2.7	2.1	2.0
A14	7.3	14.7	6.8	8.4	7.9	5.8	5.8	3.3	11.8	7.5	4.3	14.2	5.1	4.2	8.4	5.6	3.4	5.6	8.3	2.7	5.4	9.3	7.2	7.2
A15	24.2	45.3	22.6	26.2	24.5	18.3	18.3	11.6	38.7	18.5	16.2	50.0	16.8	15.1	27.7	17.9	9.0	17.0	28.6	9.4	17.6	30.1	23.7	23.6
A16	10.7	21.2	9.9	12.0	11.7	8.5	8.5	4.8	18.3	10.6	6.3	21.8	7.5	6.5	12.9	7.9	6.2	9.5	13.1	6.9	8.8	14.2	10.8	10.9
A24	7.7	15.7	7.3	8.7	8.0	6.7	6.7	4.2	13.2	7.4	4.5	15.8	5.3	4.9	9.2	5.7	4.5	6.7	9.3	3.4	5.9	10.2	8.0	8.2
A25	10.0	19.6	9.2	10.8	10.0	7.6	7.6	4.5	15.8	10.3	5.4	19.7	6.8	6.1	11.3	6.8	5.2	8.3	11.6	4.1	7.2	12.2	9.7	9.8
A26	8.2	16.5	7.9	9.0	8.6	6.5	6.5	4.3	13.2	7.8	4.3	16.2	5.4	4.6	9.5	5.8	4.1	6.8	9.5	4.9	6.2	11.1	8.1	8.0
A27	54.2	98.0	64.7	59.7	54.0	35.3	17.6	24.0	31.1	66.0	33.2	124.2	54.8	74.4	43.1	42.9	27.1	51.6	58.8	20.7	35.4	75.4	57.4	51.6
A28	17.6	33.5	15.8	18.9	17.9	13.6	13.6	8.2	28.3	17.2	9.6	34.2	11.5	10.7	20.5	13.4	8.7	14.8	20.9	7.6	13.2	22.6	16.6	17.5
A30	45.5	83.1	52.9	50.1	44.5	31.6	10.6	17.7	22.1	25.2	25.3	94.4	32.3	60.6	30.4	29.8	21.0	43.7	51.8	17.0	28.7	62.2	45.9	45.0
A31	17.3	34.7	16.4	19.4	17.5	13.7	13.7	8.8	29.3	18.9	10.3	34.5	13.2	11.0	20.2	14.0	9.0	14.9	20.6	7.0	13.9	23.2	17.3	17.7
A32	32.8	64.4	29.0	34.7	33.1	26.4	26.4	15.7	52.6	29.9	17.3	62.3	23.2	20.1	36.8	23.6	16.0	27.1	37.1	13.3	23.8	40.9	32.3	32.5
I-2	20.0	41.0	17.7	25.0	25.3	19.4	19.4	12.3	34.6	19.8	18.2	54.6	32.6	16.7	30.1	20.4	15.4	19.3	30.2	15.6	21.5	37.2	27.2	25.5
I-11	18.4	38.1	15.4	23.0	22.4	16.9	16.9	11.0	31.8	19.3	13.3	45.9	17.4	12.8	26.0	17.3	11.6	17.2	27.1	13.7	20.9	34.0	25.7	22.8
R-1	25.5	51.1	21.0	31.3	30.2	22.9	22.9	14.6	41.1	22.9	22.2	67.1	33.2	15.6	42.5	23.9	17.0	22.4	35.3	17.0	26.2	44.5	33.0	31.5
R-7	29.2	59.4	24.0	35.3	36.4	27.8	27.8	17.7	51.0	30.6	20.3	72.2	27.0	16.1	47.4	27.5	20.2	26.5	42.8	15.9	30.7	54.3	39.2	35.2

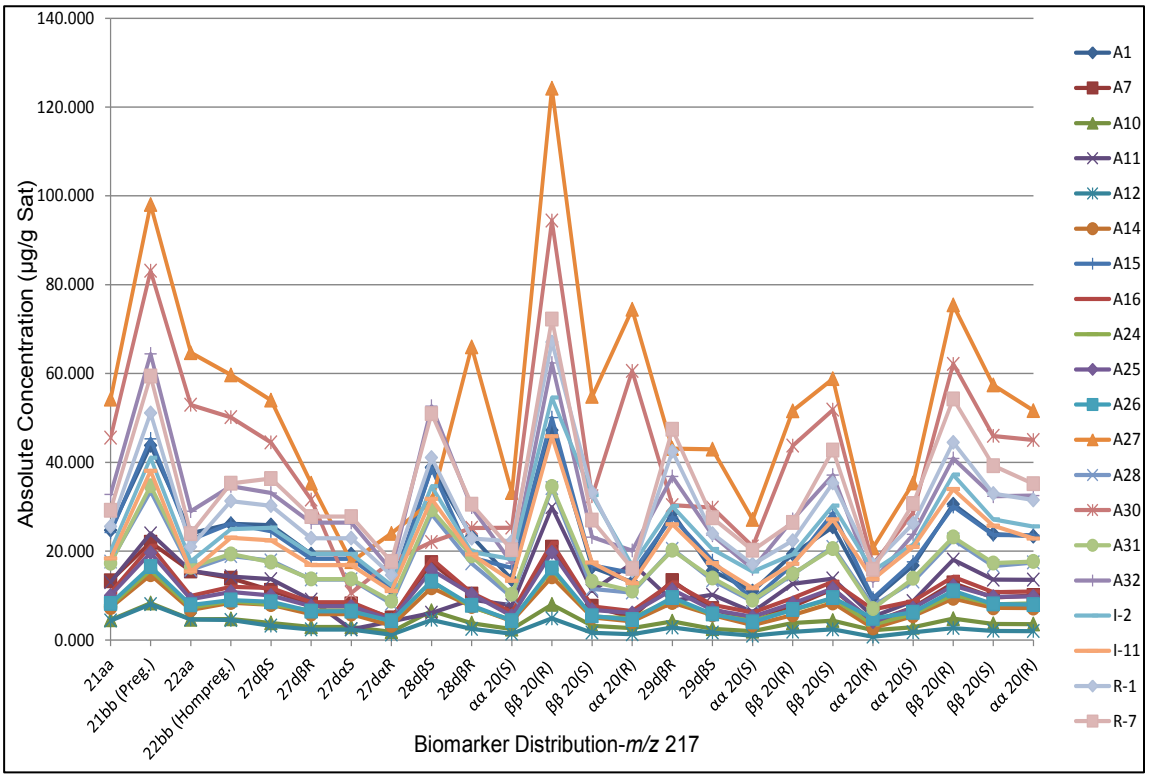

Figure 4.24. The relative distribution of sterane concentrations for crude oil from the *m/z* 217 chromatograms. Murzuq Basin, S.W. Libya.

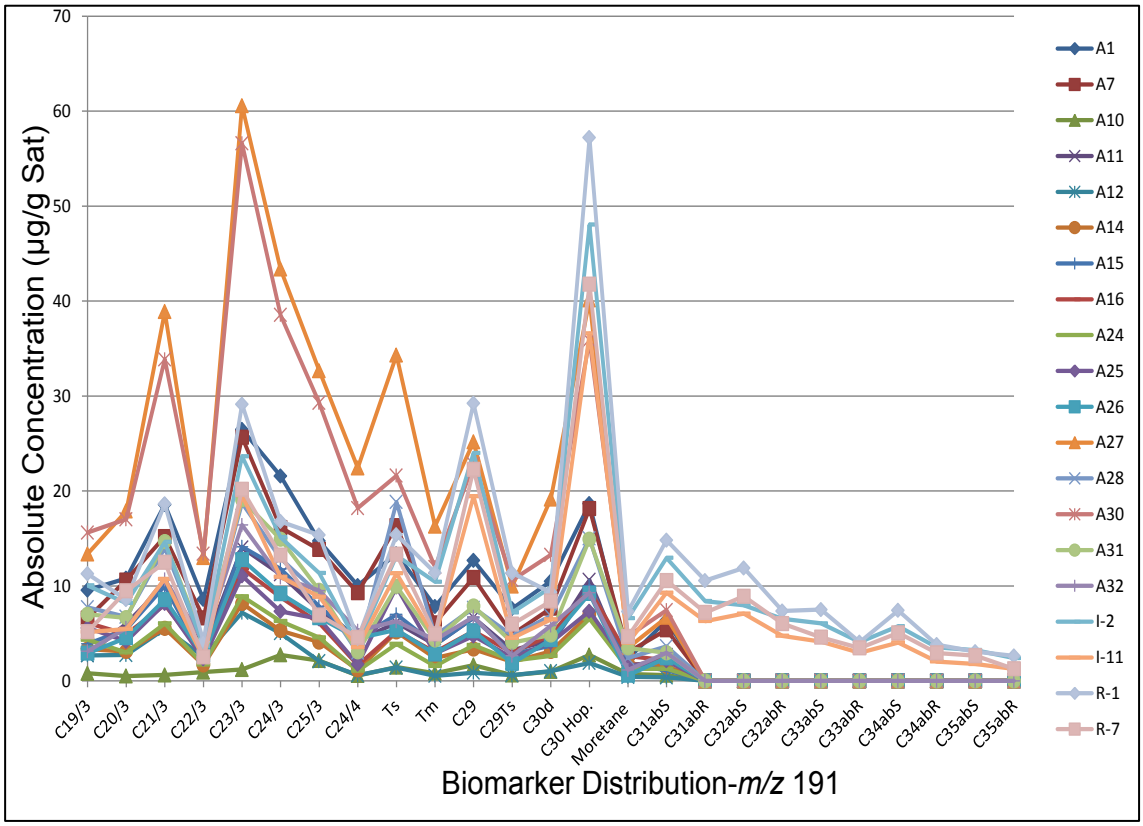

Figure 4.25. The relative distribution of triterpane concentrations for crude oil from the *m/z* 191 chromatograms. Murzuq Basin, S.W. Libya.

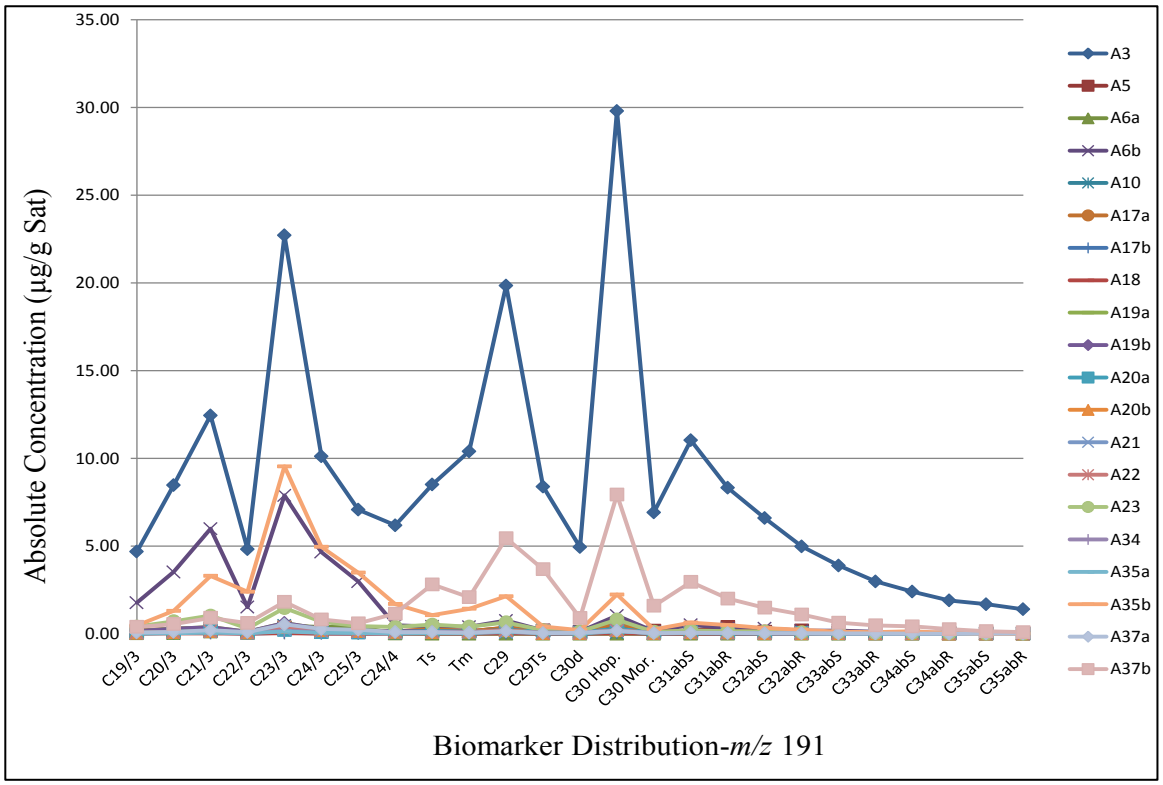

Figure 4.26. The relative distribution of triterpane concentrations for Tanezzuft 'cool' shale samples from the *m/z* 191 chromatograms. Murzuq Basin, S.W. Libya.

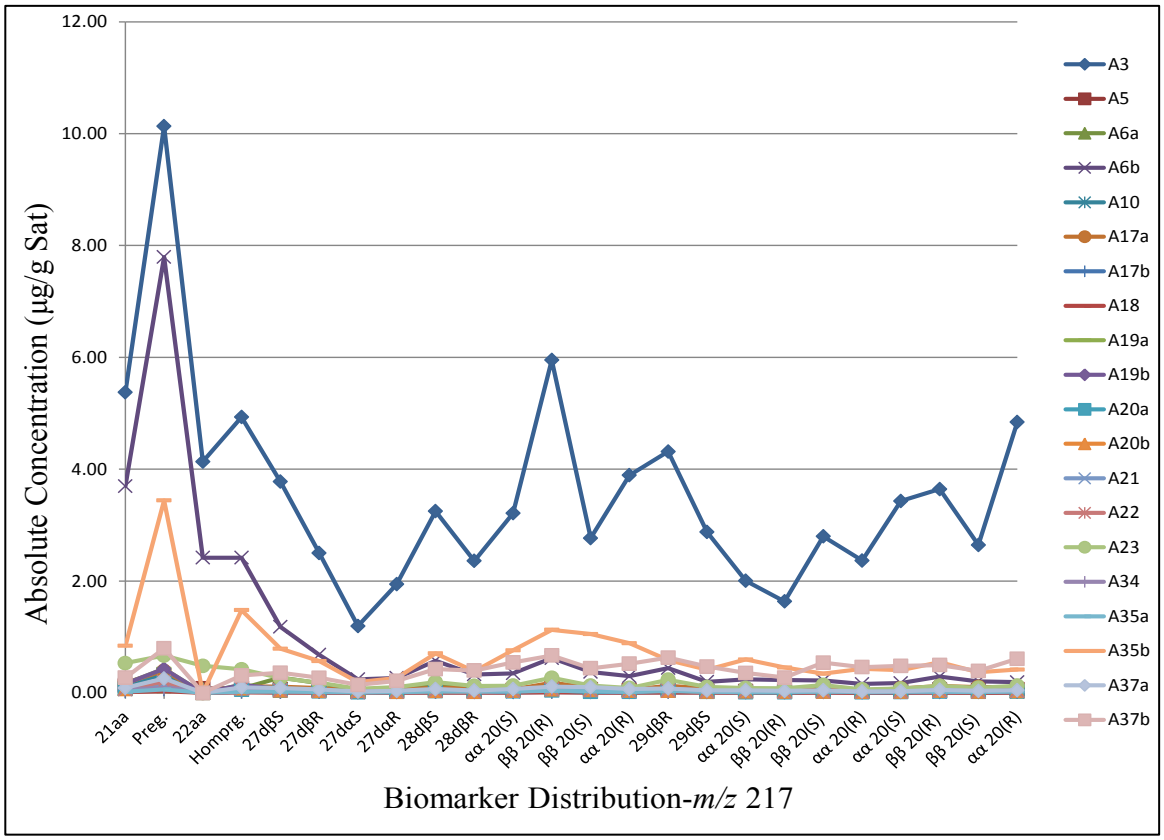

Figure 4.27. The relative distribution of sterane concentrations for Tanezzuft 'cool' shale samples from the *m/z* 217 chromatograms. Murzuq Basin, S.W. Libya.

for all samples, suggesting sub-oxic depositional environment conditions (Peters and Moldowan, 1993) as indicated by the low quality organic matter (e.g. low hydrogen index; Dahl et al., 1994) for these samples. Based on the distribution of relative sterane concentrations (Figure 4.27), sample A3 shows different patterns of sterane distributions than the other samples. Hence, variation of organic facies is a factor to be considered since the majority of samples are at early maturity.

4.2.4.1 Oil-oil correlation and classification

Oil/oil correlations were undertaken using stable carbon isotopic compositions ($\delta^{13}C$), and biomarker distributions, isoprenoids (Pr & Ph) and *n*-alkanes (C_{17} & C_{18}), as well as aromatic maturity parameters (e.g. MPI, MA(I)/MA(I+II), and TA(I)/TA(I+II) ratios). Bulk isotopic compositions for selected oils (e.g. A11, A12, A31, I-2, R-1) showed similar values (–29.30 ‰, –29.30‰, –29.09‰, –29.80‰, –29.68‰, respectively), suggesting they were all genetically related. This conclusion was further supported by the distribution of relative sterane concentrations, where all of the oils showed nearly identical sterane distributions (Figure 4.24). However, on the basis of terpane chromatograms (Figure 4.18), aromatic maturity parameters (Figures 4.20; 4.21; and 4.22), and Pr/C_{17} vs. Ph/C_{18} crossplot (Figure 4.14), oils can be divided into two subfamilies; (i) Subfamily-A is represented by oils from A-Field and (ii) Subfamily-B is represented by oils from R- and I-Fields. Oils in Subfamily-A are at high levels of thermal maturities, and are characterized by high concentrations of tricyclic terpanes relative to hopanes. Homohopanes in these oils are below the detection limit. Oils of

Subfamily-B are characterized in general by intermediate levels of thermal maturities and lower concentrations of tricyclic terpanes relative to hopanes compared to Subfamily-A. However, both subfamilies have very similar sterane distributions (Figures 4.15). This is probably due to the advanced levels of maturities for these oils and/or due to the effect of diagenetic conditions. The high levels of thermal maturities in Murzuq Basin were probably due to the burial depth of source rock and/or to a heat pulse caused by tectonism and volcanism during the Eocene (Echikh and Sola, 2000). Burial history modeling by Aziz (2000), based on the assumption of rapid burial during the Permian, suggested that oil generation in Block NC-115 began in the Carboniferous-Permian. However, Belaid et al. (2009) indicated that the most important phase of hydrocarbon generation in Murzuq Basin occurred during the Late Jurassic or Cretaceous, when burial was at its maximum, before Hercynian erosion took place.

4.2.4.2 Oil-source rock correlation

Oil/source rock correlations were undertaken using the relative biomarker concentrations (e.g. triterpane and sterane distributions) along with the thermal maturity levels. The relative biomarker concentrations of both Tanezzuft 'cool' shale samples and crude oils were normalized to the saturate fractions in order to be able to undertake the correlation study. Based on maturity biomarkers (e.g. $C_{29}\alpha\beta\beta/(\alpha\beta\beta+\alpha\alpha\alpha)$, $C_{29}\alpha\alpha\alpha 20S/(20S+20R)$, homohopane isomerization ratios $C_{32}22S/(22S+22R)$, Ts/(Ts+Tm) ratios, and C_{30}-moretane/C_{30}-hopane ratios) along with Rock-Eval Pyrolysis and reflectance measurements of graptolite, the thermal maturity of the Silurian Tanezzuft

'cool' shale from NC-115 is generally assessed as early-intermediate levels of thermal maturity (Tables 4.5 and 4.7). As mentioned above, the maturity of oil samples are mainly assessed on the basis of aromatic maturity parameters (e.g. MPI and mono- and triaromatic steroid hydrocarbons; Figure 4.22) along with terpane and sterane biomarkers (e.g. tricyclic/hopane and diasterane/sterane ratios) (Table 4.9 and 4.10). Oils from A-Field are characterized by high levels of thermal maturity, whereas, oils from I- and R-Fields are at intermediate levels of thermal maturity. Therefore, highly mature A-Field oils along with early mature rock samples can be excluded from this correlation due to their differences in maturity levels. Thus, intermediate mature oils (I- and R-Fields) should correlate with rock samples that show similar levels of maturity although the Tanezzuft 'cool' shale (organically lean shale) has not generated, and probably will not generate significant volumes of hydrocarbons in the Murzuq basin (Hodairi and Philp, 2011).

The distributions of steranes and triterpanes have been widely used as correlation tools (Moldowan et al., 1985; Philp et al., 1989; Moldowan et al., 1992). Based on the relative concentrations of triterpane of the Tanezzuft 'cool' shales and crude oils (Figures 4.28), the distribution trends of homohopanes and tricyclic terpanes in oils (I- and R-Fields) appear to be different than in rock samples. The highest peak in Figure 4.28 is at C_{30} hopane, where crude oils is characterized by high concentrations ranging from 36.58 to 57.21 ppm, and the concentrations of C_{30} hopane for rock samples fall between 0.03 and 7.93 ppm, except for the sample A3, which has a relatively high value of 29.79 ppm (Figure 4.28; Tables 4.13 and 4.14). The second major peaks in Figure 4.28 are the C_{29} hopanes and C_{23} tricyclic terpanes. C_{29} Hopane concentrations in crude oils fall between

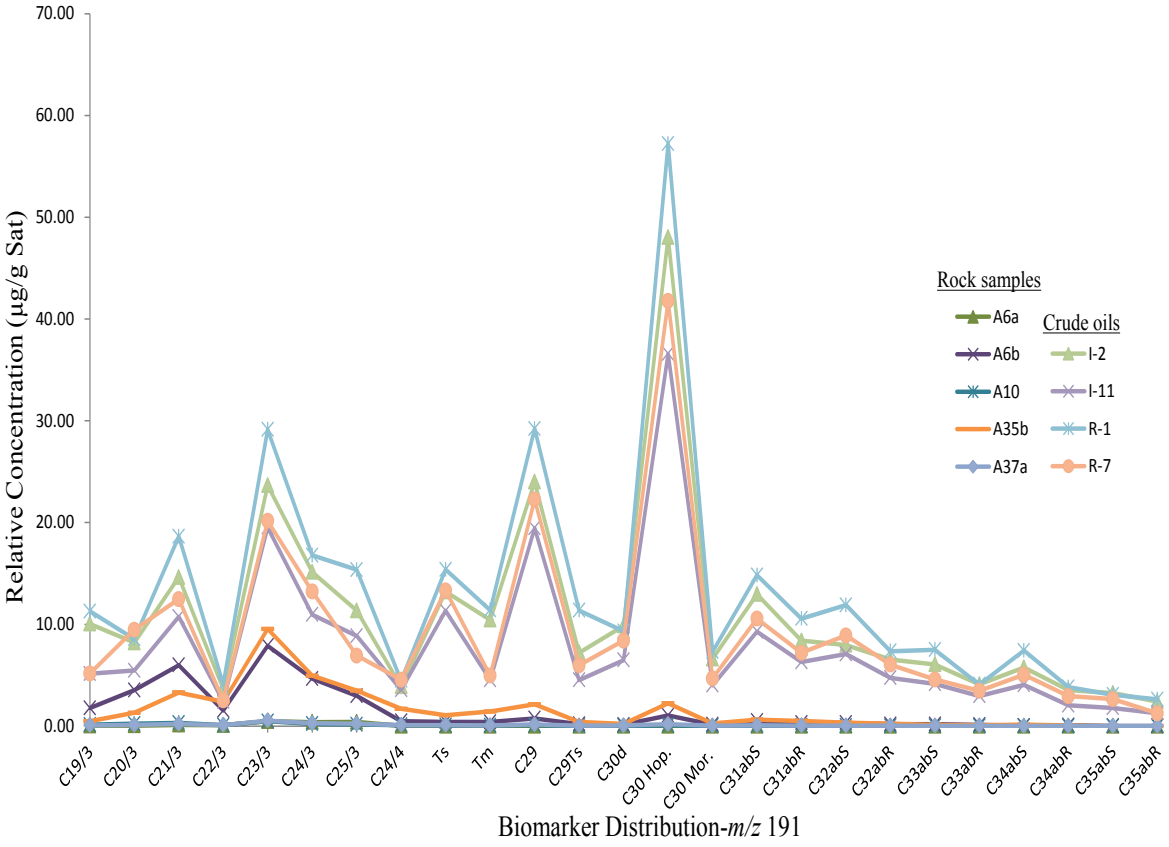

Figure 4.28. Distribution and relative concentration of triterpane in oils (I & R Fields) and Tanezzuft 'cool' shales from the *m/z* 191 chromatograms. Block NC-115, Murzuq Basin, S.W. Libya.

19.45 and 29.22 ppm, whereas in rock samples range from 0.02 to 2.14 ppm, except for the sample A3, which shows value of 19.84 ppm. C_{23} tricyclic terpane concentrations in oils range from 19.53 to 29.13 ppm. Whilst, in rock samples range between 0.03 and 7.89 ppm, except for sample A3 with value of 22.71 ppm (Tables 4.13 and 4.14). This means that the relative biomarker concentration of the Tanezzuft 'cool' shale in the present study is much lower than of the crude oils (I- and R-Fields). These differences in the patterns of biomarker distribution can be further seen in Figure 4.29, where crude oils (I- and R-Fields) show generally high sterane concentrations relative to Tanezzuft 'cool' shales. Also, the sterane distribution patterns in oils are not consistent with Tanezzuft 'cool' shales (Figure 4.29), suggesting a lack of correlation, where the sterane distributions of oils do not fit the envelope at all, which may suggest that there is no genetic relationship between the oils and the Tanezzuft "cool" shale samples in this study. However, the differences in concentrations between oils and rock samples in this study are not related to maturity although the concentrations of biomarker decrease with increasing maturity. Because the majority of rock samples plotted in Figures 4.28 and 4.29, which show very low concentration of biomarkers relative to oils are still at lower maturity levels than oils from I- and R-Fields. Usually, the concentration of biomarker decreases with increasing maturity levels (Fu et al., 1985; Requejo, 1992). The diversity in biomarker concentrations illustrates differences in sources, depositional environments and quality of the source rocks and oils (Wang, 1993; Wang and Philp, 1997). However, based on the relative concentration of C_{27}, C_{28}, and C_{29} regular steranes shown in the ternary diagram (Figure 4.30), rock samples (e.g. A6a-b, A10, A35b and A37a) that may have similar maturity levels with crude oils (I- and R-Fields) also show a lack of correlation with

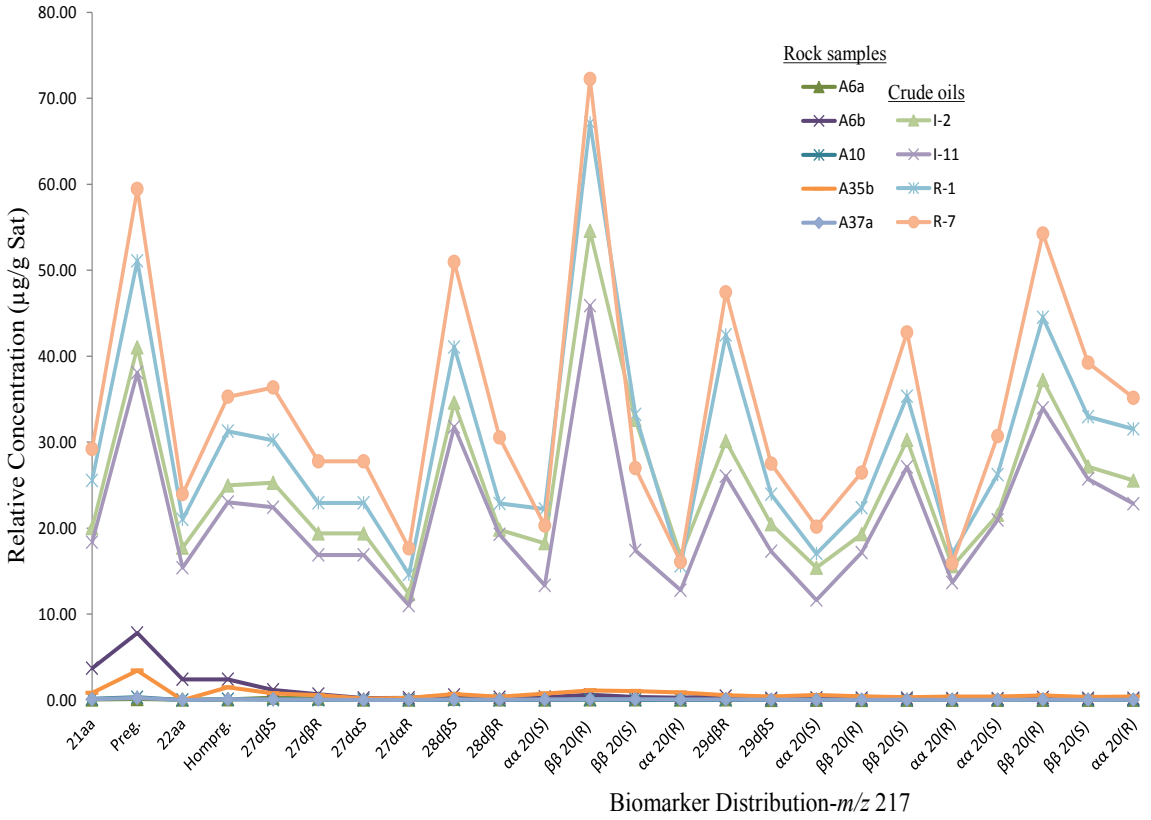

Figure 4.29. Distribution and relative concentration of sterane in oils (I & R Fields) and Tanezzuft 'cool' shales from the *m/z* 217 chromatograms. Block NC-115, Murzuq Basin, S.W. Libya.

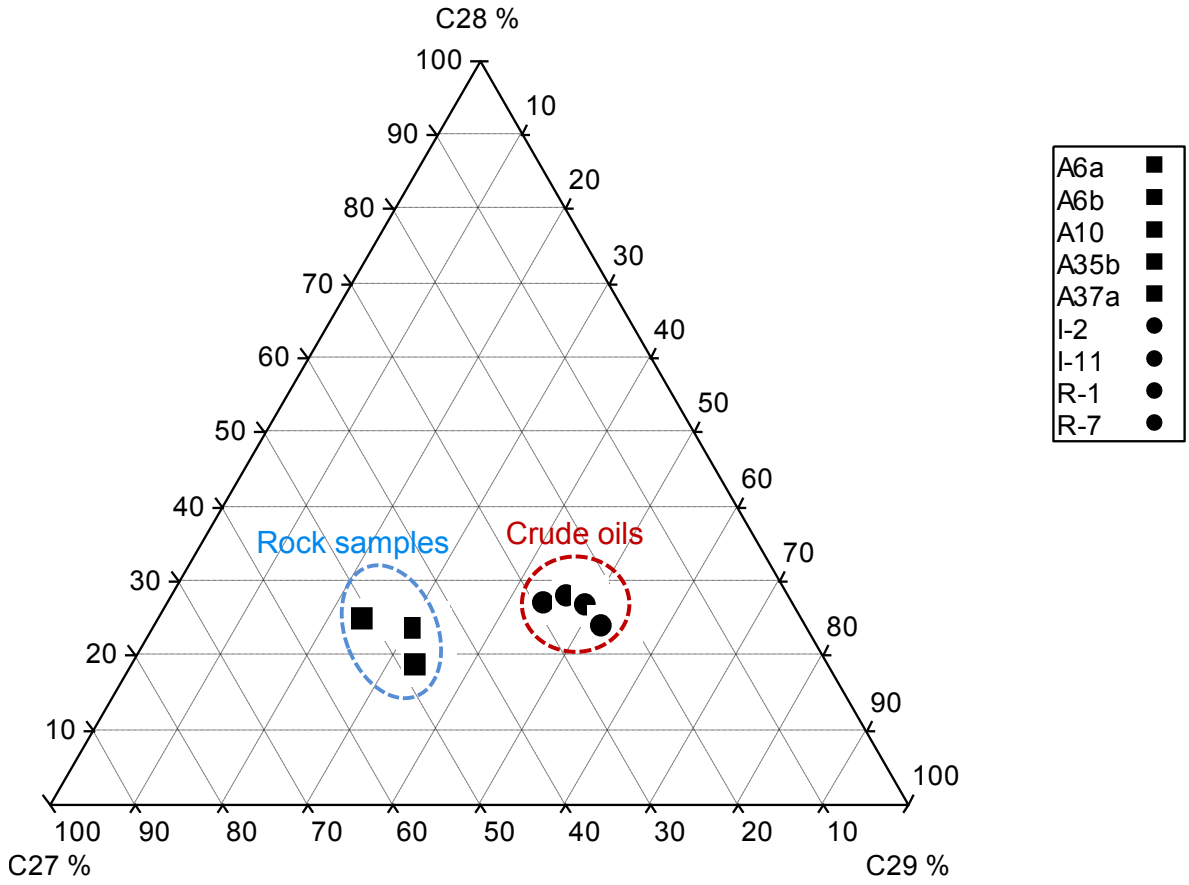

Figure 4.30. Sterane ter00nary diagram of crude oils (I&R Fields) and Tanezzuft 'cool' shale samples using C_{27} to C_{29} 14α(H),17α(H) 20R regular sterane isomers based on the relative biomarker concentrations.

crude oils, where all the rock samples plotted fall away from the oil samples on the ternary diagram (Figure 4.30).

According to several authors, all oils in the Murzuq Basin are thought to be generated from the lowermost Tanezzuft 'hot' shale (Hamyouni, 1991; Echikh and Sola, 2000; Lüning et al., 2000). In an attempt to correlate the depositional environment conditions of Tanezzuft 'hot' shales with crude oils from A-, I- and R-Fields, the relatively high values of Pr/Ph ratios (1.36–2.10) of crude oils are in agreement with the values of Pr/Ph ratio of the Tanezzuft 'hot' shale, which is characterized by values of Pr/Ph ratio (1.8–2.2) suggesting mild anoxic conditions (Hall et al., 2010). However, these values of Pr/Ph ratio for the Tanezzuft 'hot' shale are not consistent with the sedimentological interpretations, where the Rhuddanian 'hot' shale Tanezzuft Formation is interpreted as having been deposited under anoxic conditions during the early Silurian transgression (marine inner shelf environments) as indicated by the high content of uranium (U) associated with abundant TOC (Echikh and Sola, 2000; Lüning et al., 2000). As mentioned above in Section 1.1.4.2, sediments enriched in U indicate deposition under anoxic conditions that allow both large amounts of organic matter to accumulate and U to be fixed (Wignall and Myers, 1988). However, the presence of the earliest Silurian organically lean shale underlying the hot shale in several wells in the Libyan Murzuq Basin emphasizes that the sea floor was oxic during the very first part of the early Silurian transgression and hot shale deposition commenced only shortly thereafter (Lüning et al., 2000). The inconsistency of the Pr/Ph values for both oils and hot shale samples along with sedimentological interpretation is probably due to the advanced levels of thermal maturity (intermediate-high) for both oils and hot shale samples. This is because the pristane/ phytane ratios are known to be affected by maturation (Tissot and Welte, 1984;

Koopmans et al., 2002), and by the differences in possible precursors (Volkman and Maxwell, 1986; ten Haven et al., 1987). Furthermore, parameters such as C_{30}-diahopane, diasterane, and C_{35} homohopane are also affected by thermal maturity. Therefore, precise values cannot be given to define redox conditions for highly mature samples. However, Peters et al. (2005) pointed out that values of Pr/Ph ratio between 0.8 and 3.0 are not recommended to be used as an indicator of redox conditions and additional data are acquired to support this interpretation.

Based on several reports (e.g. Belaid et al., 2009 and Hall et al., 2010), maturity of the Tanezzuft 'hot' shales ranges from early mature in the southern parts of the basin to late mature in the central area of the basin and are intermediate to late mature levels in the deeper central parts of the basin (Belaid et al., 2009; Hall et al., 2010). It has also been observed that maturity increases northwards of the basin to reach the mid to late oil window, which is probably due to higher heat flows (Hall et al., 2010), because the hot shale is at shallower depths on the northern uplifted rim of the basin. However, the Tanezzuft 'hot' shales in the deeper central parts of the basin display similar thermal maturity levels with oils from both R-, and I-Fields (mid mature) together with oils from A-Field (highly mature). However, it is hard to predict from this limited data set whether or not these oils have been generated from the lowermost Tanezzuft 'hot' shale (only based on the similarities in maturity levels). Therefore, further data from the lowermost Tanezzuft 'hot' shales are needed to support any correlation study with oils.

CHAPTER V. CONCLUSIONS AND RECOMMENDATIONS

1. Source Rock

The results from this study confirm that organic matter in the "cool" shales of Tanezzuft Formation within Murzuq Basin is mainly Type III kerogen (gas prone) with some contribution of mixed Type II and III kerogens (gas/oil prone), but in general it has poor to fair hydrocarbon potential. The predominance of C_{27} and C_{29} steranes and values of Pr/nC_{17} vs. Ph/nC_{18} in most of the samples studied along with the stable carbon isotopic composition for saturate and aromatic hydrocarbons of selected extracts indicate that organic matter in these sediments is characterized by mixed marine/terrigenous sources. A slightly higher contribution of marine organic matter is suggested by the presence of C_{30} steranes and a high abundance of tricyclic terpanes in most of samples. The values of Pr/Ph ratios (0.83–2.32), the occurrence of C_{30}-diahopane, low values of C_{35} to C_{34} homohopanes ratios, and high diasterane/sterane ratios together with low quality organic matter, indicate that these sediments were deposited in sub-oxic conditions with a slight hypersaline influence indicated by the presence of pregnane and homopregnane as well as C_{24} tetracyclic terpanes. Furthermore, results of maturity parameters together with Rock-Eval data and organic petrography indicate that most of rock samples studied were generally at early to intermediate levels of maturity indicated by the ratios of 22S/(22S+22R), ββ/(ββ+αα), 20S/(20S+20R), and the C_{30}-moretanes/C_{30}-hopanes ($C_{30}\beta\alpha/C_{30}\alpha\beta$) ratios together with Tmax, HI vs. Tmax crossplot, and graptolite reflectance data. Therefore, it is proposed that the uppermost Tanezzuft Formation ('cool'

shale) has not generated, and probably will not generate significant volumes of hydrocarbons in the Murzuq basin.

2. Crude oils

This investigation confirms that the crude oils in this study were produced from source rocks characterized by mixed terrigenous/marine organic matter suggested by the distribution of C_{27}–C_{29} steranes, Pr/nC_{17} vs. Ph/nC_{18} crossplot and the stable carbon isotopic composition for saturate and aromatic hydrocarbons of selected crude oils. The source rocks were deposited under sub-oxic conditions indicated by the values of Pr/Ph ratios (1.36–2.10), C_{30}-diahopane/C_{29}Ts, and diasterane/sterane. The latter coupled with the low values of C_{29}/C_{30} hopane ratios along with the crossplot of DBT/P vs. Pr/Ph indicate that the oils were probably derived from marine clay-rich source rocks. Furthermore, the thermal maturity levels for oils vary from intermediate to high levels. Oils from A-Field are highly mature, whereas oils from R- and I-Fields are at intermediate levels of thermal maturity as indicated by the aromatic maturity parameters [e.g. MPI, MA(I)/MA(I+II) and TA(I)/TA(I+II)] as well as tricyclic/hopane and diasterane/sterane ratios. Oils do not appear to have been biodegraded as indicated by the normal distribution of *n*-alkanes, and the absence of 25-norhopanes in all oils. Oil to oil correlations, based on stable carbon isotope values, triterpane and sterane distributions, thermal maturity levels, and Pr/C_{17} vs. Ph/C_{18} crossplot, permit the establishment of one genetic family of oils that can be further divided into two subfamilies; Subfamily-A represents all oils from A-Field, and Subfamily-B, typifies both oils from R- and I-Fields. Both subfamilies were generated from similar source rocks. We assume that both subfamilies of oils represent two different phases of hydrocarbon generation; where oils

of Subfamily-A may indicate a late phase of crude oil generation, whilst, oils of Subfamily-B may represent an early phase of hydrocarbon generation in the Murzuq Basin. The differences in thermal maturities between the two subfamilies were probably dependent upon the characteristics of the basin, such as, burial history and heat flow rate. According to the relative concentration of biomarkers, the Tanezzuft 'cool' shales show a lack of correlation with crude oils.

3. Recommendations

This study covers only the Tanezzuft 'cool' shale in the Murzuq Basin along with crude oils. Therefore, further work is needed on the lowermost part of Tanezzuft Formation 'hot' shale, which is thought to be the main source rock for all oils in the Murzuq Basin. Moreover, other formations which could be potentially good source rocks include the Middle-Late Devonian Awaynat Wanin Formation.

It is recommended to accomplish further geochemical analysis on a larger suite of samples, particularly core samples in Block NC-115 (e.g. B- and H-Fields) and nearby blocks (e.g. NC-186 and NC 101) from the Tanezzuft Formation 'hot' shale. This may help us further to have better understanding over a large area of the basin, as well as to be able to generate maturity maps for the lowermost part of Tanezzuft 'hot' shale that would be very helpful in having a good decision-making process for new drilling locations.

Integrating geochemical data with sequence stratigraphic frameworks for the source rocks within the Murzuq Basin will give more support information in determining depositional environment conditions and the nature of organic matter input.

Correlation between the Silurian Tanezzuft Formation within the Murzuq basin and similar shale plays in other basins (e.g. Arabian Peninsula, N. Africa, and NE. U.S.A) would help understanding the relationship between the continents.

REFERENCES

Alexander, R., Kagi, R.I., Volkman, J.K., Woodhouse, G.W., 1983. The geochemistry of some biodegraded Australian oils. Australian Petroleum Production and Exploration Association (APEA) Journal 23, 53-63.

Angelin, M.L., Collignan, A., Bellocq, J., Oudin, J.-L., Ewald, M., 1983. Empreinte par degré d'aromaticité des hydrocarbures aromatiques polycycliques extraits de la matière organique d'une roche mère ou d'un pètrole obtenue par chromatographie liquide haute performance (µ-silice-NH2). C.r. Academie des Sciences Paris III 296, 705-708.

Aquino Neto, F.R., Trendel, J.M., Restle, A., Albrecht, P., Connan, J., 1983. Occurrence and formation of tricyclic and tetracyclic terpanes in sediments and petroleum. In Advances in Organic Geochemistry 1981 Bjoroy M. et al. ed, Wiley, Chichester.

Arfaoui, A., Montacer, M., 2007. New potential hydrocarbon source-rocks in the Lower Eocene Metlaoui Formation (Central-Northern Tunisia, Northern Africa) Geologica Acta 5, 245-254.

Armanios, C., Alexander, R., Kagi, R.I., 1992. High diahopane and neohopane abundances in a biodegraded crude oil from the Barrow sub-basin of Western Australia. Organic Geochemistry 18, 641—645.

Aziz, A., 2000. Stratigraphy and hydrocarbon potential of the lower Palaeozoic succession of licence NC 115, Murzuq Basin, S.W. Libya. In: Sola, M.A., Worsley, D. (Eds.), Geological Exploration in the Murzuq Basin Elsevier, Amsterdam, pp. 349-368.

Banerjee, S., 1980. Stratigraphic Lexicon of Libya. Industrial Research Centre, Tripoli 13, 300.

Beach, F., Peakman, T.M., Abbott, G.D., R., S., Maxwell, J.R., 1989. Laboratory thermal alteration of triaromatic steroid hydrocarbons. Organic Geochemistry 14, 109-111.

Belaid, A., Krooss, B.M., Littke, R., 2009. Thermal history and source rock characterization of a Paleozoic section in the Awbari Trough, Murzuq Basin, SW Libya. Marine and Petroleum Geology, 1-21.

Belaid, A., Krooss, B.M., Littke, R., 2010. Thermal history and source rock characterization of a Paleozoic section in the Awbari Trough, Murzuq Basin, SW Libya. Marine and Petroleum Geology 27, 612-632.

Bellini, E., Massa, D., 1980. A stratigraphic contribution to the Palaeozoic of the southern basins of Libya. Second Symposium on the Geology of Libya, Academic Press, London, eds. M.J. Salem and M.T. Busrewil ed, pp. 3-56.

Bishop, W.F., 1975. Geology of Tunisia and adjacent parts of Algeria and Libya American Association of Petroleum Geologists (AAPG) Bulletin 59, 413-450.

Boote, D.R.D., Clark-Lowes, D.D., Traut, M.W., 1998. Palaeozoic petroleum systems of North Africa. In: Petroleum Geology of North Africa. (*e.d. D.S. MacGregor, R.T.J. Moody, D.D. Clark-Lowes*). Geological Society of London, Special Publication No.132, p. 7-68.

Borghi, P., 1939. Fossili Devonici del Fezzan. Ann. Mus. Libico Scoria Naturale 1, 115-184.

Borghi, P., Chiesa, C., 1940. Cenni geologici e paleontologici sul Paleozoico dell'Egghidi Uan Caza ne1 deserto di Taita (Fezzan occidentale) Ann. Mus. Libico Scoria Nat. 2, 122-137.

Brassell, S.C., 1992. Biomarkers in recent and ancient sediments: the importance of the diagenetic continuum. In: Whelan JK, Farrington JW, editors. Organic matter-productivity, accumulation, and preservation in recent and ancient sediments. University Press, New York: Columbia, p. 339-367.

Brassell, S.C., Eglinton, G., 1983. The potential of organic geochemical compounds as sedimentary indicators of upwelling. In E. Suess and J. Thiede (Eds.) Coastal upwelling: its Sediment Record, Part A. Plenum, pp. 545-571.

Briggs, D.E.G., 1999. Molecular taphonomy of animal and plant cuticles: selective preservation and diagenesis. Philosophical Transactions of the Royal Society, London 354, 7-17.

Brooks, J.D., Gould, K., Smith, J.W., 1969. Isoprenoid hydrocarbons in coal and petroleum. Nature 222, 257-259.

Bulman, O.M.B., 1970. Graptolithina, In." TEICHERT, C. (ed.) Treatise on Invertebrate Palaeontology, V (2nd ed.). Geological Society of America and University of Kansas Press.

Burollet, P.F., 1963. Reconnaissance geologique dans le sud-est du bassin de Kufra. First Saharan Symposium. Rev. Inst. Fran. Pet. special volume. 219-227.

Burollet, P.F., Manderscheid, G., 1967. Le Devonien en Libye et en Tunisie. Symp. Devonian System, Calgary 1, 285-302.

Castro, J.C., Della Favera, J.C., EL-Jadi, 1985. Palaeozoic sedimentary facies, Murzuk Basin, SPLAJ. Internal report Braspetro-Petrobras, Rio De Janeiro, 117

Chang, Z.H., Chen, Z.H., Zhang, Y.T., 2007. Study on geochemical characteristics of crude from Dongpu Depression in Bohai Gulf Basin (in Chinese). Petroleum Exploration Geology 29, 178-182.

Chosson, P., Connan, J., Dessort, D., Lanau, C., 1992. In vitro biodegradation of steranes and terpanes: a clue to understanding geological situations. In: Moldowan, J.M., Albrecht, P., Philp, R.P. (Eds.), Biological Markers in Sediments and Petroleum. Prentice Hall, 320-349.

Clark, J.P., Philp, R.P., 1989. Geochemical characterization of evaporate and carbonate depositional environments and correlation of associated crude oils in the black Creek Basin, Alberta. Bulletin of Canadian Petroleum Geology 37, 401–416.

Connan, J., Bouroullec, J., Dessert, D., Albrecht, P., 1986. The microbial input in carbonate–anhydrite facies of sabkha paleoenvironment from Guatemala: A

molecular approach. In: Leythauser, D. & Rulkötter, J. (eds) Advances in Organic Geochemistry. Organic Geochemistry 10, 29-50.

Connan, J., Dessort, D., 1987. Novel family of hexacyclic hopanoid alkanes (C_{32}-C_{35}) occurring in sediments and oils from anoxic paleoenvironments. Organic Geochemistry 11, 103-113.

Cornford, C., Morrow, J.A., Tarrington, A., Miles, J.A., Brooks, J., 1983. Some geological controls on oil composition in the UK North Sea. In Petroleum Geochemistry Oil Exploration of Europe, Edited by Brooks, J. ed. Blackwell Scientific Publications, Oxford, pp. 175-195.

Czochanska, Z., Gilbert, T.D., Philp, R.P., Sheppard, C.M., Weston, R.J., Wood, T.A., Woolhouse, A.D., 1988. Geochemical application of sterane and triterpane biomarkers to a description of oils from the Taranaki Basin in New Zealand. Organic Geochemistry 12, 123-135.

Dahl, J.E., Moldowan, J.M., Teerman, S.C., McCaffrey, M.A., P., S., Pena, M., Stelting, C.E., 1994. Source rock quality determination from oil biomarkers I. - An example from the Aspen Shale, Scully's Gap, Wyoming. American Association of Petroleum Geologists (AAPG) Bulletin 78, 1507-1526.

Davidson, L., Simon, B., Jonathan, C., Martin, E., Andy, F., Ali, H., Jhoon, J., Bashir, M., Jerry, S., 2000. The structure, stratigraphy and petroleum geology of the Murzuq Basin, southwest Libya. In: Sola, M. A. and Worsley, D. (Eds.) Geological Exploration in Murzuq Basin. Elsevier Amsterdam.

de Leeuw, J.W., Sinnighe Damste, J.S., 1990. Organic sulfur compounds and other biomarkers as indicators of palaeosalinity: A critical evaluation. In: Orr W.L. and White C.M. (Eds.), Geochemistry of Sulfur in Fossil Fuels American Chemical Society, Washington, DC 249, 417-443.

Demaison, G., Moore, G.T., 1980. Anoxic environments and oil source bed genesis. American Association of Petroleum Geologists (AAPG) Bulletin 64, 1179-1209.

Dembicki, J.H., 2009. Three common source rock evaluation errors made by geologists during prospect or play appraisals. American Association of Petroleum Geologists Bulletin 93, 341-356.

Desio, A., 1936a. Prime notizie sulla presenza del Silurico fossiliferonel Fezzan. Bolletino della Societa Geologica Italiana 55, 116-120.

Desio, A., 1936b. Riassunto sulla presenza del Silurico fossilifero ne1 Fezzan Bolletino della Societa Geologica Italiana 55, 319-356.

Didyk, B.M., Simoneit, B.R.T., Brassell, S.C., 1978. Geochemical indicators of palaeoenvironmental conditions of sedimentation. Nature 272, 216-222.

Durand, B., Monin, J.C., 1978. Geochemical indicators of palaeoenvironmental conditions of sedimentation. Nature 272, 216-222.

Echikh, K., 1998. Geology and hydrocarbon occurrences in the Ghadames Basin, Algeria, Tunisia, Libya. In: D.S. Macgregor, R. T.J. Moody, D.D. Clark-Lowes (Eds.) Petroleum Geology of North Africa. Geological Society, London, Special Publications pp. 109-130.

Echikh, K., Sola, M.A., 2000. Geology and hydrocarbon occurrences in the Murzuq Basin, S.W. Libya. Symposium on Geological Exploration in Murzuq Basin, M.A. Sola and D. Worsley ed. Elsevier, Amsterdam, pp. 175-222.

Eglinton, G., Calvin, M., 1967. Chemical fossils. Scientific American 261, 32-43.

Eglinton, G., Hamilton, R.J., 1969. Leaf epicuticular waxes. Science 156, 1322–1334.

Eglinton, G., Scott, P.M., Belsky, T., Burlingame, A.L., Calvin, M., 1964. Hydrocarbons of a biological origin from a one-billion-year-old sediment. Science 145, 263-264.

Eglinton, L.B., Lim, D., Slater, G., Osinski, G.R., Whelan, J.K., Douglas, M., 2006. Organic geochemical characterization of a Miocene core sample from Haughton

impact structure, Devon Island, Nunavut, Canadian High Arctic. Organic Geochemistry 37, 688-710.

Eglinton, T.I., Douglas, A.G., 1988. Quantitative Study of Biomarker Hydrocarbons Released from Kerogens during Hydrous Pyrolysis. Energy & Fuels 2, 81-88.

Elkelani, M., Reichart, G., Kurschner, W., Sinninghe Damsté, J.S., Nierop, K.G.J., Brinkhuis, H., Smeenk, J., Nederlof, P., 2011. Plant microfossils from the early Silurian (Llandoverian) from western Libya. Geophysical Research Abstracts, EGU General Assembly 2011 13, 1.

Engel, M.H., Macko, S.A., 1993 Organic geochemistry. Principles and Applications. Plenum Press, NewYork, p. 861.

Engel, M.H., Maynard, R.J., 1989. Preparation of organic matter for stable carbon isotope analysis by sealed tube combustion: A cautionary note. Analytical Chemistry 61, 1996-1998.

Espitalié, J., Laparte, J., Madec, M., Marquis, F., Leplat, P., Paulet, J., Bontefou, A., 1977. Method rapide de characterisation des rocties meres, leur potentiel petrolier et de leur degre d'evolution Rev. Institut français du pétrole 32, 23-42.

Espitalié, J., Madec, M., Tissot, B., 1984. Geochemical logging, in Voorhees, K.J., (ed.), . Analytical Pyrolysis—Techniques and Applications, Boston, Butterworth, 276-304.

Fan Pu, King, J.D., Claypool, G.E., 1987. Characteristics of biomarker compounds in Chinese crude oils. In: R. K. Kumar, P. Dwivedi, V. Banerjie, and V. Gubta (Eds.) Petroleum Geochemistry and Exploration in the Afro-Asian Region, Dehradun, 25-27 November 1985, Rotterdam, Balkema, p. 197-202.

Fello, N., Lüning, S., Storch, P., Redfern, J., 2006. Identification of early Llandovery (Silurian) anoxic palaeo-depressions at the western margin of the Murzuq Basin, (southwest-Libya) based on gamma-ray spectrometry in surface exposures. GeoArabia, Gulf PetroLink, Bahrain 11, 101-118.

Fello, N.M., 2001. Depositional environments, diagenesis and reservoir modelling of concession NC115, Murzuq Basin, SW Libya (PhD thesis, University of Durham, England) (unpublished). 1-336.

Fowler, M.G., Douglas, A.G., 1987. Saturated hydrocarbon biomarkers in oils of late Precambrian age from eastern Siberia. Organic Geochemistry 11, 201-213.

Freulon, J.M., 1964. Etude geologique des series primaires du Sahara central (Tassili n'Ajjer et Fezzan). Centre National Recherche Scientifique, Paris. Ser. Geologie 3, 198.

Fu, J.M., Xu, F.F., Maxwell, J.R., Liang, D.G., 1985. Quantitative analysis of steranes, terpanes and other biomarkers. In: Organic Geochemistry and Origin of Oil from Continental Deposits. 29-38.

Goodarzi, F., 1982. A brief hydrocarbon potential study of Southeast Turkey using petrography. Report to Turkish Petroleum Research Centre, Ankara, Turkey, 28.

Goodarzi, F., 1986. Dispersion of optical properties of graptolites epiderms with increased maturity in early Paleozoic organic rich sediments. Fuel 64, 1735-1740.

Goodarzi, F., Brooks, P.W., Embry, P.F., 1989a. Regional maturity as determined by organic petrology and geochemistry of the Schei Point Group (Triassic) in Western Sverdrup Basin, Canadian Archipelago. Marine and Petroleum Geology 6, 290-302.

Goodarzi, F., Norford, B.S., 1989b. Variation of graptolite reflectance with depth of burial. International Journal of Coal Geology 11, 127-141.

Goudarzi, G.H., 1980. Structure of Libya. In: Salem, M. J. and Busrewil, M. T. (eds) Geology of Libya. Academic Press London, 879-892.

Grantham, P.J., Wakefield, L.L., 1988. Variations in the sterane carbon number distributions of marine source rock derived crude oils through geological time. Organic Geochemistry 12, 61-73.

Gumati, Y., Kanes, W., Schamel, S., 1996. An evaluation of the hydrocarbon potential of the sedimentary basins of Libya. Journal of Petroleum Geology 19, 95-112.

Hall, P.B., Bjoroy, M., Ferriday, I.L., Ismail, Y., 2010. Libyan Murzuq Basin Source Rocks. Adapted from poster presentation at AAPG Convention, New Orleans, Louisiana, April 11-14, 2010, 24.

Hallett, D., 2002. Petroleum Geology of Libya, 1st (eds) ed. Elsevier Science B. V., London, p. 503.

Hamyouni, E., Amar, I., Riani, B., El-Ghull, A., Rahoma, S., 1984. Petroleum source rock evaluation and timing of hydrocarbon generation, Murzuq Basin, Libya. National Oil Corporation paper, In: Symposium on the Source and Habitat of Petroleum in the Arab Countries, Kuwait. OAPEC, Kuwait, 125-148.

Hamyouni, E.A., 1991. Petroleum source rock evaluation and timing of hydrocarbon generation, Murzuk Basin, Libya: A case study In: M.J. Salem and M.N. Belaid, (Eds.) Geology of Libya. Elsevier, 183-211.

Han, J., Calvin, M., 1969. Hydrocarbon distribution of algae and bacteria and microbiological activity in sediments. Proceedings of the National Academy of Science of the United States of America 64, 436-443.

Hassi, I.A., 1998. Sequence stratigraphic analysis of the Tahara in Hamada Basin, western Libya (abstract only). Symposium on Geological Exploration in Murzuq Basin, Sabha, 20-22nd September 1998. Book of abstract.

Hodairi, T.A., Philp, R.P., 2011. Geochemical Investigation of Tanezzuft Formation, Murzuq Basin, Libya. Adapted from expanded abstract presentation at AAPG Annual Convention and Exhibition, Houston, Texas, USA, April 10-13, 2011, 22.

Hoffmeister, W.S., 1959. Lower Silurian plant spores from Libya. Micropaleontology 5, 331-334.

Huang, H.P., Lu, S.N., Yuan, P.L., 1994. Diahopanes newly detected in ancient sediments and their significance to hydrocarbon exploration (in Chinese). Natural Gas Geochemistry 5, 23-28.

Huang, W.Y., Meinschein, W.G., 1979. Sterols as ecological indicators. Geochimica et Cosmochimica Acta 43, 739-745.

Huang, Y., Li, B., Bryant, C., Bol, R., Eglinton, G., 1999. Radiocarbon dating of aliphatic hydrocarbons: a new approach for dating passive-fraction carbon in soil horizons. Soil Science Society of American Journal 63, 1181-1187.

Hughes, W.B., Holba, A.G., Dzou, L.I.P., 1995. The ratio of dipenzothiophene to phenanthrene and 261 ristine to phytane as indicators of depositional environment and lithology of petroleum source rocks. Geochimica et Cosmochimica Acta 59, 3581-3598.

Hughes, W.B., Holba, A.G., Miller, D.E., Richardson, J.S., 1985. Geochemistry of greater Ekofisk crude oils. In: Thomas, B. M., Dore´, A.G., Eggen, S.S., Home, P.C. & Larsen, R.M. (Eds.) Petroleum Geochemistry in Exploration of the Norwegian Shelf. Graham and Trotman, London, 75–92.

Isaksen, G.H., Bohacs, K.M., 1995. Geological controls on source rock geochemistry through relative sea level; Triassic, Barents Sea. In: Katz, B.J. (Ed.), Petroleum Source Rocks. Springer-Verlag, New York, 25-50.

Ivanov, V., Golovko, A.K., 1992. Phenanthrene hydrocarbons in SSSR crude oils Siberian Chemical Journal, Russia 1, 94-102.

Jacqué, M., 1962. Reconnaissance geologique du Fezzan oriental. Notes et mémoires du compagnie francais des pétroles 5, 43.

Jarvie, D.M., 1991. Total organic carbon (TOC) analysis, in R. K. Merrill, ed., Source and migration processes and evaluation techniques: . AAPG Treatise of Petroleum Geology, Handbook of Petroleum Geology, 113–118.

Jobson, A.M., Cook, F.D., S., W.D.W., 1979. Interaction of aerobic and anaerobic bacteria in petroleum biodegradation. Chemical Geology 24, 355-365.

Jones, P.J., Philp, R.P., 1990. Oils and source rocks from Pauls Valley, Anadarko Basin, Oklahoma, U.S.A. Applied Geochemistry 5, 429-448.

Kirk, D.M., Shaw, P.M., 1975. Backbone rearrangement of steroidal 5-enes.-J. Chemical Society, Perkin Transactions 1, 2284-2294.

Klett, T.R., Ahlbrandt, T.S., Schmoker, J.W., Dolton, G.L., 1997. Ranking of the worlds oil and gas provinces by known petroleum volumes. U. S. Geological Survey Open File Report, 97-463.

Klitzsch, E., 1969. Stratigraphic section from the type areas of Silurian and Devonian strata at western Murzuk Basin (Libya). In: Kanes, W. H.(ed.) Geology, archaeology and prehistory of the southwestern Fezzan, Libya . Eleventh Annual Field Conference. Petroleum Exploration Society of Libya, 83-90.

Klitzsch, E., 1981. Lower Palaeozoic rocks of Libya, Egypt and Sudan. In: C.H. Holland (ed.) Lower Palaeozoic of Middle East, eastern and southern Africa and Antartica. John Wiley, New York, 131-163.

Kolaczkowska, E., Slougui, N.-E., Watt, D.S., Maruca, R.E., Michael Moldowan, J., 1990. Thermodynamic stability of various alkylated, dealkylated and rearranged 17α- and 17β-hopane isomers using molecular mechanics calculations. Organic Geochemistry 16, 1033-1038.

Koopmans, M.P., Larter, S.R., Zhang CM, et al., 2002. Biodegradation and mixing of crude oils in Eocene Es3 reservoirs of the Liaohe basin, northeastern China. American Association of Petroleum Geologists (AAPG) Bulletin 86, 1833-1843.

Kvalheim, O.M., Christy, A.A., Telnes, N., Bjørseth, A., 1987. Maturity determination of organic matter in coals using the methylphenanthrene distribution. Geochimica et Cosmochimica Acta, 51, 1883-1888.

Landis, C.R., Castaño, J.R., 1995. Maturation and bulk chemical properties of a suite of solid hydrocarbons. Organic Geochemistry 22, 137-149.

Lelubre, M., 1946a. Le Tibesti septentrionale. Esquisse morphologique et structural Comptes Rendus de l'Academie des Sciences. Paris 6, 337-357.

Lelubre, M., 1946b. Sur la Paleozoique du Fezzan. Comptes Rendus Hebdomadaire des Seances de l'Academie des Sciences. Paris 222, 1403-1404.

Lelubre, M., 1948. Le Paleozoique du Fezzan sud-oriental. C.R. Société Géologique de France 18, 79-81.

Lelubre, M., 1952. Apercu sur la geologie du Fezzan. Bull Serv. Carte Geol. d' Algerie, Trav. Rec. Coll. 3, 109-148.

Lijmbach, G.W.M., 1975. On the origin of petroleum. Proceedings Ninth World Petroleum Congress. Applied Sciences Publisher, London 2, 357–369.

Lüning, S., Craig, J., Fitches, B., Mayouf, J., Busrewil, A., El Dieb, M., Gammudi, A., Loydell, D.K., 2000. Petroleum source and reservoir rock re-evaluation in the Kufra Basin (SE Libya, NE Chad, NW Sudan) in: Geological Exploration in Murzuq Basin., M. A. Sola & D. Worsley ed. Elsevier, Amsterdam, pp. 151-173.

Lüning, S., N. M. , Fello, J., Craig, D.P., Le Heron, S., Lubeseder, G., Pyke, S., Schulz, A.J., Dunford, Abutarruma, Y., 2007. 1001 Million Saharan Nights – Petroleum Geology of Southern Libya. Documentary film, 4h 30 min, Seven Continents Science Productions, Bremen, Germany, www.seven-continents.com/libya.htm.

Mackenzie, A.S., Brassell, S.C., Eglinton, G., R., M.J., 1982. Steroid hydrocarbons and the thermal history of sediments Nature, London 295, 223-226.

Mackenzie, A.S., Patience, R.L., Maxwell, J.R., 1981. Molecular changes and the maturation of sedimentary organic matter In: Atkinson G. and Zuckerman J. J. (Eds.) Origin and Chemistry of Petroleum. Pergamon Press, Oxford, pp. 1-31.

Mackenzie, A.S., Patience, R.L., Maxwell, J.R., Vandenbroucke, M., Durand, B., 1980. Molecular parameters of maturation in the Toarcian shales, Paris basin, France, I: Changes in the configuration of acyclic isoprenoid alkanes, steranes and triterpanes. Geochimica et Cosmochimica Acta 44, 1709-1721.

Marzi, R., Rullkötter, J., 1989. Application of biological marker reactions to the reconstruction of geothermal histories: implications of recent pyrolysis results, 14th International Meeting on Organic Geochemistry, Paris, September 18-22, Abstracts, No.125.

Massa, D., Collomb, G.R., 1960. Observations nouvelles sur la region d' Aouinet Ouenine et du Djebel Fezzan, Libya. 21st International Geology Congress Report. 12, 65-73.

Massa, D., Jaeger, H., 1971. Données stratigraphiques sur le Silurien de l'Ouest de la Libye. Coll. Ordovicien-Silurien, Brest (France), September 1971, Memoir Bureau de Recherches Géologiques et Minières. 73, 313-321.

Massa, D., Moreau-Benoit, A., 1976. Essai de synthese stratigraphiqu et palynologique du systeme devonien en Libya occidentale. Revue da linstitute France Pétrole 31, 287-333.

Massa, D., Termier, G., Termier, H., 1974. Le Carbonifere de Libya occidentale Company France de Petrole. Notes et memmer 11, 139-206.

McDonald, T.J., Kennicutt, M.C., 1992. Fractionation of crude oils by HPLC and quantitative determination of aliphatic and aromatic biological markers by GC-MS with selected ion monitoring. LC/GC 10, 935-938.

McKirdy, D.M., Aldridge, A.K., Ypma, P.J.M., 1983. A geochemical comparison of some crude oils from pre-Ordovician carbonate rocks. In M. Bjoroy et al. (Ed.) Advances in Organic Geochemistry 1981. Organic Geochemistry, London: Wiley, 99-107.

McKirdy, D.M., Cox, R.E., Volkman, J.K., Howell, V.G., 1986. Botryococcane in a new class of Australian non-marine crude oils Nature 328, 57-59.

McKirdy, D.M., Kantsler, A.J., Emmett, J.K., Aldridge, A.K., 1984. Hydrocarbon genesis in Cambrian carbonates of the eastern Officer Basin, South Australia. In: Palacas, J.G. (Ed.) Petroleum Geochemistry and Source Rock Potential of Carbonate Rocks American Association of Petroleum Geologists (AAPG), Studies in Geology 18, 13-31.

Meister, E.M., Ortiz, E.F., Pierobon, E.S.T., Arruda, A.A., Oliveira, M.A.M., 1991. The origin and migration fairways of petroleum in Murzuq Basin, Libya, an alternative exploration model. In: Salem, M.J., Busrewil, M.T., Ben Ashour, A.M. (Eds.)The geology of Libya. Elsevier, Amsterdam, VII, 2725-2741.

Mello, M.R., Gaglianone, P.C., Brassell, S.C., Maxwell, J.R., 1988a. Geochemical and biological environment using brasilian offshore oils. Marine and Petroleum Geology 5, 205–223.

Mello, M.R., Telnaes, N., P.C., G., Chicarelli, M.I., Brassell, S.C., Maxwell, J.R., 1988b. Organic geochemical characterization of depositional environment in Brazilian marginal basins. Organic Geochemistry 13, 31-46.

Milner, C.W.D., Rogers, M.A., Evans, C.R., 1977. Petroleum transformations in reservoirs. Journal of Geochemical Exploration 7, 101-153.

Moldowan, J.M., 1984. C_{30}-steranes, novel markers for marine petroleums and sedimentary rocks. Geochimica et Cosmochimica Acta 48, 2767-2768.

Moldowan, J.M., Fago, F.J., Carlson, R.M.K., Young, D.C., an Duvne, G., Clardy, J., Schoell, M., Pillinger, C.T., Watt, D.S., 1991. Rearranged hopanes in sediments and petroleum. Geochimica et Cosmochimica Acta 55, 3333-3353.

Moldowan, J.M., Fago, F.J., Lee, C.Y., Jacobson, S.R., Watt, D.S., Slougui, N.E., Jeganathan, A., Young, D.C., 1990. Sedimentary 24-n-propylcholestanes, molecular fossils diagnostic of marine algae. Science 247, 309-312.

Moldowan, J.M., Seifert, W.K., 1980. First discovery of botryococcane in petroleum. Journal of the Chemical Society, Chemical Communications (J.S.C. Chem. Commun.) 9, 912-914.

Moldowan, J.M., Seifert, W.K., Gallegos, E.J., 1985. Relationship between petroleum composition and depositional environment of petroleum source rocks. American Association of Petroleum Geologists (AAPG) Bulletin 69, 1255-1268.

Moldowan, J.M., Sundararaman, P., Schoell, M., 1986. Sensitivity of biomarker properties to depositional environment and/or source input in the Lower Toarcian of S.W.-Germany. Organic Geochemistry 10, 915-926.

Moldowan, M.L., Lee, C.Y., Sundrararaman, P.e.a., 1992. Sources correlation and maturity assessment of selected oils and rocks from the central Adriatic basin (Italy and Yugoslavia). In: Moldowan, M.J., Albrecht, P., & Philip, R.P. (Eds.) Biological markers in sediments and petroleum. Prentice-Hall, Englewood Cliffs, N.J., 370-401.

Mueller, E., Philp, R.P., Allen, J., 1995. Geochemical characterization and relationship of oils and solid bitumens from S.E. Turkey. Journal of Petroleum Geology 18, 289-308.

Murray, A.P., Boreham, C.J., 1992. Organic Geochemistry in Petroleum Exploration. Australian Geological Survey Organization, Canberra, 230.

Nissenbaum, A., Kaplan, I.R., 1972. Chemical and isotopic evidence for the in situ origin of marine humic substances. Limnology and Oceanography 17, 570-582.

Ourisson, G., Albrecht, P., Rohmer, M., 1979. The hopanoids, paleochemistry and biochemistry of a group of natural products. Pure and Applied Chemistry 51, 709-729.

Ourisson, G., Albrecht, P., Rohmer, M., 1982. Predictive microbial biochemistry-from molecular fossils to procaryotic membranes. Trends in Biochemical Sciences 7, 236- 239.

Ourisson, G., Albrecht, P., Rohmer, M., 1984. The microbial origin of fossil fuels. Scientific American 251, 34-41.

Palacas, J.G., Anders, D.E., King, J.D., 1984. South Florida basin-a prime example of carbonate source of Petroleum Geochemistry and source rock potential of carbonate rocks. AAPG Studies in Geology, Palacas J. G. ed. American Association of Petroleum Geologists (AAPG), Tulsa, 71-96.

Palmer, S., 1984. Effect of water washing on C_{15+}hydrocarbon fraction of crude oils from Northwest Palawan, Philippines. American Association of Petroleum Geologists (AAPG) Bulletin 68, 137-149.

Peakman, T.M., Maxwell, J.R., 1988. Acid catalysed rearrangements of steroid alkenes--Part I. Rearrangement of 5a-cholest-7-ene. J. L. Journal of the Chemical Society, Perkin Transactions, 1065-1070.

Peakman, T.M., ten Haven, H.L., Rechka, J.A., de Leeuw, J.W., Maxwell, J.R., 1989. Occurrence of (20R)- and (20S)-$\Delta^{8(14)}$ and Δ^{14}5α(H)-sterenes and the origin of 5a(H),14b(H),17b(H)-steranes in an immature sediment. Geochimica et Cosmochimica Acta 53, 2001–2009.

Pepper, A.S., Corvi, P.J., 1995. Simple kinetic models of petroleum formation. Part I: oil and gas generation from kerogen. Marine and Petroleum Geology 12, 291-319.

Peters, K.E., 1986. Guidelines for evaluating petroleum source rock using programmed analysis. American Association of Petroleum Geologists (AAPG) Bulletin 70, 318-329.

Peters, K.E., Moldowan, J.M., 1991. Effects of source, thermal maturity, and biodegradation on the distributions and isomerization of homohopanes in petroleum. . Organic Geochemistry 17, 47-61.

Peters, K.E., Moldowan, J.M., 1993. The Biomarker Guide: Interpreting Molecular Fossils in Petroleum and Ancient Sediments. Prentice Hall, Englewood Cliffs, N.J., 363.

Peters, K.E., Moldowan, J.M., Sundararaman, P., 1990. Effects of hydrous pyrolysis on biomarker thermal maturity parameters: Monterey Phosphatic and Siliceous members. Organic Geochemistry 15, 249-265.

Peters, K.E., Snedden, J.W., Sulaeman, A., Sarg, J.F., Enrico, R.J., 2000. A new geochemical-sequence stratigraphic model for the Mahakam delta and Makassar slope, Kalimantan, Indonesia. American Association Petroleum Geologists (AAPG) 84, 12-44.

Peters, K.E., Walters, C.C., Moldowan, J.M., 2005. The Biomarker Guide: Biomarkers and Isotopes in Petroleum Exploration and Earth History, Sec. Edition. ed. Cambridge University Press UK, v. 2, 1155.

Philp, R.P., 1982. Correlation of crude oils from the San Jorges Basin, Argentina. Geochimica et Cosmochimica Acta 47, 267-275.

Philp, R.P., 1985. Fossil Fuel Biomarker. Elsevier Science Publishers New York, p. 294.

Philp, R.P., 2003. Formation and Geochemistry of Oil and Gas in Treatise on Geochemistry. Elsevier Ltd., pp. 223-256.

Philp, R.P., Chen, J.H., Fu, J.M., Sheng, G.Y., 1992. A geochemical investigation of crude oils and source rocks from Biyang Basin, China. Organic Geochemistry 18, 933-945.

Philp, R.P., Gilbert, T.D., 1986. Biomarker distributions in Australian oils predominantly derived from terrigenous source material. In Leythauser D. and Rullkötter JAdvances (Eds.)Organic Geochemistry 1985. Pergamon Press, Oxford, 73-84.

Philp, R.P., Li Jingui, Lewis, C.A., 1989. An organic geochemical investigation of crude oils from Shanganing, Jianghan, Chaidamu and Zhungeer Basins, People's Republic of China. Organic Geochemistry 14, 447-460.

Pierobon, E.S.T., 1991. Contribution to the stratigraphy of the Murzuq basin, S.W. Libya, in The geology of Libya, Vol. V, Salem, M.J., et al., (Eds.), Proc. of 3rd Symposium on the Geology of Libya, Sept. 27-30, 1987 Tripoli, V, 1, 767-783.

Powell, T.G., McKirdy, D.M., 1973. Relationship between ratio of pristane to phytane, crude oil composition and geological environment in Australia. Nature 243, 37-39.

Price, P.L., O'Sullivan, T., Alexander, R., 1987. The nature and occurrence of oil in Seram, Indonesia. In: Proceedings of the Indonesian Petroleum Association, 16th Annual Convention. Indonesian Petroleum Association, Jakarta 1, 141-173.

Radke, M., 1987. Organic geochemistry of aromatic hydrocarbons. In: Brooks, J. and Welte, D. H. (Eds.) Advances in Petroleum Geochemistry. Academic Press, London 2, 14-207.

Radke, M., Welte, D.H., 1983. The Methylphenanthrene Index (MPI): A maturity parameter based on aromatic hydrocarbons. In Advances in Organic Geochemistry1981, Organic Geochemistry, eds. M. Bjorøy et al. ed, pp. 504-512.

Radke, M., Welte, D.H., Willsch, H., 1982a. Geochemical study on a well in the Western Canada: Relation of the aromatic distribution pattern to maturity of organic matter. Geochimica et Cosmochimica Acta 46, 1-10.

Radke, M., Willsch, H., Leythaeuser, D., 1982b. Aromatic components of coal: relation of distribution pattern to rank. Geochimica et Cosmochimica Acta 46, 1831–1848.

Radulovic, P., 1984. Explanatory booklet for the Geological map of Libya 1:250,000, Sheet Wadi Ghat, Industrial Research Centre, Tripoli, NG32-15 87

Ramón, J.C., Dzou, L.I., 1999. Petroleum geochemistry of Middle Magdalena Valley, Colombia. Organic Geochemistry 30, 249–266.

Ramos, E., Marzo, M., de Gibert, M., J., Tawengi, K.S., Khoja, A.A., Bolatti, N.D., 2006. Stratigraphy and sedimentology of the Middle Ordovician Hawaz Formation

(Murzuq basin, Libya). American Association of Petroleum Geologists (AAPG) Bulletin 90, 1309-1336.

Requejo, A.G., 1992. Quantitative analysis of triterpane and sterane biomarkers: methodology and applications in molecular maturity studies: In J. M. Moldowan, P. Albrecht and R. P. Philp (Eds.) Biomarkers in Sediments and Petroleum. Prentice Hall, New York, pp. 222-239.

Requejo, A.G., Hollywood, J., Halpern, H.I., 1989. Recognition and source correlation of migrated hydrocarbons in Upper Jurassic Hareelv Formation, East Greenland. American Association of Petroleum Geologists (AAPG) Bulletin 73, 1065-1088.

Richardson, J.B., Ioannides, N., 1973. Silurian Palynomorphs from the Tanezzuft and Akakus Formation, Tripolitania. Micropaleontology 19, 257-307.

Robert, P., 1980. The optical evaluation of kerogen and geothermal histories applied to oil and gas exploration. B. Durand (ed.). Technip, Paris, 385-414.

Robinson, K.J., 1987. An overview of source rocks and oils in Indonesia. In: Proceedings of the Indonesian Petroleum Association, 16th Annual Convention, Indonesian Petroleum Association, Jakarta. 1, 97-122.

Ronov, A.B., 1958. Organic carbon in sedimentary rocks (in relation to the presence of petroleum). Organic Geochemistry 5, 497–509.

Rubinstein, I., Sieskind, O., Albrecht, P., 1975. Rearranged sterenes in shale: occurrence and simulated formation. Journal of the Chemical Society, Perkin Transactions 1, 1833-1836.

Rullkötter, J., Aizenshtat, Z., Spiro, B., 1984a. Biological markers in bitumens and pyrolyzates of Upper Cretaceous bituminous chalks from the Ghareb Formation (Israel). Geochimica et Cosmochimica Acta 48, 151-157.

Rullkötter, J., Mackenzie, A.S., Welte, D.H., Leythaeuser, D., Radke, M., 1984b. Quantitative gas chromatography mass spectrometry analysis of geological

samples. In Schenck P. A., de Leeuw J. W. and Lijmbach G. W. M. (Eds.) Advances in Organic Geochemistry 1983. Pergamon Press, Oxford, pp. 817-827.

Rullkötter, J., Marzi, R., 1988. Natural and artificial maturation of biological markers in Toarcian shale from northern Germany. In: L. Mattavelli and L. Novelli, (Eds.) Advances in Organic Geochemistry 1987 Oxford, Pergamon Press, pp. 639-645.

Rullkötter, J., Spiro, B., Nissenbaum, A., 1985. Biological marker characteristics of oils and asphalts from carbonate source rocks in a rapidly subsiding graben, Dead Sea. Geochimica et Cosmochimica Acta 49, 1357-1370.

Sammy, N., 1985. Biological systems in northern Australia solar salt and fields. In: B.C. Schreiber and L. Harner (Eds.) 6th International Symposium on Salt. Salt Institute, Alexandria, Virginia 1, 207-215.

Schou, L., Eggen, S., Schoell, M., 1985. Oil-oil and oil-source rock correlation, Northern North Sea. In: Thomas, B. M. (Ed.) Petroleum Geochemistry in Exploration of the Norwegian Shelf. Graham & Trotman London, pp. 101-117.

Seifert, W., Moldowan, J.M., 1986. Use of biological markers in petroleum exploration. In Johns, R. B (Ed.) Biological Markers in the Sedimentary Record. Methods in Geochemistry and Geophysics, Elsevier, Amsterdam, pp. 261-290.

Seifert, W.K., Moldowan, J.M., 1978. Application of steranes, terpanes and monoaromatics to the maturation, migration and source of crude oils. Geochimica et Cosmochimica Acta 42, 77-95.

Seifert, W.K., Moldowan, J.M., 1979. The effect of biodegradation on steranes and terpanes in crude oils. Geochimica et Cosmochimica Acta 43, 111-126.

Seifert, W.K., Moldowan, J.M., 1981. Paleoreconstruction by biological markers. Geochimica et Cosmochimica Acta 45, 783-794.

Seifert, W.K., Moldowan, J.M., Jones, R.W., 1980. Application of biological marker chemistry to petroleum exploration. In Proc. Tenth World Petroleum Congress, Bucharest, Romania. September 1979. Paper SP8. 425-440.

Shanmugam, G., 1985. Significance of coniferous rain forests and related organic matter in generating commercial quantities of oil, Gippsland Basin, Australia. . American Association of Petroleum Geologists (AAPG) Bulletin 69, 1241-1254.

Sieskind, O., Joly, G., Albrecht, P., 1979. Simulation of the geochemical transformations of sterols: superacid effect of clay minerals. Geochimica et Cosmochimica Acta 43, 1675-1679.

Sikander, A.H., Basu, S., Rasul, S.M., 2000. Geochemical source-maturation and volumetric evaluation of lower Palaeozoic source rocks in the west Libyan basins (abstract only). Second Symposium on the Sedimentary Basins of Libya. The Geology of northwest Libya. Book of abstracts, 88.

Sofer, Z., 1980. Preparation of carbon dioxide for stable carbon isotope analysis of petroleum fractions. Analytical Chemistry 52, 1389-1391.

Strachan, M.G., Alexander, R., Van Bronswijk, W., Kagi, R.I., 1989. Source and heating rate effects upon maturity parameters based on ratios of 24-ethylcholestane diastereomers. Journal of Geochemical Exploration 31, 285-294.

Summons, R.E., Thomas, J., Maxwell, J.R., Boreham, C.J., 1992. Secular and environmental constraints on the occurrence of dinosterane in sediments. Geochimica et Cosmochimica Acta 56, 2437–2444.

Tegelaar, E.W., de Leeuw, J.W., Derenne, S., Largeau, C., 1989. A reappraisal of kerogen formation. Geochemica et Cosmochimica Acta 53, 3103-3106.

ten Haven, H.L., de Leeuw, H.L., Sinninghe Damste, J.S., Schenk, D.A., 1985. Organic geochemical studies of a Messinian evaporite basin, northern Apennines (Italy), I. Hydrocarbon biological markers for a hypersaline environment. Geochimica et Cosmochimica Acta 43, 739-745.

ten Haven, H.L., de Leeuw, J.W., Peakman, T.M., Maxwell, J.R., 1986. Anomalies in steroid and hopanoid maturity indices. Geochimica et Cosmochimica Acta 50, 853-855.

ten Haven, H.L., De Leeuw, J.W., Rullkötter, J., Sinninghe Damste, J.S., 1987. Restricted utility of the pristane/phytane ratio as a palaeoenvironmental indicator. Nature 330.

ten Haven, H.L., De Leeuw, J.W., Schenck, P.A., Klaver, G.T., 1988. Geochemistry of Mediterranean sediments. Bromine/ organic carbon and uranium/organic carbon ratios as indicators for different sources of input and post depositional oxidation, respectively. Organic Geochemistry 13, 255-261.

Tissot, B., Durand, B., Epitalié, J., Combaza, A., 1974. Influence of nature and diagenesis of organic matter in formation of petroleum. American Association of Petroleum Geologists (AAPG) Bulletin 58, 499-506.

Tissot, B.P., Welte, D.H., 1984. Petroleum Formation and Occurrence, 2nd ed. ed. Springer Verlag, New York, p. 699.

Tissot, B.P., Welte, D.H., Durand, B., 1987. The role of geochemistry in exploration risk evaluation and decision making. In Proc. 12th World Petroleum Congress 2, 99-112.

Tyson, R.V., 1995. Sedimentary organic matter; Organic facies and palynofacies. Chapman & Hall, London, 615.

Van Bergen, P.F., Collinson, M.E., Briggs, D.E.G., de Leeuw, J.W., Scott, A.C., Evershed, R.P., Finch, P., 1995. Resistant biomacromolecules in the fossil record. Acta Botanica Neerlandica 44, 319-342.

van Graas, G.W., 1989. New biomarker maturity parameters: extension of the working range to higher maturity levels. 14th International Meeting on Organic Geochemistry, Paris, September 18-22. Abstracts, Number 56.

van Graas, G.W., 1990. Biomarker maturity parameters for high maturities: Calibration of the working range up to the oil/condensate threshold. Organic Geochemistry 16, 1025-1032.

Vandenbroucke, M., Largeau, C., 2007. Kerogen origin, evolution and structure. Organic Geochemistry 38, 719-833.

Volkman, J.K., 1986. A review of sterol markers for marine and terrigenous organic matter. Organic Geochemistry 9, 83-99.

Volkman, J.K., 1988. Biological marker compounds as indicators of the depositional environments of petroleum source rocks. In Fleet, A.J., Kelts, K., and Talbot, M.R. (Eds.), Lacustrine Petroleum Source Rocks. Geological Society, London, Special Publications 40, 103-122.

Volkman, J.K., Alexander, R., Kagi, R.I., Noble, R.A., Woodhouse, G.W., 1983a. A geochemical reconstruction of oil generation in the Barrow Sub-Basin of Western Australia. Geochemica et Cosmochimica Acta 47, 2091-2105.

Volkman, J.K., Alexander, R., Kagi, R.I., Noble, R.A., Woodhouse, G.W., Woodhouse, G.W., 1983b. Demethylated hopanes in crude oils and their applications in petroleum geochemistry. Geochemica et Cosmochimica Acta 47, 785-794.

Volkman, J.K., Gillan, F.T., Johns, R.B., Eglinton, G., 1981. Sources of neutral lipids in a temperate intertidal sediment. Geochimica et Cosmochimica Acta 45, 1817-1828.

Volkman, J.K., Maxwell, J.R., 1986. Acyclic isoprenoids as biological markers In: R.B. Johns (Ed.) Biological Markers in the sedimentary Record Elsevier, New York, pp. 1-42.

Vos, R.G., 1981. Sedimentology of an Ordovician Fan Delta complex, Western Libya Sedimentary Geology 29, 153-170.

Wakeham, S.G., 1990. Algal and bacterial hydrocarbons in particulate matter and interfacial sediment of the Cariaco Trench. Geochimica et Cosmochimica Acta 54, 1325–1336.

Wang, H.D., 1993. A geochemical study of potential source rocks and crude oils in the Anadarko Basin, Oklahoma. Unpublished Thesis. University of Oklahoma, 269.

Wang, H.D., Philp, R.P., 1997. Geochemical Study of Potential Source Rocks and Crude Oils in the Anadarko Basin, Oklahoma. American Association of Petroleum Geologists (AAPG) Bulletin 81, 249-275.

Waples, D.W., Machihara, T., 1990. Application of sterane and triterpanes biomarkers in petroleum exploration. Bulletin of Canadian Petroleum Geology 38, 357-380.

Waples, D.W., Machihara, T., 1991. Biomarkers for geologists. AAPG Methods in Exploration Series 9, 91.

Welte, D., 1974. Recent advances in organic geochemistry of humic substances and kerogen. A review. In: Tissot, B., Bienner, F. (Eds.), Advances in Organic Geochemistry 1973. Editions Technip, Paris, 3-13.

Wenger, L.M., Davis, C.L., Isaksen, G.H., 2002. Multiple controls on petroleum biodegradation and impact on oil quality. Society of Petroleum Engineering (SPE) Reservoir Evaluation and Engineering 5, 375-383.

Wignall, P.B., Myers, K.J., 1988. Interpreting benthic oxygen levels in mudrocks: a new approach. Geology 16, 452-455.

Yahia, A.M., Van Dijk, P.M., Erren, J.W.M.G., 2000. Surface and Subsurface Characteristics of Al-Qarqaf Arch and Adjacent Parts of the Ghadamis and Murzuq Basins, West Libya: An Integration of Remote Sensing, Aeromagnetic and Seismic Interpretation. In: Salem, M. J., Khaled, M. Oun. & Hussein, M. S. (Eds.), the Geology of North-West Libya National Library, Benghazi, Libya, GSPLAJ., pp. 171-190.

Yang, B., 1991. Geochemical characteristics of oil from well Shacan 2 in the Tarim Basin. Journal of Southeast Asian Earth Sciences 5, 401-406.

Zhang, W.Z., Yang, H., Hou, L., Liu, F., 2009. Distribution and geological significance of 17α(H)-diahopanes from different hydrocarbon source rocks of Yanchang Formation in Ordos Basin. Science in China Series D: Earth Sciences 52, 965-974.

Zumberge, J.E., 1984. Source rocks of the La Luna (Upper Cretaceous) in the Middle Magdalena Valley, Colombia. In: J.G. Palacas (ed.) Geochemistry and Source Rock Potential of Carbonate Rocks. AAPG Studies in Geology 18, 127-133.

Zumberge, J.E., 1987. Prediction of source rock characteristics based on terpane biomarkers in crude oils: A multivariate statistical approach. Geochimica et Cosmochimica Acta 51, 1625-1637.

APPENDICES

APPENDIX I. Extraction and Fractionation Data of Crude Oils and Source Rocks from Murzuq Basin, S.W. Libya.

Crude Oil Sample:

Oil Samples	sample weight (gr)	Maltene (mg)	Maltene (%)	Asph (mg)	Asph (%)	SAT (mg)	SAT (%)	ARM (mg)	ARM (%)	NSO (mg)	NSO (%)
A1	2	1146.43	99.06	0.0109	0.94	5.03	58	2.92	34	0.71	8
A7	2	1258.11	99.12	0.0112	0.88	5.55	68	2.09	26	0.54	7
A10	2	1073.35	98.85	0.0125	1.15	6.42	68	2.67	28	0.38	4
A11	2	1198.78	98.90	0.0133	1.10	7.68	64	3.1	26	1.28	11
A12	2	1225.07	90.77	0.1245	9.23	9.27	80	1.9	16	0.49	4
A14	2	1227.06	98.69	0.0163	1.31	10.25	90	0.85	7	0.27	2
A15	2	1402.69	98.48	0.0217	1.52	5.99	82	0.9	12	0.4	5
A16	2	1227.38	97.72	0.0286	2.28	1.87	49	1.76	46	0.16	4
A24	2	983.11	98.59	0.0140	1.41	7.39	74	1.86	19	0.7	7
A25	2	965.68	91.29	0.0922	8.71	3.69	63	1.71	29	0.47	8
A26	2	1164.29	98.68	0.0156	1.32	7.17	84	1.09	13	0.3	4
A27	2	1285.84	98.74	0.0164	1.26	2.84	37	4.75	61	0.17	2
A28	2	1267.49	98.80	0.0154	1.20	7	76	1.94	21	0.23	3
A30	2	1121.74	98.05	0.0223	1.95	1.13	35	1.69	52	0.41	13
A31	2	1164.60	98.24	0.0209	1.76	4.18	82	0.73	14	0.19	4
A32	2	2068.19	99.20	0.0166	0.80	5.49	66	1	12	1.78	22
R-1	2	1289.18	93.93	0.0833	6.07	8.65	80	1.78	17	0.32	3
R-7	2	1263.81	91.62	0.1156	8.38	8.8	87	1.16	11	0.14	1
I-2	2	1028.14	78.48	0.2819	21.52	8.74	80	1.78	16	0.39	4
I-11	2	1278.32	91.72	0.1154	8.28	8.29	79	1.79	17	0.38	4

Saturate, aromatic and polar (NSO) fractions was calculated based on the following equations:

% Asphaltene= Weight of asphaltene/Weight of sample *100

% Sat= Wsat/ (Wsat + Waro +Wnso) * (100-%Asph)

% ARO= Waro/ (Wsat + Waro +Wnso) * (100-%Asph)

% NSO= Wnso/ (Wsat + Waro +Wnso) * (100-%Asph)

APPENDIX I. (continued)

Rock Samples:

Rock sample	Rock sample weights (gr)	Maltenes (mg)	Maltenes (%)	Asph (mg)	Asph (%)	SAT (mg)	SAT (%)	ARM (mg)	ARM (%)	NSO (mg)	NSO (%)
A3	55.8	29.49	71.63	11.68	28.37	3.7	3.2	1.3	1.2	84.5	73.0
A5	48.2	39.52	80.83	9.37	19.17	4.5	32.8	0.2	1.7	6.5	47.2
A6a	59.1	480.92	98.23	8.69	1.77	2.5	24.0	2.3	22.0	5.6	53.8
A6b	43.5	289.16	92.43	23.68	7.57	7.9	28.8	1.4	5.0	16.1	58.7
A10	59.0	82.86	87.40	11.95	12.60	5.2	39.4	0.8	6.3	5.6	41.9
A17a	41.2	33.62	86.96	5.04	13.04	4.6	19.9	0.8	3.6	14.4	62.6
A17b	25.1	29.79	88.11	4.02	11.89	5.3	73.5	0.3	3.6	0.7	9.4
A18	40.7	27.35	99.45	0.15	0.55	5.4	74.0	0.9	12.3	1.0	13.0
A19a	58.4	20.56	75.39	6.71	24.61	3.9	15.0	0.4	1.6	15.7	60.1
A19b	65.4	39.91	88.71	5.08	11.29	4.6	35.9	1.0	7.4	5.8	44.9
A20a	54.0	41.86	85.12	7.32	14.88	6.0	43.1	0.7	5.0	5.1	36.4
A20b	55.0	35.33	83.58	6.94	16.42	4.6	35.5	0.6	4.5	5.6	43.3
A21	27.9	8.79	73.43	3.18	26.57	1.9	6.9	0.7	2.6	15.4	55.5
A22	35.0	26.42	82.05	5.78	17.95	5.4	36.8	0.7	4.9	5.6	38.7
A23	58.0	41.25	88.94	5.13	11.06	4.7	77.1	0.3	4.6	0.4	6.7
A34	8.0	8.78	66.67	4.39	33.33	3.0	18.4	0.2	1.2	5.3	32.9
A35a	25.8	15.5	85.59	2.61	14.41	3.1	28.4	0.3	3.1	5.5	50.8
A35b	47.4	25.54	76.54	7.83	23.46	2.2	18.9	0.2	2.1	6.2	53.6
A37a	47.0	24.73	76.73	7.5	23.27	4.2	53.2	0.2	2.2	1.6	20.5
A37b	21.5	30	79.70	7.64	20.30	4.1	62.5	0.2	3.7	0.8	11.6

APPENDIX II. Gas chromatograms of aliphatic fractions showing the n-alkanes and acyclic isoprenoids for selected rock samples from 'cool' shale Tanezzuft Formation, Murzuq Basin, NC-115, A-Field.

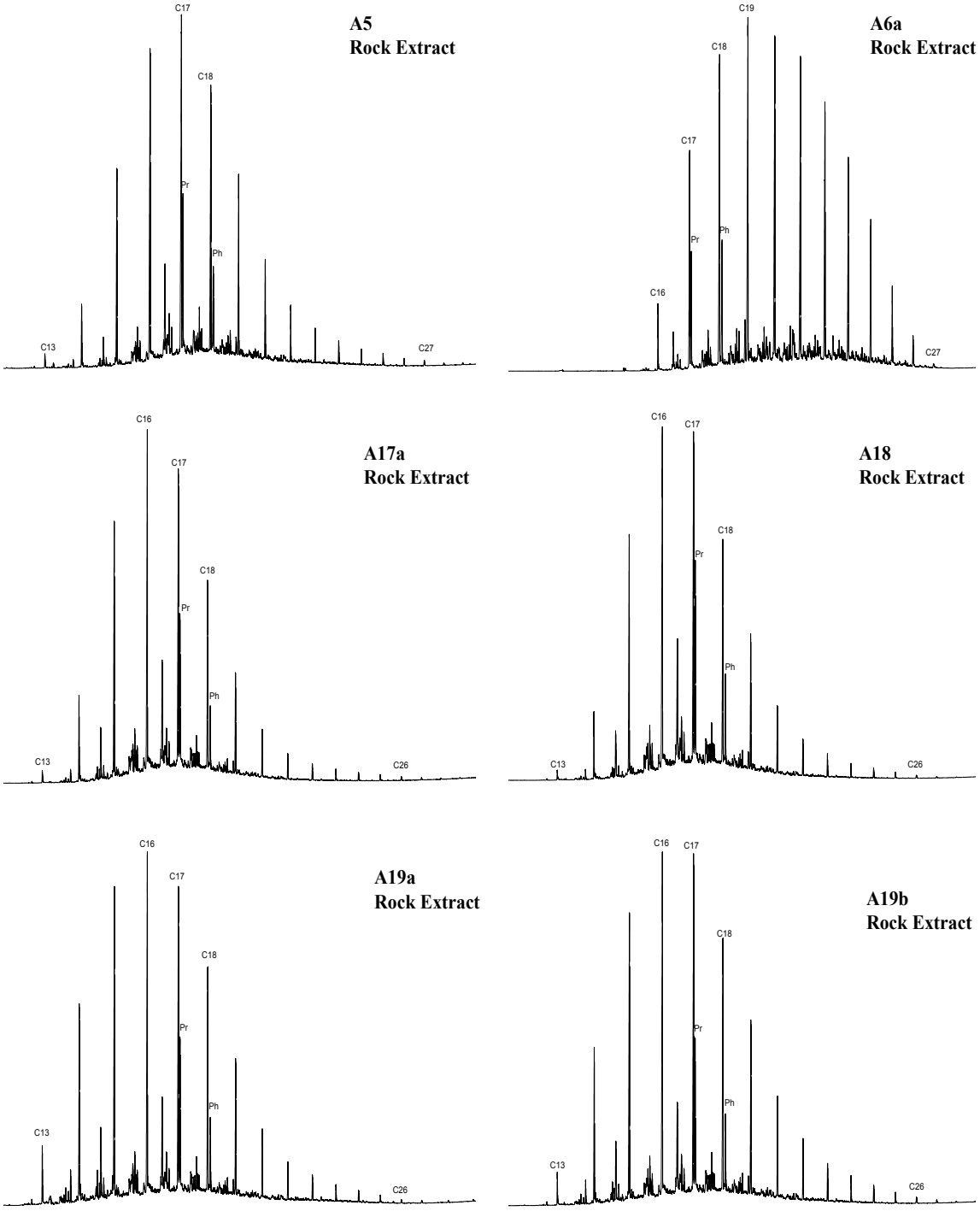

APPENDIX II. (continued)

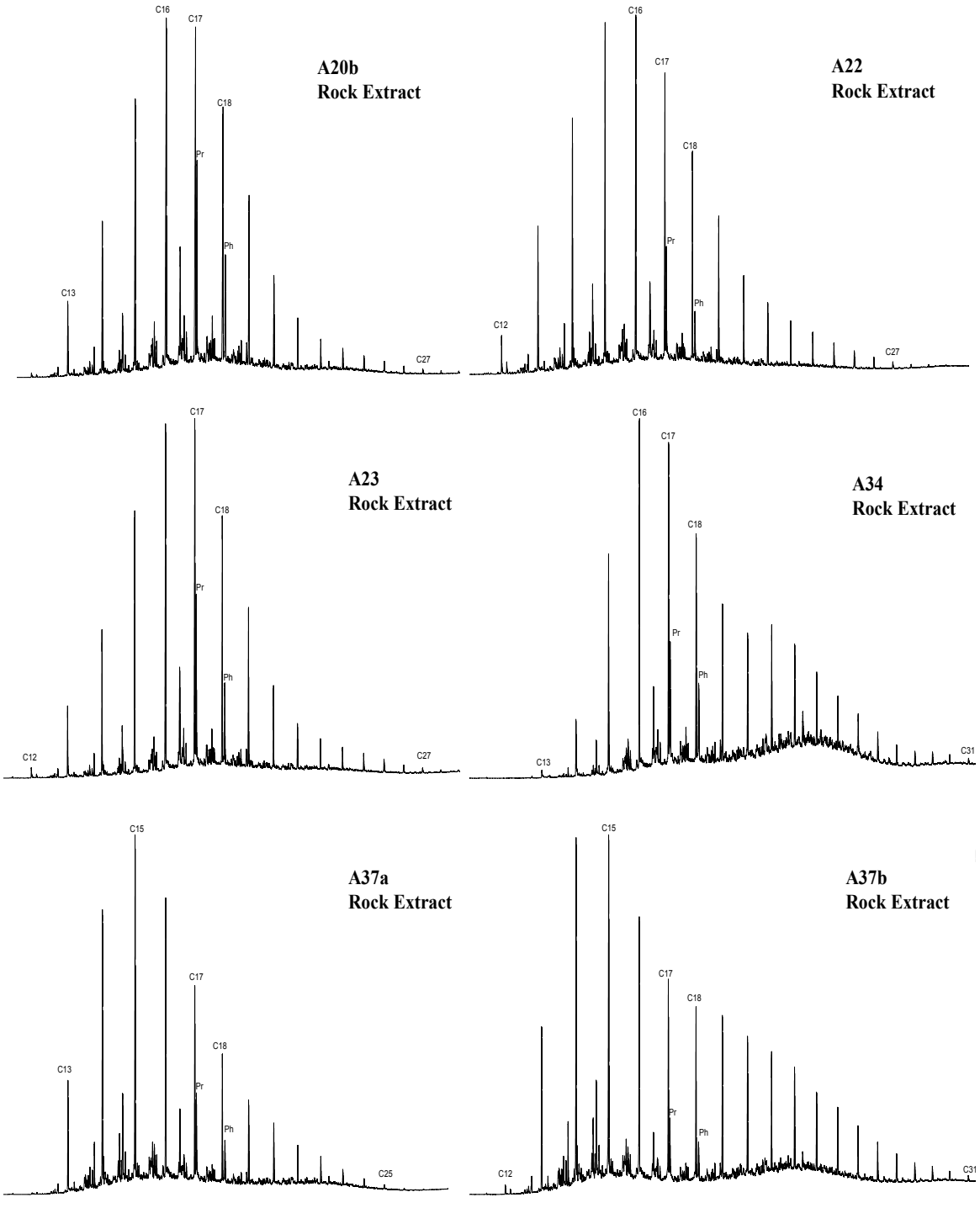

APPENDIX III. Mass chromatograms showing the distribution of steranes (*m/z* 217) of the samples from the Tanezzuft Formation "cool" shale, A-Field, NC-115 in the Murzuq Basin, S.W. Libya. (*) Deuterated Internal Standard ($C_{24}D_{50}$).

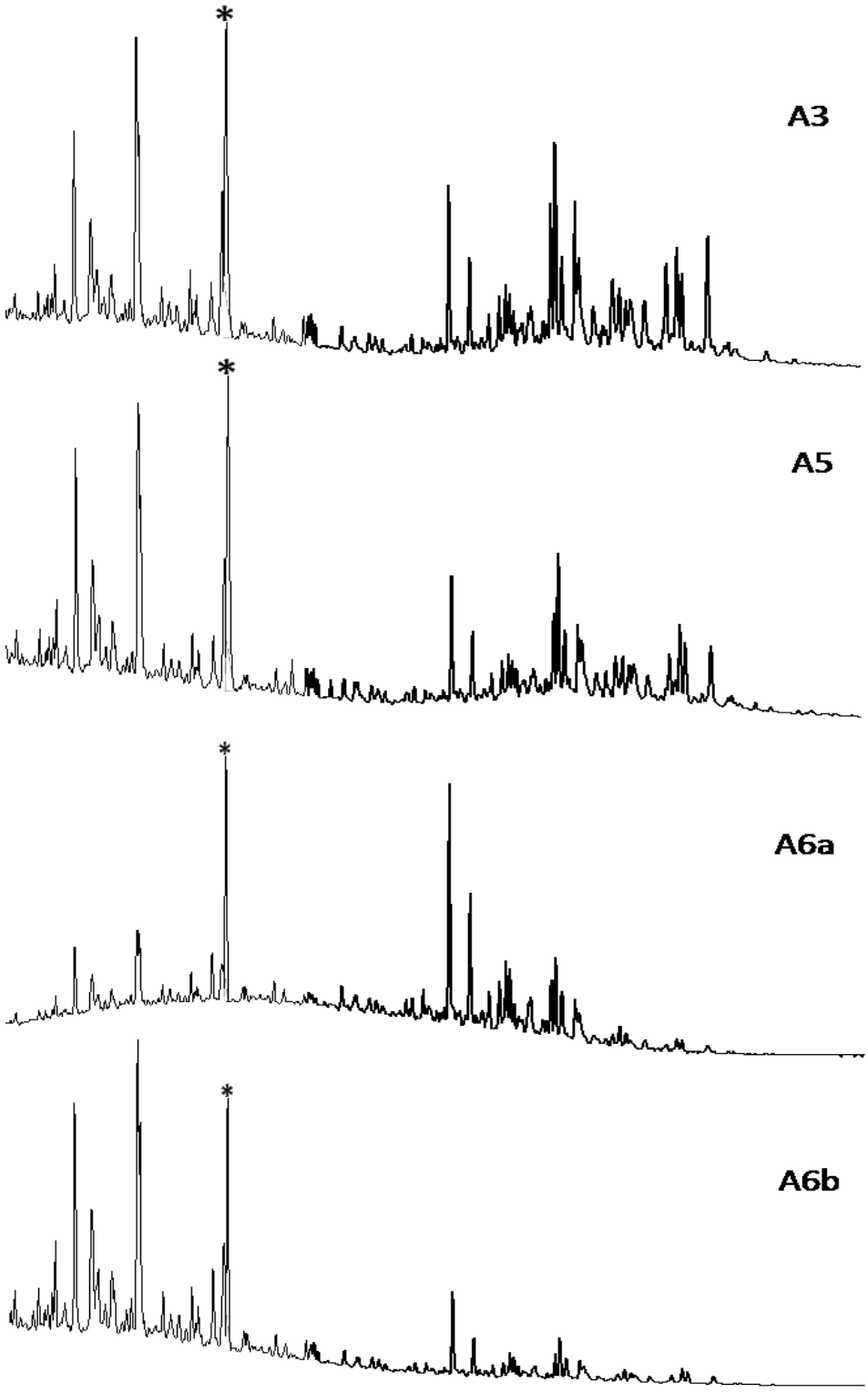

APPENDIX III. (continued)

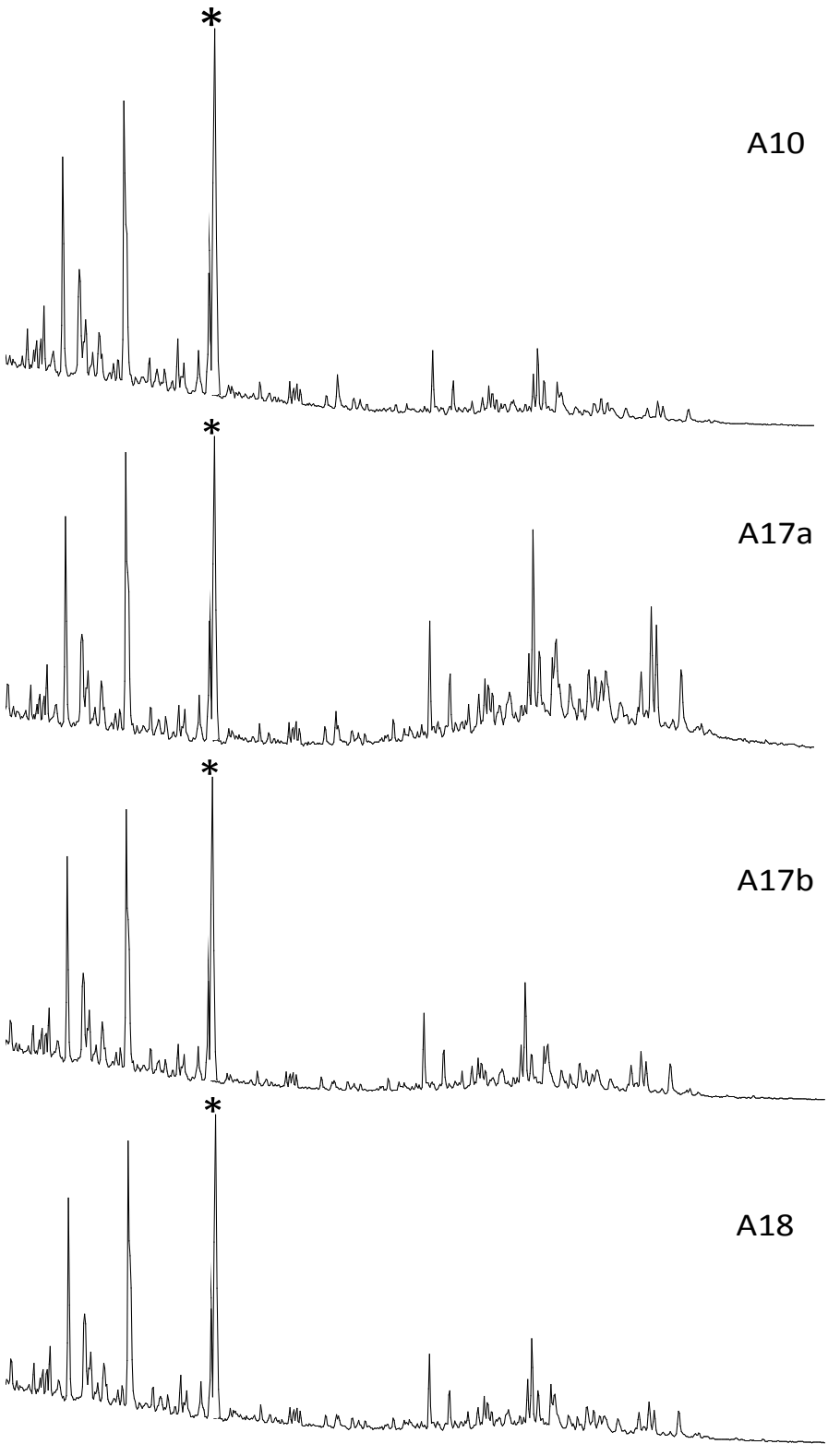

APPENDIX III. (continued)

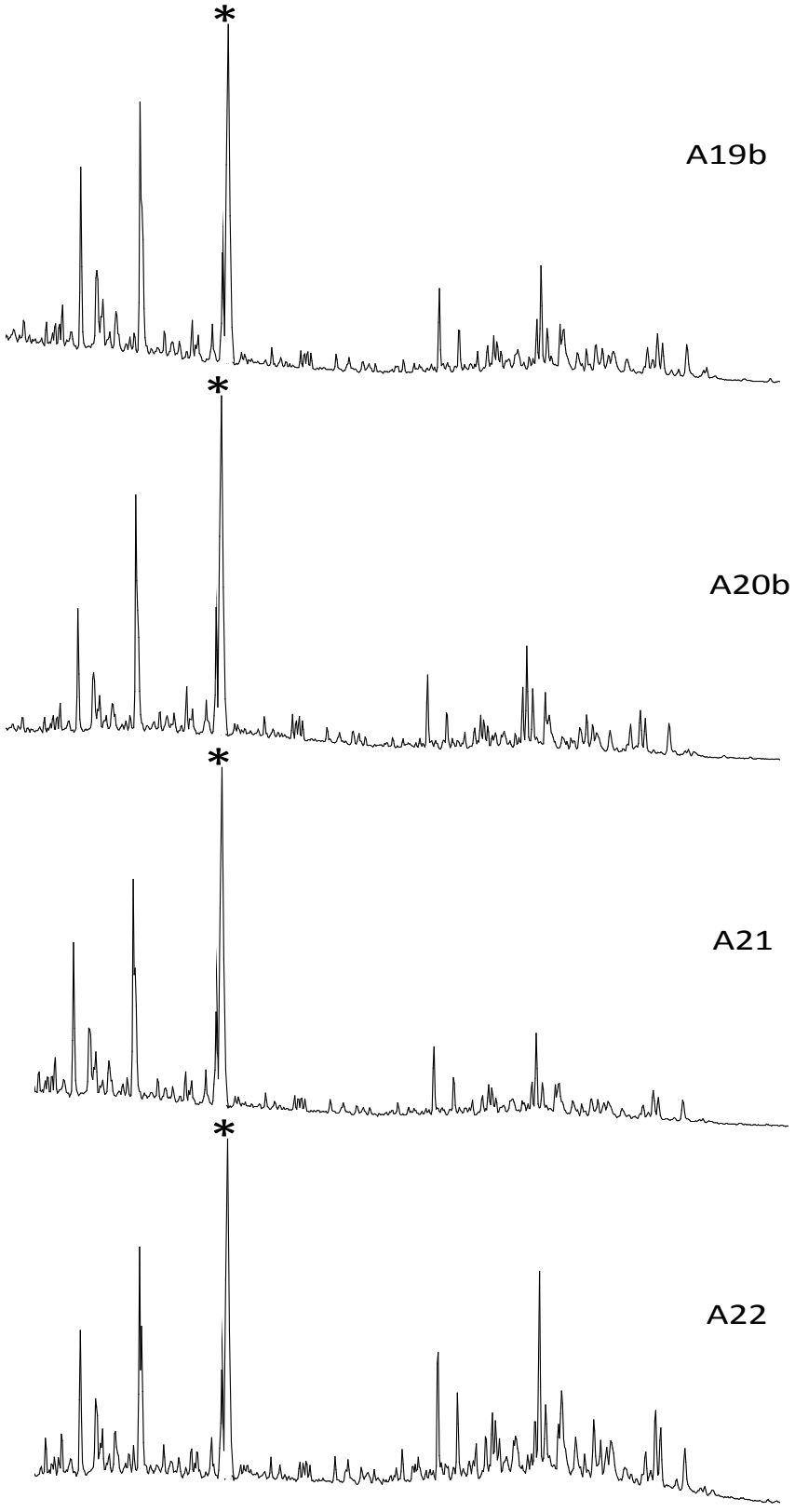

APPENDIX III. (continued)

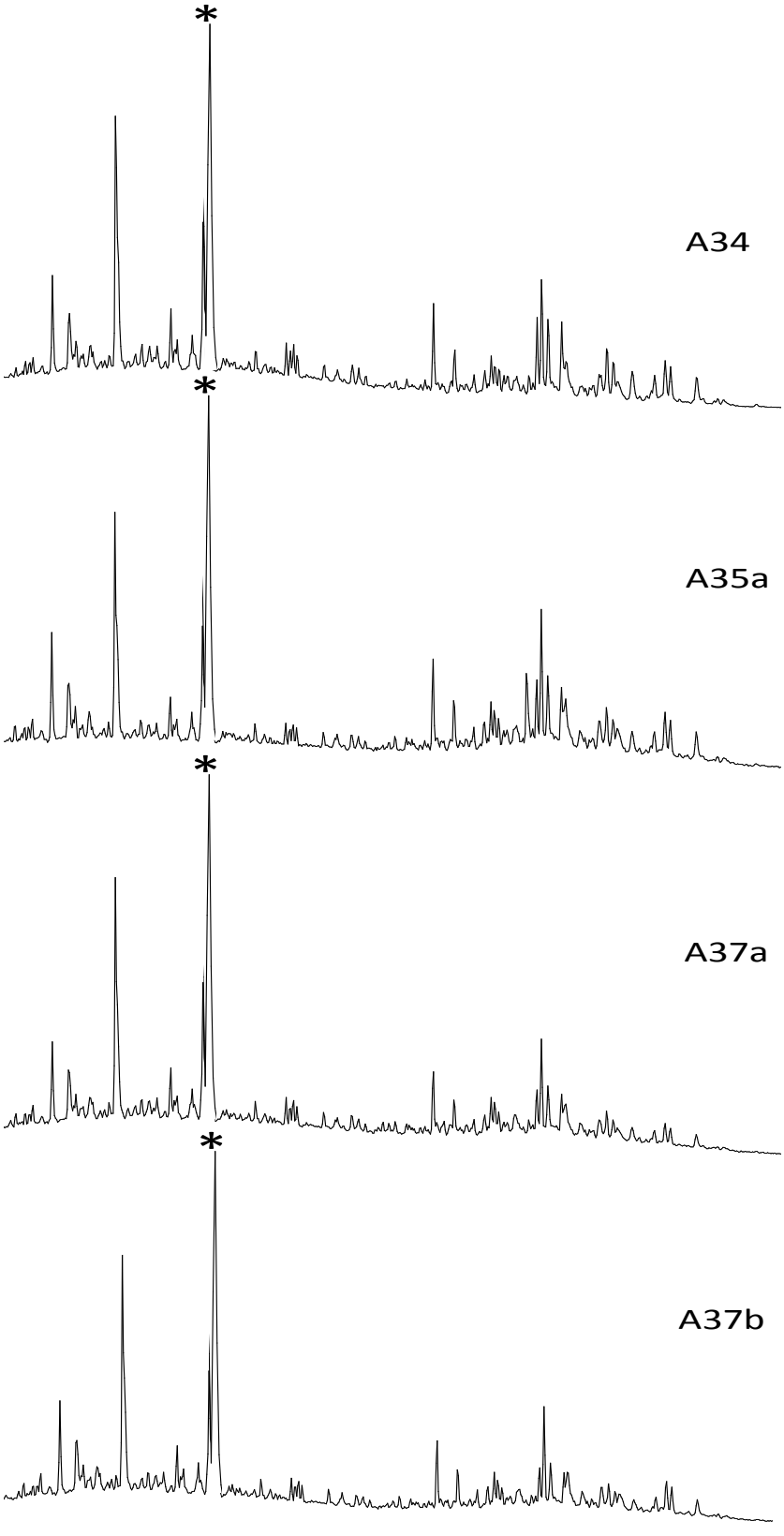

APPENDIX IV. Mass chromatograms showing the distribution of hopanes (*m/z* 191) of selected samples from the Tanezzuft Formation "cool" shale, A-Field, NC-115 in the Murzuq Basin, S.W. Libya. (*) Deuterated Internal Standard ($C_{24}D_{50}$).

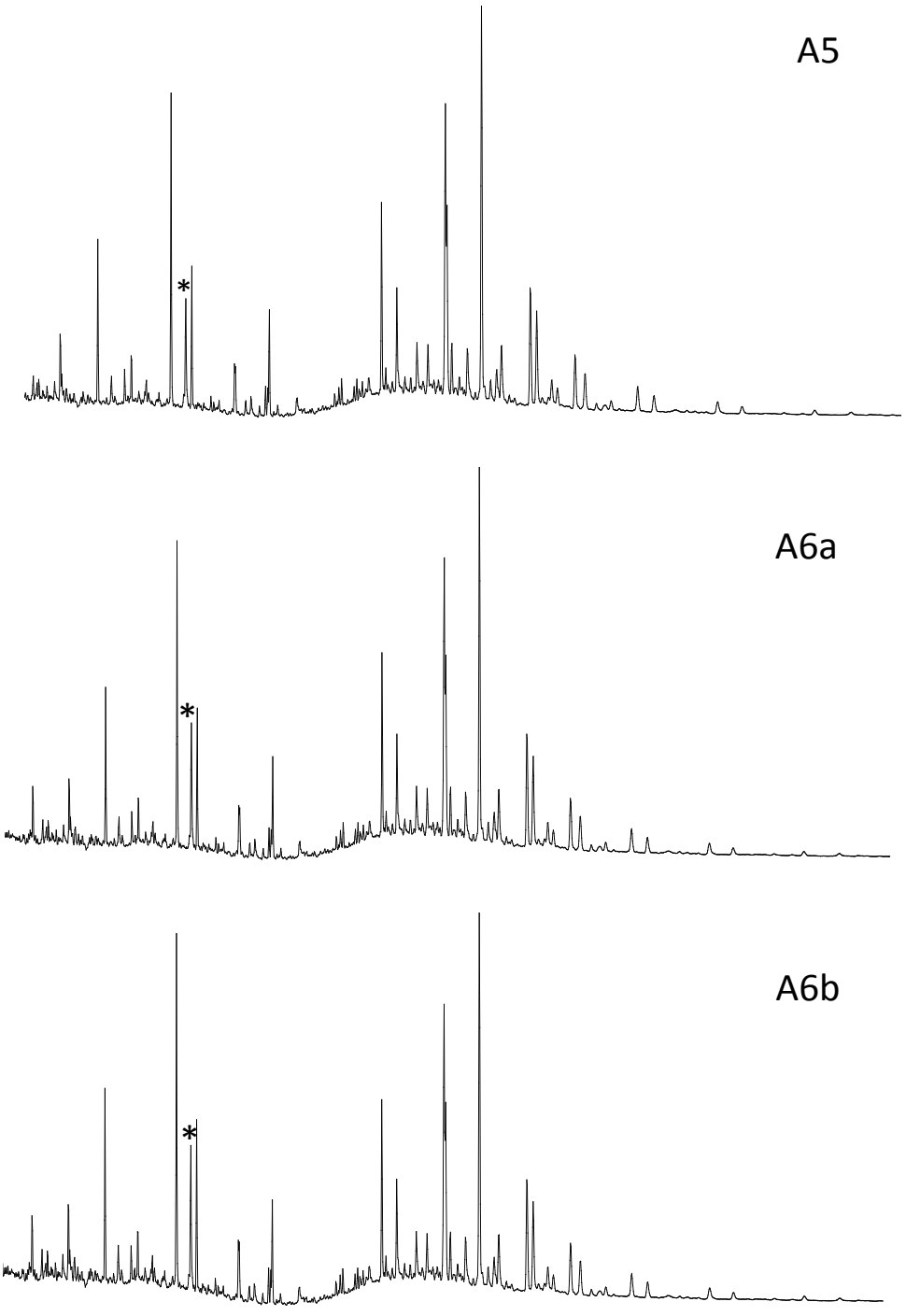

APPENDIX IV. (continued)

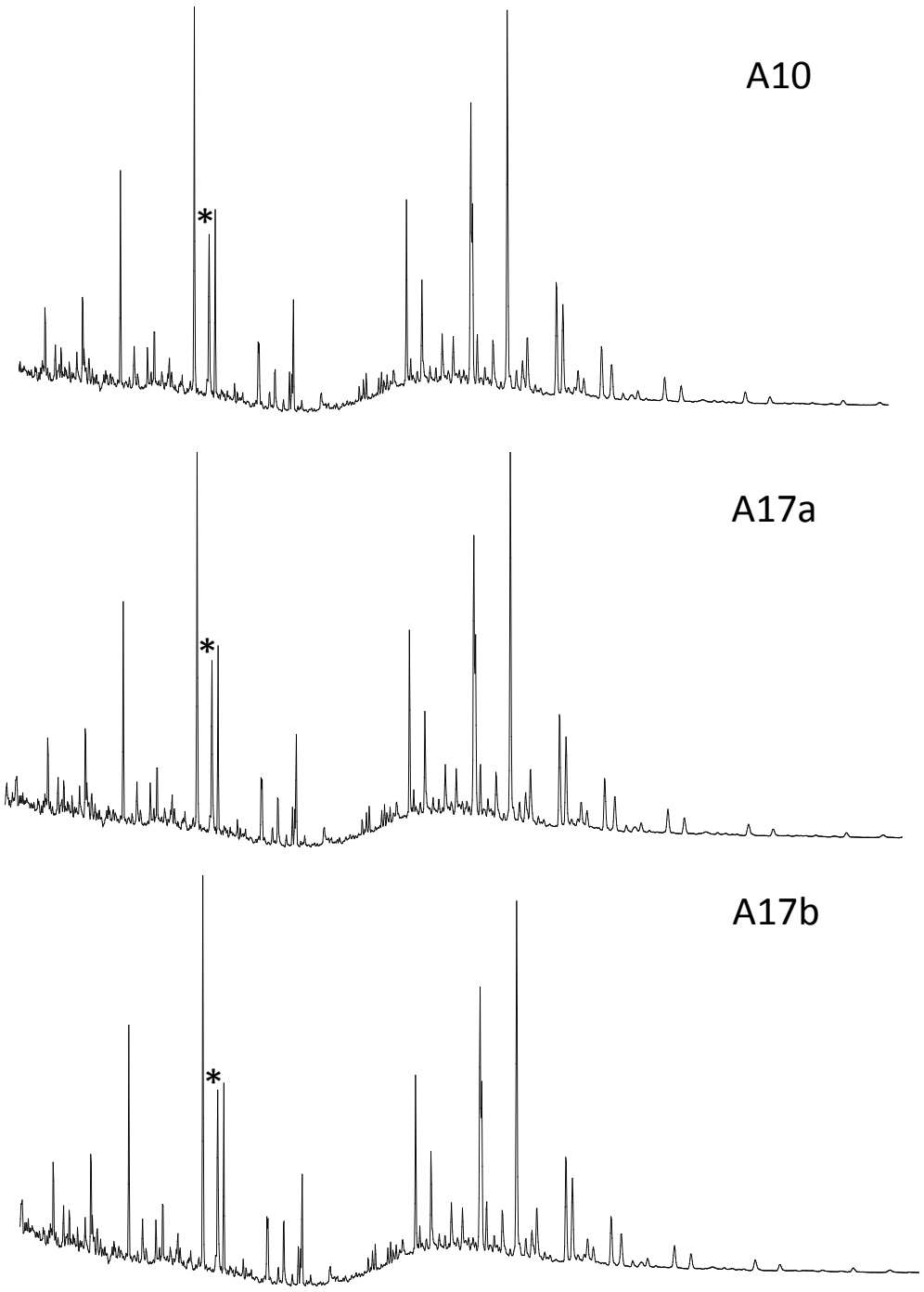

APPENDIX IV. (continued)

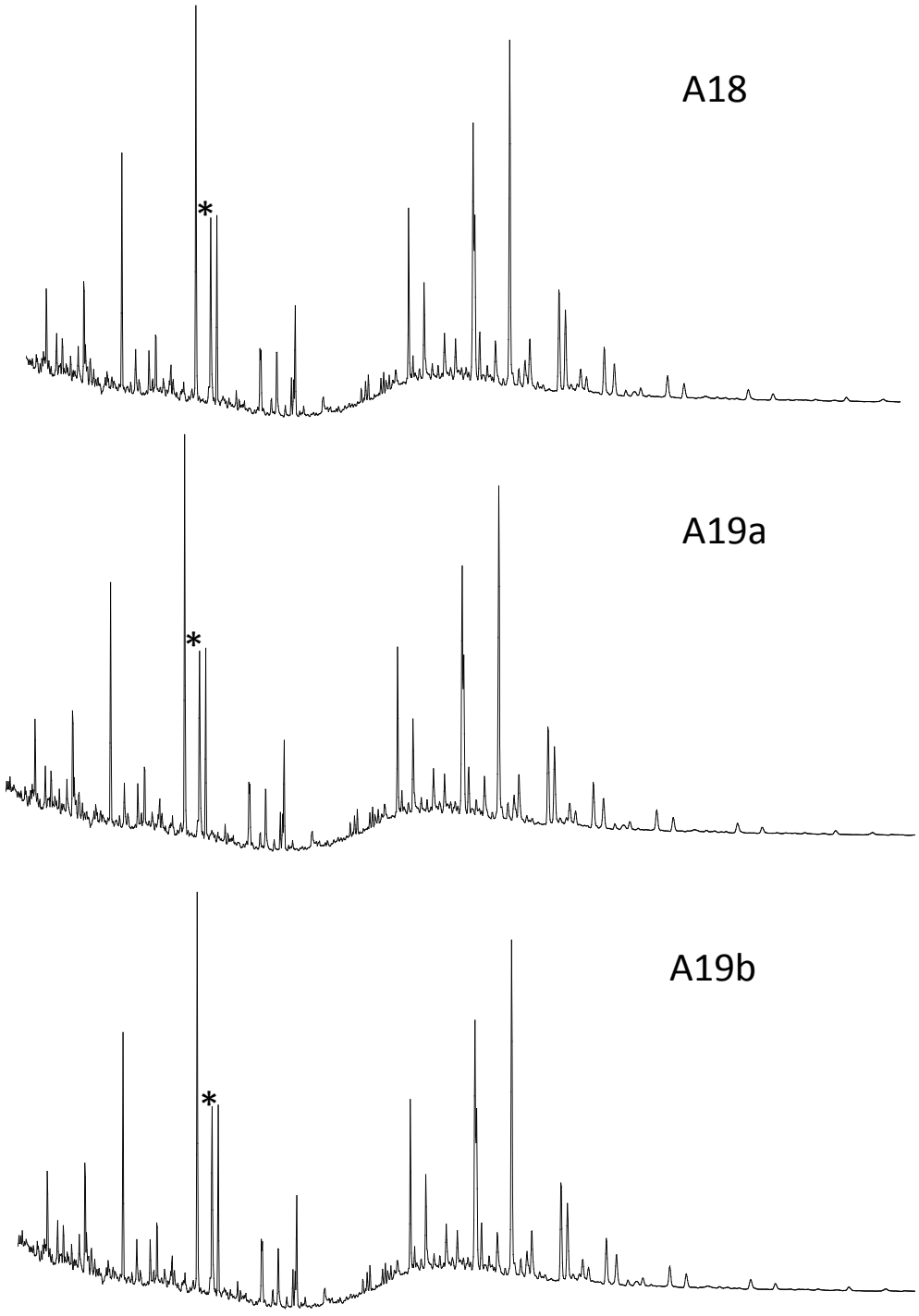

APPENDIX IV. (continued)

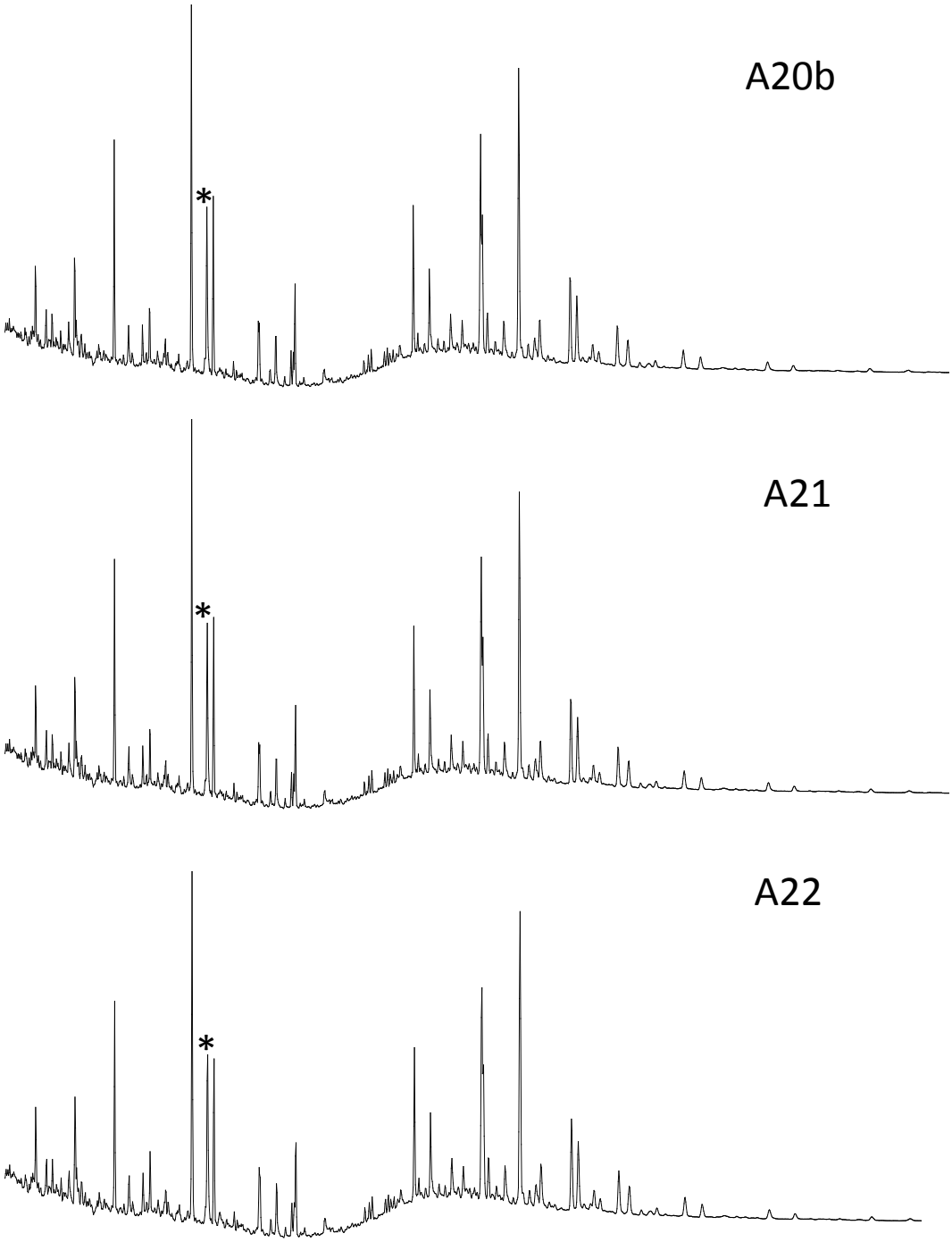

APPENDIX IV. (continued)

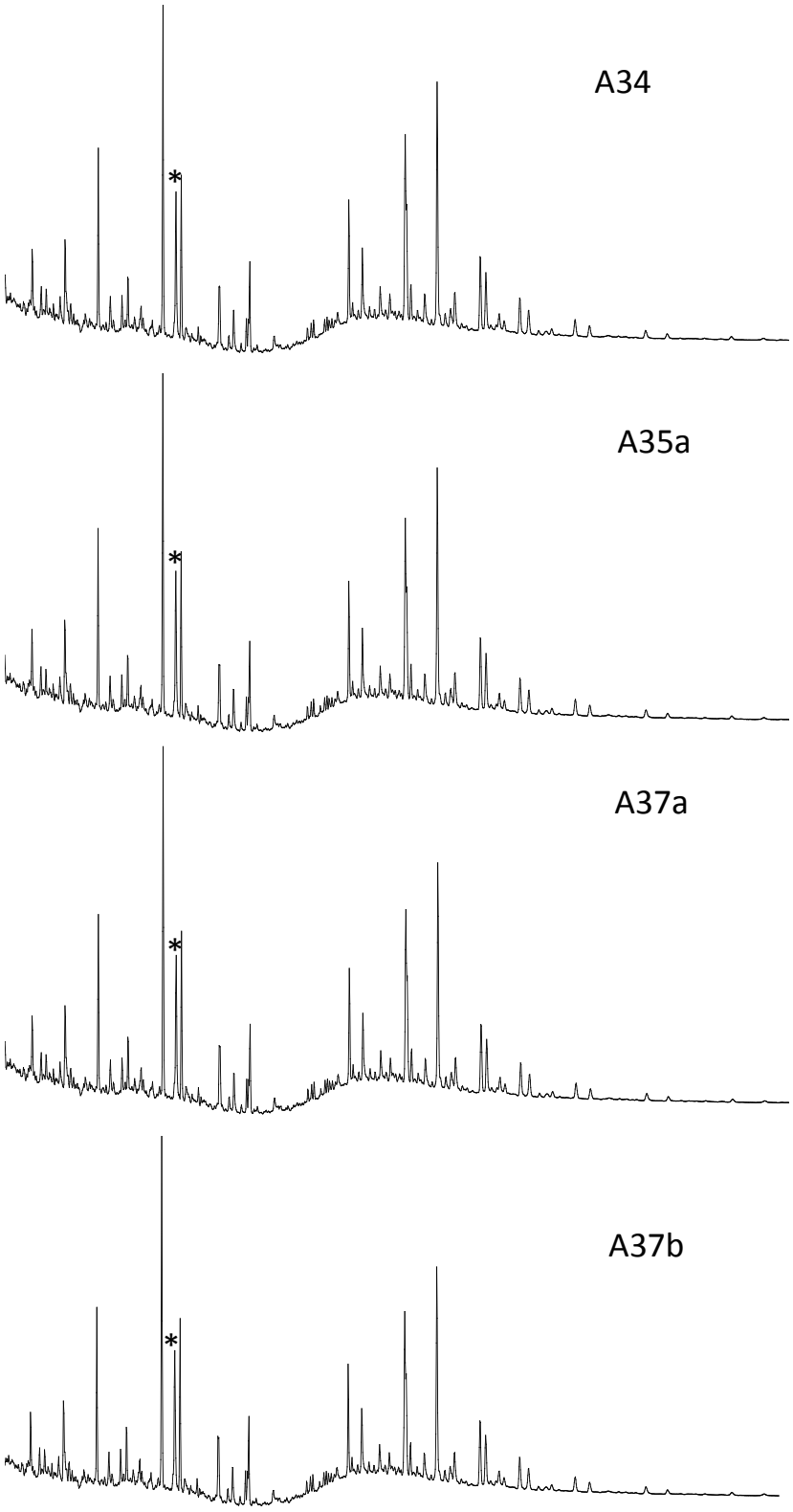

APPENDIX V. Gas chromatograms of aliphatic fractions showing the *n*-alkanes and acyclic isoprenoids for the crude oils from Murzuq Basin, Block NC-115, A Field and Block NC186, I and R Fields.

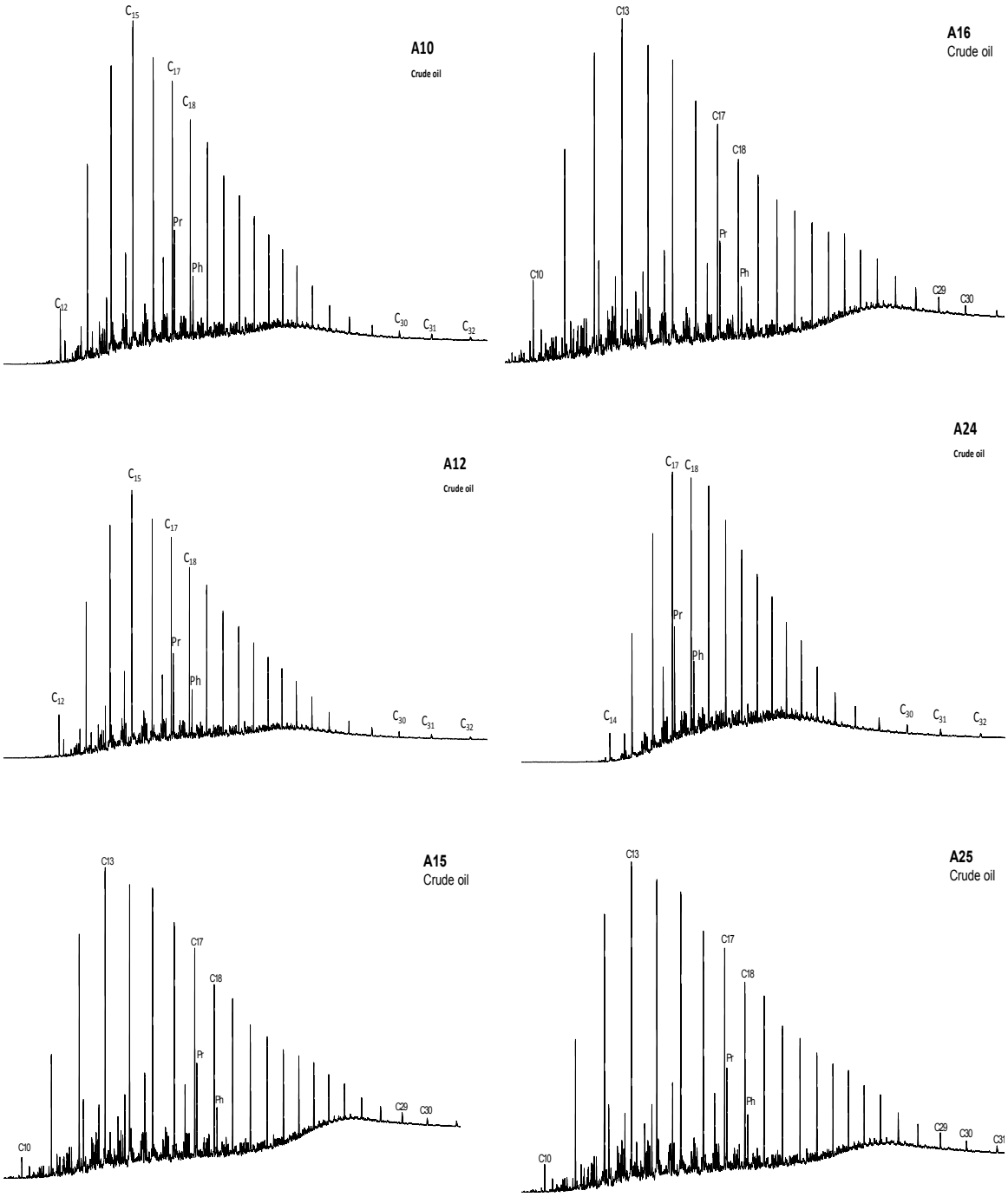

APPENDIX V. (continued)

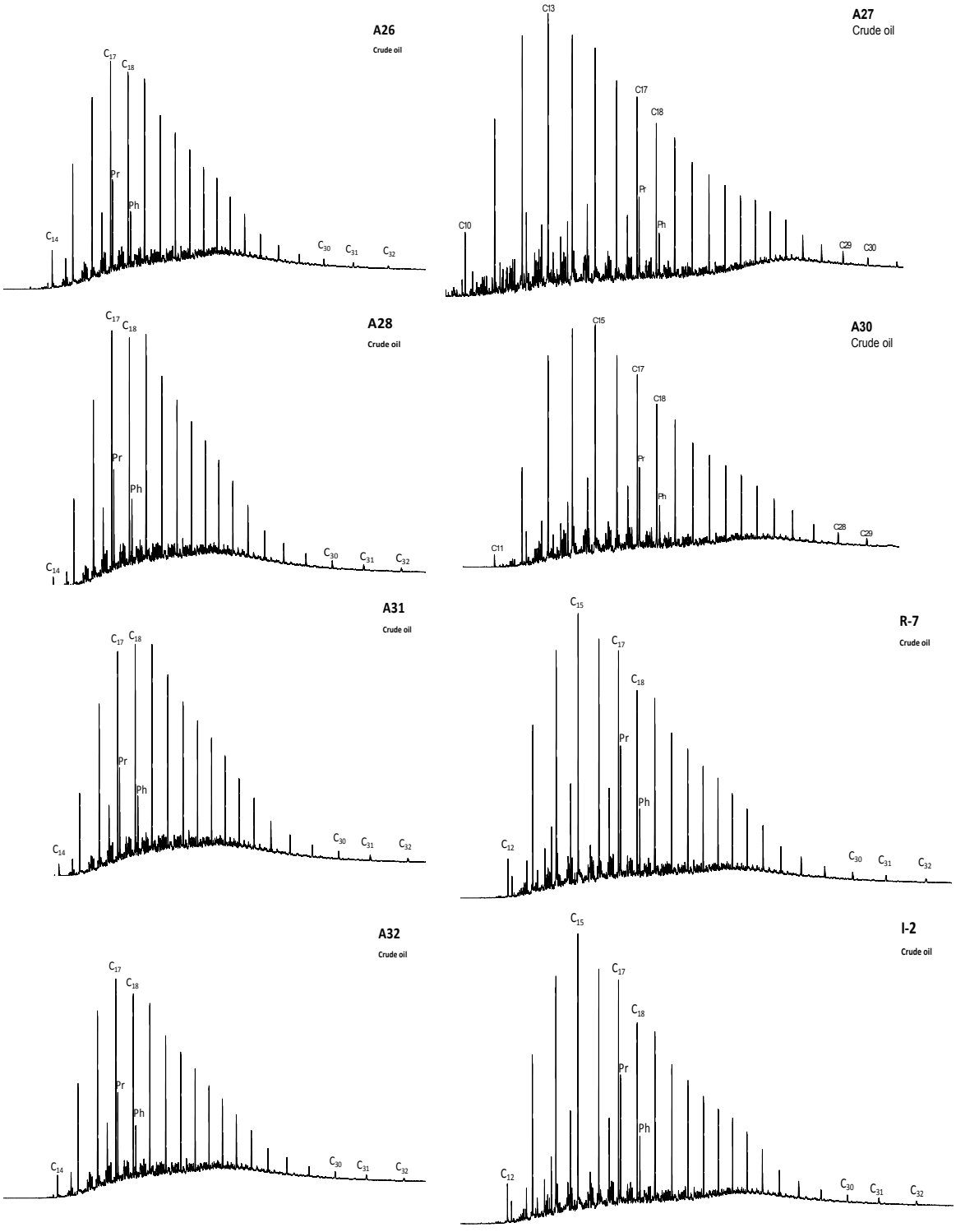

APPENDIX VI. Mass chromatograms showing the distribution of steranes (*m/z* 217) of the crude oil samples from the Murzuq Basin, Block NC-115, A Field and Block NC186, I and R Fields. (*) Deuterated Internal Standard ($C_{24}D_{50}$).

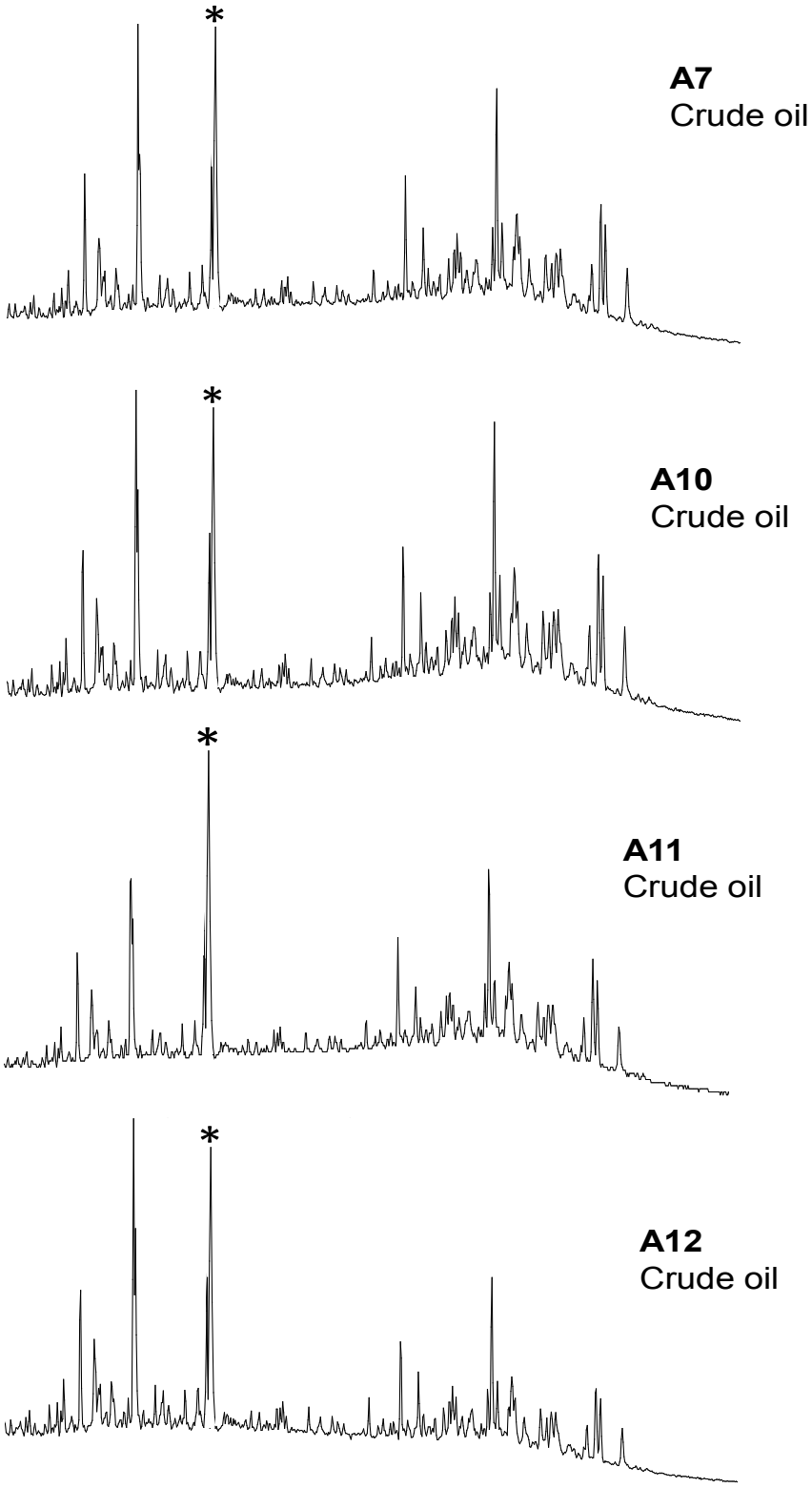

APPENDIX VI. (continued)

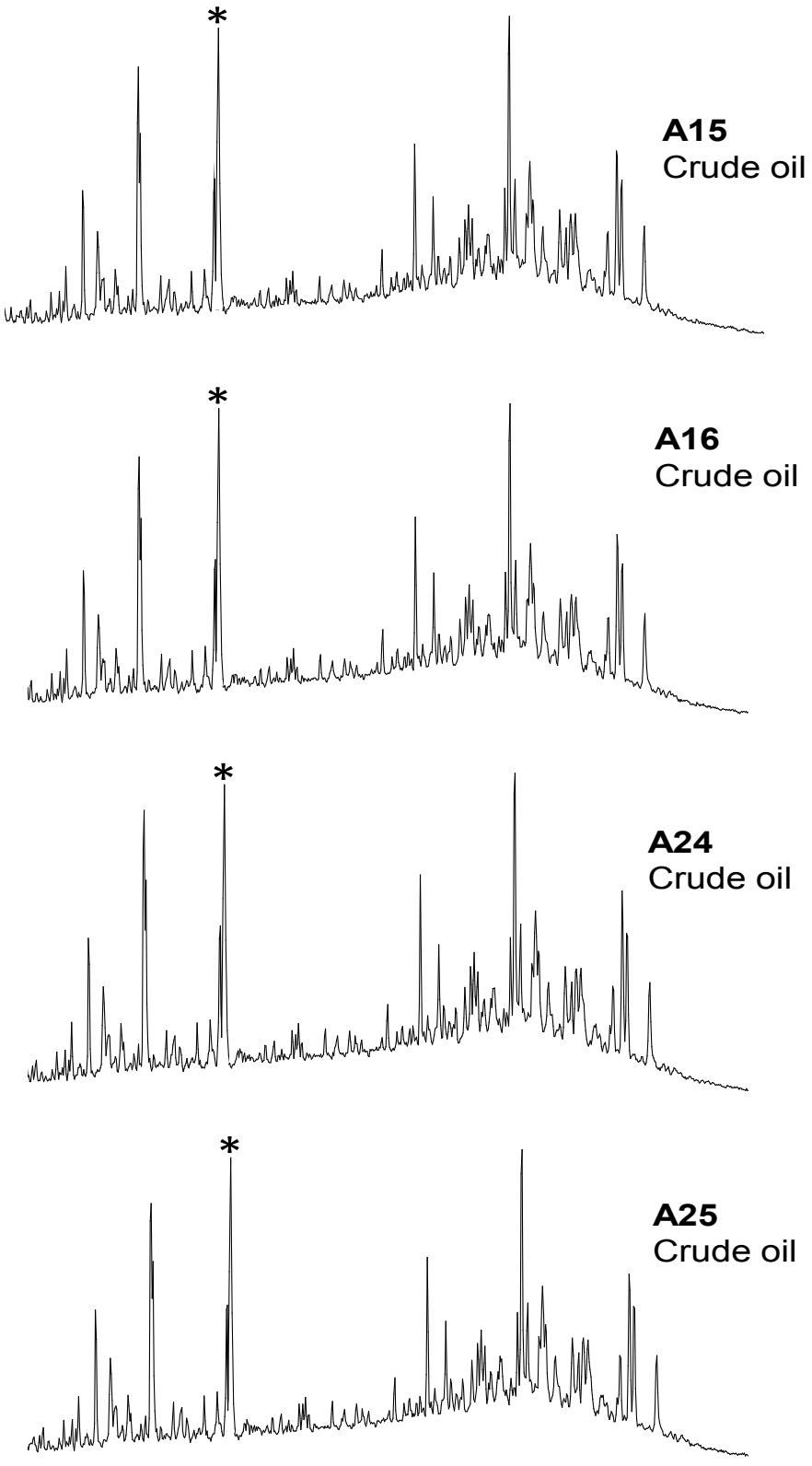

APPENDIX VI. (continued)

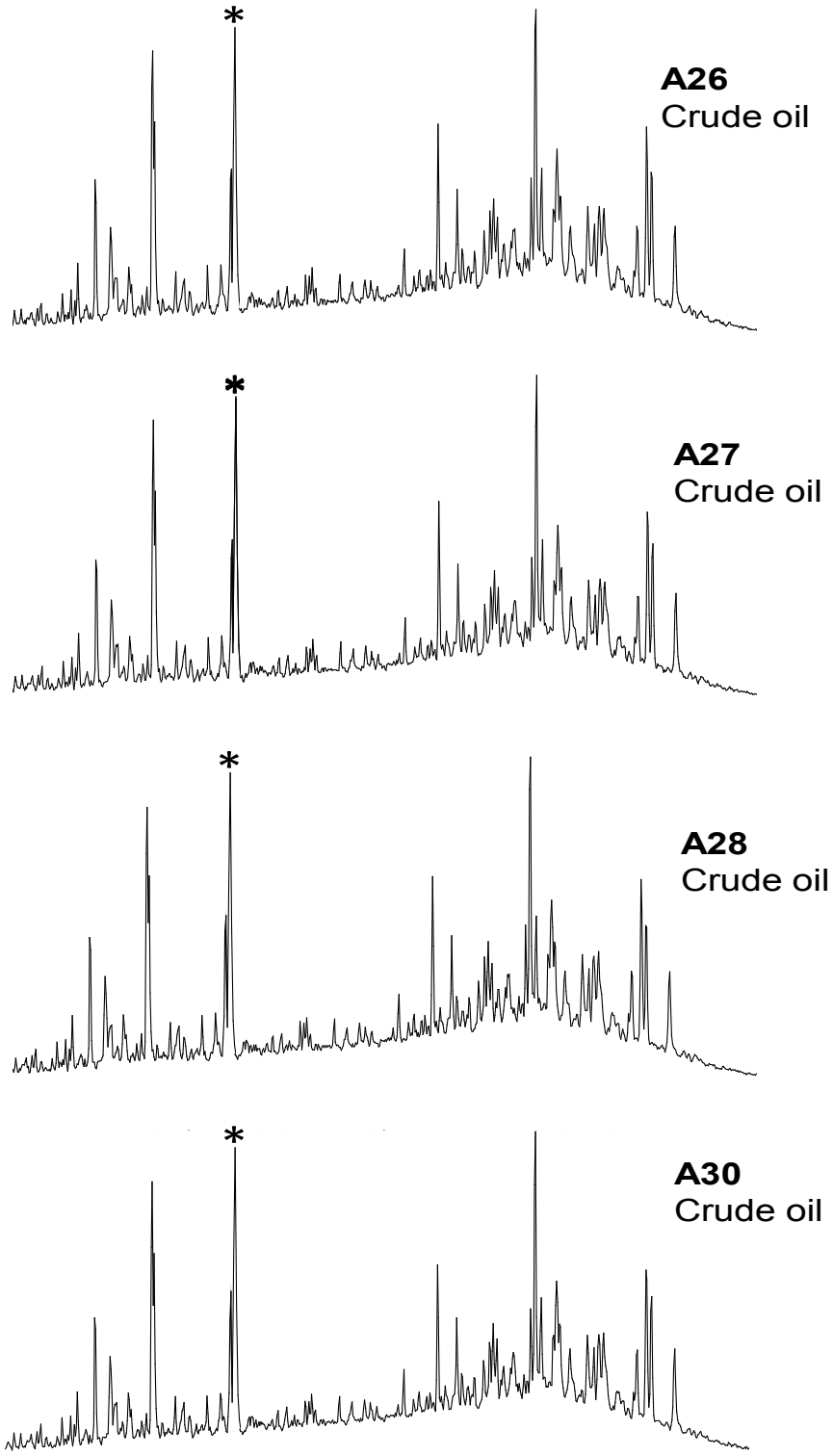

APPENDIX VI. (continued)

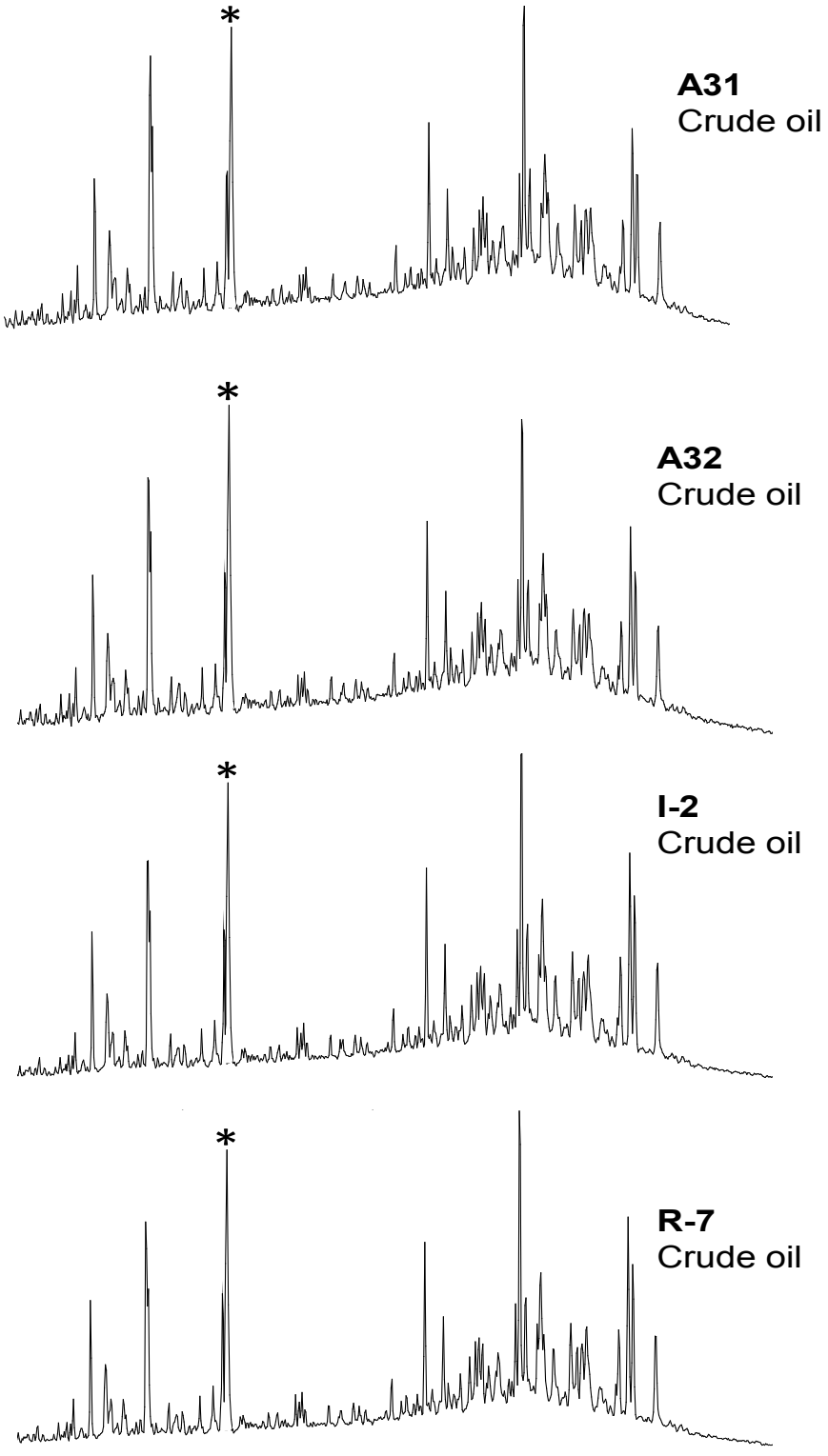

APPENDIX VII. Mass chromatograms showing the distribution of hopanes (*m/z* 191) of the crude oil samples from the Murzuq Basin, Block NC-115, A Field and Block NC186, I and R Fields.

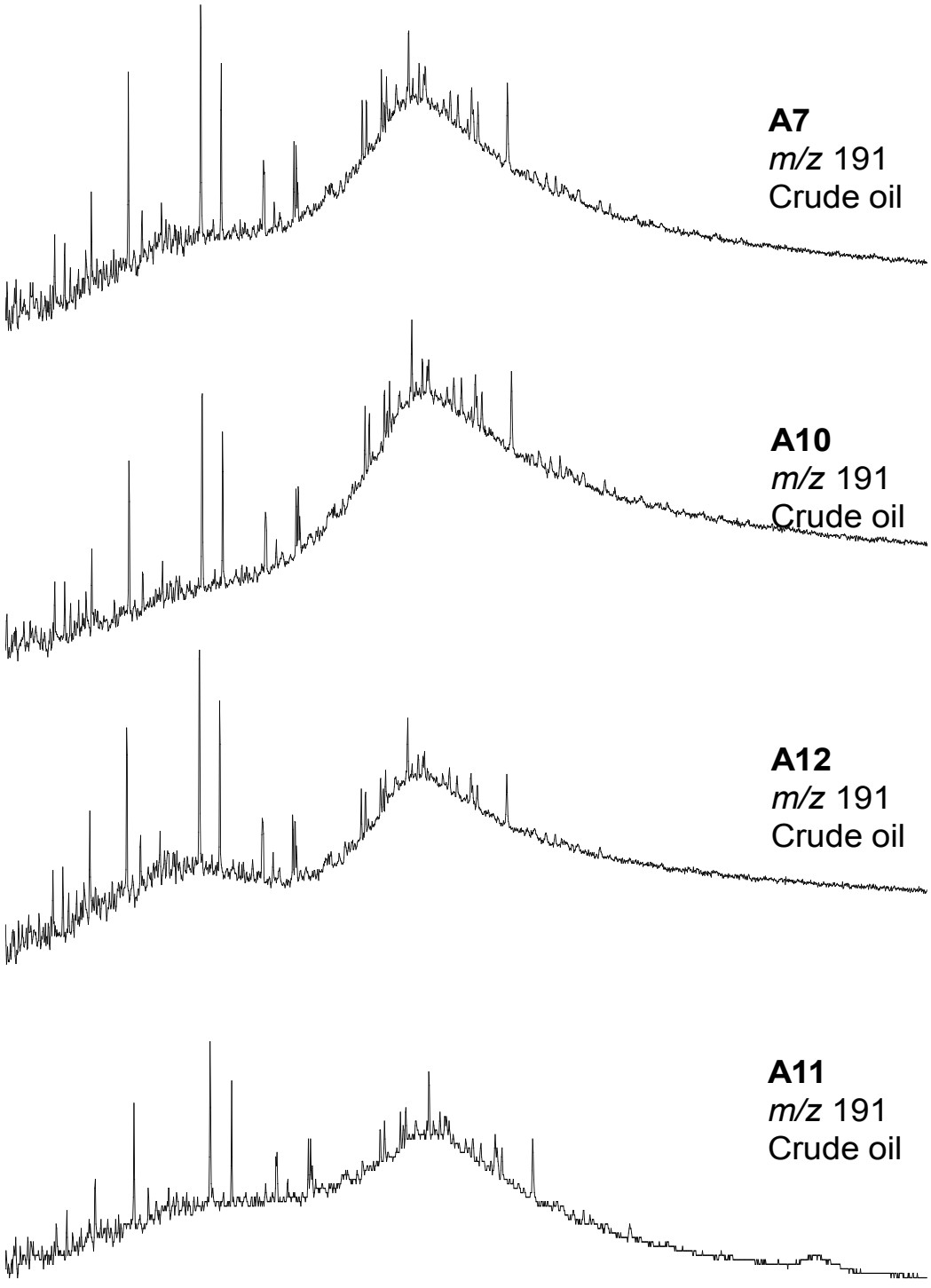

APPENDIX VII. (continued)

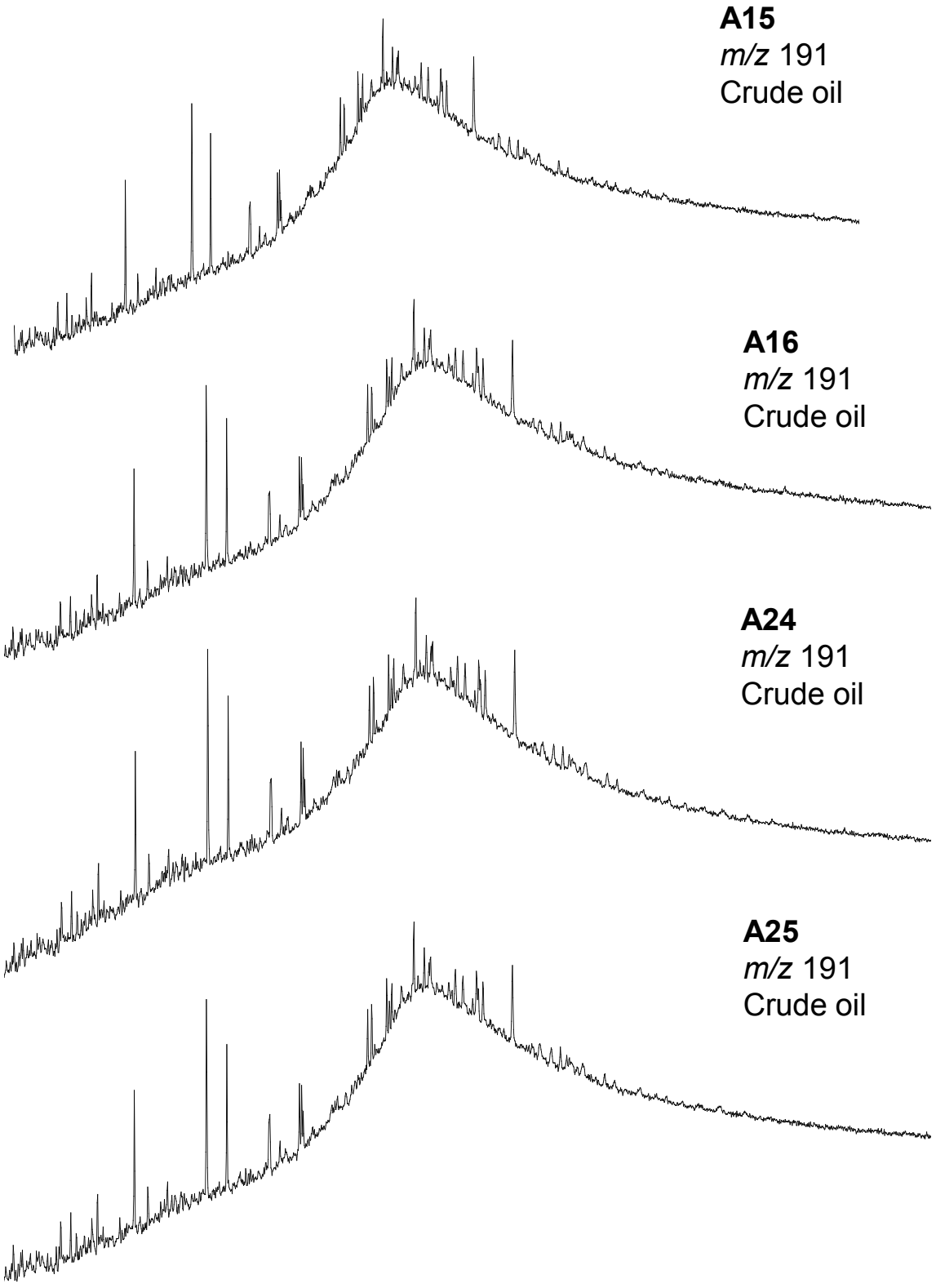

APPENDIX VII. (continued)

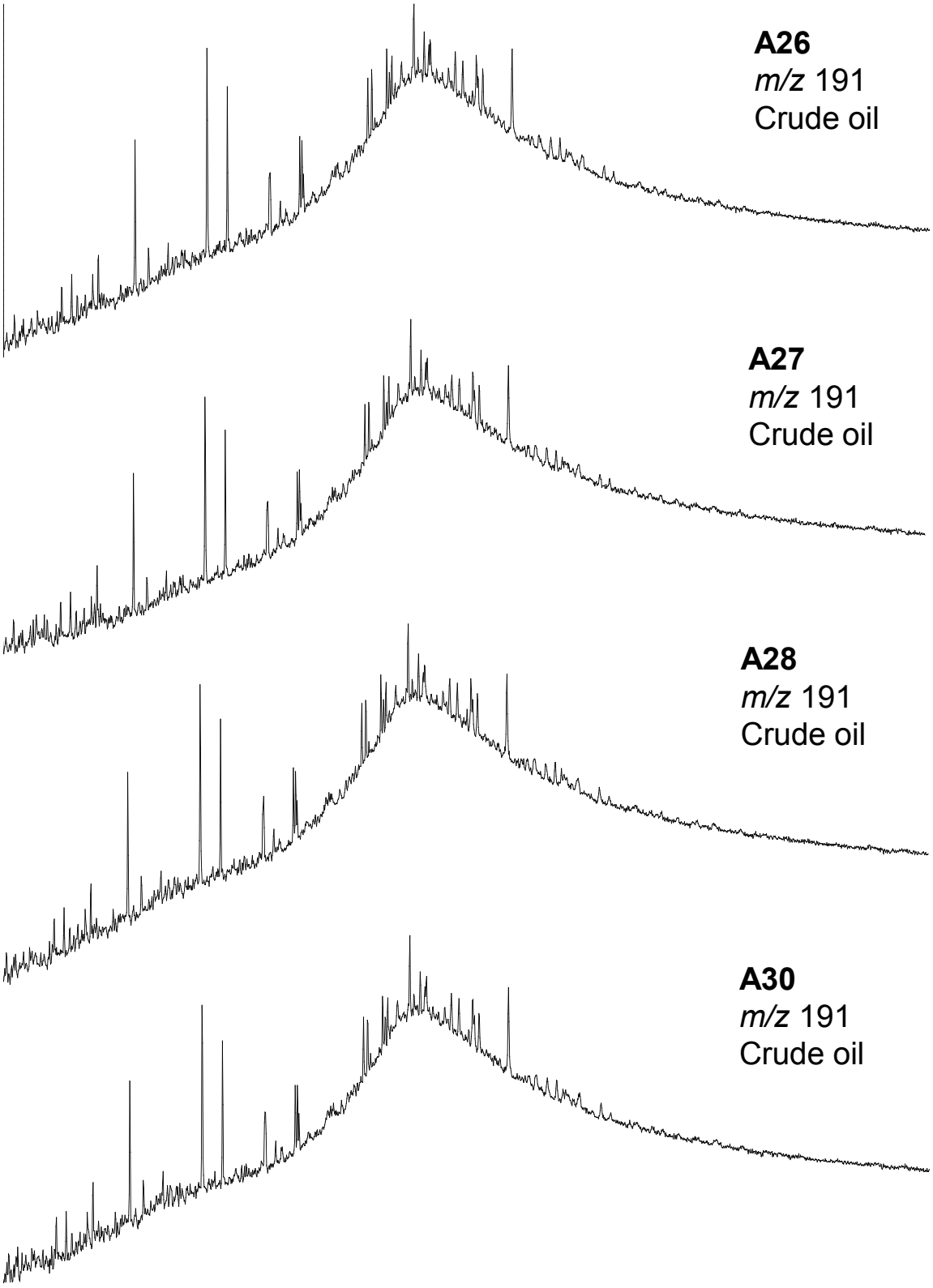

APPENDIX VII. (continued)

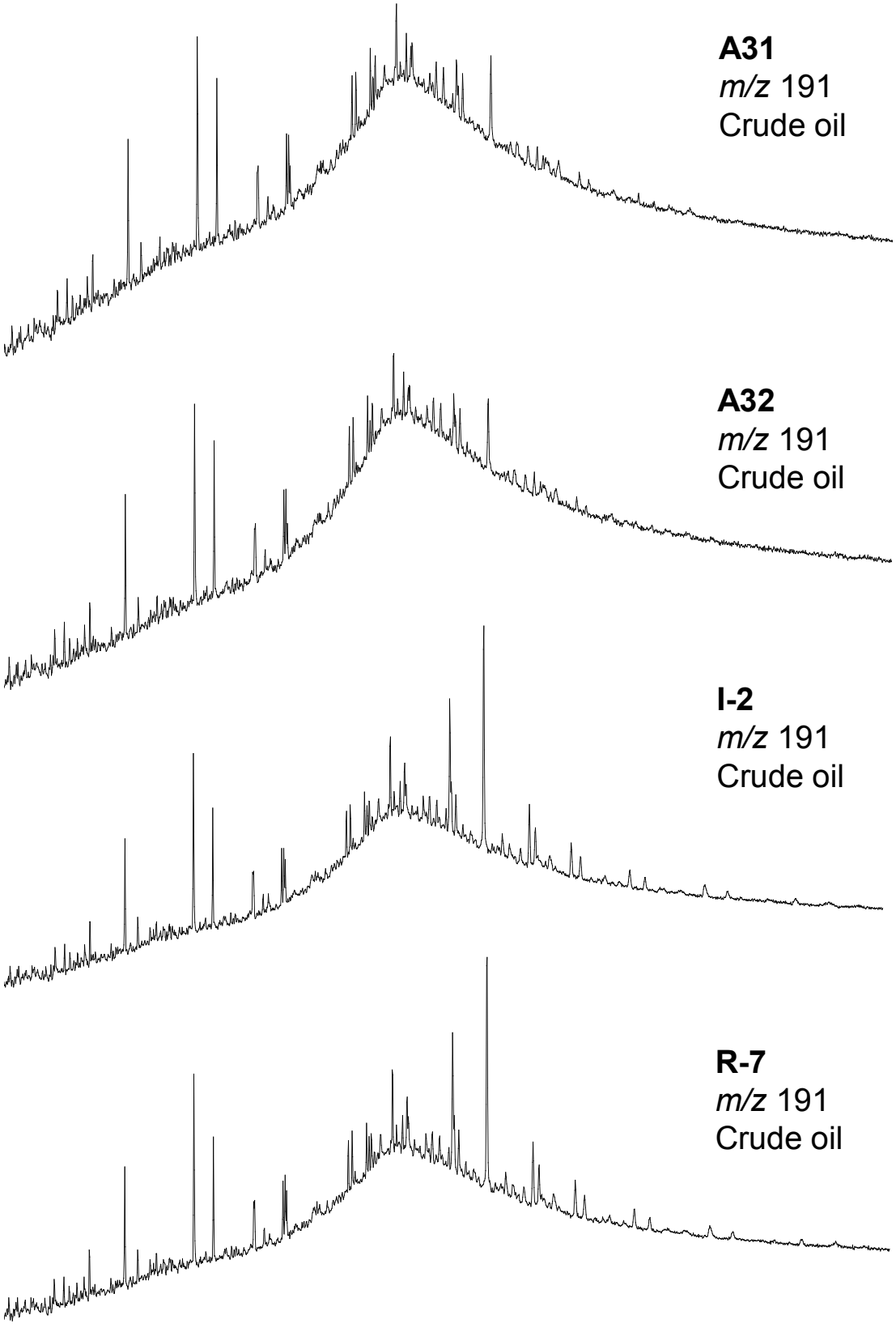

APPENDIX VIII. Mass chromatograms (*m/z* 178+192+206) showing the phenanthrene compounds in the aromatic fractions of Murzuq Basin crude oils.

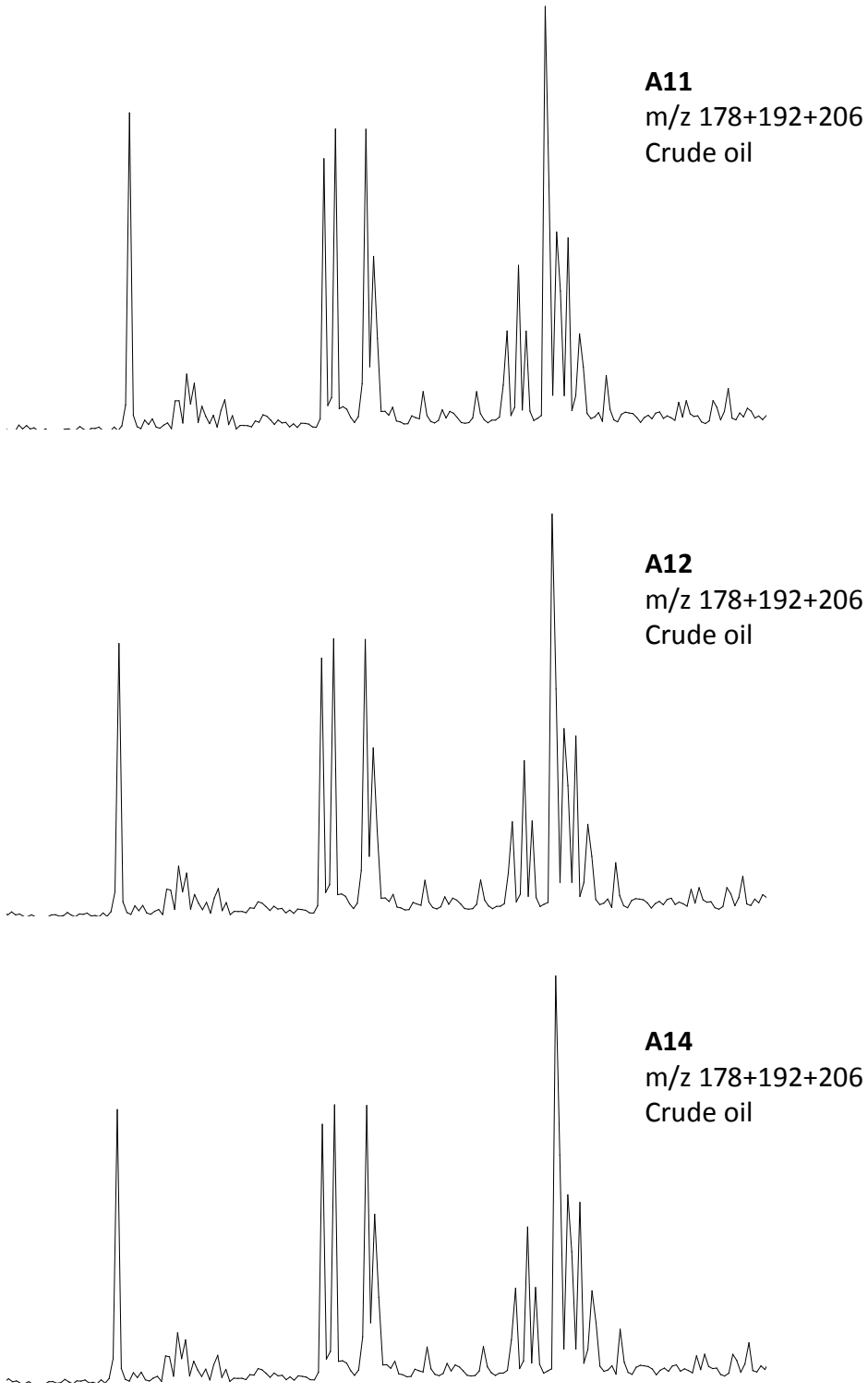

APPENDIX VIII. (continued)

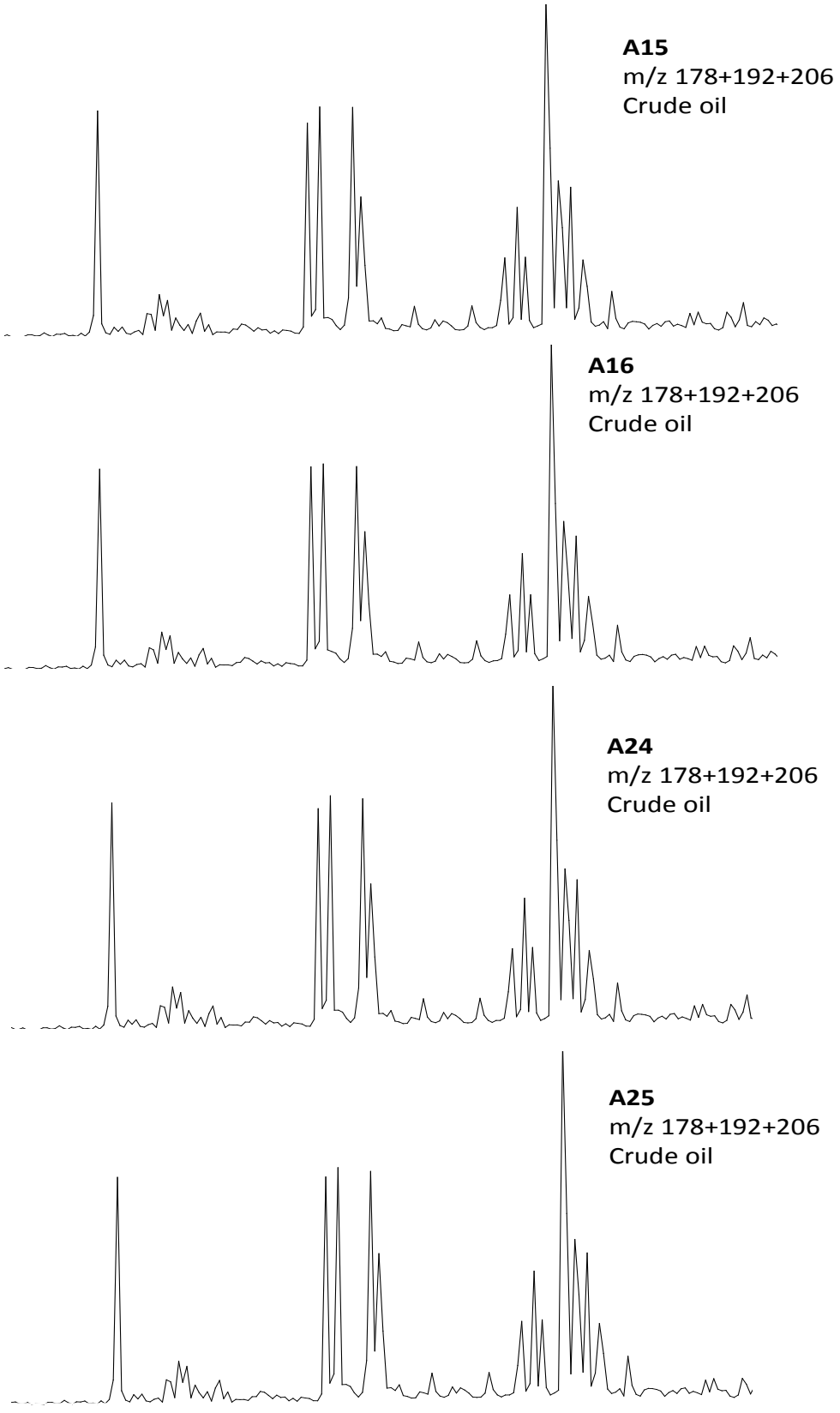

APPENDIX VIII. (continued)

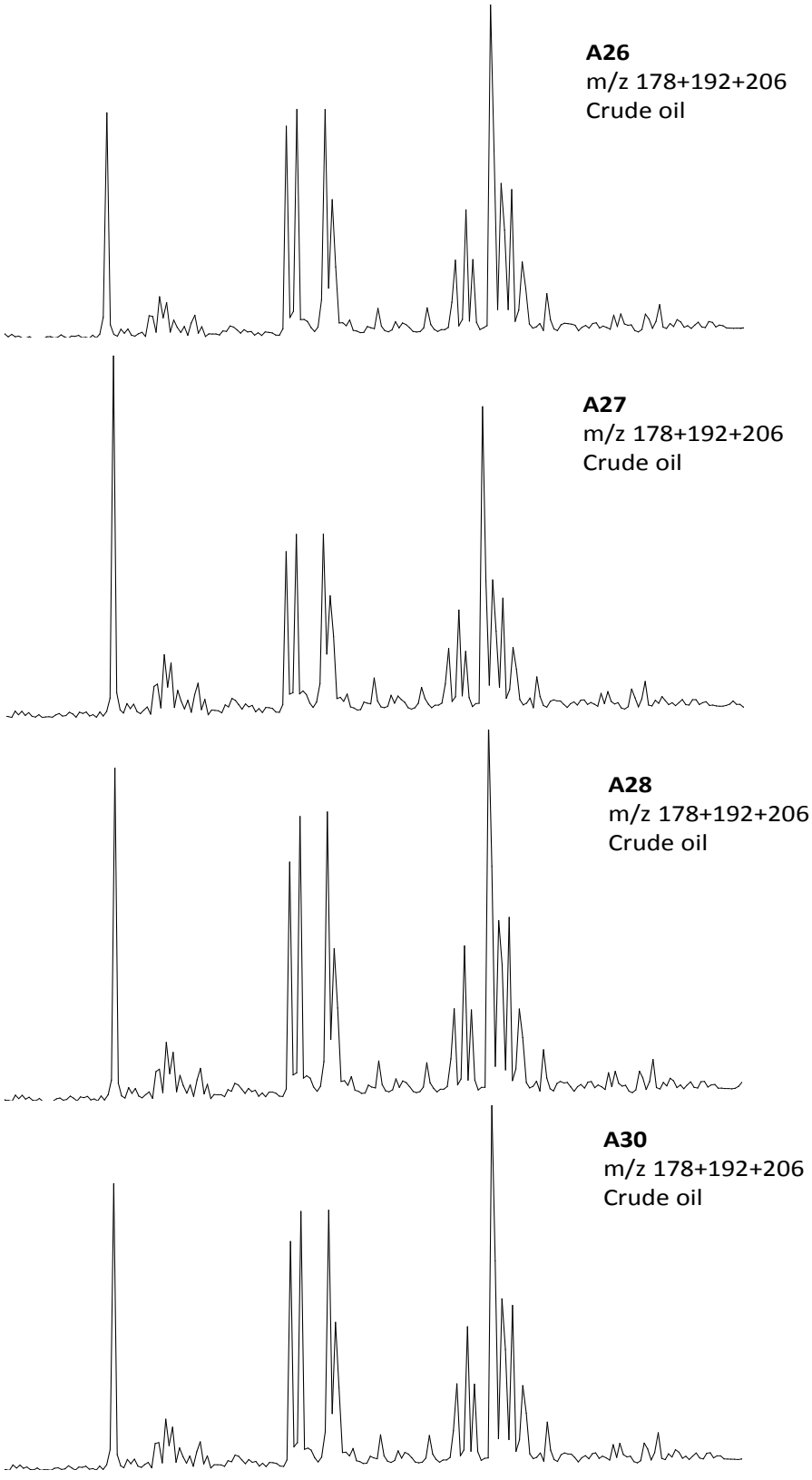

APPENDIX VIII. (continued)

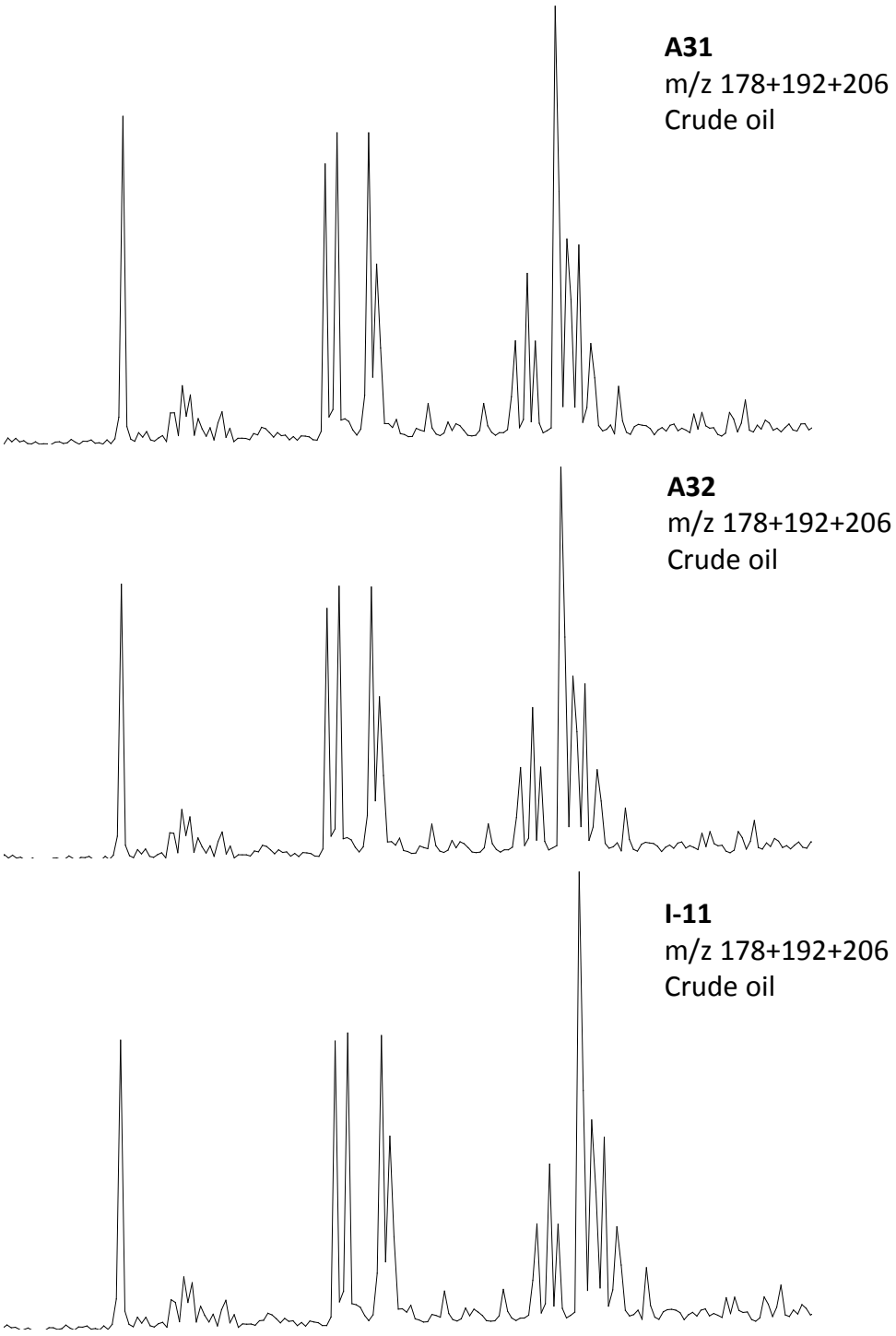

APPENDIX IX. Mass chromatograms of *m/z* 253 showing the distribution of the monoaromatic steroid hydrocarbons in the aromatic fractions of crude oil samples.

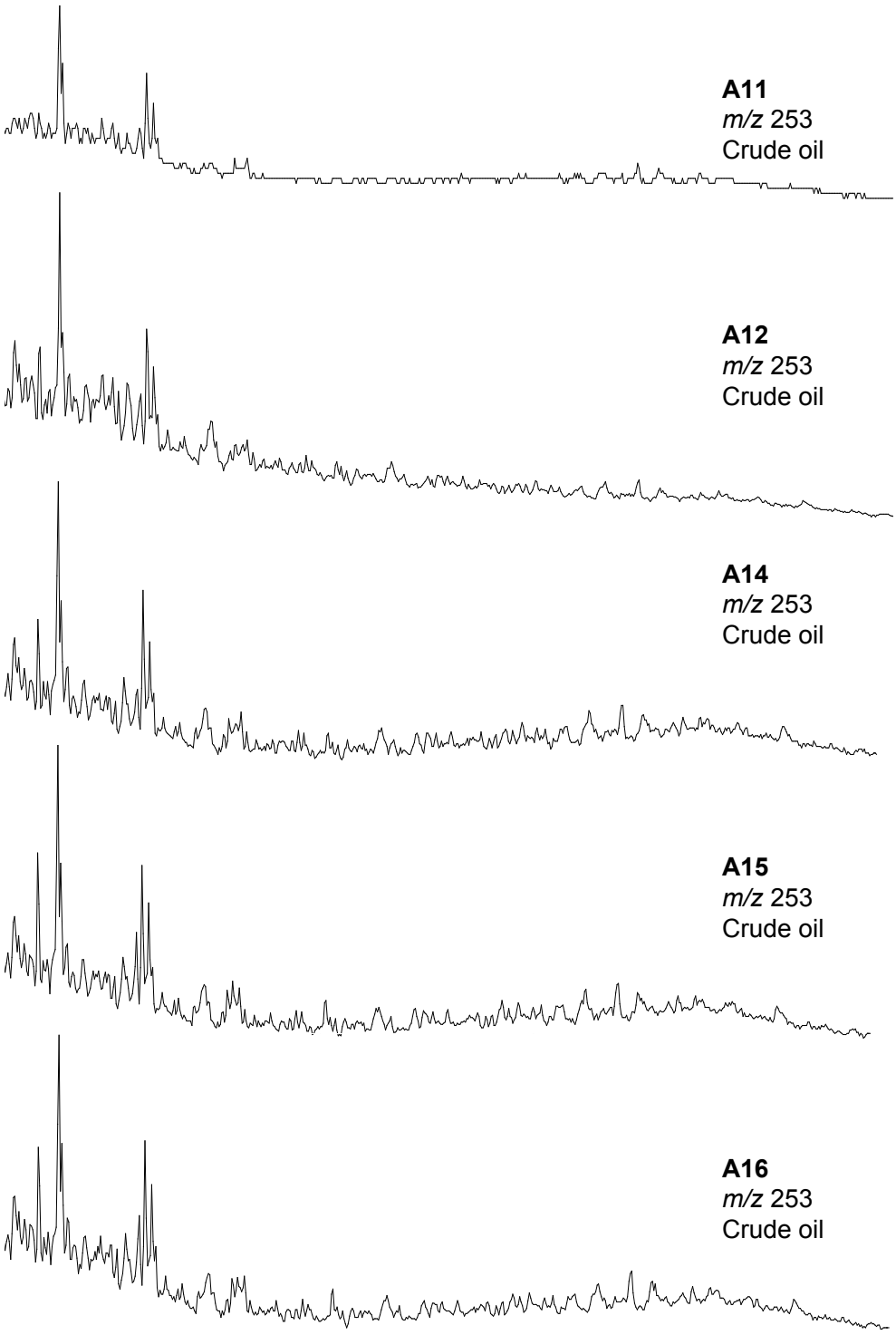

APPENDIX IX. (continued)

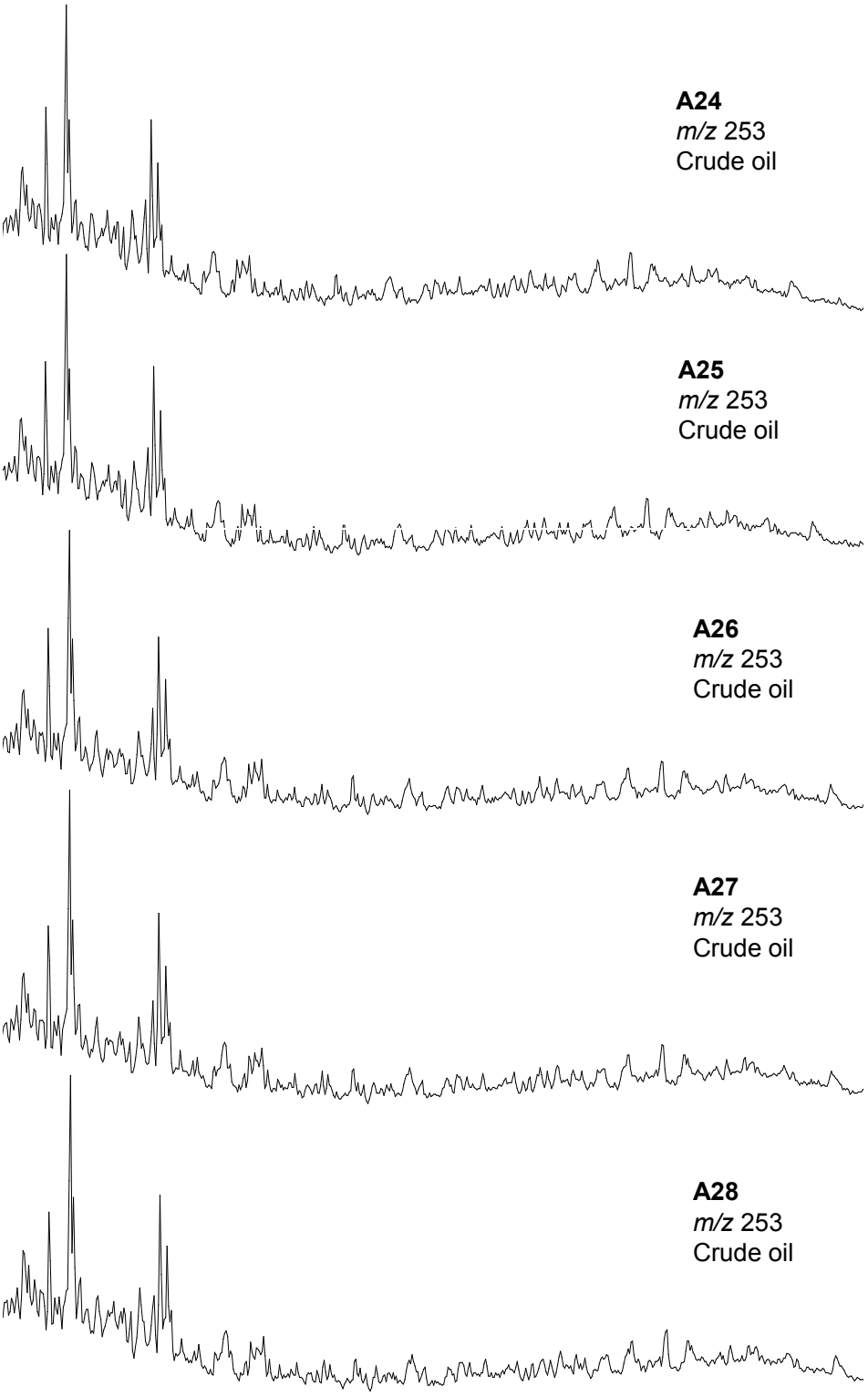

APPENDIX IX. (continued)

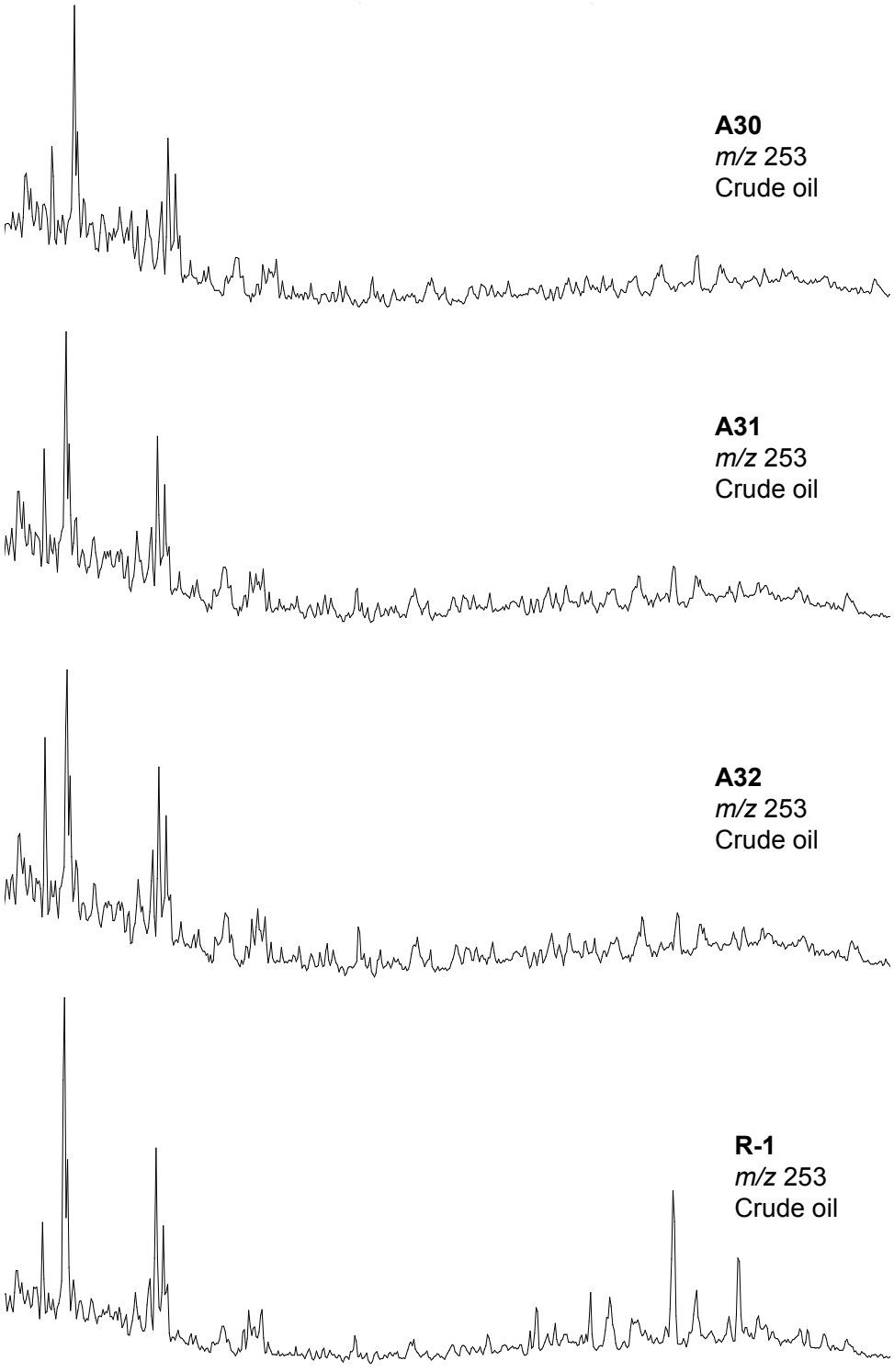

APPENDIX X. Mass chromatograms of *m/z* 231 showing the distribution of the triaromatic steroid hydrocarbons in the aromatic fractions of crude oil.

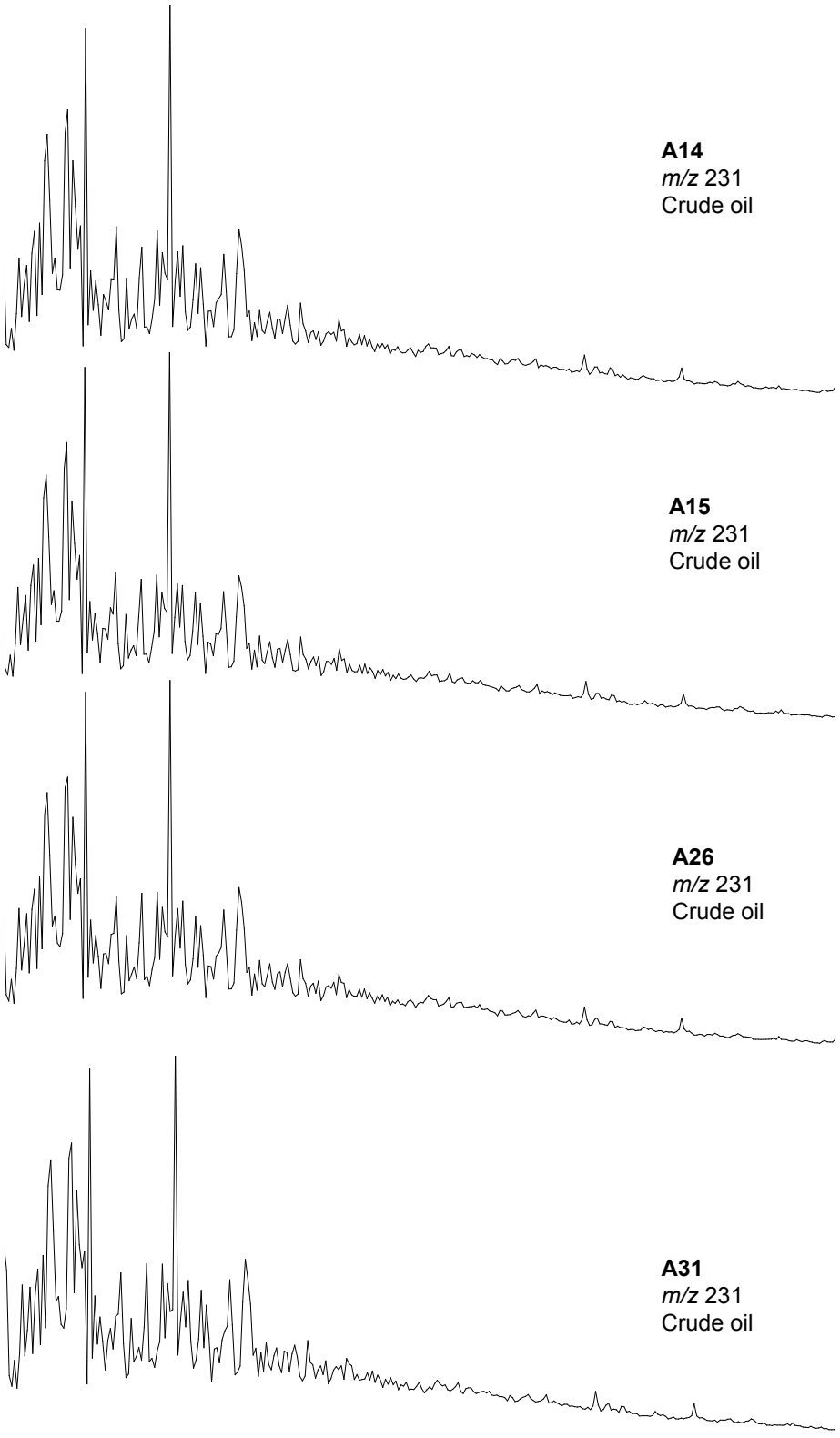

APPENDIX X. (continued)

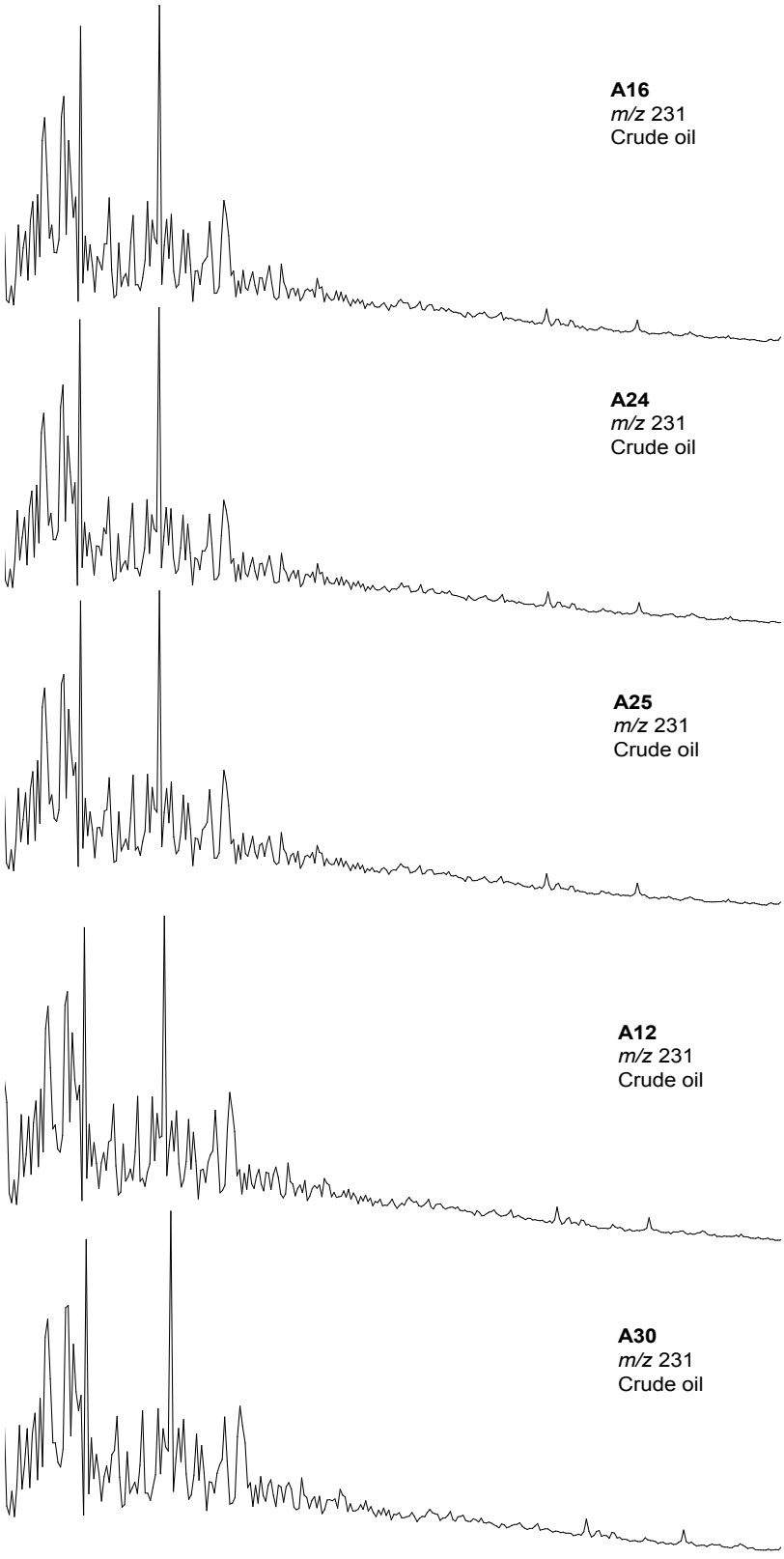

APPENDIX X. (continued)

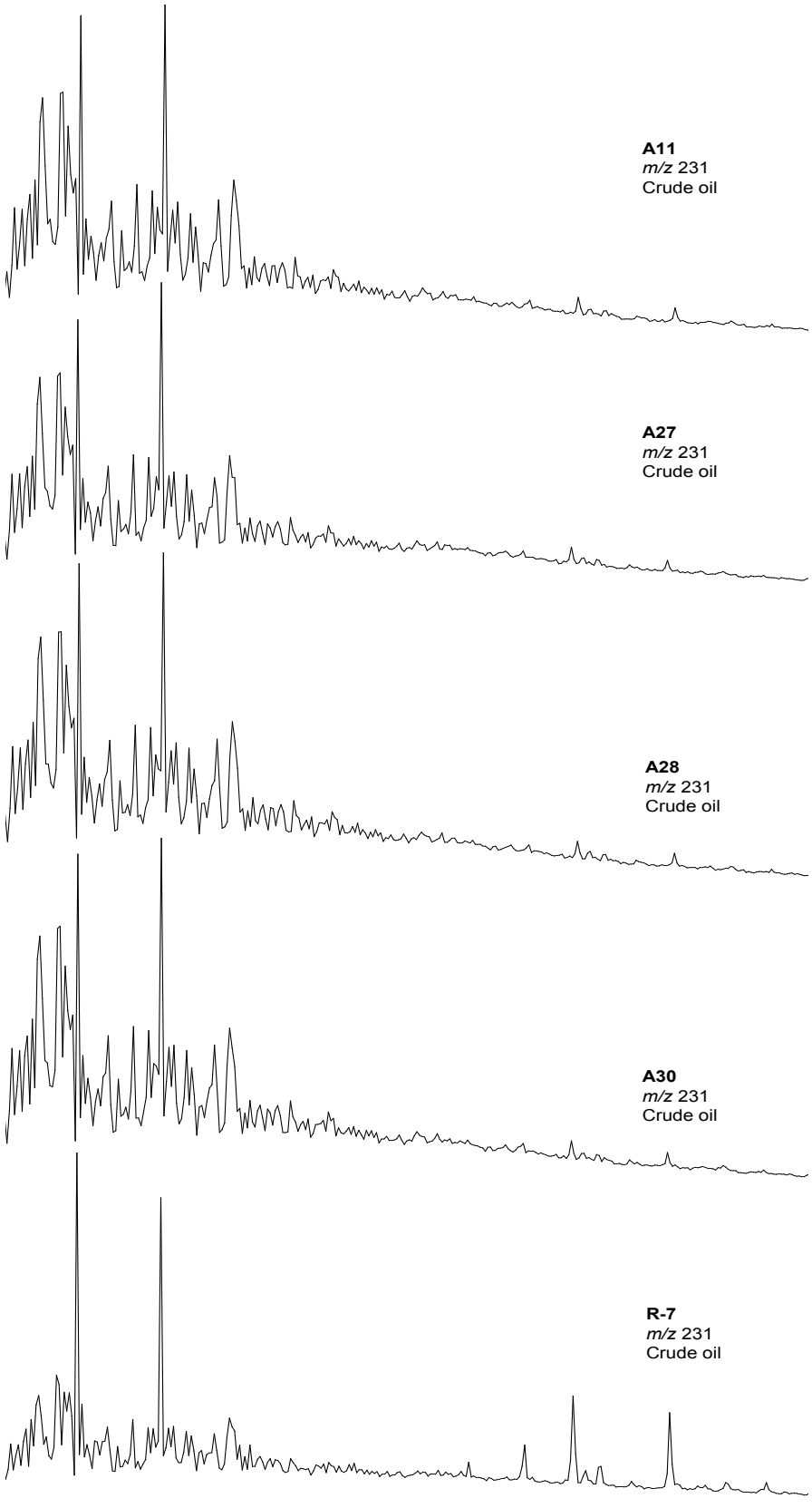

APPENDIX XI. Mass chromatograms showing: the absence of 25-norhopanes (*m/z* 177) in all crude oils from A-, I-, & R-Fields within Murzuq Basin, S.W. Libya.

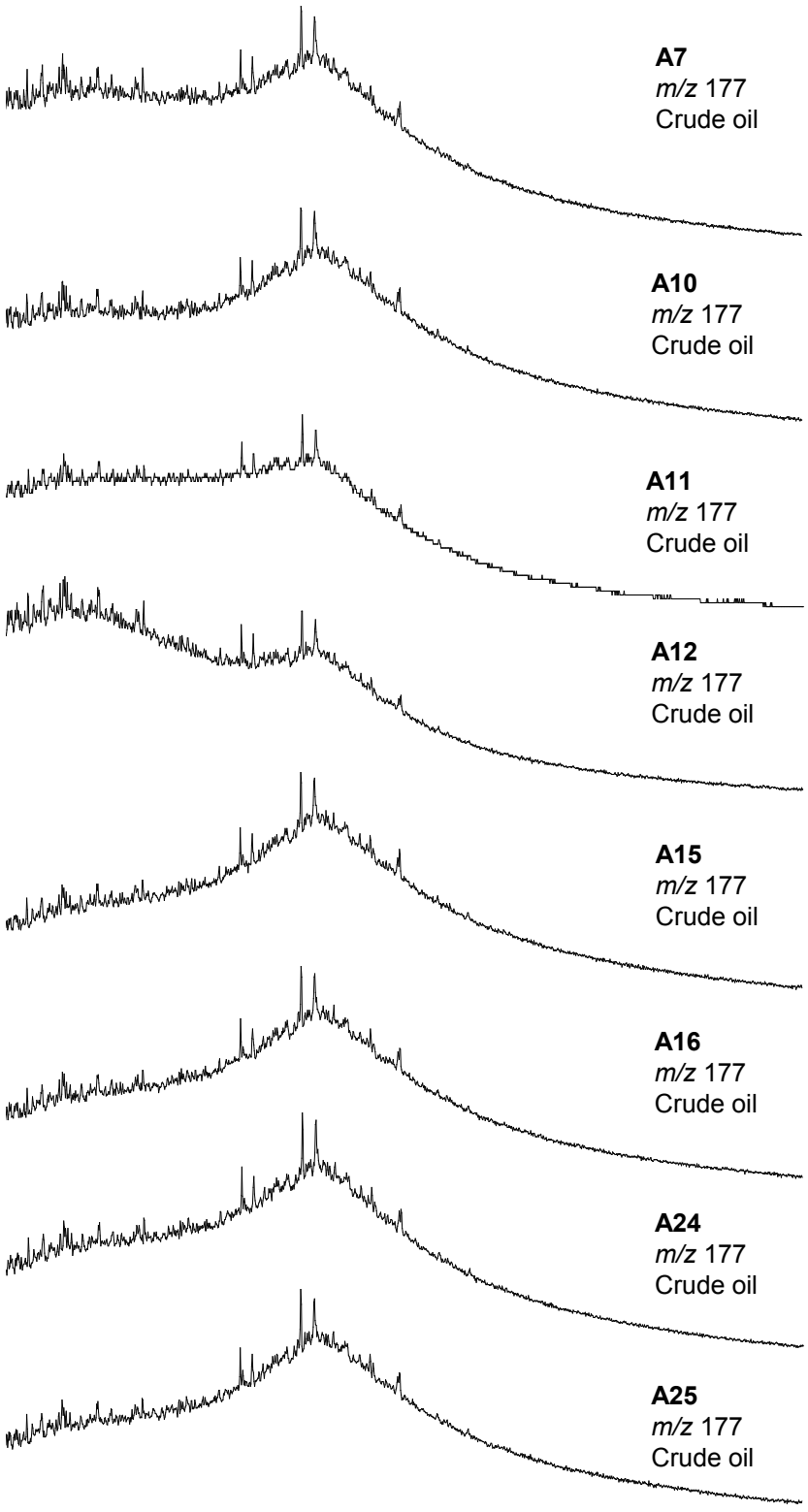

APPENDIX XI. (continued)